Trinity College Dublin
Coláiste na Tríonóide, Baile Átha Cliath
The University of Dublin

Large scale compound parabolic concentrator for building integrated façade

Anita Lorena Ortega

16313458

March 2023

A dissertation submitted in partial fulfilment of the degree of

Doctor of Philosophy

Department of Civil, Structural and Environmental Engineering,
School of Engineering

Declaration

I have read and I understand the plagiarism provisions in the General Regulations of the University Calendar for the current year, found at **http://www.tcd.ie/calendar**.

I have also completed the Online Tutorial on avoiding plagiarism 'Ready Steady Write', located at **http://tcd-ie.libguides.com/plagiarism/ready-steady-write**.

_____

Abstract

This thesis presents the design, fabrication, performance and analysis of two façade-integrated compound parabolic concentrator (CPC) for two different locations: Ferrara, Italy and Mayo Ireland. The research involves comparing the performance of CPC, CPC/PCM (CPC with Phase Change Material) and Reference systems.

The first, CPC, designed for Ferrara, Italy, had an acceptance half angle of 22 º - 68 º, concentrator ratio of 3, and contained 32 solar cells. It was fabricated in Trinity College Dublin and tested at University of Ferrara (UNIFE), Italy. The results showed 928 W/m^2 CPC/PCM system reached 113 W (target power), this value was a factor of 1.79 higher when compared with the Reference system. A record solar cell efficiency was achieved for CPC/PCM system of 24 %, this was 10 % more than the Reference system.

Maximum electrical power production between CPC/PCM system and CPC system were 80 W and 72 W, respectively at 642 W/m^2 solar radiation. The solar cell efficiency reached by the CPC/PC system was 25 % and 22 % for the CPC system. It can be confirmed that heat exchange helps to improve the electrical efficiency of the concentrator compared to a concentrator without heat exchange by 3 %.

Second, a compound parabolic concentrators with acceptance half angle of 12 º - 63 º, concentrator ratio of 3, 24 solar cells and suitable in Mayo, Ireland weather climate condition were manufactured and tested at Brackloon Drummin Community Centre, Ireland.

The experimental average results showed that under direct radiation, CPC system reported better power output equal to 37 W (power ratio 1.86), while CPC/PCM and Reference systems were 33 W (power ratio 1.77) and 19 W respectively. Reference system showed more stable and better fill factor equal 0.76, while CPC and CPC/PCM system were 0.62 and 0.59 respectively. CPC system presented better solar cell efficiency equal to 20 %, while CPC/PCM and Reference system were 19 % and 12 % respectively. CPC/PCM system reported the highest solar cell temperature equal to 67 ºC.

At 824 W/m^2, CPC/PCM system reached 103 W (power target) with a power ratio equal to 2.79. The fill factor was 0.61 with a system efficiency equal to 11 %. The temperature in the solar cells was 53 ºC, this was 35 ºC more than the outdoor temperature. At 832 W/m^2, CPC system reported 104 W (power target) with power ratio of 2.65. The fill factor was 0.63 with a system efficiency equal to 11 %. The temperature in the solar cell was 50 ºC, this was 33 ºC more than the outdoor temperature.

Acknowledgements

A deep and big super thank you to my project supervisor Dr. Sarah McCormack. For your infinite patience, hours of meeting, kilometers of walks and litters of tea. Thank you for letting me be part of your team and this great project. For putting up with all my mistakes and crazy behavior. For believing in me more than I do. This is more yours than mine Professor Sarah (I think you know that). For being my guide and friend and for holding my back in difficult times. Please keep this in mind Professor Sarah *"You never forced me, I was always interested", I always will.*

Thanks for being there Professor Sarah.
My role model personally and professionally.

To the group of technicians at Civil Engineering Department for their great and hard work during the manufacturing process of the systems. A special thanks to the boss of bosses David Mc Aulay (aka Mr D), thank you for helping me in every detail of the manufacturing process, for collecting materials and for sacrificing your holidays in Cork to finish the systems on time (sorry about that). Thank you for your life advices and for letting me play with the crane when I was sad. To the rest of the team: Mary, Mark, Michael and Pat. Thank you for the infinite help, for all the teaching and for your patience dealing with my super stressful behavior and pressure. It was fun.

For them in the sky
Always with me
I miss you guys with every breath
♥

The last one standing

Contents

List of figures

List of tables

Nomenclature

a	Radius of an aperture	mm
a’	Radius of an absorber	mm
C	Geometric concentration ratio	
G	Irradiation	W/m^2
I	Current	A
P	Power	W
R	reflectivity	%
T	Temperature	°C - K
t	time	s
V	Voltage	V
θ	Acceptance-half angle	°
Ø	diameter	mm
Δ	variation	
M_{pp}	Power output at maximum power point	W
I_{mpp}	Current at maximum power point	A
V_{mpp}	Voltage at maximum power point	V
PR	Power ratio	
$P_{concentrator}$	Concentrator power	W
$P_{reference}$	Reference power	W
η_{cell}	Solar cell efficiency	%
M_{pp-cpc}	Power output in the CPC	W
A_{cell}	Solar cells area	mm^2 – m^2
η_{system}	System efficiency	%
A_{apert}	CPC aperture area	mm^2 – m^2
η_{opt}	Optical efficiency	%
$I_{sc,cpc}$	Short circuit current of CPC	A
$I_{sc,ref}$	Short circuit current of Reference	A

Abbreviations

ACPPVC	Asymmetric compound parabolic photovoltaic concentrator
CPC	Compound parabolic concentrator
2D	Two dimensional
3D	Three dimensional
Al	Aluminium
BIPV	Building integrated photovoltaics
CNC	Computer numerical control
CPC	Compound parabolic concentrator
CdTe	Cadmium telluride
LDS	Luminescent down shifting
PCM	Phase change material
PMMA	Polymethylmethacrylate
PV	Photovoltaics
Refl.	Reflector
UV	Ultraviolet
PLA	Polylactic Acid
ABS	Acrylonitrile Butadiene Styrene
LCA	Life Cycle Assessment
STC	Standard Test Conditions
ASTM	American Society for Testing and Materials
a.u.	Arbitrary unit

Chapter 1 Introduction

1.1 Background

Global energy policy and national initiatives, such as the Climate Action Plan targets are increasingly focused on clean energy sources. This emphasis on sustainability raises the question of why solar energy should be considered. Solar energy is a renewable and abundant source, making it an attractive option for addressing energy security and reducing greenhouse gas emissions. Photovoltaic technologies, in particular, offer a versatile and efficient method for harnessing solar energy.

Irelands Climate Action Plan, published in 2022(Government of Ireland, 2023), aimed to achieve a more sustainable, low-carbon future by 2030. The main targets related to renewable energy included:

- Increasing the share of renewable energy in electricity generation to 70 % by 2030.
- Increasing from 1.5 GW to 8 GW of electricity from solar energy by 2030.

Photovoltaics convert solar radiation to electrical energy. The efficiency and power output depend on the solar radiation intensity which reaches the solar cell surface. The amount of solar radiation over the solar cell surface can be increased using concentrators. PV concentrators can be classified in four types: Lens concentrator, Mirror concentrator, Reflector concentrator, Static concentrator (McCormack, 2016). An example of a reflector concentrator is the compound parabolic concentrator (CPC). In this concentrator, a large portion of the reflector area can be eliminated without reducing the concentration ratio substantially, and concentration of the light into a smaller area of PV, gives the potential to reduce the electricity production cost (Rabl, 1976). However, the temperature in the CPC becomes in an important factor.

Research has been undertaken to improve the efficiency of the CPC (Winston, 1974; Rabl, 1976a; Othman et al, 2005; Mallick et al, 2007; Wu, 2009). In addition, researchers have been working to integrate CPCs in building façades (Zacharopoulos et al, 2000; Mallick et al, 2004, Wu, 2009). Results showed power and optical losses in the CPC system affected the system efficiency.

Truncation of CPC creating an asymmetric CPC has been found to be the most suitable for use in building facades for a range of angular acceptance angles and is an excellent option for electricity generation in buildings. However, there is much scope for enhancement and improvement.

1.2 Scope of the research

To achieve building EU target of at least a 40 % reduction in greenhouses gas emissions (GHG) by 2030 (IDEAS, 2023), it is essential to apply integrated renewable energy systems (RES) to buildings, a critical step for the wider integration and deployment of renewable energy, however, traditional solar and geothermal technologies often require more space than is

practical in urban setting such as apartment blocks and offices, where roof space and surrounding building footprints are limited.

This PhD project is part of a larger H2020 project 'IDEAS'. The Integrated Design of Efficiency Approaches and Systems (IDEAS) project addresses this challenge by incorporating efficiency and scale improvements to solar PV, thermal and geothermal RES enabling more energy efficiency with less space. As a result, buildings will be able to meet more of their needs sustainably (IDEAS, 2023). Trinity College Dublin is leading the IDEAS research project, which is supported by EU Commissions Horizon 2020 research and innovation programme through grant agreement No. 815271. The aims in IDEAS research project are:

- Integrating PV with heat energy trapping coating into building facades
- Optimizing Heat Pump technologies with PV/PCM
- Novel integration and Demand-side Management

The subject of this thesis forms part of work package 1 on the development of novel solar technology "Integrating a concentrating CPC with PV with into the building façade with luminescent layers and thermal energy storage for enhanced efficiency". Two demo-sites were used in order to integrate these technologies and subsequent testing:

- Ferrara, Italy: University of Ferrara (UNIFE) (44º49`54.12" N, 11º35`59.48" E)
- Mayo, Ireland: Brackloon Drummin Community Centre (53º44'16.46" N, - 9º33'13.10" O)

The design criteria for work package 1 are described in table 1.1.

Table 1. 1 Design criteria for IDEAS project – Work package 1

Design Criteria	Description
1. Novel Solar Technology	Development of large-scale compound parabolic concentrators (CPCs)
	Integration of luminescent down-shifting layers coating on top of the solar cell
	Incorporation of phase change material for heat collection
2. Power Output	Target power output of 100 W at noon throughout the year
3. Concentrator Ratio	Concentrator ratio higher than 2
4. Efficiency Improvement	Address the challenges posed by low efficiency PV systems
5. Building Integration	Integration of PV system into building façades
	Efficient use of limited building surface area
6. Demo Sites	Ferrara, Italy
	Mayo, Ireland

IDEAS project proposed the implementation of large scale compound parabolic concentrators (CPCs) using luminescent down shifting layers on top of the solar cell and integrated with phase change material (PCM) for heat collection. These CPCs possess a power output of 100 W at noon during the year and a concentrator ratio higher than 2. The purpose of this proposed implementation is to address the challenges posed by low efficiency photovoltaic (PV) systems and limited building surface area in the integration of PV system building façade To enhance and improve the CPC and also to demonstrate a new option for integration in buildings, a new compound parabolic concentrator system suitable for façade installation was proposed in this research.
This research will involve exploring the design, optimization and performance of CPCs for two different locations: Ferrara, Italy and Mayo, Ireland, taking into consideration the local weather patterns, solar radiation and building design. The research also examines the potential challenges and limitations of implementing CPCs in buildings such as their maintenance requirements, durability and impact on the building aesthetics.
Overall, the scope of research in CPCs for building façade in Ferrara, Italy and Mayo, Ireland will require a comprehensive review of the current literature in CPCs and their applications in building, experimental studies to evaluate the performance of different CPC design and expertise in areas such solar energy, building design, material science, manufacturing as well as knowledge of the local climate.

The 100 W power output chosen as a design criterion for the Compound Parabolic Concentrator (CPC) was determined by a number of factors, including efficiency, cost, size, and potential integration with existing building structures.

- Efficiency: The goal of a CPC is to maximize the amount of solar radiation that can be captured and converted into electricity by the photovoltaic (PV) cells. A 100 W output at peak solar noon suggests that the CPC design is highly efficient and can harness a significant amount of solar energy. This makes it a valuable component of the PV system, particularly in areas where solar radiation levels may not be very high.

- Cost: The power output of a PV system directly impacts its cost. Larger, higher power systems tend to be more expensive due to the larger amount of PV material required. By setting a target of 100 W, the project aims to strike a balance between power output and system cost, making the technology more affordable and thus more accessible for widespread adoption.

- Size and Integration: The size of the PV system is directly related to its power output. A system designed to output 100 W would have a reasonable size that can be seamlessly integrated into building facades without causing too much disruption or requiring significant structural modifications. This is particularly important when considering the aesthetic impact and the practicality of retrofitting existing structures.

- IDEAS project demand: In the context of the IDEAS project, the selection of 100 W as a power output for the Compound Parabolic Concentrator (CPC) has a specific purpose. The project plans to utilize this power to operate a heat pump, which is a device that transfers heat from one place to another. Heat pumps require a certain amount of energy to function effectively. In this case, the IDEAS project has determined that a 100 W power output is sufficient to run the intended heat pump system. This is a significant design consideration because it ties the performance of the photovoltaic (PV) system directly to the operational needs of the heat pump. By designing the CPC system to meet this target, the project ensures that the generated solar power is put to optimal use. It also implies that the PV system and heat pump are designed to work in tandem, creating an integrated solution for heating that is powered by renewable energy. This design requirement thus helps in achieving the project's goals of increasing the efficiency of photovoltaic systems, while also addressing heating needs in a sustainable manner. The careful matching of PV output to heat pump input requirements is an example of system-level design thinking, which aims to optimize the overall performance of interconnected components rather than just their individual performances.

Remember, the 100 W power output is not a strict limit, but rather a design guideline that allows for optimization of these factors. The actual output of the implemented system may vary depending on various factors such as local weather conditions, building orientation, and the specific design of the CPCs.

1.3 Research aims

The primary aim of this thesis is to meet the requirements of IDEAS project increasing power output, power ratio and efficiencies of the solar cell using a compound parabolic contractor for building integrated façade with a power of 100 W for two locations (Ferrara, Italy and Mayo, Ireland).
The research aims of the thesis are:

- To design two Compound Parabolic Concentrators (CPC) for façade integration to produce 100 W power output at noon during the year for two locations: Ferrara, Italy and Mayo, Ireland.
- To undertake ray tracing to predict the power and optical performance for different CPC systems and chose a CPC system suitable for the maximum and minimum altitude of the sun for Ferrara, Italy and Mayo, Ireland.
- To undertake a ray tracing simulation to predict the annual behavior that leads to the production of 100 W at noon for both CPC systems in Ferrara, Italy and Mayo, Ireland.
- To design, manufacture and characterise two small scale prototype CPCs systems for the two demo site locations and compare with a Reference system, in order to validate the results obtained from ray tracing simulation.

- To design and manufacture large scale CPC systems and the Reference systems for Ferrara, Italy and for Mayo, Ireland.
- To investigate the power output, power ratio, efficiencies and thermal behavior in outdoor conditions by comparing the largescale CPC systems with the Reference systems in Ferrara, Italy and Mayo, Ireland.

1.4 Contributions to knowledge

The proposed research aims to develop innovative designs for two CPCs specifically tailored for façade integration, capable of producing 100 W of power output at noon throughout the year in two distinct locations. This ground breaking approach to CPC design has never been done before and represents a novel contribution to the field of solar energy.

Integrating CPCs into building façade is a relatively new concept, and previous studies have primarily focused on improving efficiency and exploring integrations possibilities. The development of CPC designs tailored to different geographical locations, while maintaining a consistent power output of 100 W, will push the boundaries of what has been achieved thus far.

This research not only demonstrates the versatility of CPCs but also showcases their potential to be optimized for diverse environments, thereby enabling more widespread adoption of solar energy. By designing CPCs with location-specific considerations in mind, this study breaks new ground and opens up exciting opportunities for further advancements in solar energy technologies and building integrated photovoltaics.

The contributions to knowledge of this research are:

1. Design of CPCs: The research will produce designs of two CPCs for façade integration, which will be able to produce 100 W power output at noon during the year in the two different locations.
2. Ray tracing: The research undertakes ray tracing to predict the power and optical performance for different CPC systems and choose a CPC system suitable for each location. The ray tracing will also be used to predict the annual behaviour that leads to the production of 100 W at noon for the CPC system for each location.
3. Prototype testing: The research designs, manufacture and characterises two small prototype systems for the two locations and compare them with a Reference system to validate results obtained from ray tracing. This will help to ensure that the predicted performance of the CPCs is accurate.
4. Large scale system design and manufacture: The research will design and manufacture large scale CPC systems and Reference systems for each location. This will enable to investigate the power output, the power ratio, efficiencies and thermal behaviour of the CPC systems in outdoor conditions.

5. Investigating the power output and efficiencies: The research will investigate the power output, power ratio, efficiencies and thermal behaviour of the CPC systems by comparing them with the Reference systems in outdoor conditions for both locations. This will help to determine the effectiveness of the CPC systems in increasing power output and efficiencies.

The research described in this thesis will contribute to development for higher efficiency for building integrated photovoltaic façades, which can have a significant impact on reducing the carbon footprint of buildings and promoting sustainable energy sources.

1.5 Thesis outline

Chapter 2 presents a comprehensive literature review to identify the latest research and developments in the field of large scale compound parabolic concentrators for building façade.

Chapter 3 outlines the methodology used in this research and presents details such as description of the demo-sites, experimental techniques, software and characterization equipment.

Chapter 4 presents the ray tracing simulation to predict the power and optical performance for different CPC systems and choose a CPC system suitable for each location. Also, describe the use of ray tracing to predict the annual behavior that leads to the productions of 100 W at noon for the CPC system for Ferrara, Italy and Mayo, Ireland.

Chapter 5 describes the design, manufacture and characterisation of two small prototype CPC systems for the two locations and compare them with a Reference system to validate the results obtained from ray tracing.

Chapter 6 contains the design and manufacturing of large scale CPC systems and Reference systems for Ferrara, Italy and Mayo, Ireland.

Chapter 7 presents the installation and characterisation of the CPC systems and References systems in outdoor conditions in Ferrara, Italy and Mayo, Ireland. It presents the data collected such as on the power output, power ratio, efficiencies and thermal behaviour of the CPC systems and Reference systems for both locations. Analysis of data is presented to determine the effectiveness of the CPC systems in increasing the power output and efficiency compared with Reference systems.

Chapter 8 draws conclusions based on the results obtained and provides recommendations for future research and development in the field.

Chapter 2 Literature review

In recent years, the use of photovoltaics (PV) as an integral part of the building e.g. façade, windows, walls, roofs, has significantly increased and is one of the fastest growing PV markets worldwide. Building integrated photovoltaic (BIPV) products differ from PV systems used for field applications and have potential to reduce the cost of the PV system (Mallick et al., 2006).

The cost reduction of the BIPV system can be made either by increasing the system efficiency or using the concentrating system if the cost of the concentrating system is comparable with the replaced BIPV components (Mallick et al., 2006). Concentrating solar energy onto a photovoltaic material reduces the cell area per unit output and, for certain cell materials and designs, it can increase the PV conversion efficiencies. This will allow the total cost of the system to be reduced per unit of energy which is delivered (Collares-Pereira et al., 1978). Concentration can be achieved using reflective or refractive devices in order to increase the luminous flux on the solar cell surface (Luque et al., 1995; Zacharopoulos et al., 2000).

2.1 Practical development of Compound Parabolic Concentrator (CPC)

Compound parabolic concentrators (CPC), concentrate radiation from the aperture to the receiver (Norton et al, 2011) and most of the incoming beam and diffuse radiation can be collected and/or reflected onto the absorber surface (Kessentini and Bouden, 2013). The performance of the solar cell can be improved significantly increasing the electric power yield for a unit area of PV (Norton et al., 2011).

The schematic diagram of a CPC is shown in Figure 2.1 and it consists of two different parabolas (A and B), the axis of which are inclined at an angles $\pm\ \theta_c$ with respect to the optical axis.

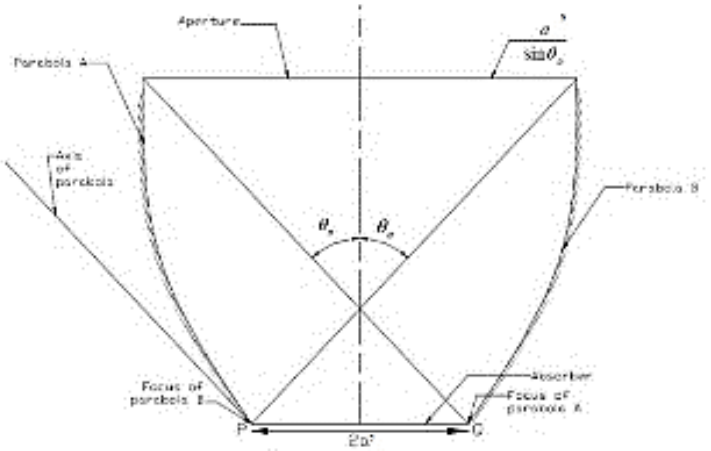

Figure 2. 1 Sectional view of the compound parabolic concentrator (CPC) (Welford and Winston, 1978)

The parameters which defined in CPC systems are:

- Acceptance half-angles: The angle $\pm \theta_c$ is defined as a collector half-acceptance angle (Devanayanan and Murugavel, 2014). It is the maximum angle at which light can enter the concentrator and still be reflected onto the target area. This angle depends on the design of the CPC and can vary depending on the specific application.

- Geometrical concentration ratio: The geometrical concentration ratio is defined as the ratio of the area of aperture to the area of the receiver (Duffie and Beckman, 1991). The concentration ratio determines the increase in relative radiation at the surface of the exit aperture/absorber.

- Optical concentration ratio: The optical concentration ratio indicates the proportion of incident rays within the collecting angle that emerge from the exit aperture (Rabl A, 1976a).

- Power output: CPC system power output depends on a number of factors, including the intensity of the incoming light, the efficiency of the solar cell and losses due to reflection and absorption. It can be calculated using the following equation, where I_{mpp} and V_{mpp} are the current and voltage at maximum power point:

  $M_{pp} = I_{mpp} \times V_{mpp}$ (2.1)

- Power ratio: CPC system power ratio is the ratio of power of the concentrator to the power output of flat plate collector with the same area. It is a measure of the effectiveness of the CPC in increasing the amount of energy collected. The power ratio can be calculated using the following equation, where $P_{concentrator}$ and $P_{reference}$ are the power of the concentrator and reference respectively:

  $$PR = \frac{P_{concentrator}}{P_{reference}} \quad (2.2)$$

- Solar cell efficiency: In a CPC system this is the ratio of the electrical power output of the cell to the incident solar power. It can be calculated using the following equation, where $M_{pp\ -\ cpc}$ is the power output of solar cell in the CPC system, G is the solar radiation intensity at the aperture and A_{cell} is the area of the solar cell:

  $$\eta_{cell} = \frac{M_{pp-cpc}}{GA_{cell}} \quad (2.3)$$

- System efficiency: The system efficiency of the CPC is the ratio of the electrical power output of the system to the incident solar power. This include losses due to reflection and absorption in the concentrator, losses due to electrical resistance in the wiring and losses due to inefficiencies in the solar cell. The system efficiency can be

calculated using the following equation, where A_{aper} is the area of the aperture of the CPC system:

$$\eta_{system} = \frac{M_{pp-cpc}}{GA_{apert}} \tag{2.4}$$

- Optical efficiency: CPC optical efficiency is the ratio of the amount of light that enters the concentrator to the amount of light that reaches the receiver. This includes losses due to reflection and absorption in the concentrator. The optical efficiency can be calculated using the following equation, where C is the concentration ratio, $I_{sc,cpc}$ and $I_{sc,ref}$ are short circuit currents for the CPC and Reference systems respectively:

$$\eta_{opt} = \frac{1}{C}\frac{I_{sc,cpc}}{I_{sc,ref}} \tag{2.5}$$

A CPC can be designed for different absorber shapes as shown in Figure 2.2 and gives rise to a range of different reflector designs (Norton et al., 2011).

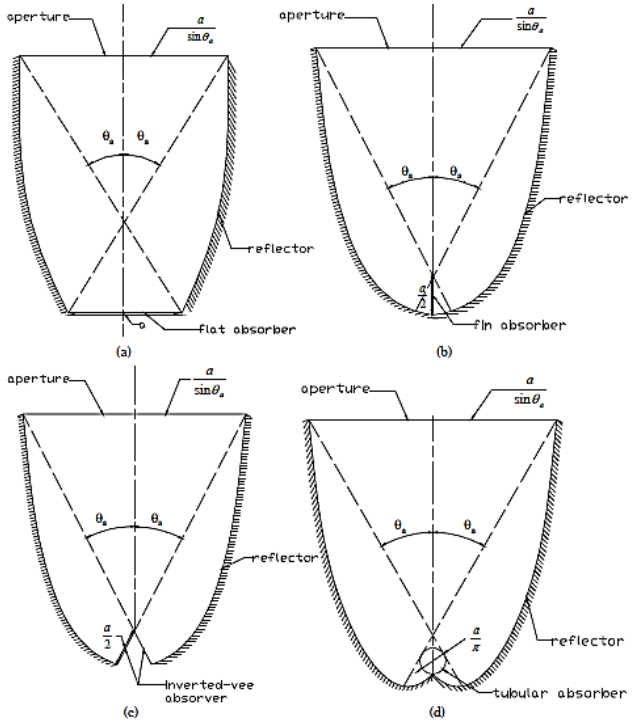

Figure 2. 2 Different CPC configurations (Mallick, 2003)
(a) CPC with flat absorber, (b) CPC with fin,
(c) CPC with "inverted vee" absorber, (d) CPC with tubular absorber

2.1.1 CPC Development

Over the past 50 years, many researchers have been working with CPCs to improve the efficiencies (Mallick et al., 2002; Othman et al., 2005; Rabl A, 1976a; Winston, 1974; Wu Y., 2009; Zacharopoulos et al., 2000).

In 1960, Winston discovered CPC as a light collector for Čerenkov radiation counters and it was accepted for solar energy collection in the USA in 1974 (Devanayanan and Murugavel, 2014).
In 1976, Rabl calculated the convective and radiative heat transfer through a CPC, and the equations for evaluating the performance of solar collectors based on the CPC principle were presented (Rabl A, 1976b). For the first time a truncated CPC was used. The results show that a large portion of the reflector area can be eliminated without seriously reducing the concentration ratio. The results also indicate that the ideal concentrator CPC was different from conventional systems such as focusing parabolas and act as a radiation funnel with no focusing element. For a given acceptance angle, a CPC has a concentration ratio of two to four times compared to other solar concentrators, however it requires a larger reflector area (Wu Y., 2009). In 1976, Rabl also designed new concentrators, including the use of compound parabolic concentrators as second stage concentrators for the conventional parabolic or Fresnel mirrors. Such a combination approaches the performance of an ideal concentrator without demanding a large reflector (Rabl A, 1976a).

In 1978, Winston et al., proposed two types of CPC collectors with concentration ratios of 3.0 (requiring two tilt adjustments per year) and 6.5 (requiring about one tilt adjustment per week). The results showed that the optical efficiency of both collectors was 60%, the U-value was 3.0 W/m^2K and 1.6 W/m^2K respectively. Under full sunshine these numbers imply operating efficiencies of 45% at $\Delta T=50K$ and $\Delta T=100K$, respectively (Winston et al., 1978). In 1978 Winston also confirmed that the conduction losses between absorber and reflector can be reduced by creating gaps between them (R. Winston, 1978). In 1978, Mills and Giutronich examined both Parabolic and Non-Parabolic Asymmetrical Concentrators and compared with symmetrical designs. The results revealed that the focus and end points of the two parabolas of an asymmetric compound parabolic concentrator make different maximum acceptance-half angles with the absorber surface (Mills and Giutronich, 1978).

In 1986, Winston integrated evacuated CPCs for high temperature solar thermal systems (Winston et al., 1986). In 1986, Winston also investigated the potential to maximize concentrating optics for solar electricity generation by using a secondary concentrator placed in the focal zone of a primary lens or paraboloidal mirror (Winston and O'Gallagher, 1986). Two stage concentrators for both solar thermal and photovoltaic electricity generation were tested. The first design used a Fresnel lens primary combined with totally internally reflecting Dielectric Compound Hyperbolic Concentrator secondary. The second design was a facetted paraboloidal primary combined with a Compound Parabolic Concentrator (CPC). The results showed that the solar flux concentration improved by a factor of 2 to 15 above that achievable by the primary alone (Winston and O'Gallagher, 1986).

2.1.2 CPC Design categorization

There have been variations in the design of CPC in order to improve different aspects such as concentration ratio and irradiance distribution as illustrated in Figure 2.3, (Shanks et al., 2016). The location, incident sun light conditions and tracker options decide which CPC type suits an application best (Shanks et al., 2016) .

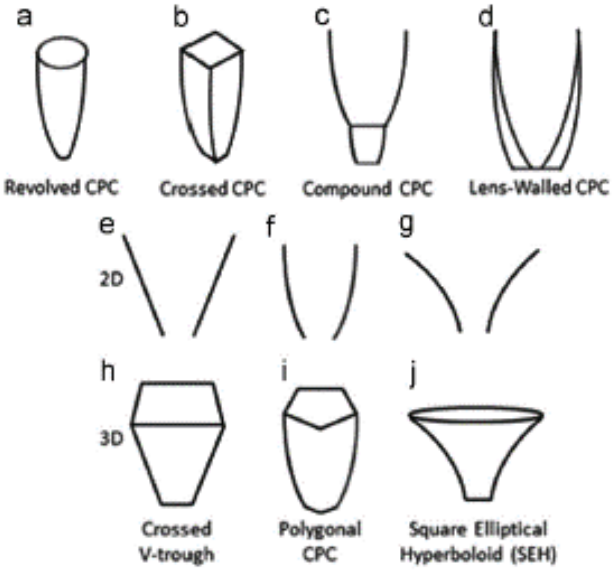

Figure 2. 3 Variations of CPC (Shanks et al., 2016)
(a) The revolved CPC (b) The Crossed CPC (c) The Compound CPC (d) The Lens-Walled CPC (e) V-trough (f) CPC (g) Compound Hyperbolic Concentrator (h) 3D square aperture V-trough (i) Polygonal aperture CPC (j) Hyperboloid with an elliptical entry aperture and square exit aperture

2.2 Design, development and performance of a CPC

In 2000, Zacharopoulos et al., showed that an asymmetric concentrator is more suitable for use in building facades. The authors proposed an optical analysis of three-dimensional dielectric-field symmetric and asymmetric compound parabolic PV concentrators for building façade integration. The first concentrator was a symmetric CPC with a geometrical concentration ratio of 3.0 including a silvered circular section. A silvered dielectric circular reflector section was included between the lower reflector and the absorber to achieve the vertical orientation required for use on building facades. The second type was an asymmetric CPC with a concentration ratio of 2.5. Both concentrators had an optical efficiency over 90 %. The results revealed that the asymmetric design maintained optical efficiencies over 40 % even for the incidence angles outside the two-dimensional angular acceptance range. For both concentrators angular acceptance was enhanced due to refraction and most solar energy collected by the photovoltaic material left the concentrators at exit angles less than 40º. The performance of symmetric, asymmetric and flat plate devices with the same photovoltaic surface area was also compared. The results showed that the symmetric cover collected the most energy at all aperture tilt angles over 40 ° (Zacharopoulos et al., 2000).

Mallick et al (2002) used ray trace techniques to predict the optical characteristics of non-imaging asymmetric compound parabolic photovoltaic concentrators (ACPPVC) suitable for south facing façades in the UK (52° N) (Figure 2.4). The truncated air filled ACPPVC had a geometric concentration ratio of 2.0 with acceptance angles of 0° and 50°. The results showed that approximately 91% optical efficiency of the ACPPVC system was achieved for a wide range of solar incidence angles (Mallick et al., 2002).

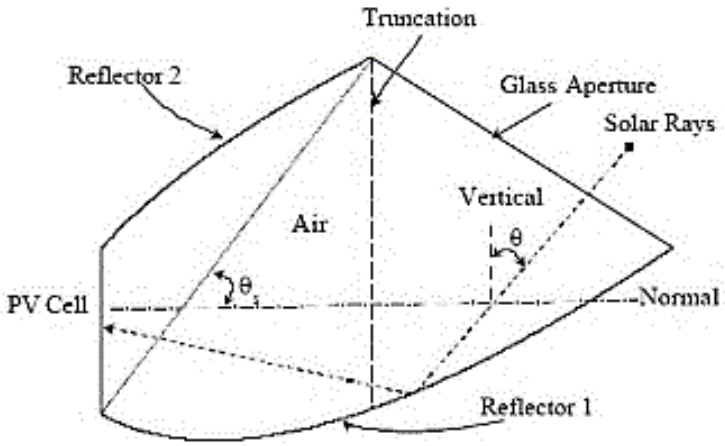

Figure 2. 4 Modelled photovoltaic concentrator for building façade integration in the UK (Mallick et al., 2002)

Mallick et al (2004) designed, constructed and experimentally characterized a novel non-imaging asymmetric compound parabolic photovoltaic concentrator (ACPPVC) (Figure 2.5) (Mallick et al., 2004). An electrical and thermal analysis of the ACPPVC was undertaken. The reflector system was removed from the PV panel to provide a non-concentrating PV panel for comparison against the concentrator panel. In both instances the active solar cell area was kept constant. The results revealed that the power produced by the ACPPVC was 1.62 times of the power generated by the flat PV panel. Although the power increased by a factor of 1.62, the aluminium back plate temperature of the concentrator panel was only 12 °C higher than the flat panel. Approximately 8.5 % electrical efficiency was achieved by the flat system compared to 6.8% for the ACPPVC with a fill factor of 65% (Mallick et al., 2004). A maximum

system efficiency of 7.8 % was obtained at a solar radiation level of 800 W/m^2, and the maximum power generated by the system was 26 W (Wu Y., 2009).

a)

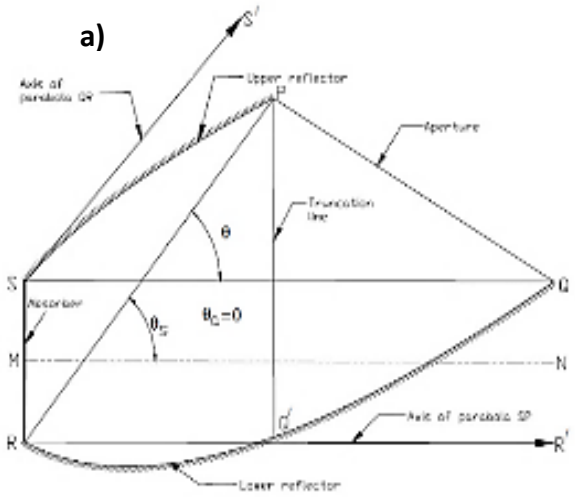

b)

Acceptance-half angles	50° & 0°
Absorber width (mm)	50.0
Aperture width (mm)	100.0
Length of upper reflector (mm)	84.0
Length of lower reflector (mm)	71.0
Concentration ratio	2.0
Truncation (%)	54

Figure 2. 5 Asymmetric compound parabolic concentrator for building integration in the UK with acceptance-half angles of 0ºand 50º (Mallick et al., 2004)
(a) Geometrical design (b) Physical and geometrical properties of a single trough ACPPVC

Mallick et al (2007a) undertook a detailed parametric analysis of the heat transfer in an experimentally characterized asymmetric compound parabolic photovoltaic concentrator suitable for building facade integration in the UK, using a comprehensive validated unified model for optics and heat transfer in line-axis solar energy systems. The results showed that free and forced convection at the rear of the PV concentrator provided a significant temperature reduction in the PV. An inlet air velocity of 1.0 m/s in a 20 mm wide channel between the aperture cover and the reflector could decrease the PV cell temperature by 25.4 K. A maximum temperature reduction of 34.2 K is predicted for a front and rear air gap of 20 mm with an inlet air velocity of 1.0 m/s. (Mallick et al., 2007a). Mallick et al (2007b) also analysed the power loss in an Asymmetric Compound Parabolic Photovoltaic Concentrator with a geometric concentration ratio of 2.0. The power loss of the system is explained by a comparative analysis of the non-concentrating photovoltaic system for long-tabbed and short-tabbed solar cell strings. The results revealed an average of 3.4% electrical power loss due to resistance in the interconnections between each individual solar cell and 0.6 % occurred due to the increased temperature of the PV cells in the ACPPVC system. The optical losses of the ACPPVC were 15 % caused by the combined effect of the number of reflections at the reflectors and the misalignment of the imperfection in the reflector geometry. Due to a combination of optical and electrical resistance losses, the maximum output power achieved was only 1.62 times of non-concentrating counterpart (Mallick et al., 2007b).

In 2009, Wu designed, fabricated and experimentally characterised an Asymmetric Compound Parabolic Photovoltaic Concentrator (ACPPVC) for building façade integration (Figure 2.6). Extensive indoor experiments were used to investigate the thermal behaviour and the I-V characterisation of a truncated Asymmetrical Compound Parabolic Photovoltaic Concentrator. Phase Change Material (PCM) was integrated to the rear of the PV panel to moderate the temperature rise of the PV and maintain good solar-electrical conversion efficiency. The results confirmed that the truncated ACPPVC system with a geometric concentration ratio of 2.0 was more suitable for the UK climate compared to the other ACPPVC systems simulated, due to the range of angular acceptance. For the ACPPVC with PCM system, it can be observed that for an incident solar radiation intensity of 280 W/m^2, the average solar cell temperature of the system was reduced by 7 °C and the electrical conversion efficiency increased by approximately 5 %. For an incident solar radiation intensity of 672 W/m^2, the average solar cell temperature of the system was reduced by 18° C and the electrical conversion efficiency increased by around 10 % (Wu Y., 2009).

a)

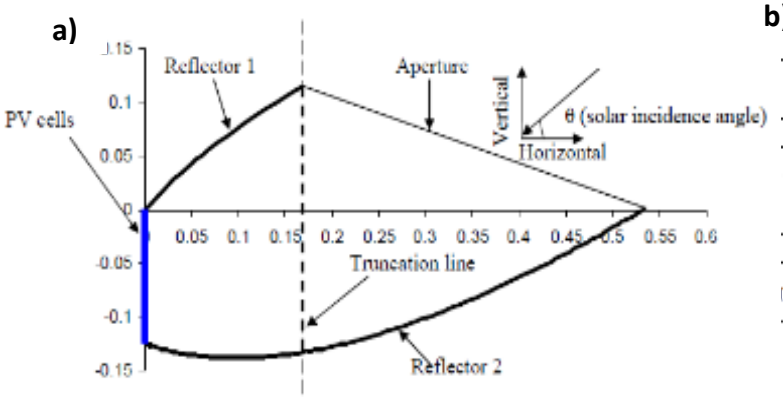

b)

Parameters		Values
Acceptance-half angles		38° & 55°
Absorber width(mm)		125
Aperture width(mm)		248.5
Length of reflector1(R1)(mm)		204.5
Length of reflector2(R2)(mm)		169.8
Concentration ratio		1.99
Truncation (%)	Ref1	0
	Ref2	69.7

Figure 2. 6 ACPPVC-55 system with acceptance-half angle of 0° and 55° (Wu Y., 2009)
(a) Geometrical design (b) Geometrical characteristics of the truncated ACPPVC-55

2.2.1 Large Scale CPC development

In 2016, Xie at al developed a concentrating flat-plate photovoltaic-thermal (CPV/T) system of low cost and high output, eliminating multiple reflections CPC (EMR) with a geometric concentration ratio 4. The best concentration plane of EMR, full CPC (FUL) and half truncation CPC (HAL) were defined to conduct optical performance study. The theoretical data showed that the material consumption of EMR is about one-half less than that of FUL. Theoretical and test result showed that EMR, PV/T can exceed 71% the optical efficiency. The table 2.1 showed the initial condition of the test for the three types of CPCs highlighting the hight reduction for the EMR syetm. The Figure 2.7 a and b ilustrated the experimental test of 12 units EMR PV/T Sytems (Xie et al., 2016)

Table 2. 1 Initial conditions of EMR, FUL AND HAL CPCs system (Xie et al., 2016)

	EMR	FUL	HAL
C	4.0	4.0	3.6
H (mm)	703.2	1510.4	755.2
$\overline{BF}$ (mm)	156.0	156.0	156.0

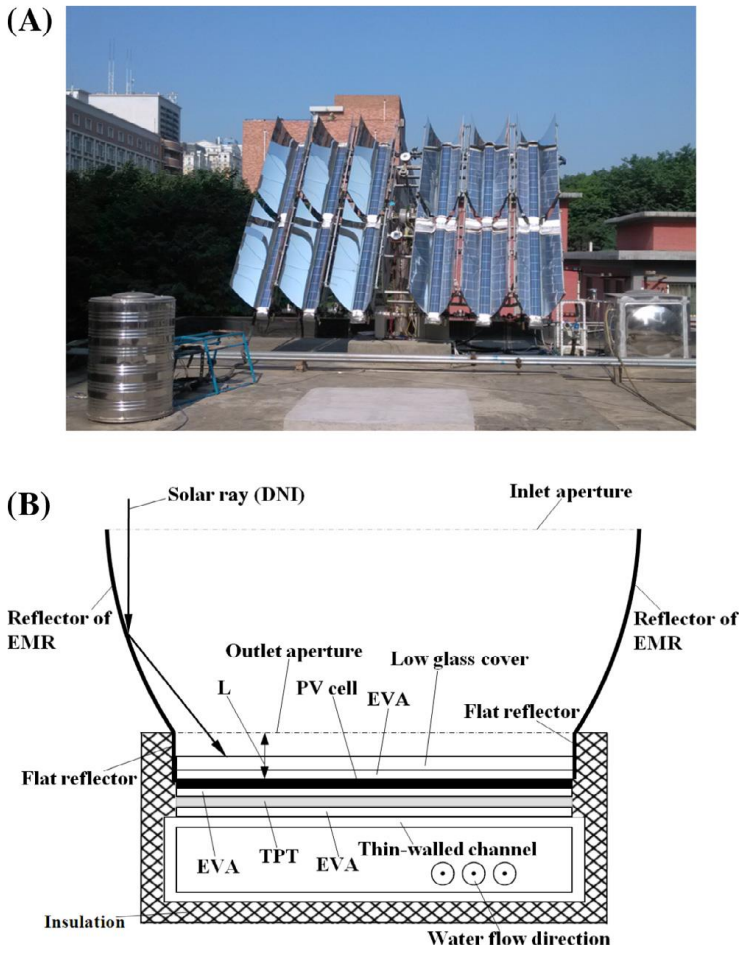

Figure 2. 7 Experimental platform of EMR assembled with PV/T (Xie et al., 2016)
(a) EMR assembled with PV/T (12 units) and (b) schematic of one unit of EMR assembled with PV/T

Jaaz et al realized a physically test of a compound parabolic concentrator (CPC) with a thermal photovoltaic module (PVT) where the cooling process of the CPC is conducted using a novel technique of water jet. The test includes the effect of water jet impingement on the total power, electrical efficiency, thermal efficiency, and total efficiency on CPC-PVT system. The result showed an improvement in the electrical efficiency by 7 %, total output power by 31 % and the thermal efficiency by 81 % (Jaaz et al., 2018). The Figures 2.8 (a) and (b) revel the characterization of the CPC with 36 solar cell and maximum power output of 135 W.

a)

b)

Characteristic	Value
Cell type	Polycrystalline silicon
Number of cells	36 cells
Maximum power (P_{max})	135 W
Open circuit voltage (V_{oc})	21.80 V
Short circuit current (I_{sc})	7.97 A
Maximum power voltage (V_{mp})	18.12 V
Maximum power current (I_{mp})	7.45
Cell open circuit voltage	0.6 V
Module efficiency (at STC)	15%
Cell size	156 × 156 mm

Figure 2. 8 Characterization pf CPC-Collector with 36 solar cell (Jaaz et al., 2018)
(a) PVT-CPC Collector and (b) Specification of PV module

A large scale hybrid CPV/T was designed for (Wang et al., 2019). A large-scale south-north tracking hybrid CPV/T system with sunlight collecting area of 810m^2 was built to explore practical application of this CPV/T unit. The results showed that the whole-day thermal efficiency and total thermal output of the large-scale hybrid CPV/T system were 55% and 1,730,039 kJ respectively on April 14, 2017 (Wang et al., 2019). An aerial photograph of the large scale system is shown in Figure 2.9.

Figure 2. 9 Large-scale hybrid CPV/T test (Wang et al., 2019)

2.3 Luminescent Down-Shifting Layers (LDS)

Spectral losses due to limited spectral response of solar cells represent a downside to the electrical generation (Ahmed, 2012). Luminescent down shifting layer reduce these losses by converting high energy photons to lower energy photons making better use of the short wavelength light before the interaction with the solar cells, improving the absorption and the electrical output and controlling the temperature of the system (Ahmed, 2012). It is an optical approach to increasing the ultra-violet/blue response of a solar cell by shifting short wavelength light to longer wavelengths for which the external quantum efficiency of solar cell is higher (Hovel et al., 1979, Klampaftis et al., 2009, Ross et al., 2014). In the 1970s, LDS was used as a luminescent solar concentrator (LSC) and in 1979, Hovel realised the first investigation using LDS with PV cell.

In 2014, Ahmed tested 0.15 % dye concentration with violet, yellow, orange and red lumogen used an excitation wavelength of 380, 380, 443 and 535 nm respectively. From the absorption and emission measurements, the results revealed that lumogen violet downshifted photons from 375 nm to 413 nm, lumogen yellow from 476 nm to 495 nm. Lumogen orange from 524 nm to 539 nm and lumogen red from 574 nm to 613 nm. From Figure 2.10 it was confirmed that the lumogen violet and yellow have suitable spectral properties for transfer of photons from UV range to visible range.

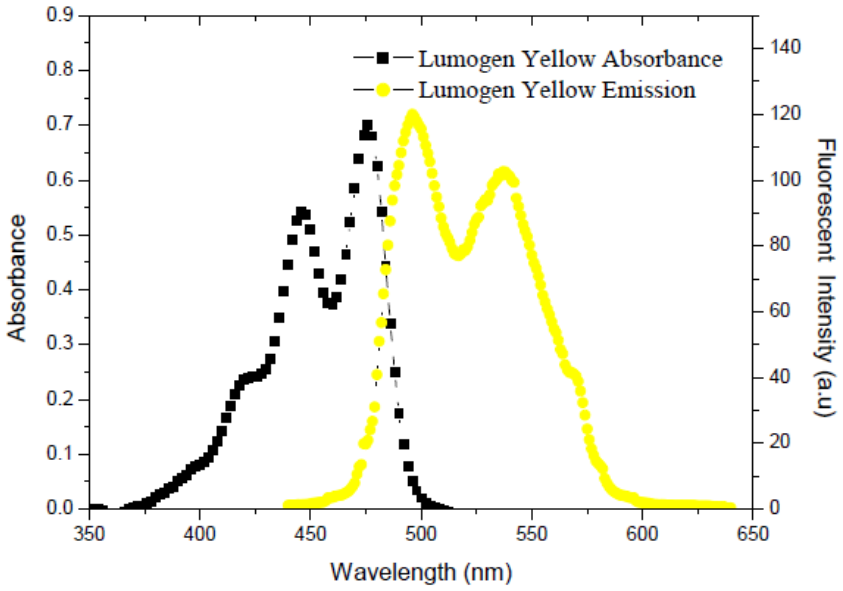

Figure 2. 10 Absorbance and emission spectra of Lumogen Yellow (Ahmed, 2014)

In 2017, Ahmed et al investigated the plasmonic coupling between lumogen yellow and silver nanoparticles (Ag NPs) to produce lumogen yellow luminescent down shifting layer. A 100 µm thickness was fabricated with a dye concentration of 0.9%. The results showed that when the PLDS was deposited on the top of CdTe mini-modules increased the short circuit current of CdTe device between 300 and 500 nm. In addition, the external quantum efficiency measurements improved by 25 - 40 % below 500 nm. Figure 2.11 shows the emission spectra

for the yellow dye LDS for different concentration. It can be seen that the optimum concentration for the yellow dye. Higher than this concentration the emission intensity starts to decrease (Ahmed et al., 2017).

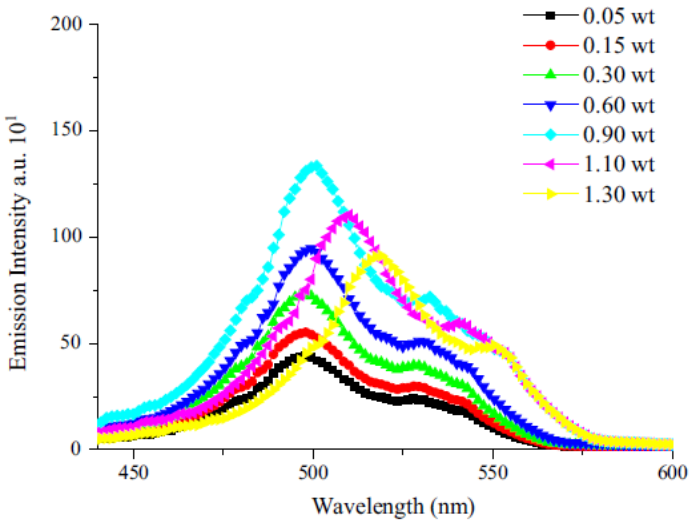

Figure 2. 11 Emission spectra for lumogen yellow dye LDS layers of different concentrations (Ahmed et al., 2017)

2.4 Phase Change Material (PCM)

The idea that Phase Change Materials (PCM) could potentially be utilized as a thermal storage when combined with a Photovoltaic system (PV) was first mooted in 1978. This innovative concept received patent protection in 1983 (Ames, 1983). Despite this initial interest, the exploration of PCM for the cooling of PV systems was not undertaken until the mid-1990s. A considerable number of experimental and computational research initiatives have been launched to study the efficacy of PCM in managing PV temperature (Ling et al., 2014). The earliest known research endeavor assessing PCM as a feasible strategy for controlling PV temperature is depicted in Figure 2.12 (Stultz and Wren, 1978). In his study, Stultz used Eicosane, a material with a melting point of 36.7 ºC, in conjunction with a Spectrolab PV module (Stultz and Wren, 1978). The experiment yielded a 1.4 % rise in the PV's electrical efficiency. However, it was observed that this could potentially be amplified through improved heat transfer from the PV to the PCM, facilitated by enhanced thermal conductivity of the PCM. Stultz hypothesized that if the PCM efficiently absorbed the surplus thermal energy, a power increase of 2 % to 3.5 % might be achievable. Although a PV/PCM system was not deemed economically viable, the combination of a PV and a thermal storage system appeared to have the potential for cost effectiveness.

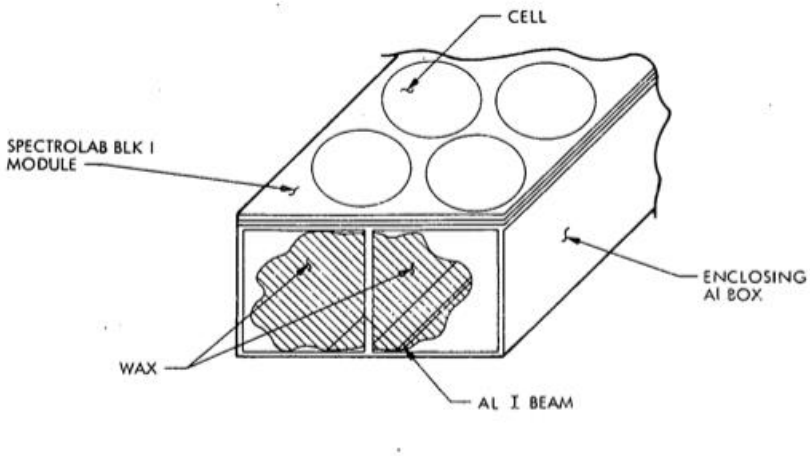

Figure 2. 12 Phase change material integrated with a photovoltaic model (Stultz and Wren, 1978)

Huang and his team (Huang et al., 2004) independently advanced the concept through comprehensive experimental work and simulation studies. The initial PV/PCM numerical model was effectively validated through a comparison with small-scale experiments. Three different systems were subjected to various environmental conditions for analysis: (i) an aluminium plate was used to mimic a PV cell; (ii) an aluminium plate coupled with a container of PCM was used to represent a PV/PCM system; and (iii) an aluminium plate paired with a container of PCM and integrated fins was analyzed, as shown in Figure 2.13. The observed temperature fluctuations within the PCM, as well as the solid-liquid transition of the PCM, were found to align well with the predicted outcomes. The integrated PCM system, complete with fins, showcased efficient temperature management of the plate (Huang et al., 2004).

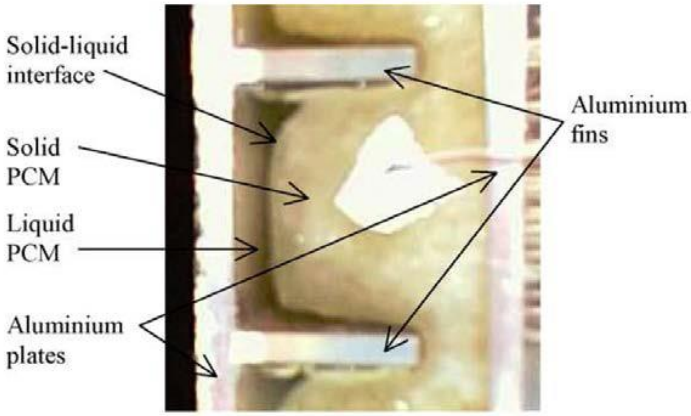

Figure 2. 13 Photographic image of melting front of PV/PCM system (Huang et al., 2004)

Hasan and his team (Hasan, 2010) conducted an experimental study on the usage of various types of Phase Change Materials (PCMs) to improve thermal regulation of Building Integrated Photovoltaics (BIPV) through a series of small scale indoor experiments. Five PCMs were tested - RT20, capric:palmitic acid, capric:lauric acid, calcium chloride, and SP22 - in conjunction with four distinct systems: System A (Aluminium, with an internal width of 5 cm), System B (Perspex, with an internal width of 5 cm), System C (Aluminium, with an internal width of 3 cm), and System D (Perspex, with an internal width of 3 cm), as represented in

Figure 2.14. These setups were tested under three different levels of simulated sunlight intensity (500 W/m^2, 750 W/m^2, and 1000 W/m^2), in a small-scale indoor experiment. A solar simulator was employed to replicate solar conditions, with an ambient temperature held constant at ± 1 ºC. When subjected to insolation of 500 W/m^2, System A, paired with capric: lauric and capric: palmitic acid, was found to sustain a lower PV temperature for the longest duration, specifically up to 2.5 hours at 10 ºC less than the control system. When the insolation increased to 750 W/m^2 and 1000 W/m^2 (as is presented in Figure 2.15), System A, this time in combination with calcium chloride, consistently held PV front surface temperatures 10 ºC beneath the reference for an extended period in comparison to the other systems.

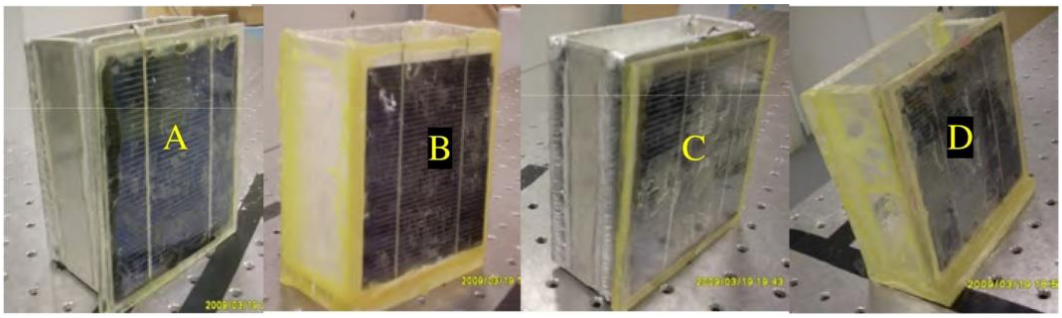

Figure 2. 14 System A, B, C and D (Hasan, 2010)

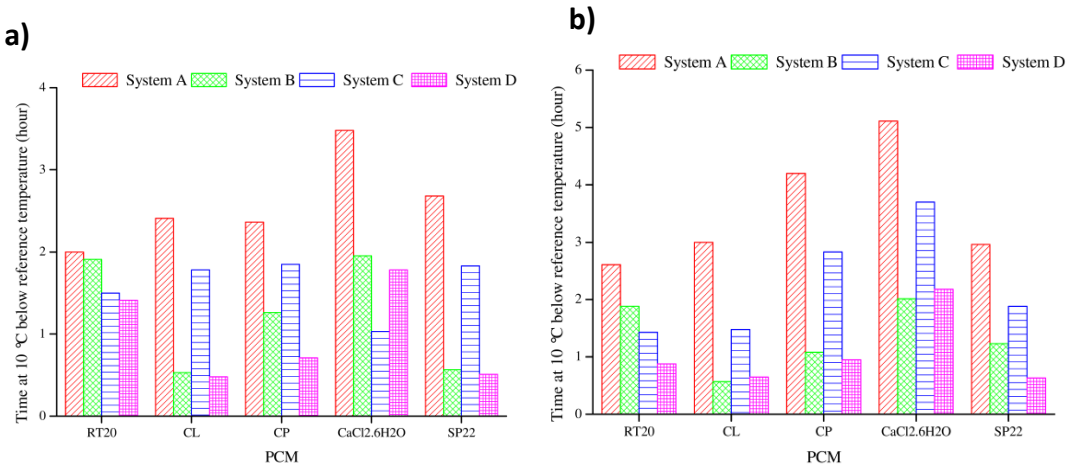

Figure 2. 15 Results from experiments at (a) 750 W/m^2 and (b) 1000 W/m^2 (Hasan, 2010)

Hasan (Hasan et al., 2014) carried out full-scale outdoor experiments in Dublin, Ireland, and Vehara, Pakistan to investigate the application of Phase Change Materials (PCM) in regulating the temperature of Photovoltaic (PV) systems. In the experiment, three 65 W PV modules were utilized as show in Figure 2.16. One of these modules served as a reference, while the other two were integrated with PCM systems; one with a eutectic mixture of capric-palmitic and the other with salt hydrate. The performance of these PV-PCM systems was assessed by comparing their peak instantaneous temperatures with that of the reference PV module. The capric:palmitic PV-PCM system managed to maintain the PV temperature 7 °C lower than the reference. The PV-PCM system with salt hydrate achieved a temperature reduction of 10 °C

relative to the reference. A similar pattern was observed in Vehari, where the capric:palmitic system maintained a temperature 10 °C lower than the reference, while the salt hydrate system achieved a remarkable temperature reduction of 21 °C (Hasan et al., 2014).

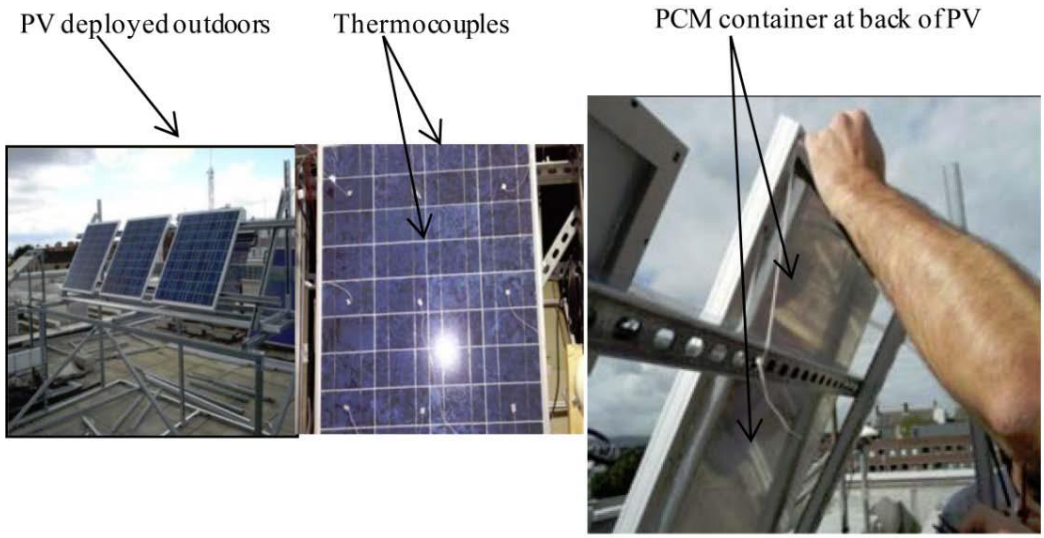

Figure 2. 16 Experimental set-up of PV-PCM systems, location of thermocouples and attachment of PV to PCM container (Hasan et al., 2014)

In a novel investigation, Browne and colleagues (Browne et al., 2016) explored a PV/T/PCM system designed to generate electricity, store heat, and pre-heat water, under the climatic conditions prevalent in Dublin, Ireland. This system integrates a Photovoltaic (PV) module with a thermal collector, where heat is extracted from a heat exchanger embedded within the Phase Change Material (PCM) via a thermosyphon flow. The performance of this system was evaluated against three alternative setups: (a) the same system, but without the inclusion of PCM; (b) the same system, excluding both the heat exchanger and PCM; and (c) the lone PV module, as demonstrated in figure 2.17. The results revealed that the water temperature achieved in the novel system was approximately 5.5 °C higher than that in a PV/T system that lacked PCM. This underscores the effectiveness of PCM as a method for storing heat for subsequent extraction in a PV/T system.

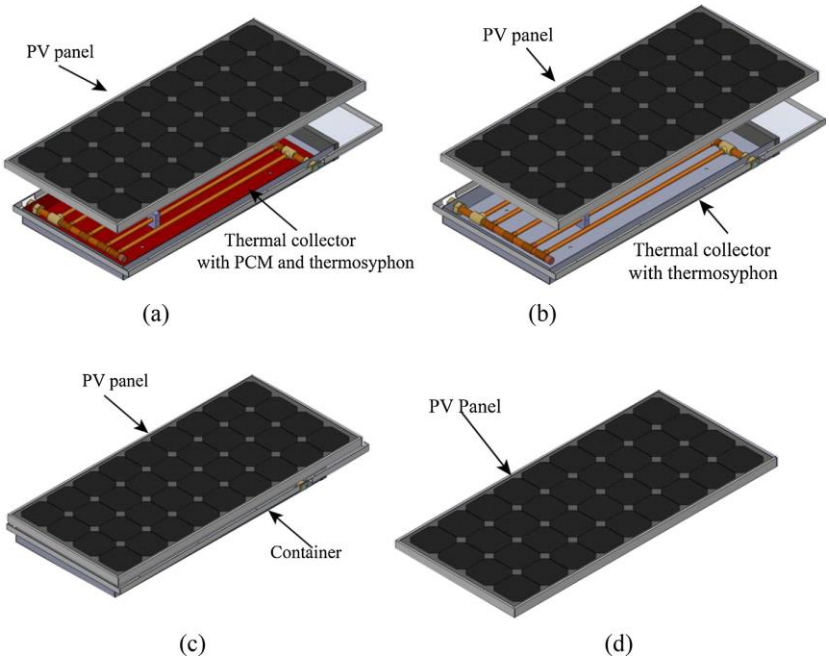

Figure 2. 17 Schematic illustrating the design of (a) System 1 (PV/T/PCM) (b) System 2 (PV/T) (c) System 3 (PV with container) and (d) System 4 (PV) in the experiment (Browne et al., 2016)

2.5 Conclusion

In this chapter compound parabolic concentrators and their applications in building integration for electricity generation have been reviewed. The broad variety of practical realized design and performance of CPCs for building integrated has been presented. From this chapter, it can be concluded that truncated Asymmetric Compound Parabolic Photovoltaic Concentrator (ACPPVC) is more suitable for use in building facades for the range of angular acceptance; however, the power and the optical losses in ACPPVC system must be taken into account in order to improve the system efficiency. Building integrated compound parabolic concentrators (BICPC) has been proven time and again to be an excellent option for electricity generation in buildings, however there is much scope for enhancement and improvement.

The given literature review described the research and development of Asymmetric Compound Parabolic Concentrator (ACPPVC) for build façade integration. The authors of the studies discussed in the literature review proposed and designed various types of ACPPVC with different concentration ratios, geometries and optical and thermal characteristics. They used ray trace techniques and experimental methods to investigate the optical and electrical efficiencies of the ACPPVC systems, as well as their thermal behavior and effect of different factors, such as convection and interconnections between solar cells, on their performance. The results showed that ACPPVC systems can achieve high optical and electrical efficiency and improve the power output of photovoltaic panels compared to flat systems. They also demonstrated the importance of optimizing the design and using techniques such as Phase

Change Materials (PCM) integration to maintain good solar electrical conversion efficiency and reduce the temperature rise of the PV cells. This review shows that the ACPPVC systems can be a promising solution for integrating photovoltaic technology into building facades.

On the other hand, the application of LDS layers is another exciting approach to improving PV performance. LDS layers work by absorbing higher-energy (shorter wavelength) photons and re-emitting them at lower energies (longer wavelengths) that are more efficiently converted to electricity by the PV cell. This process can effectively increase the number of photons available for conversion to electricity within the optimal energy range of the PV material, thereby enhancing the overall efficiency of the solar cell. In addition to efficiency enhancement, LDS layers can also contribute to a reduction in the thermal load on the PV cell by shifting the photon energy to the lower end of the spectrum where less heat is generated per photon absorbed. The integration of PCMs and LDS layers represents a promising strategy to tackle two of the main challenges facing CPC technology - thermal management and the efficient utilization of the solar spectrum. The research and development in these areas are of substantial relevance and have the potential to significantly contribute to the advancement of solar energy conversion technologies.

The scope for enhancement and improvement of BICPCs lies in optimizing their efficiency, improving their durability and reducing their manufacturing and installation cost. One area of future research could focus on improving the optical efficiency performance of BICPCs by using advanced optical materials to reduce reflection and absorptions losses. Another area of research is exploring the use of new materials or deigns to increase the mechanical strength and durability of BICPCs, allowing them to withstand harsh weather conditions and extend their lifespan. The scope for enhancement and improvement of BICPCs is significant and has the potential to significantly increase their viability and impact as a renewable energy solution for building integration.

Chapter 3 Methodology

3.1 Demo-sites

As outlined in chapter 1 this research is part of a wider IDEAS project and contains 2 demo site locations, Ferrara, Italy and Mayo Ireland for the integration and subsequent testing of the proposed renewable energy systems.

The demo-site in Ferrara is situated at the University of Ferrara (UNIFE) and is located at 44°49`54.12" N, 11°35`59.48" E. The city of Ferrara is located in the Emilia-Romagna region of northern Italy and has a temperate climate with hot summers and cold winters. The demo-site will provide a testing ground for the proposed compound parabolic concentrator (CPC) system suitable for façade installation in an urban setting.

The demo-site in Mayo, Ireland is located at Brackloon Drummin Community Centre at 53º44'16.46" N, - 9º33'13.10" O. Mayo is located on the west coast of Ireland and has a temperate oceanic climate with mild winters and cool summers. The demo-site will provide as opportunity to test the proposed integrated renewable energy system in a rural setting where traditional solar geothermal technologies may not be practical due to space limitations. Figure 3.1 presents the locations of the two IDEAS demo-sites in Europe. Figure 3.2 and 3.3 shows the building for the installations of the CPCs in Mayo, Ireland and Ferrara, Italy respectively.

Figure 3. 1IDEAS demo-sites locations in Europe

Figure 3. 2 Demo-site Mayo, Ireland at Brackloon Drummin Community Centre

Figure 3. 3 Demo-site Ferrara, Italy at University Ferrara (UNIFE)

3.2 External collaboration

As part of IDEAS project the work package 1 has the participation of three groups of researchers integrating the technologies to the CPC systems. Figure 3.4 shows the diagram of the parts involved that make up this section of the project. First is the CPC parabolic reflectors composite system, in which LDS layers and PCM containers are integrated in order to improve the efficiency of the solar collector.

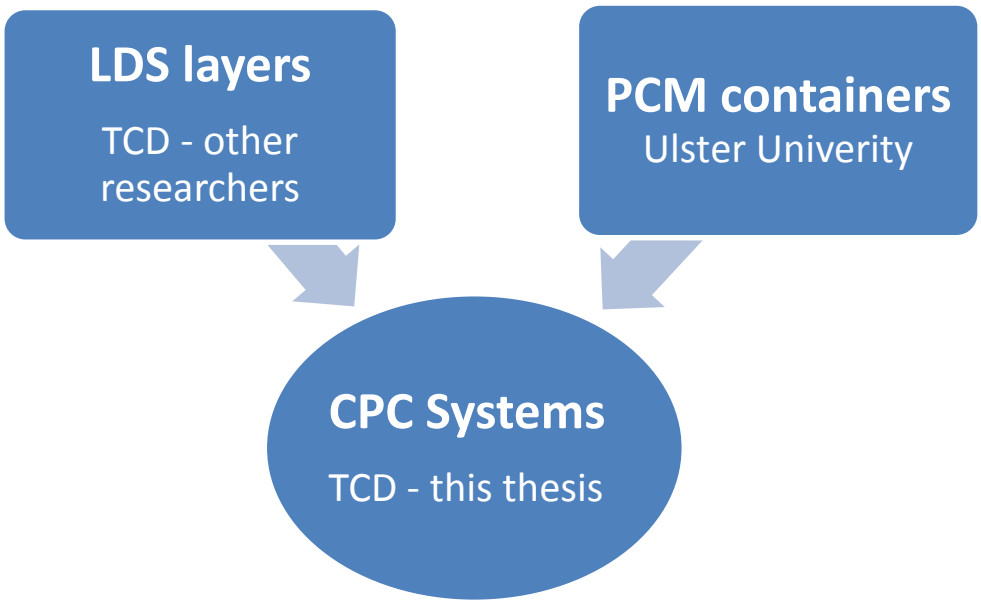

Figure 3. 4 Researchers involve as a part of work package 1

Luminescent Down-Shifting (LDS) is a photonic process that is being used to improve the performance of photovoltaic (PV) cells, which convert sunlight into electricity. In an LDS layer, special luminescent materials are used to absorb higher energy, shorter-wavelength light (such as blue or ultraviolet light) and re-emit it at a lower energy, longer wavelength (often in the visible range). This process is called "down-shifting." The down-shifted light is then more efficiently absorbed by the underlying PV cell. The key advantage of this process is that it can help to overcome some of the limitations of PV cells. For example, many PV materials are less efficient at converting high-energy photons to electricity and may suffer from increased heat generation and degradation when exposed to high-energy light. By converting this high-energy light to wavelengths where the PV cell's performance is optimal, the LDS layer can potentially increase the cell's overall efficiency and lifespan. So in a nutshell, LDS is a technology that's used to modify the spectrum of light absorbed by a photovoltaic cell in order to improve its performance. Luminescent downshifting layer (LDS) was designed and manufactured for researchers from Trinity College Dublin. LDS is an array of newly developed PV cells using a downshifting coating to increase solar energy collection and transference to electrical energy. The LDS layer uses specially formulated dyes which absorb more energy from the sun than traditional coatings. Figure 3.5 shows one LDS layers used in this project.

Several crucial steps are associated with the creation of the Luminescent Down-Shifting (LDS) layer:

- Polymer Concentration: A concentration of 3.8 g of PMMA (Poly methyl methacrylate), representing 21.2 wt%, is mixed with 10 ml of chloroform (78.6 wt%). This specific ratio ensures an even thickness when applied to larger PV cells.

- Stirring Speed & Duration: Given the addition of PMMA, the stirring speed is increased from 600 to 650 rpm. The duration of stirring is extended to a minimum of 60 minutes, with 90 minutes being optimal where feasible.

- Dye: Lumogen Orange dye from BASF, mixed with chloroform at a concentration of 0.1 wt%, is utilized for the process. A stock solution of this dye mixture is prepared in 1 wt% batches and subsequently diluted with the stock solution. This method ensures that the polymer solution does not begin to polymerize before its application to the PV cell is completed.

- Layer Application: A G3P-12 Systems spin coater is utilized for fabricating LDS layers. It provides the most consistent and easily adjustable approach for the application of the LDS layer to a PV cell. Films varying in thickness from 10 µm to 60 µm are directly spin-coated onto the Si solar cells for a duration of 180 seconds at speeds of 1000 rpm and 750 rpm, respectively. The thickness of these layers is then measured at various points using a digital micrometer, and an average is calculated. From these measurements, it is found that a thickness of 20 µm is the most beneficial, since this thin layer facilitates the absorption process from the LDS.

Figure 3. 5 One Luminescent down shifting layer (LDS)

Phase Change Materials (PCMs) are substances with a high heat of fusion which, undergoing phase change, are capable of storing or releasing large amounts of energy. They can be very useful in thermal energy storage due to their ability to absorb and emit heat at a constant temperature, or over a range of temperatures. PCMs work on the principle of latent heat storage and release. They absorb heat causing them to change from solid to liquid (melting), and when they solidify (freeze), they release the stored heat. This phase change occurs at

relatively constant temperatures, which makes them very effective for thermal regulation applications. There are various types of PCMs including organic materials, such as paraffins and non-paraffin organics, and inorganic materials, such as salt hydrates. Each type has its own benefits and drawbacks in terms of thermal storage properties, cost, availability, and environmental impact. PCMs can play a significant role in thermal management. Excessive heat can reduce the efficiency of PV cells, but by integrating PCMs, this excess heat can be absorbed and the temperature of the PV cells can be kept within optimal operating ranges.

Phase Change Materials (PCM) containers, a unique component of the CPC/PCM system, were designed and manufactured at the University of Ulster to help extract excess heat from the solar cells. The heat exchanger consists of 3 and 4 aluminum containers connected by copper piping and filled with a PCM composite. The composite used for this study was a mixture of paraffin with melting points of 36 ºC and 28 ºC, combined with expanded graphite in a 1:3 ratio. In this system, the heat exchanger is capable of absorbing thermal energy generated by the solar cells in two ways: passively, by absorbing the latent heat inside the PCM composites, or actively, through water circulation inside the tubes. Additionally, a water pipe network was integrated into the design for active cooling. This network helped to enhance the heat extraction process by circulating water through the copper pipes, further improving the overall efficiency and thermal management of the solar cells. The PCM containers were placed behind the backplate in the exact position of the solar cell strings, ensuring optimal heat transfer between the components. Figure 3.6 illustrates the design of the heat exchanger during a pretest, showcasing the integration of both passive and active heat extraction mechanisms in the CPC/PCM system.

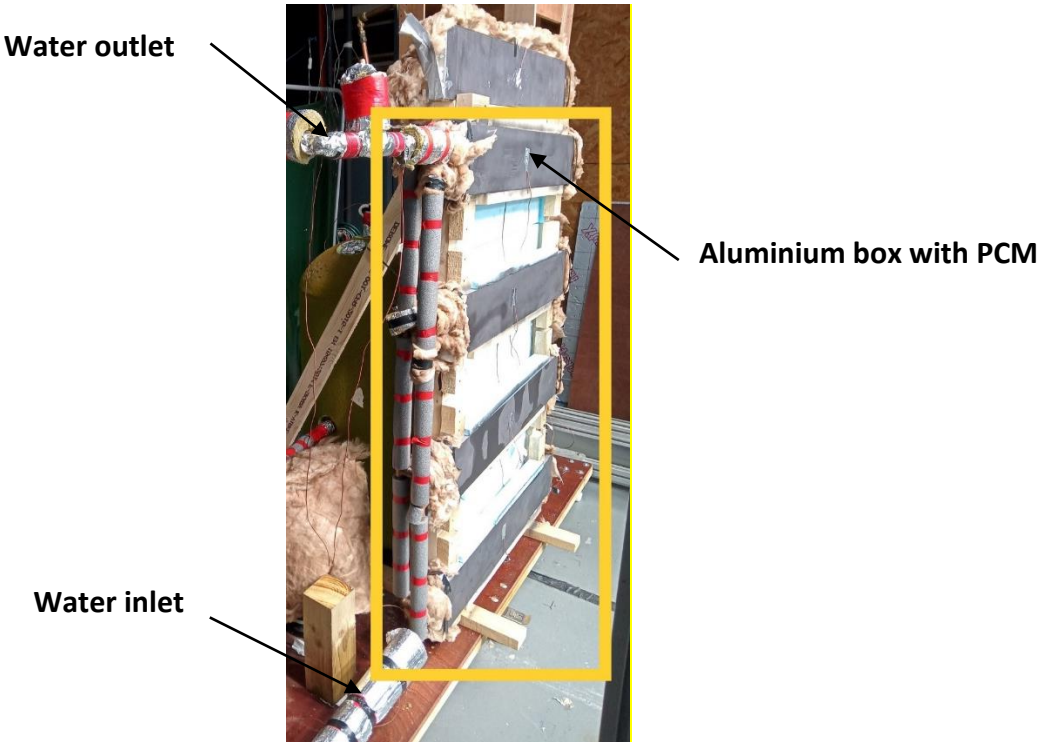

Figure 3. 6 PCM containers during a pre-test

3.3 Experimental techniques

The experimental techniques in this research include the design, manufacture and testing of two small prototype CPC systems for both locations Ferrara, Italy and Mayo Ireland, as well as large-scale CPC systems and the Reference system for both locations.

The prototypes will be tested to validate the results obtained from the ray tracing simulation and to evaluate the performance of the CPCs in outdoor conditions. Large-scale CPC systems and Reference systems were designed and manufactured for both locations to investigate the power output, power ratio, efficiencies and thermal behavior of the CPCs in outdoor conditions.

To evaluate the performance of the CPCs in outdoor conditions, power output and efficiency under different weather conditions was measured and, thermal behavior was evaluated.

These experimental techniques were used to evaluate the performance of the CPCs in real-world conditions and validate the results obtained from simulations.

3.4 Software

As a part of the design process for the CPCs, software such Solidworks and AutoCad were used to created 2D and 3D models of the CPCs, as well as to make accurate material selection and other design decisions. Solidworks is a powerful 3D design software that can be used to create complex shapes and models with ease. The software has a range of tools and features that allow for accurate modelling of parts and assemblies, as well as simulating testing design. The use of Solidworks was important in designing the complex shapes of the CPCs, as well as optimizing the optical performance of the system.

AutoCad is widely used in architecture and engineering fields and is particularly useful in creating 2D and 3D models of building components. AutoCad was used in the design the façade integration of the CPCs, as well as ensuring that the design fitted within the overall building design.

As a part of the ray tracing process for this research, TracePro was used. TracePro is a comprehensive optical simulation software and was used to model the behaviour of light in complex optical systems, such as CPCs. TracePro utilizes a ray tracing algorithm to simulate the behavior of the light in the CPCs. The software simulates reflection, refraction and absorption of light within the CPCs, as well as predicting the power output and optical performance of the system under different weather conditions.

In using TracePro, a 3D model of the CPCs needs to be created in the software or integrated from Solidworks using STL format. The model should include all relevant components, such as the mirrors, absorber, glass and any other optical elements. Once the model is complete, it can use the software to simulate the behavior of light within the CPCs under different conditions, such as different times of day, weather conditions and other variables. Using TracePro was used in evaluating different design options for the CPCs and selecting the optimal design for each location. The software provided predictions of power output and

optical performance of the CPCs, allowing to make informed decisions about the design systems as outlined in Chapter 4.

TracePro has a built in Solar Emulator tool that was used to simulate the solar spectrum and intensity for a given location and time of day. It took into account the atmospheric conditions, latitude and longitude of the locations as well as the time of the day and date. By using the Solar Emulator tool from TracePro, accurate simulations of the behavior of light within CPCs for Ferrara, Italy and Mayo, Ireland were generated. This was used to select the optimal design for each location, and in evaluating different design options and in order to select the optimal design that produces the highest power output and optical performance under these specific site conditions.

3.5 Characterization equipment

The solar module analyzer used was ISO – TECH ISM 490. This equipment was used to measure the electrical performance of the PV cells used in the CPCs. The analyzer can measure and record the short circuit current, open circuit voltage, instantaneous current and voltage. Figure 3.7 (a) presents the solar module analyzer used for testing.

ORIEL Sol3A Class AAA Solar Simulator was used to provide a controllable and consistent light source for testing the solar cell using in the CPCs. This equipment can simulate the solar spectrum and intensity, allowing for controlled testing of the solar cells under different conditions. Figure 3.7 (b) shows ORIEL Sol3A Class AAA Solar Simulator used for indoor characterization.

“K” type thermocouples (chromel-alumel) were used to measure temperature at different locations in the CPCs, allowing for characterization of thermal performance and temperature distribution. K thermocouples were chosen due to their wide temperature range (-200 ºC to 1372 ºC) and high sensitivity. They are also known for their accuracy, stability and durability making them popular choice for temperature measurement in many applications, including those related to solar energy. Additionally, K thermocouples are affordable and readily available, which makes them a practical choice for experimental setups that require multiple measurements. Figure 3.7 (e) presents a K thermocouple used for thermal performance.

Kipp and Zonen Sp Lite 2 pyranometer measured the solar irradiance received by the CPCs. It provides data on the solar radiation incident on the CPCs, which is essential for evaluating their performance. Vertical solar radiation was recorded using a Kipp and Zonen Sp Lite 2 pyranometer with a sensitivity of 10.2 µV/Wm. Figure 3.7 (d) shows the Kipp and Zonen pyranometer used for outdoor testing.

Agilent 3472ALXI data logger with three cards with twenty-two channels each was used to record and monitor the various measurements taken during the testing process, such as

temperature, solar irradiance and electrical performance. The data logger provides a way to collect and store the data for later analysis. Figure 3.7 (e) presents the Agilent 3472A LXI data logger used in this research.

The data acquisition control codes were written in ‘‘Visual-Basic’’ and each set of I–V measurements were stored on a dashboard along with the solar radiation and temperature measurements.

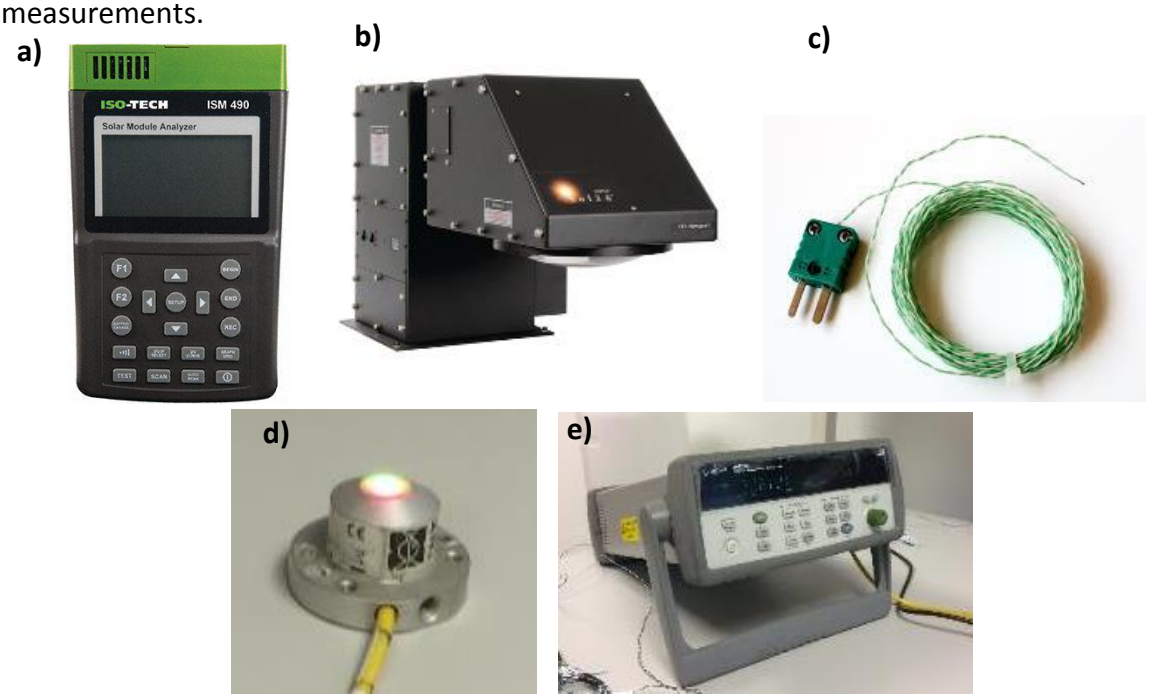

Figure 3. 7 (a) ISO – TECH ISM 490 solar module analyser (b) ORIEL Sol3A Class AAA Solar Simulator (c) K thermocouple (d) Kipp and Zonen pyranomet (e) Agilent 3472A LXI data logger

A labsphere integrated sphere was utilized to measured the reflectivity of differents reflectors. This especific equipment setup allows for accurancte and reliable measurements of the samples optical properties. The light sources employed was an Ocean Optics light source, which offers a broad wavelength range of 200 to 2500 nm. This wide range ensures that a comprehensive spectrum of light is available for the testing and characterization of the samples response to various wavelenths.

Colum heater Beckman is a laboratory instrument used to control and maintain the temperature of an environment. It is designed to provide precise temperature control and uniform heating to ensure accurate and reliable temperature measurements. This device was used to test the “K” thermocouples at various temperatures, such as 21 ºC, 40 ºC, 50 ºC and 60ºC. The objective was to verify their accuracy and performance by comparing the measured temperatures to those obtained with a Thermometer HD 2307.0 RTD, a highly accurate temperature measuring device. An example of the thermocouple characterization is shown in figure 3.8.

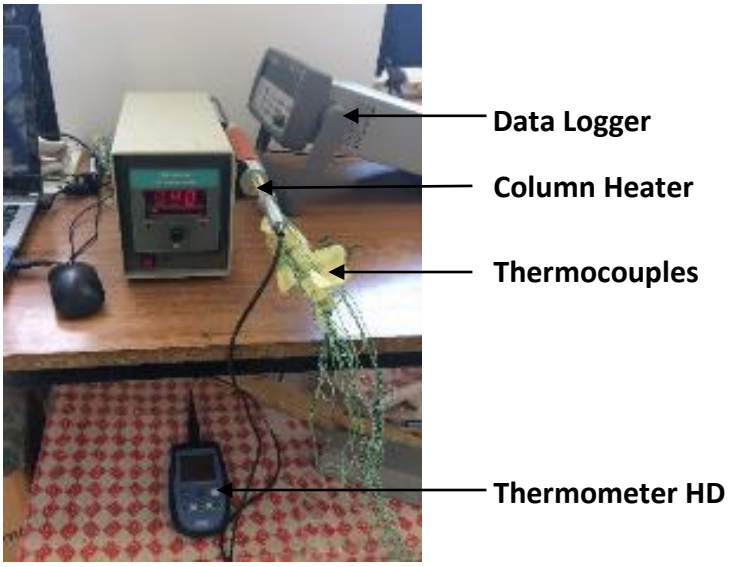

Figure 3. 8 Thermocouples characterization at 40°C using column heater

The outdoor experimental performance of the solar systems at the University of Ferrara (UNIFE) was monitored using a programmable DC electronic load, the EA-EL 3000 B high-speed data acquisition system. This advanced electronic load allowed for precise control and measurement of the electrical characteristics of the solar systems, ensuring accurate and reliable data collection during the testing process. SR20 pyranometer was used to record solar radiation levels during the experiments. The SR20 pyranometer is a high-quality instrument known for its accuracy and durability, making it an ideal choice for measuring solar irradiance in outdoor testing environments. By integrating this device into the experimental setup, researchers were able to accurately measure and correlate the solar system's performance with real-time solar radiation data, allowing for a comprehensive understanding of the system's efficiency and potential improvements.

3.6 Manufacturing equipment

Four 3D printer machines (Anycubic Mega S, Anycubic Mega X and two Prusa MK3S) were used for manufacturing some of the CPC parts.

Anycubic Mega S is a budged-friendly 3D printer that offers reliable performance and ease of use. It is known for its sturdy construction, which ensures stability during the printing process and its compatibility with various filament materials. Anycubic Mega X is larger version of the Mega S, offering a more expansive build volume, making it more suitable for creating bigger prototypes. Like its smaller counterpart, Mega X is compatible with a wide range of material and maintains a stable printing process. Prusa MK3S is a well-established, high-quality 3D printer known for its precision and reliability. This open-source printer is equipped with numerous advanced features, such as automatic bed leveling, power loss recovery and a filament sensor, which contribute to an accurate printing experience.

In order to print, the Solidworks design is saved as an STL file, then the design is converted to the p'inter's language using Prusa Slicer for the Prusas 3D printers and Cura for the Anycubics

3D printers. Parameters such as base and nozzle temperature are selected in each software and depends of the filament used. Figure 3.9 shows the 3D printers used.

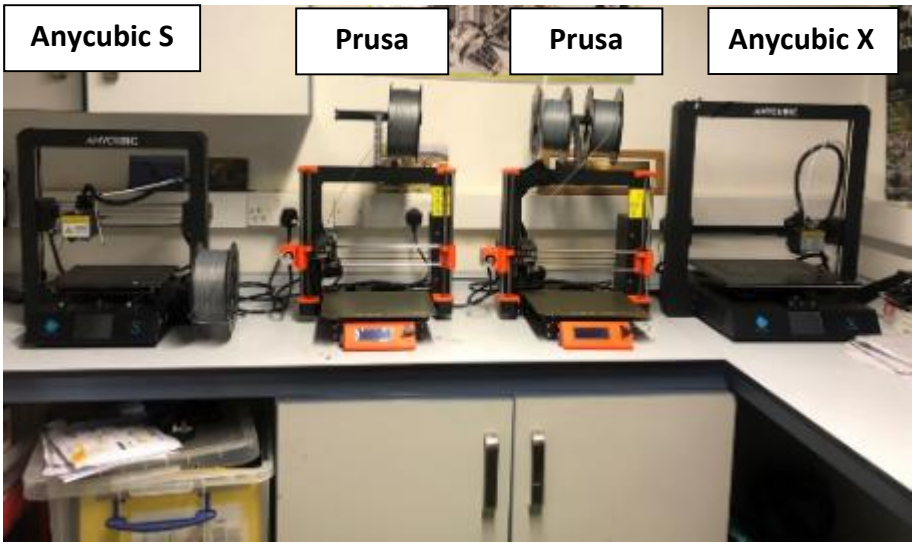

Figure 3. 9 3D Printers used for manufacturing

Two types filament were used in order to print some part of the CPC system: PLA (Polylactic Acid) and ABS (Acrylonitrile Butadiene Styrene). Thermal resistance and softening temperature are important material properties that affect the performance and suitability of PLA and ABS filaments in various applications. Thermal resistance refers to a material's ability to resist the flow of heat. It is essential property to consider when selecting materials that will be subjected to high temperatures or applications where temperature stability is crucial.

Softening temperature is the temperature at which a material starts to soften and lose its rigidity, becoming more pliable and susceptible to deformation. It is crucial to consider the softening temperature when selecting material for applications that involve exposure to elevated temperatures.

PLA is one of the most widely used materials for 3D printing due to its ease use, low odor and minimal warping. PLA exhibits good strength, stiffness and also offers a smooth finish and high detail resolution. PLA has lower thermal resistance compared to ABS. It is more sensitive to heat and is not suitable for high-temperature applications. The softening temperature is typically between 55 ºC to 60 ºC. Above this temperature, PLA starts to soften and may lose its structural integrity. ABS is a petroleum-based thermoplastic known for its durability, impact resistance and high-temperature tolerance. It is commonly used in various industries for making robust and long lasting components. ABS has higher thermal resistance than PLA, making it suitable for applications where parts may be exposed to elevated temperatures. The softening temperature is approximately 100 ºC. This means ABS can maintain its rigidity and structural integrity at higher temperatures compared with PLA. While ABS can be more challenging to print due to its propensity to wrap, using a heated printed bead, heated printing room and enclosed printer chamber can help maintain dimensional stability during the printing process. Table 3.1 comparing the key printing parameters for PLA and ABS filament used.

Table 3. 1 Printing parameters for PLA and ABS filaments

Parameter	PLA	ABS
Nozzle Temperature	180°C to 220°C	220°C to 250°C
Bed Temperature	40°C to 60°C	90°C to 110°C
Bed Adhesion	Blue painters tape, glue stick	Kapton tape, ABS slurry
Cooling	100% fan speed (active cooling)	Minimal or no cooling
Print Speed	40 to 60 mm/s	40 to 60 mm/s (can vary)

3.7 Process techniques

Back monocrystalline silicon solar cells (SunPower), 125 mm^2 were selected for the IDEAS project. According to technical specification the solar cells dimensions are 125 X 125 mm, with an efficiency of 22 %, open circuit voltage of 0.582 V and short circuit current of 6 A. The manufacturer specifies that the temperature losses in the solar cells is equal to 0.32 %/ºC (SunPower, 2023).

For the solar cell interconnection, two dog bone solar cell interconnectors were used. For the soldering process, a leaded solder wire with alloy metal Sn-43Pb-14Bi (Almil Serie: KR-15) of 0.65 mm diameter was used with the soldering iron heated to 400 °C. A flux pen ECO-WORTHY was used to mark the flux of the dog bones interconnectors in order to improve the soldering performance. For the connection of solar cells, first, the solar cells were cleaned and placed in the solar cell holders, then the welding process occurs. All the connections are series in order to increase the voltage and maintain a constant electrical current. As the solar cells are back contact, the complete string is faced downward on a table of low iron glass, in this way, the connection can be made by looking at the back of the cells. Below the low iron glass, two 100 W halogen lamps are used to test each connection of the solar cells in order to identify short circuits or error in the connections. Figure 3.10 shows the back section solar cell along with the dog bones connectors.

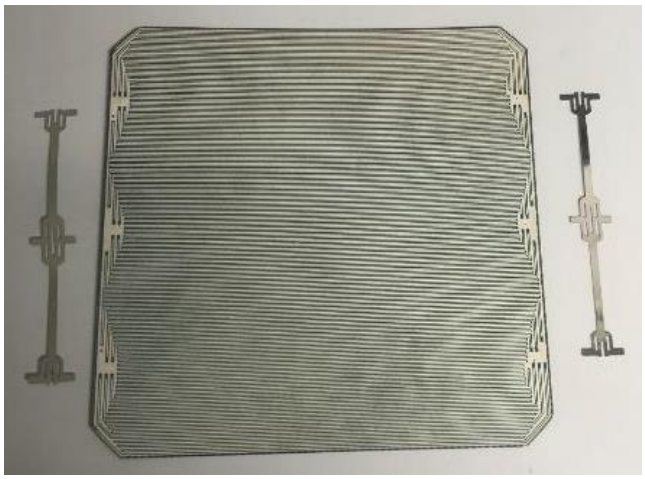

Figure 3. 10 Back section of the cells with dog bones connectors

Solar cell strings were welded and tested to verify their conductivity as is shown in figure 3.11.

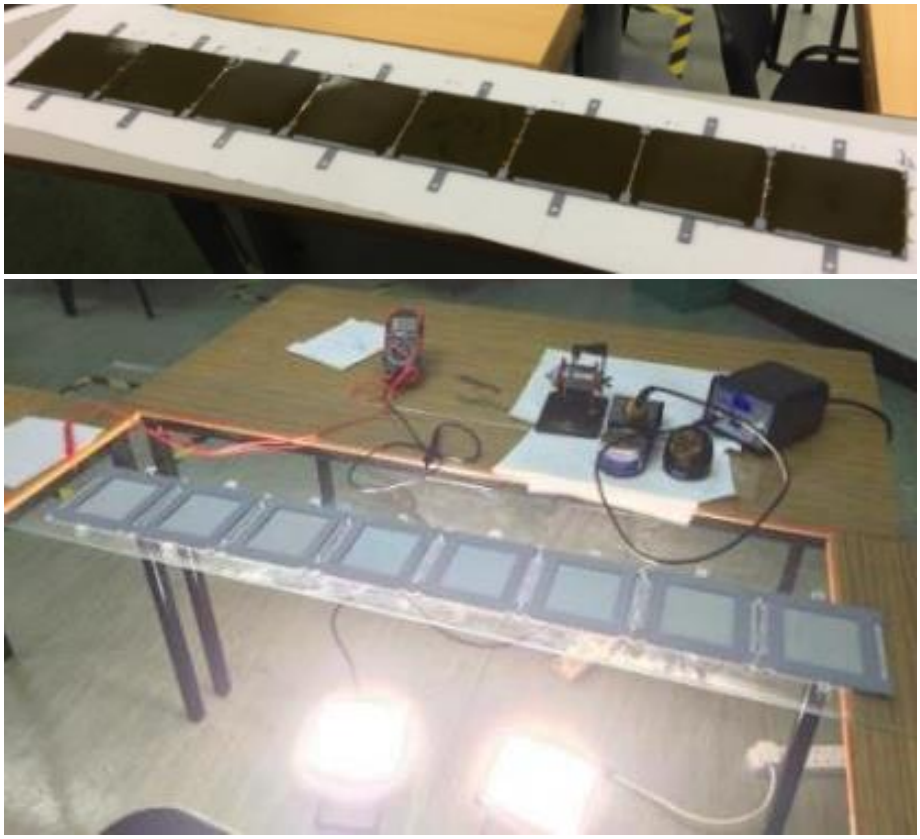

Figure 3. 11 Connection table with halogen lamps

Before installing the solar cells on the backplate, 1 mm thick thermal patches are glued on the back of the cells in order to avoid an air gap between the solar cells and the backplate generated by the solar cells holder. Thermal Interface Sheet, 2.2 W/m·K, Self-Adhesive was used for the process. The figure 3.12 show a string with the thermal patches.

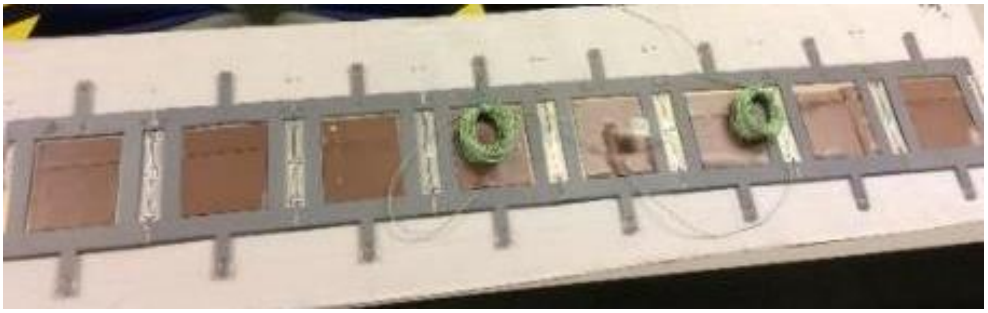

Figure 3. 12 Thermal interface sheet located in the back of the solar cells

A silicon elastomer Sylgard-184 was used to encapsulate and attach the solar cells to the aluminum back plate, to prevent short circuit between the PV cells and the aluminum back plate, and to protect the PV cells from the environment. This coating provides the following benefits (Wu Y., 2009):

- Effective, durable protection,
- High transparency,
- UV stable and moisture resistant,
- Easy application, by spray, brush, flow, dip or automated pattern coating and
- Continuos processing.

The procedures for encapsulation of the solar cells were as follows:

- The soldered solar cells strings were tested using a multimeter to determine and avoid short circuits.
- The two components of the Sylgard were thoroughly mixed using a weight ratio of 10:1 (Part A and Part B), and the mixture was placed inside a vacuum chamber for 45min to vacuum gas the mixture.
- The aluminum back plate surface was cleaned using acetone wipes. It was covered with insulation duct tape where solar cells strings were to be attached.
- The aluminum back plate was coated with a thin layer of 1.5 mm thickness of the Sylgard mixture and the solar cell strings were placed on top
- Sylgard mixture was added to cover the top of the solar cells strings and systems were left for 48 hrs. at room temperature to allow curing of the encapsulant.
- the solar cell strings were again tested to determine if short circuits were present.

Figure 3.13 shows an encapsulated solar cell in the backplate.

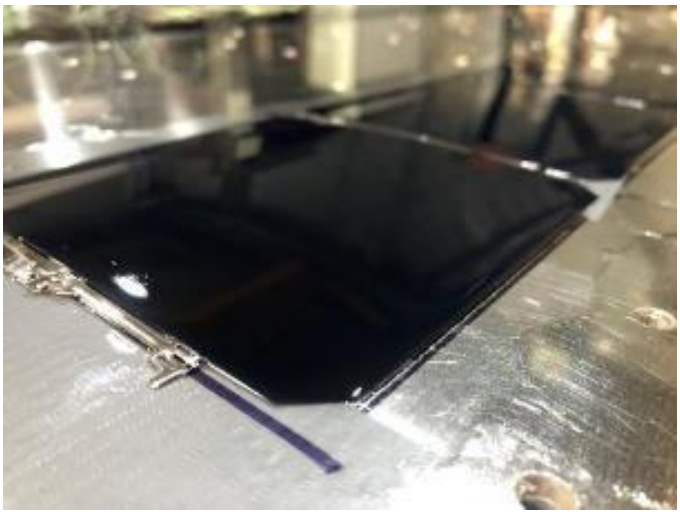

Figure 3. 13 One solar cell encapsulated on the backplate

3.8 Conclusion

The methodology employed in this study involved a comprehensive approach that combined various locations, collaborations, experimental techniques, software, characterization equipment, and manufacturing processes. The demo-sites in Ferrara, Italy, and Mayo, Ireland, provided diverse geographical settings for evaluating the performance of the solar concentrator systems. External collaborations with researchers from TCD and Ulster University allowed for an exchange of knowledge and expertise, which contributed to the robustness of the study.

The experimental techniques utilized in this research included a range of software tools such as SolidWorks, Autocad, TracePro, and Solar Emulator for system design, simulation, and analysis. Characterization equipment like solar module analyzers, solar simulators, thermocouples, pyranometers, data loggers, integrated spheres, and column heaters were employed to gather precise and accurate data on the performance of the solar concentrator systems.

The manufacturing processes involved the use of advanced equipment, such as 3D printers, and various process techniques for solar cell connections and encapsulation. This multifaceted approach ensured the development and assessment of efficient and reliable solar concentrator systems.

This methodology facilitated a thorough investigation of solar concentrator systems, taking into account various factors and conditions that could influence their performance. The insights gained from this study can be applied to future research and development in the field of solar energy, leading to more efficient and sustainable solar energy solutions

Chapter 4 Simulation

This chapter describes the design of asymmetrical compound parabolic concentrator (CPC) systems for collecting solar energy in the two IDEAS demo-sites: Mayo, Ireland and Ferrara, Italy. The designed CPC systems are required to have a wide range of angular acceptance angles to collect most of the annual incident solar radiation and a suitable concentration ratio to reduce the systems initial cost. The chapter presents the design methodology and geometric characteristics of various CPC systems designed as required by H2020 IDEAS project described in Chapter 1.

In consideration of the maximum and minimum altitude angles of the sun in each location, as well as the IDEAS project requirement to design a CPC with concentration ratio greater than 2 and power output of 100 W, six different CPC systems with varying acceptance half-angles were derived for Mayo, Ireland and eight CPC system for Ferrara, Italy. The 100 W power output mentioned refers to power generated under standard test conditions (STC), which include an irradiance of 1000 W/m^2, a solar cell temperature of 25 ºC, air mass (AM) of 1.5 and using the "Standard Tables for Reference Solar Spectral Irradiances" stablished by the American Society for Testing and Materials ASTM G-173.

The emphasis on achieving a concentration ratio greater than 2 is to push the boundaries of existing CPC designs, surpassing the current state of the art and making a valuable contribution to the field of solar energy technology. A higher concentration ratio implies that more sunlight can be focused onto a small PV cell area, resulting in enhanced efficiency and reduced cost of electricity production.

By designing a CPC system with concentration ratios greater than 2, the research aims to significantly improve the performance of building-integrated photovoltaics, particularly in terms of efficiency and power. This pioneering approach will open up new possibilities for harnessing solar energy more efficiency and facilitate the widespread adoption of renewable energy in various geographical locations.

Ray tracing analysis to predict the performance for the CPC system was undertaken using the software TracePro (as described in section 3.4). The optimum system for each demo-site was chosen taking into account the following parameters (defined in section 2.1):

- Acceptance half-angles
- Concentration ratio
- Power output (target 100 W)
- Power ratio
- Solar cell efficiency
- Optical efficiency

Further to this, the annual performance of the chosen CPC system was carried out.

4.1 Optimized CPC design for Mayo, Ireland

4.1.1 Parabola design

Researchers in the past have used the design proposed by Rabl (Rabl et al., 1976b) where the CPC is composed of two parabolas whose focal points are the end points of the flat absorber. With this design, the ends of the absorber are the maximum points of concentration of the solar rays for the determined acceptance half-angle of the concentrator, therefore, when varying the angle of incidence of the solar rays, many rays are lost since they fall above or below the focal points. The CPC becomes larger with increasing value of geometric concentration ratio resulting in an increased reflector size. Although reflector truncation was employed to solve this problem, this leads to a reduction in geometric concentration ratio of CPC, where the location of the optimum focus on the concentration plane is not being considered. Therefore, it is important to find a better parabola combination strategy to reduce these two negative factors of traditional CPC design.

In a Compound Parabolic Concentrator (CPC), the ultimate goal is to concentrate solar radiation as efficiently as possible onto a target, known as the absorber. The typical design of a CPC incorporated a parabolic or curved shape that collected and redirected sunlight towards the absorber. One of the design principles of CPCs is the edge-ray principle. According to this principle, the focal points of the parabolic reflectors should ideally be the edges of the absorber. However, in practice, directing a large proportion of solar radiation onto the edges of the absorber leads d to a significant loss of radiation. This is due to a phenomenon known as edge loss, where radiation either overshoots the edge or is reflected off the sides, resulting in it not being absorbed.

To mitigate this issue, an adjustment was made to shift the focal points inward from the edges of the absorber. This was achieved by placing the new focal points (A1 and B1 from figure 4.1) 10 mm from the edges. This adjustment improved the concentration of solar radiation on the absorber, as the radiation was better targeted and less susceptible to edge loss. Additionally, maintaining the focal points 10 mm away from the edge also helped to counteract losses associated with the manufacturing process. During the production of the CPC, slight irregularities or imperfections may have occurred at the edges. By keeping the focal points 10 mm away from these edges, these potential inconsistencies were less impactful as they were not situated in the path of the concentrated sunlight.

The annual maximum and minimum altitude angles of the sun at noon at Mayo, Ireland (Brackloon Drummin Community Centre 53°44`16.46” N and 9º33`13.10” O) are 60° and 12°, respectively. Annual daylight hours per day vary from about 8 to 18 hours in this location, and there is a large variation in daily available solar energy between summer and winter, due to the winter having shorter daytimes and lower solar altitudes compared to those in the summer. The designed CPC system should have a wide range of angular acceptance to collect

most of the annual incident solar radiation and a suitable concentration ratio to reduce the system's initial cost.

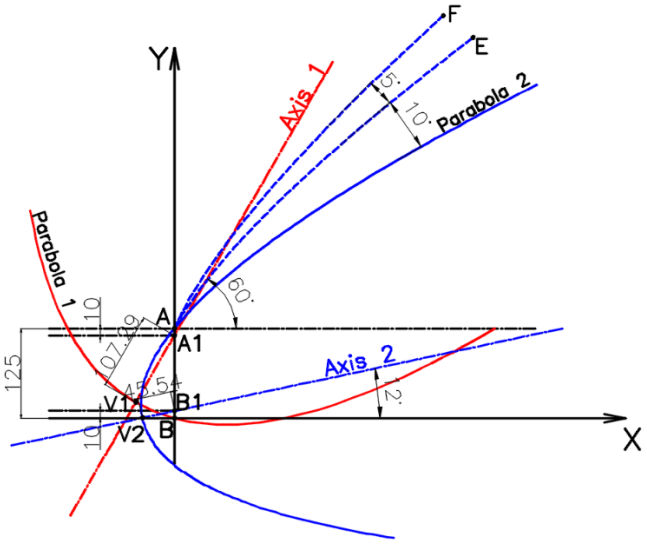

Figure 4. 1 Optimization structure of the CPC

The initial structure design of the asymmetric CPC is illustrated in figure 4.1. The profile can be described as follows:

- For the purpose of our CPC design the dimension of the absorber is 125 mm and a line parallel to the X axis is drawn at that distance.
- Points A and B represent the edges of the solar cell, whose distance AB is equal to 125 mm.
- 10 mm from these edges, the new focal points of the CPC parabolas are positioned, A1 and B1.
- Axis 1 corresponds to the axis of parabola 1 (summer parabola, red) so axis 1 is rotated 60º with the horizontal and contains point A1 that is the focus of parabola 1.
- Parabola 1 is a parabola that must pass through point B (edge of the solar cell) and whose focus is point A1. A focal length V1A1 equal to 107.29 mm meets the required condition.
- The same approach is used for parabola 2 (winter parabola, blue), whose axis 2 is rotated 12º with the horizontal and contains point B1, focus of parabola 2.
- Parabola 2 with a focal length V2B1 equal to 45.54 mm meets the required conditions.
- The segment of Parabola 2, centered at Point A, undergoes a series of rotations relative to the X-axis. Specifically, the segment is rotated to angles of 10 degrees and 5 degrees respectively. The resulting terminal points of these rotations are identified as Points E and F, respectively.

In the context of a Compound Parabolic Concentrator (CPC), rotations are often applied to parts of the parabolic structure to optimize certain performance parameters. A CPC's

performance is characterized by two important parameters: the aperture length and the acceptance half angle. The aperture length is the length of the opening through which sunrays enters the CPC, while the acceptance half angle is the maximum angle from the CPC's axis at which sunrays can still enter and be effectively concentrated onto the absorber. The segment of Parabola 2, centered at Point A, is rotated at angles of 10 degrees and 5 degrees relative to the X-axis to increase these two parameters. The reasoning behind this strategy is as follows:

- Increasing the aperture length: By rotating the parabolic segment, the overall length of the aperture can be increased. This allows for a greater collection area for the incoming sunrays, which can lead to a higher concentration of sunrays onto the absorber and, consequently, better performance of the solar collector.

- Increasing the acceptance half angle: The rotation also increases the CPC's acceptance half angle. This means that the CPC can accept sunrays from a wider range of incident angles. This is particularly useful in practical applications where the position of the sun changes throughout the day. A larger acceptance half angle ensures that the CPC can effectively collect and concentrate sunrays over a larger portion of the day, increasing its overall efficiency.

The final positions after these rotations, Points E and F, mark the endpoints of the parabolic segment and help define the shape of the CPC after these adjustments have been made. This fine-tuning process, therefore, improves the solar collector's ability to harness and concentrate sunrays, contributing to the overall efficiency and effectiveness of the CPC.

With this new arrangement of parabolas (parabola 2, solar cell AB and parabola 1; Parabola EA, solar cell AB and parabola 1; parabola FA, solar cell AB and parabola 1) six CPC systems were designed in order to obtain concentration ratios of 2, 2.5 and 3. CPC designs are shown in figure 4.2 and their geometric characteristics are presented in table 4.1.

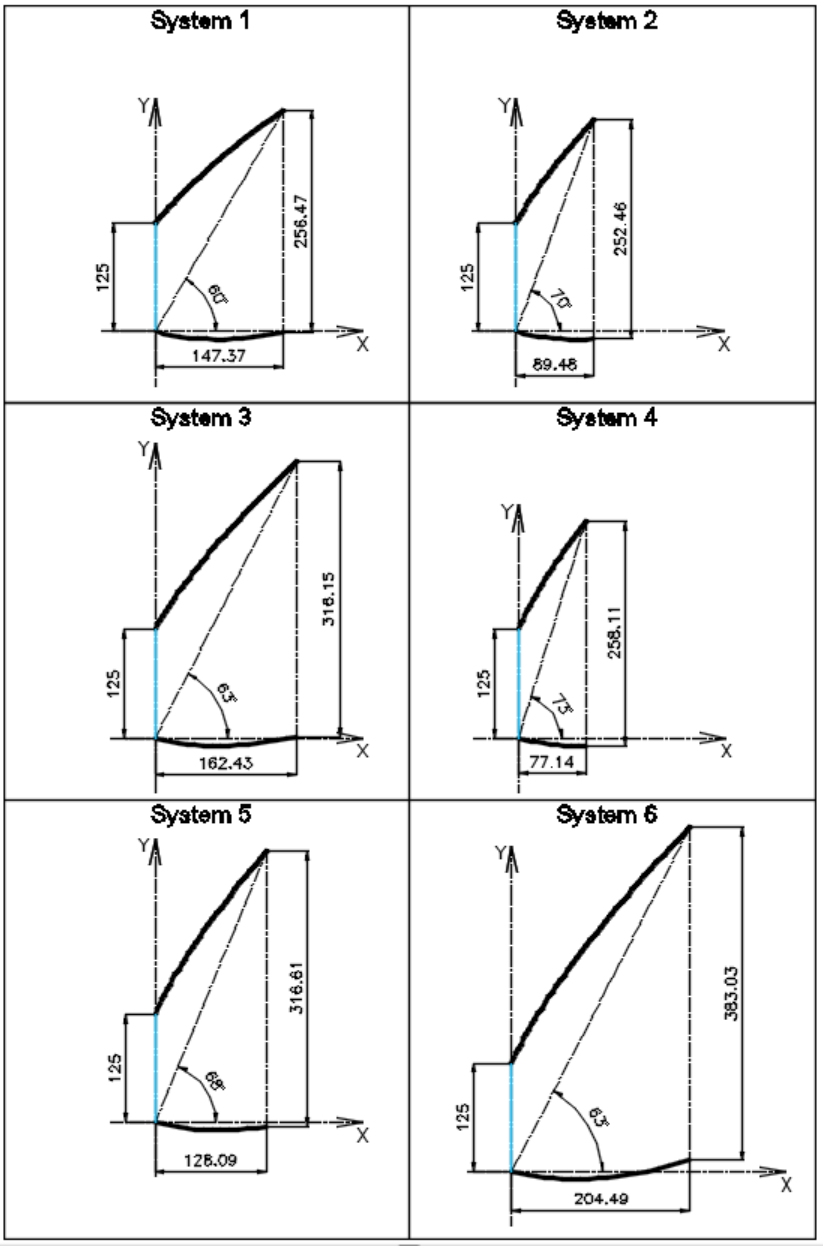

Figure 4. 2 Geometric characteristics of the CPC modelled for Mayo, Ireland

Table 4. 1 Geometrical properties of the CPCs modelled for Mayo, Ireland

System	Top reflector rotation (°)	CR	Acceptance half-angle (°)
1	0	2.0	12 - 60
2	10	2.0	12 - 70
3	10	2.5	12 - 63
4	15	2.0	12 - 73
5	15	2.5	12 - 68
6	15	3.0	12 - 63

4.1.2 Optical modelling

The angle between the normal of the absorber of the CPC and the incident ray is defined as the incidence angle. However, not every sun ray can reach the absorber by reflection, which means that a portion of solar rays may escape the concentrator. The solar rays corresponding to summer (red line and incident angle 60 º) and winter (blue line and incident angle 12 º) and the CPC module are shown in figure 4.3.

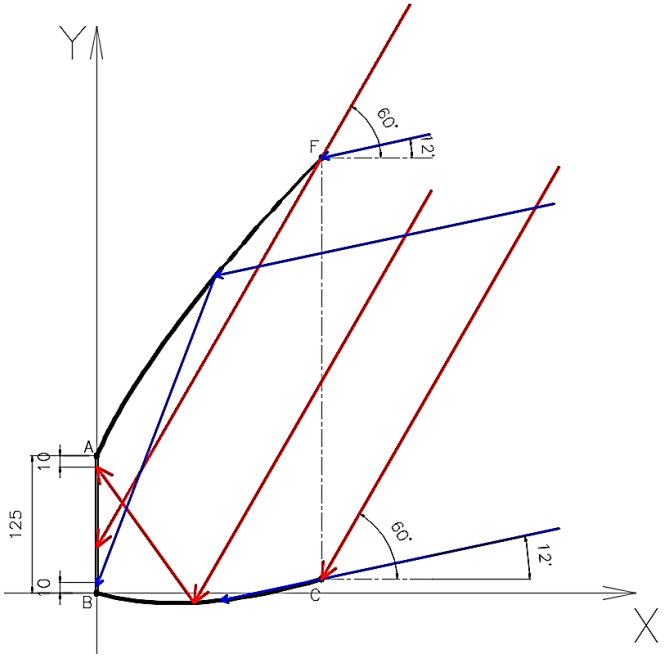

Figure 4. 3 Schematic diagram of ray paths to reach the absorber

From figure 4.3 the behavior of the solar rays through the seasons can be seen. The summer ray passes through point F on the top reflector reaches the absorber at point X, all rays parallel to the line XF and below it will reach the absorber between the points XB. The portion of the absorber between the points AX will not be reached by the direct summer sunrays as a consequence of the shadow caused by the portion of the top reflector AF. It is to be expected that the rays that reach the bottom reflector BC will be reflected at the focus point A1 of the parabola BC. The winter solar rays at 12 º will be reflected with the parabola AF at its focus B1.

4.1.3 Ray Tracing simulation

Trace Pro was used to simulate the incident rays passing through the CPC and then to get first the power output, number of solar cell and reflector area. Trace Pro is a fast and accurate ray-tracing analysis program which provides the optical system modelling and performance evaluation for the CPC design. The required design power is 100 W at noon during the year with the lowest consumption of solar cells to install in the location of Mayo for a CPC system installed in façade. Simulation parameters are:

- PV is a perfect absorber of 125 x 125 mm

- Aluminium reflectors of reflectivity of 0.92
- Aperture is unglazed
- 100,000 rays uniformly entered the aperture
- Irradiance of 1000 W/m^2
- AM 1.5 – ASTM G-173
- Solar cell efficiency 22 %
- Solar cells uncoated
- Standard temperature condition 25 ºC

Figure 4.4 shows the schematic design in Solidworks that was inserted in TracePro for simulation. The required length determined the area and number of solar cells necessary for the CPC. The results of the six CPC simulated systems are shown in Table 4.2.

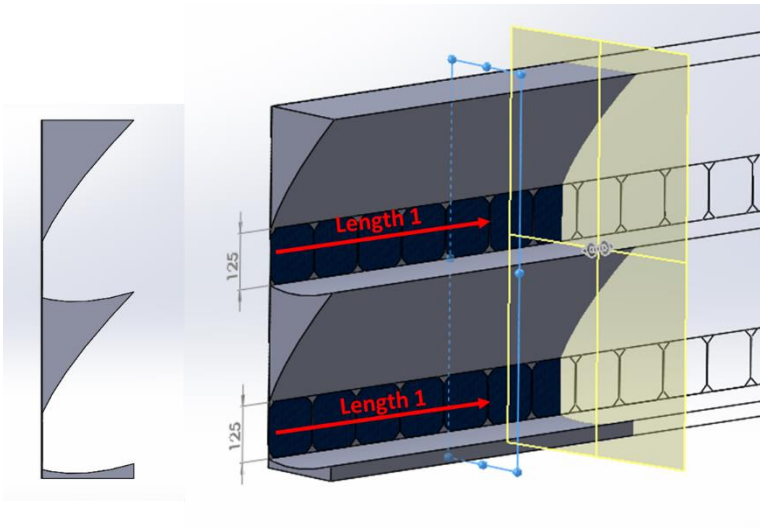

Figure 4. 4 System design inserted into Trace Pro

Table 4. 2 Season results from simulation for Mayo

System	Summer Power (W)	Spring/Autumn Power (W)	Winter Power (W)	Nº Solar cells	Reflector Area (m^2)
1	103.12	175.96	203.56	31	1.11
2	100.53	168.33	121.02	30	2.69
3	102.47	174.22	102.24	25	3.91
4	103.28	148.78	118.75	30	2.53
5	104.07	154.61	102.83	25	3.34
6	119.29	182.51	100.20	24	4.94

In the context of a building façade, the amount of incident solar radiation received varies throughout the year, with lower levels in the summer and higher levels in the winter. This is due to the varying angles of sunlight incident on the façade, which depend on the suns position in the sky during different seasons. As a result, the first principal filter for selecting

the best CPC system is to ensure that it can efficiently produce 100 W during the summer months when the façade recives lower solar radiation. Moreover, by achieving the desired 100 W during the summer, the system is likely to perform even better during the winter months, when incident solar radiation levels are higher. Consequently, this design approach contributes to a more reliable and sustainable energy source for the building throughout the year.

The power generated by a solar energy system like a Compound Parabolic Concentrator (CPC) was primarily a function of two factors: the amount of solar radiation incident on the system (measured in W/m^2), and the efficiency of the system at converting this solar radiation into electrical power. In table 4.2, to calculate the power, one multiplied the incident solar radiation (in W/m^2) by the area of the solar cells (in m^2), and then by the efficiency of the solar cell (as a fraction). This would give the electrical power output in Watts. Regarding the orientation of the systems, they were facing due south. This was the optimal orientation for solar collectors in the Northern Hemisphere as it maximized the amount of sunlight they received throughout the year. The sun move from east to west, but its highest point was towards the south. Therefore, a south-facing system could capture the most sunlight during the day. From the results in table 4.2 all the simulated systems reach 100 W in the summer with different numbers of solar cells. System 6 reached the highest value of electrical production, 119 W with the lowest number of solar cells (24). Figure 4.5 shows the power ratio of the six systems for each season and shows that system 6 reached the highest power ratio for the summer, spring and autumn seasons, and for winter is equal to systems 2, 3, 4, and 5. Therefore, System 6 was chosen as the CPC system for manufacture for Mayo, Ireland.

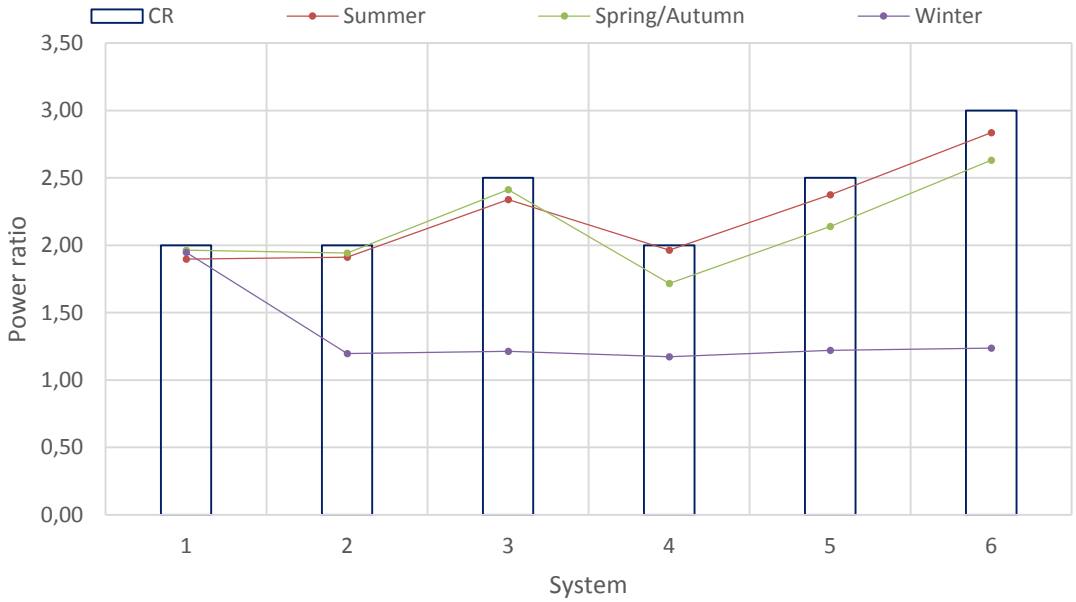

Figure 4. 5 Power ratio for the systems modelled for Mayo

Figure 4.6 shows the ray tracing simulation for all seasons, revealing the lower reflectors role as a summer reflector and its capacity to concentrate rays at the focal point. Even with the shadow generated by the top reflector during the summer, the CPC system not only meets but exceeds the target power output of 100 W. In fact, the system achieved a 119 W in the summer, which demostrates a excellent performance under the given conditions.

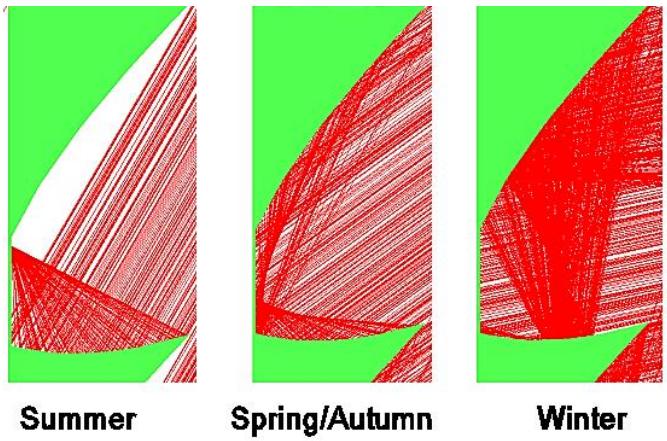

Figure 4. 6 Ray traced for CPC system for Mayo

Table 4.3 shows the geometric properties of the chosen system. The range of acceptance half-angle for the system is 12º - 63º, allowing the CPC to efficiently capture and concentrate solar rays over a broad range of incident angles in Mayo. The absorber, where the solar radiation is focused, has a width of 125 mm. The top reflector, which redirects solar rays towards the absorber, has a length of 341.08 mm. The bottom reflector, which primarily functions as summer reflector, has a length of 207.5 mm. The CPC system has a geometrical concentration ratio of 3, meaning that the solar radiation is focused onto an area three times smaller than the aperture, resulting in higher efficiency and reducing the cost of electricity production.

Table 4. 3 Geometrical properties for CPC system for Mayo

Acceptance -half angle	12º - 63º
Absorber (mm)	125
Length of top Reflector (mm)	341.08
Length of bottom Reflector (mm)	207.5
Aperture (mm)	383.03
Geometrical Concentration Ratio	3

Figure 4.7 shows the schematic design of the CPC system and shows the arrangement and interaction of these geometric properties, providing an overview of the CPC systems layout and dimensions.

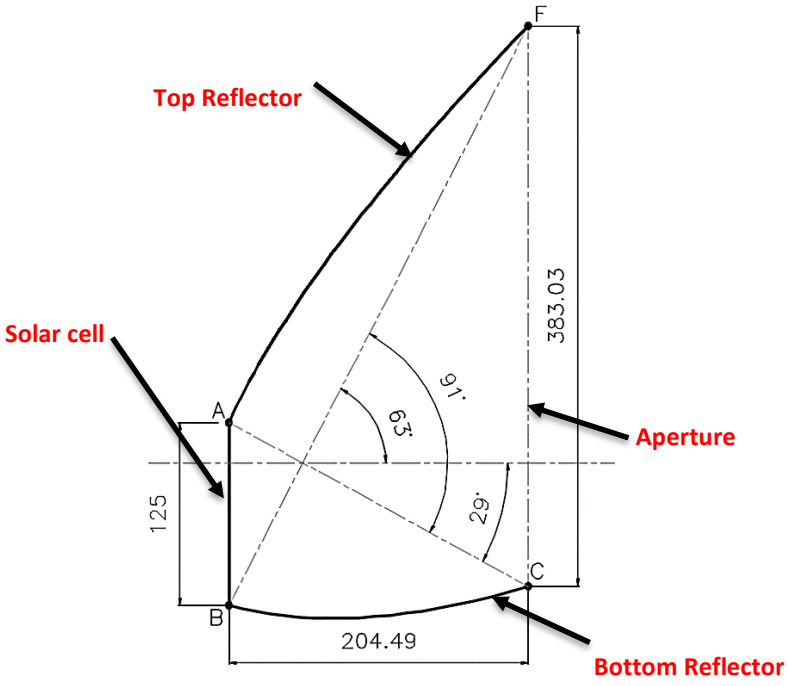

Figure 4. 7 Geometric characteristics of the CPC system for Mayo

4.1.4 CPC Annual performance

A ray trace analysis to predict the annual performance for the CPC system 6 was undertaken (as described in Tables 4.2 & 4.3 and shown in figure 4.7) and compared with a Reference system.

In this context, the Reference system was defined as a solar energy system that didn't employ a concentrator. Instead, this system captured sunrays through a flat collection area, which is a flat-plate collector or a basic photovoltaic panel. The key characteristic of this system for comparison purposes was its identical area to that of CPC system 6. The decision to compare CPC system 6 with a non-concentrator system of the same area provided a useful baseline for comparison. This allowed for an examination of the extent to which the utilization of a concentrator within the CPC system could enhance the system's efficiency and performance. A flat collector without a concentrator absorbed sunrays directly without any mechanism to focus or concentrate these rays onto a smaller area. In contrast, a CPC system used a parabolic design to concentrate the incident sunrays onto a smaller absorber area. Depending on the efficiency of the CPC design and the quantity of incident sunrays, this concentration could potentially augment the quantity of energy captured. By comparing CPC system 6 to a reference system with the same area but without a concentrator, the analysis could quantify the benefits of employing a concentrator. These benefits could include increased power output, improved efficiency, or superior performance under various sunray conditions. Consequently, the comparison would offer valuable insights into the advantages and potential trade-offs associated with using a CPC system versus a more traditional flat collector system.

Using Trace Pro, CPC system 6 and Reference system were simulated for one year (from 1st of January to 31st of December) in order to determine the hourly power production under global and diffuse radiation (AM 1.5 – ASTM G-173). Figure 4.8 shows the annual production power for the CPC and Reference system, where the CPC system clearly outperforms the Reference system under global and diffuse radiation.

Utilizing the optical simulation software, Trace Pro, both the CPC system 6 and the Reference system underwent a comprehensive simulation for a full calendar year (from the 1st of January through to the 31st of December). The goal of this extensive simulation was to establish the hourly power production of each system under conditions of both global and diffuse radiation. This was achieved using a constant solar radiation of 1000 W/m^2 following the AM 1.5 – ASTM G-173 standard spectrum.

The decision to incorporate a constant solar irradiance of 1000 W/m^2 in the Trace Pro simulation was primarily dictated by the software's inherent capabilities, which allowed solely for constant solar radiation data. This presented a limitation in the ability to simulate the dynamic nature of real-world solar radiation, which fluctuates throughout the day and across seasons. The specific selection of 1000 W/m^2 as the solar irradiance value originates from conventional practices in solar energy studies. The 'solar constant'—an estimate of the solar electromagnetic radiation received at the outer atmosphere of the Earth on a surface oriented perpendicularly to the rays—is around 1361 W/m^2. However, due to processes such as atmospheric scattering and absorption, the solar irradiance value is reduced by the time it reaches the Earth's surface. On a clear day, with the sun at zenith and at sea level, the typical solar irradiance is about 1000 W/m^2. Utilizing this value of 1000 W/m^2 for the simulations provided a standard benchmark that was representative of peak solar irradiance for many geographical locations globally. Thus, this choice represented a balance between replicating realistic conditions and accommodating the software's constraints. However, it is crucial to acknowledge that actual solar radiation varies temporally throughout the day and annually, and also spatially depending on factors like latitude, altitude, and atmospheric conditions. These variances could have significant implications on the performance of solar energy systems such as CPC system 6 or the Reference system.

The results of these simulations were plotted in Figure 4.8, showcasing the annual power production of both the CPC and reference systems. A clear pattern emerged from this data, revealing that the CPC system 6 significantly outperformed the reference system under conditions of both global and diffuse radiation. This highlighted the efficacy of the CPC system 6 in harnessing solar energy, even when compared to a similarly sized system without a concentrator. Additionally, in order to provide a robust understanding of the daily power output of these systems, the maximum power reached within each day was recorded. From these data points, an average monthly of maximum power output for each day was calculated for each system. This approach offered another useful perspective on the power production

capabilities of the CPC system 6 and the reference system, capturing their peak performance under optimal conditions each day.

The results indicated that the CPC system performed well by achieving the design output power of 100 W during the year. Under ideal conditions, the maximum electrical output for the CPC system reached 126 W in summer, whereas the Reference system only generated 45 W. This comparison highlighted the effectiveness of the CPC system. The significantly higher power output of the CPC system (126 W) compared to the Reference system (45 W) demonstrated the advantages of incorporating concentrating technologies like CPCs in solar energy systems. The CPC system was more efficient at capturing and utilizing solar radiation, leading to a higher power generation capacity.

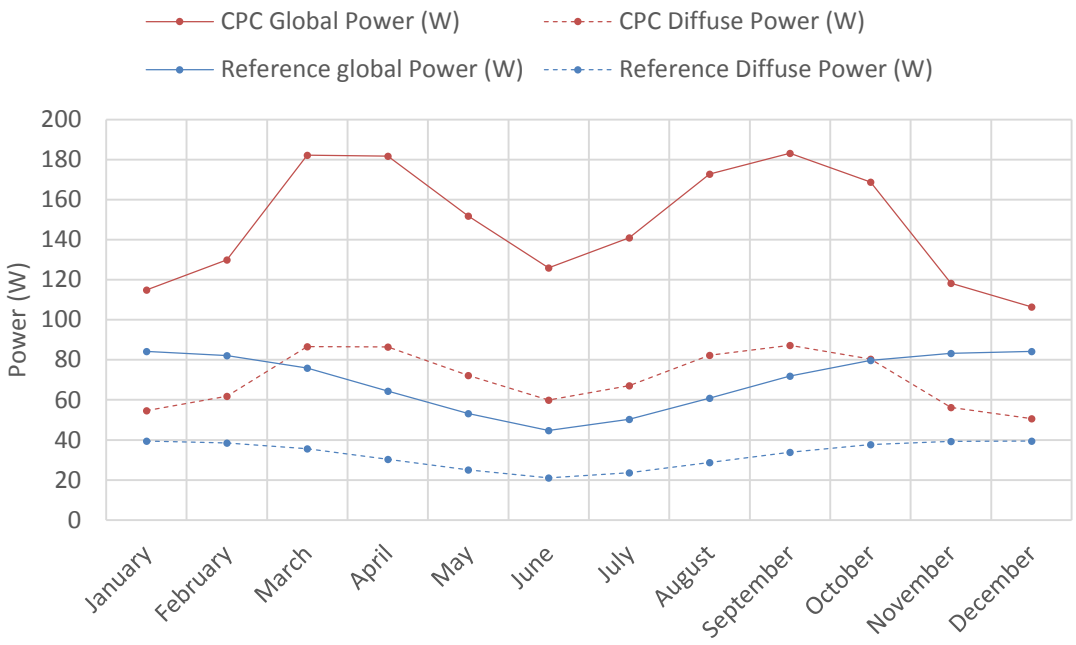

Figure 4. 8 Simulated Annual performance for the CPC and Reference systems under global and diffuse radiation for Mayo

Figure 4.9 shows the solar cells electrical efficiency of the solar cells in the CPC and Reference systems, the results show that the efficiency varies between 28 % to 49 % during the year for the CPC system while for the Reference system it varies between 12 % to 22 %. It is important to note than SunPower solar cell has an efficiency of 22 % (section 3.7), which applies under standard test conditions. However, the efficiencies mentioned in Figure 4.9 can be explained as a concentration effect. The CPC system uses a concentrator to focus ray lights onto smaller area of solar cell. This increased concentration of light raises the intensity of the incident light, which can improve the efficiency of the solar cell beyond its performance under standard test conditions.

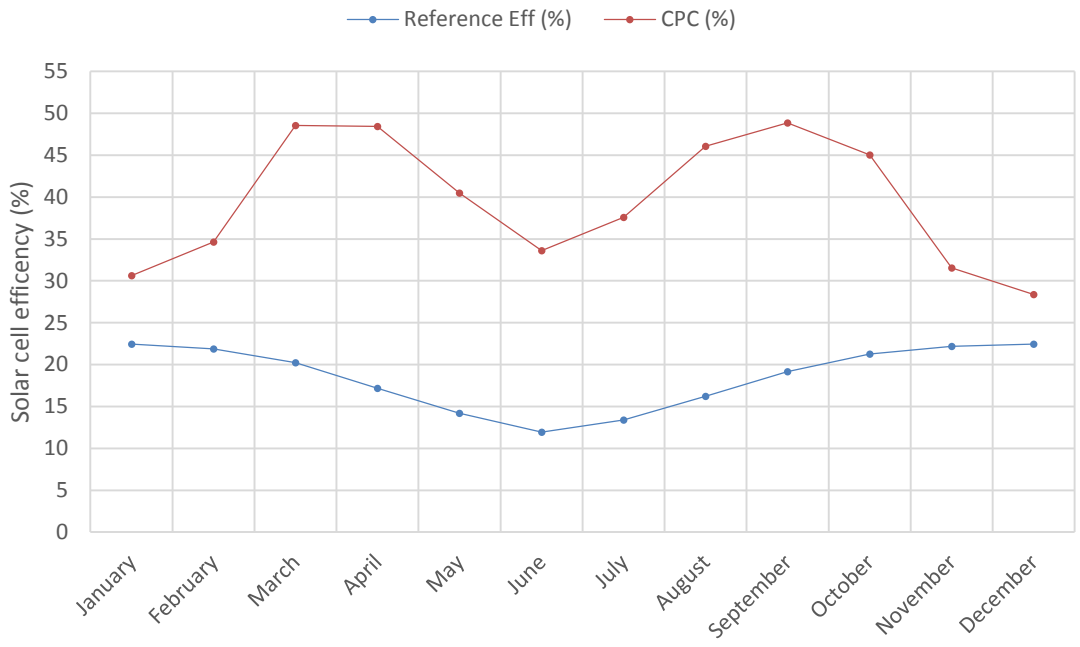

Figure 4. 9 Simulated annual solar cells electrical efficiency for CPC and Reference systems for Mayo

The CPC power ratio was stable and equal to 2.82 from February to September with the lowest value shown in December and January of 1.29 and 1.40 respectively as it is shown figure 4.10. The power ratio behaviour can be explained by considering several factors related to the solar radiation intensity, seasonal variation and CPC design. The intensity of the solar radiation varies throughout the year due to changes in the sun position and the length of the daylight hours. From February to September, the sun is generally higher in the sky, leading to increased solar radiation intensity and longer daylight hours. This increased radiation intensity is more effectively captured and concentrated by the CPC system, resulting in a stable and higher power ratio of 2.82 during these months. In December and January, the sun is lower in the sky and daylight hours are shorter, leading to less intense solar radiation. The CPC system is less effective at capturing and concentrating this lower-intensity sunlight, resulting in a reduced power ratio of 1.29 and 1.40 respectively. In addition, the design of the CPC was optimized for capturing solar radiation at higher sun altitudes, which are common from February to September. This optimization contributed to the stable and higher power ratio observed during these months. In contrast, the lower sun altitudes in December and January where solar radiation is not captured as efficiently by the CPC design, leading to lower power ratios.

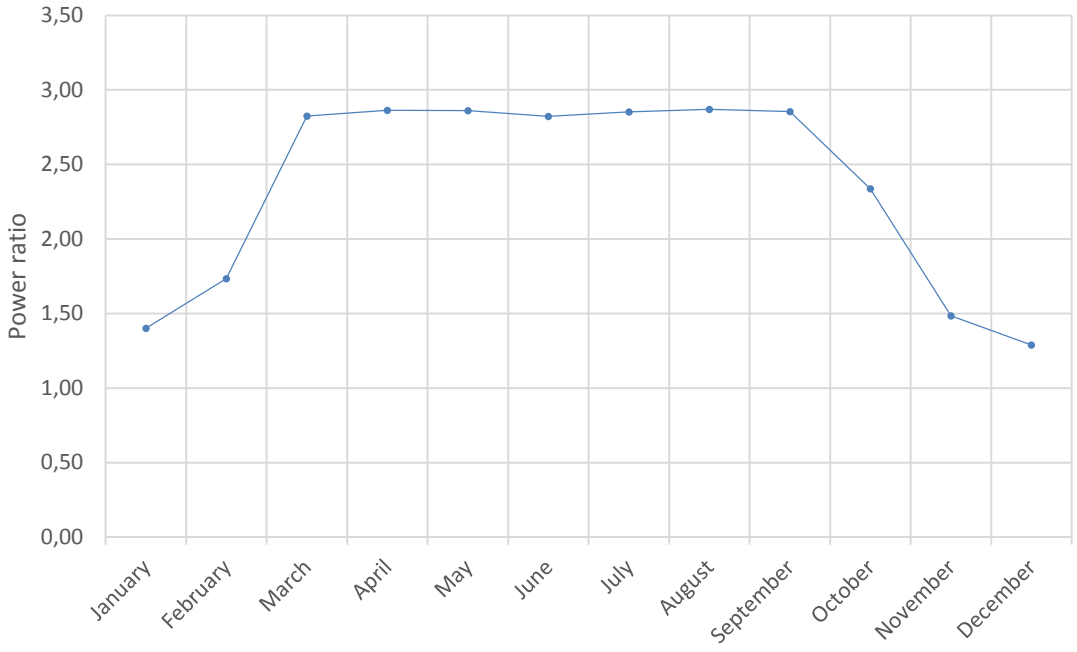

Figure 4. 10 Simulated annual power ratio for the CPC system form Mayo

Optical efficiency through the year can be observed in figure 4.11 and its variation according to the angle of incidence in figure 4.12. From figure 4.12 the optical efficiency reaches more than 90 % when the solar rays vary between 30 º to 60 º and as expected it has lower values outside the range of the acceptance of half-angle (12 º - 63 º) between the 10 º and 20 º, 80 º and 90 º.

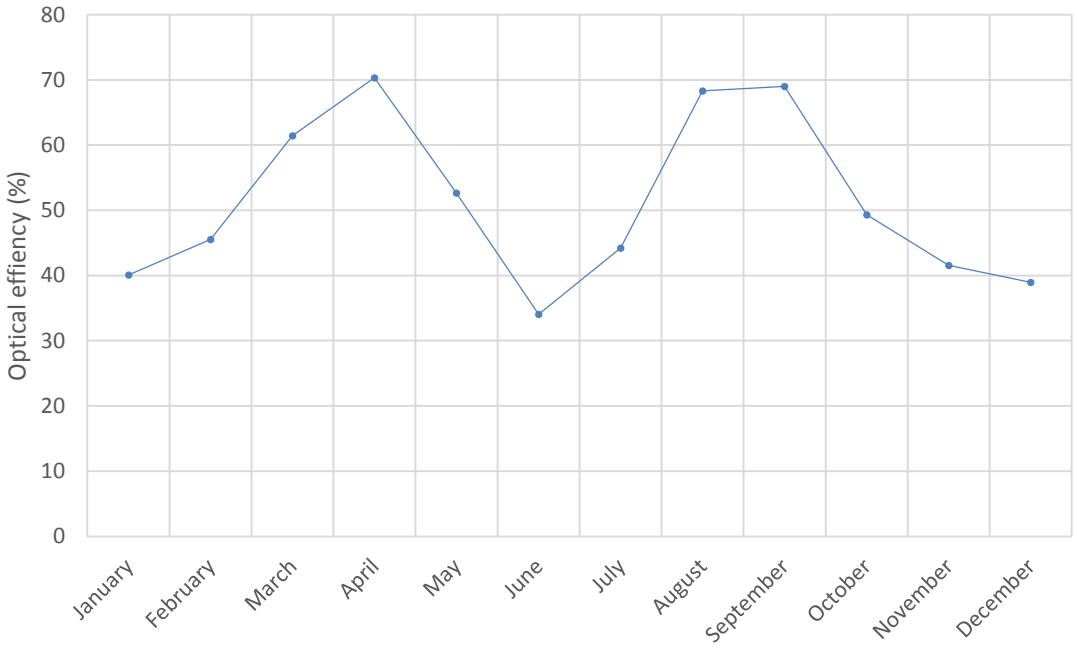

Figure 4. 11 Simulated annual optical efficiency for the CPC system for Mayo

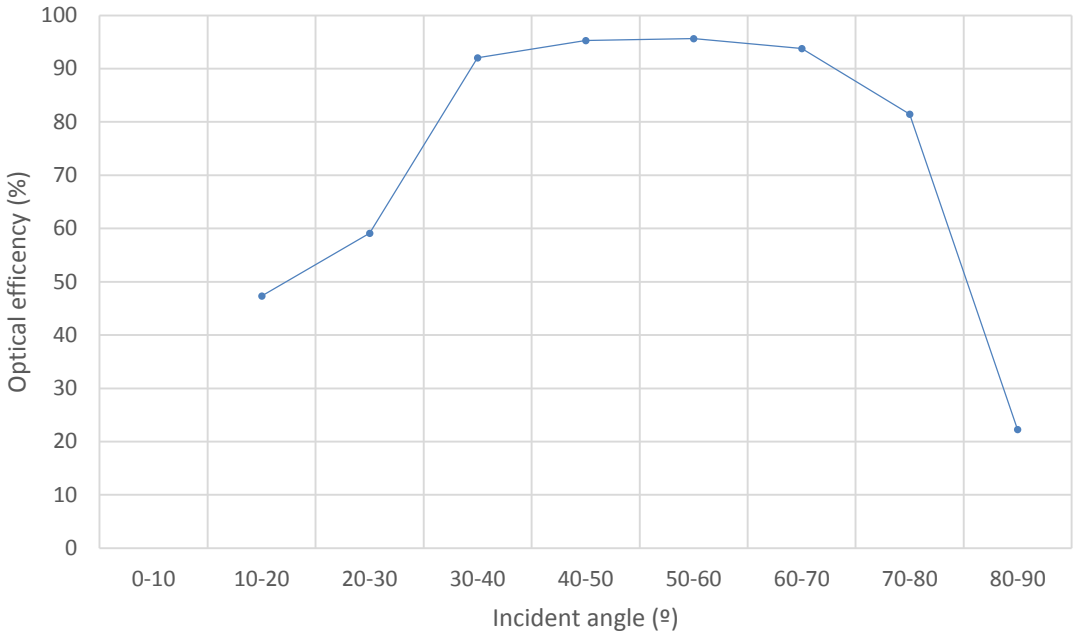

Figure 4. 12 Simulated optical efficiency for the CPC system with incident angle for Mayo

Annual flux distribution can be observed in Figure 4.13, which shows the concentration of solar radiation on the solar cells for each month. In January, February, October, November, and December, a low proportion of direct solar radiation (without reflection) reached the solar cells. This could be corroborated with Figure 4.8, where these months exhibited low electricity production. In May, June, July, and August, the presence of the focal line (parabola 2 - Bottom reflector) was clearly visible, thus verifying that it was concentrating the rays on the focal line located 10 mm from the edge of the solar cells, as per design. Finally, the top reflector played a crucial role during the months of March, April, May, September, October, and November. This can be attributed to the thoughtful design and strategic placement of the reflector, which enhanced the overall performance of the CPC system.

Flux distribution is illustrated in Figure 4.13 enabling a clear understanding of how solar radiation was concentrated on the solar cells throughout the year. By comparing Figure 4.13 with Figure 4.8, the correlation between the concentration of solar rays on the solar cells and the electricity production is evident. The presence of the focal line and the importance of the top reflector in certain months further confirmed that the CPC system was working as intended, concentrating solar radiation as per the design requirements (see Table 1.1).

Flux distribution, in this context, pertains to the dispersal pattern of solar radiation, or 'flux', as it impacts the surface of the solar cells within a given system. This distribution effectively chronicles the concentration of solar radiation that individual segments of the solar cell array receive.

Figure 4.13 present this concept further by delineating the flux distribution across a series of eight solar cells. This collection of diagrams facilitates a comprehensive understanding of the dynamics of solar radiation concentration onto the solar cells over the span of a year. Each distinct diagram corresponds to the flux distribution at noon on the 21st of each month, from January to December. In these diagrams, the X-axis represents the cumulative length of the solar cell string, which is an aggregate of eight individual solar cells each measuring 125 mm, totaling to 8 X 125 mm. In contrast, the Y-axis represents the width of a singular solar cell, which is 125 mm. Thus, the diagrams essentially provide a longitudinal cross-sectional view of the array of solar cells.

The observed non-uniformity of flux distribution at different Y-positions is attributed to the inherent asymmetry of the Compound Parabolic Concentrator (CPC) system under examination. Owing to its asymmetrical design, the CPC system does not distribute solar radiation uniformly across the solar cells; instead, the flux tends to be concentrated more towards specific areas, thereby leading to an uneven distribution. An assessment of Figure 4.13 in conjunction with Figure 4.8 revealed a distinct correlation between the concentration of solar rays on the solar cells and the subsequent electrical output of the system. The presence and significance of the focal line and the top reflector in the CPC system were further emphasized during certain months of the year (From May to August), thereby substantiating that the CPC system operated in alignment with its intended design requirements, as delineated in Table 1.1.

Given the limitations of the processing capabilities of the laptop used for simulation, the diagrams were produced with a reduced pixel quality. Despite this computational constraint, these visual aids yield invaluable insights into the performance and operational dynamics of the CPC system.

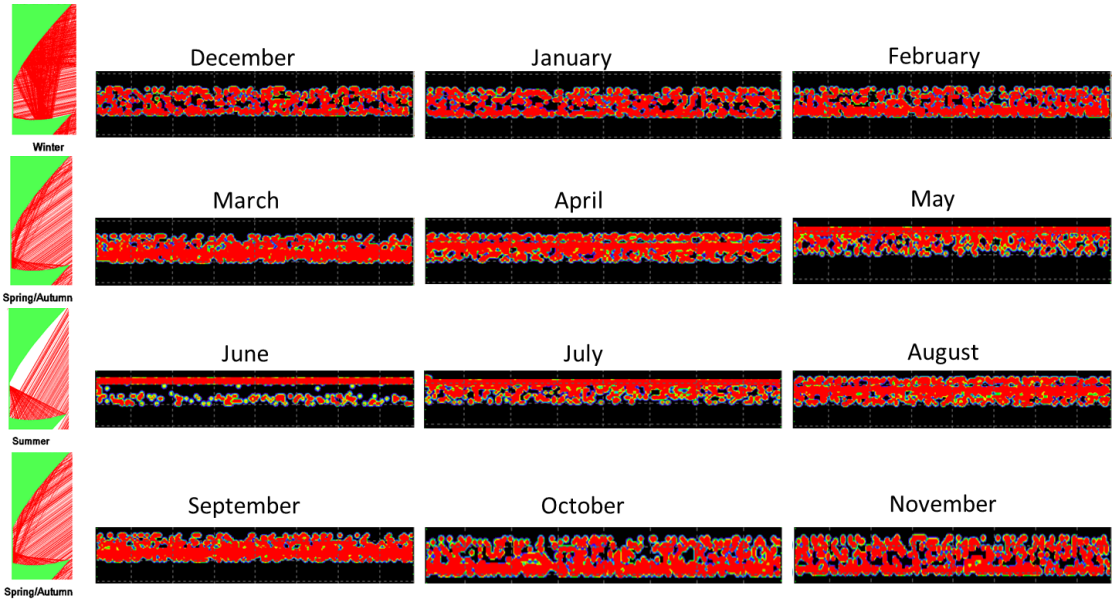

Figure 4. 13 Flux distribution obtained from simulation in a string of eight solar cells on the 21st of each month for Mayo CPC system

High intensity peaks in solar radiation can significantly influence the electrical performance of solar cells. These peaks typically result in a higher generation of electricity due to the increased photon absorption, leading to more electron-hole pairs and hence more current. However, an excessive intensity peak can potentially cause overheating, resulting in thermal stress and efficiency losses due to the temperature dependence of the solar cell performance. Solar cells operate best within a specific temperature range and exceeding this can negatively affect their performance. When solar cells get too hot, the efficiency of energy conversion (from sunlight to electricity) drops. This effect, known as the temperature coefficient, results in a decrease in power output for every degree rise in temperature beyond the cell's optimal operating range. In addition, high intensity peaks, if not managed correctly, can contribute to accelerated aging and potential degradation of the solar cells over time. This can affect the overall durability and longevity of the solar photovoltaic system.

The impact of high-intensity peaks was not accounted for in the modelling of the CPC system due to the constraints of the software used for the simulation. Specifically, the software did not offer functionality for incorporating thermal effects or the capability to simulate the influence of temperature variations on solar cells. As a result, the modelling was largely concentrated on the collection and absorption of solar radiation, without considering potential thermal impacts and the stress that could be introduced by high-intensity peaks of sunlight. While this approach served to yield valuable insights into the fundamental operation and anticipated performance of the CPC system under idealized conditions, it is essential to acknowledge that real-world conditions might deviate from these.

4.2 optimized CPC design for Ferrara, Italy

The same design methodology described in Section 4.1 was used to generate the parabolas corresponding to the CPC for Ferrara, Italy.

Annual maximum and minimum altitudes of the sun at noon Ferrara University (UNIFE) (44°49`54.12" N and 11°35`59.48" E) are 68 ° and 22 °, respectively. Annual daylight hours per day vary from ~8 to 18. Eight CPC systems were designed in order to obtain a concentration radius equal 2, 2.5 and 3 (as outlined in the design criteria in table 1.1). The designed CPCs geometric characteristics are presented in table 4.4 and are illustrated in figure 4.14.

Table 4. 4 Geometrical properties of the CPCs modelled for Ferrara

System	Top reflector rotation (°)	CR	Acceptance half-angle (°)
1	0	2	22 - 66
2	0	2.5	22 - 56
3	10	2	22 - 74
4	10	2.5	22 - 68
5	10	3	22 - 64
6	15	2	22 - 77
7	15	2.5	22 - 72
8	15	3	22 - 69

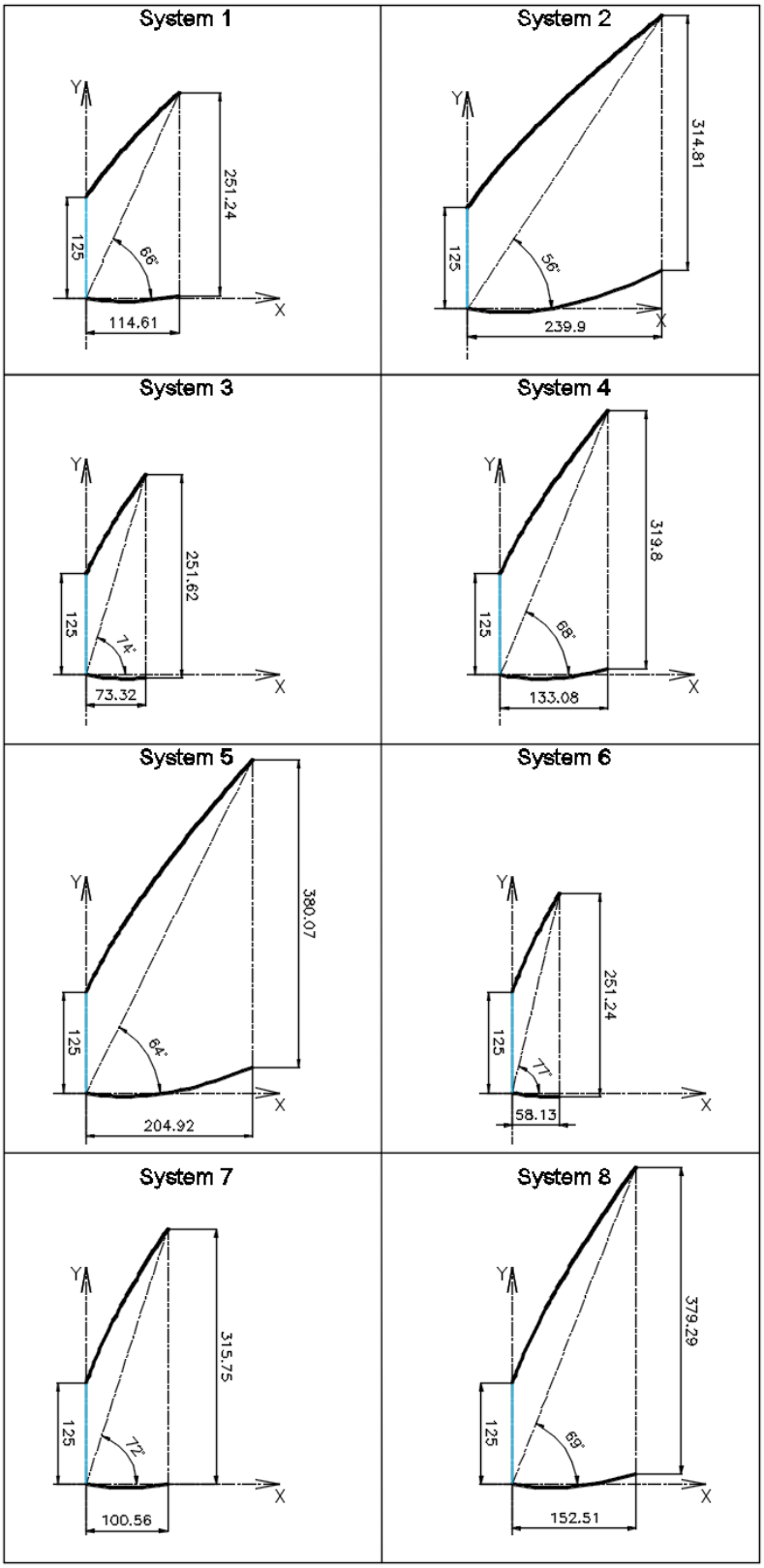

Figure 4. 14 Geometric characteristics of the CPC modelled for Ferrara

4.2.1 Ray tracing simulation

As noted in Chapter 1 (table 1.1), the design objective is to achieve a power output of 100 W at noon for a CPC system installed on a façade in Ferrara, Italy. The simulation parameters used were consistent with those outline in section 4.1.

The results of the eight CPC simulated systems are shown in table 4.5 where all the simulated systems reach 100 W in the summer with different numbers of solar cells. System 8 reached the highest value of electrical production of 102 W and with the lowest number of solar cells (28).

Table 4. 5 Season results from simulation for Ferrara

System	Summer Power (W)	Spring/Autumn Power (W)	Winter Power (W)	Nº Solar cells	Reflector Area (m^2)
1	100.55	205.01	261.50	42	1.51
2	100.71	200.12	253.44	33	7.27
3	101.61	204.09	166.73	42	3.42
4	101.22	202.21	142.60	33	4.66
5	101.70	201.88	122.21	28	5.92
6	100.69	162.49	157.41	41	2.98
7	102.20	175.08	141.68	34	4.04
8	102.66	177.30	120.92	28	4.86

Figure 4.15 shows the power ratio of the eight systems during the seasons. The graph shows that system 8 reached the highest power ratio of more that 2 for summer, spring/autumn, equal to 2.83 and 2.51 respectively, but was almost equal to systems 3 – 7 in winter with values equal to aproximately to 1.31

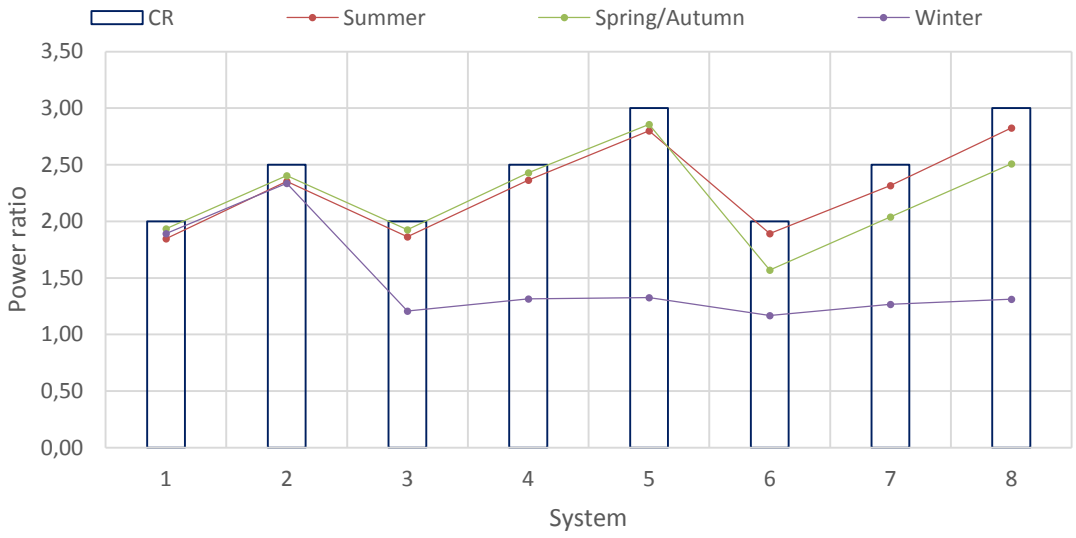

Figure 4. 15 Power ratio for the systems modelled for Ferrara

Finally, System 8 was chosen as the CPC system for manufacture for Ferrara, Italy. Figure 4.16 shows the tracing of the rays for each season. This figure illustrates how the CPC system captures and concentrates solar radiation throughout the year. It can be observed in the summer how the bottom reflector concentrates the solar radiation at the designated focus.

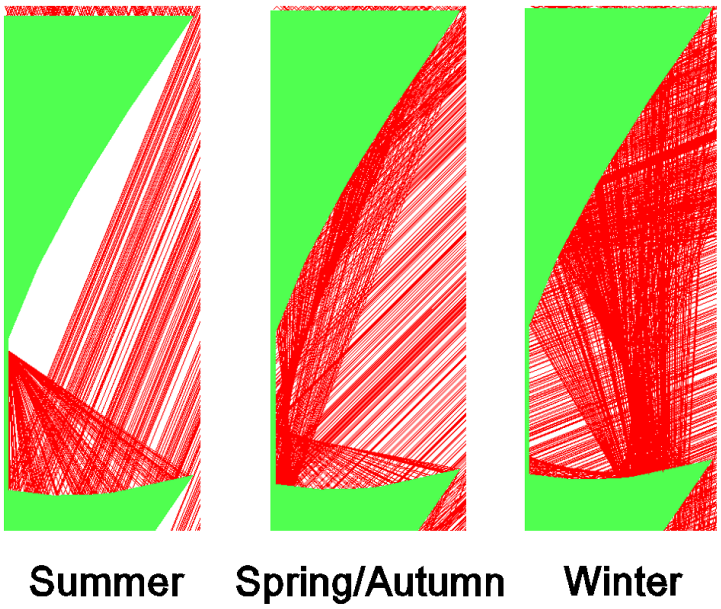

Figure 4. 16 Ray traced for CPC system for Ferrara

Table 4.6 shows the geometric properties of the chosen system, including the acceptance half-angle, absorber dimensions, reflector lengths, aperture size and geometrical concentration ratio. These properties are crucial for understanding the systems design and its ability to effciency concentrate the ray lights onto the solar cells, ultimately influencing the systems performance.

Table 4. 6 Geometrical properties for CPC system for Ferrara

Acceptance -half angle	22º - 69º
Absorber (mm)	125
Length of top Reflector (mm)	378.13
Length of bottom Reflector (mm)	154.57
Aperture (mm)	379.29
Geometrical Concentration Ratio	3

Figure 4.17 shows the schematic design of the CPC system for Ferrara, Italy illustrating the arrangement of the reflectors and the solar cell absorber.

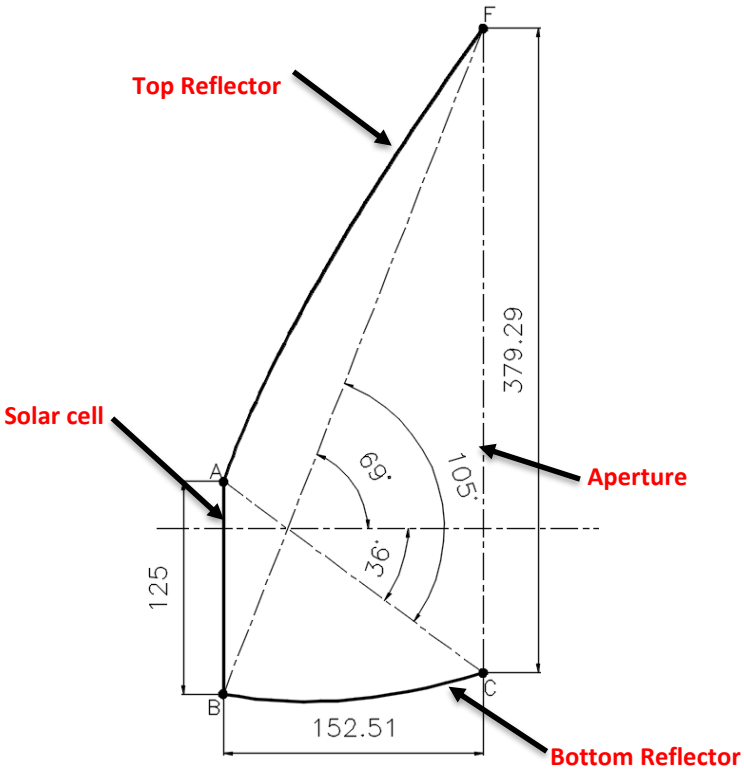

Figure 4. 17 Geometric characteristics of the CPC system for Ferrara

4.2.2 Annual CPC performance

Figure 4.18 shows the annual simulated power production where the selected CPC system performs better than the reference PV system throughout the year by a factor of 2.48 in summer. A reduction in power production to ~ 80 W in June can be observed in the CPC System, where it does not reach the design target of 100 W.

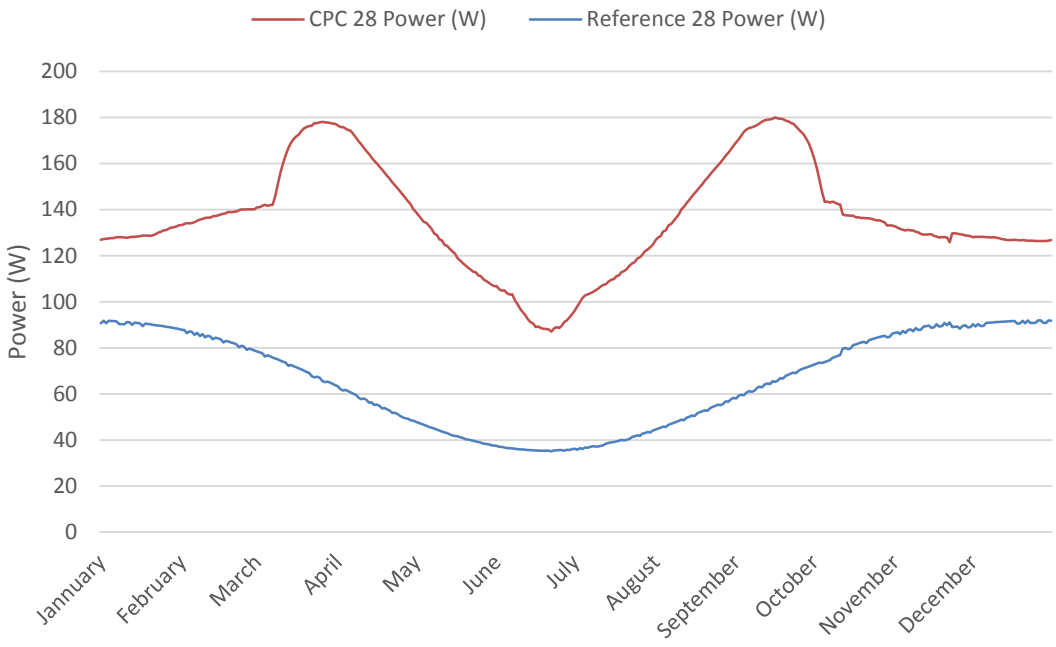

Figure 4. 18 Annual performance for the selected system with 28 solar cells for Ferrara along with the Reference system

To reach the power target of 100 W, four more solar cells were added to the system, thus increasing the total number of solar cells to 32. This new system was simulated, and its annual power production is shown in figure 4.19. From the figure, the 100 W target is reached throughout the year by adding four additional solar cells and the system continues to outperform the reference system throughout the year. Due to these results, system 8 with a concentration ratio of 3, acceptance half angle between 22º and 69º, and 32 solar cells was chosen as the CPC system for demonstration at Ferrara, Italy.

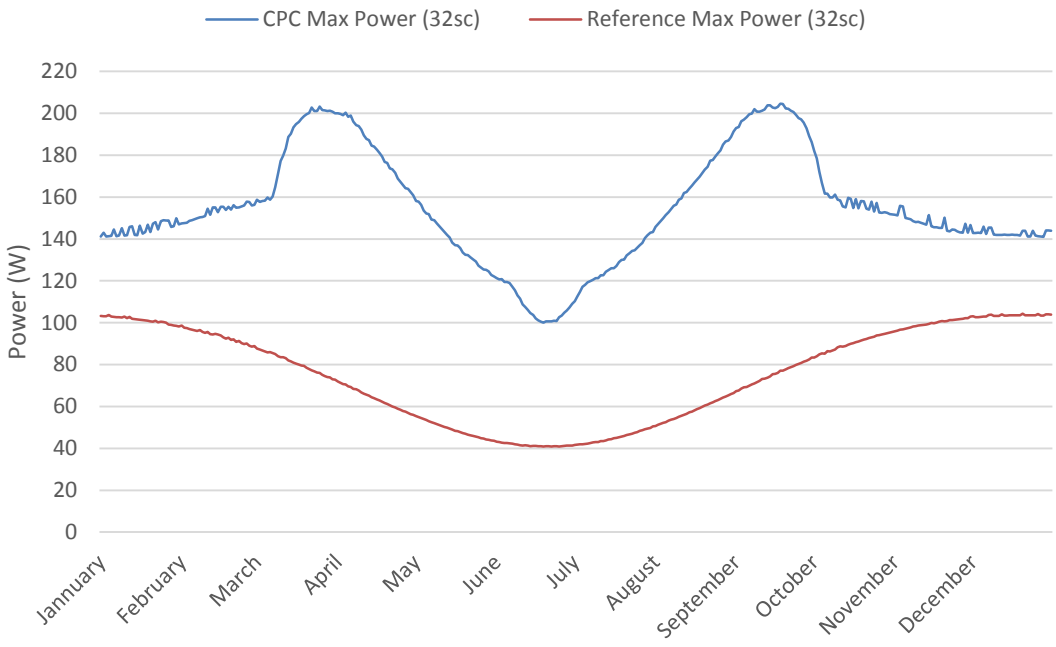

Figure 4. 19 Annual performance for the selected system with 32 solar cells for Ferrara along with the Reference system

4.2.3 Annual CPC performance with correction

The selected CPC system 8 as described in table 4.6 and figure 4.17 was simulated in Trace Pro for one year to determine the hourly power production under global and diffuse radiation AM 1.5 – ASTM G-173 and with a constant 1000 W/m^2 solar radiation (explained in section 4.1.4)

Figure 4.20 shows the annual production power for the CPC and Reference system where the CPC system is better than the Reference system during the year under global and diffuse radiation by a factor of 2.8 in summer. The results show that the CPC system reached the design output power of 100 W at noon throughout the year. As expected, May, June and July (summer) presented lower electricity production compared to the rest of the year, with 121 W in June and 150 W in January. March, April, August, September and October presented the highest values of electrical production (spring/autumn). Under ideal conditions (AM 1.5 – ASTM G-173), the maximum electrical output in summer by the CPC system was 121 W and 43 W for the Reference system.

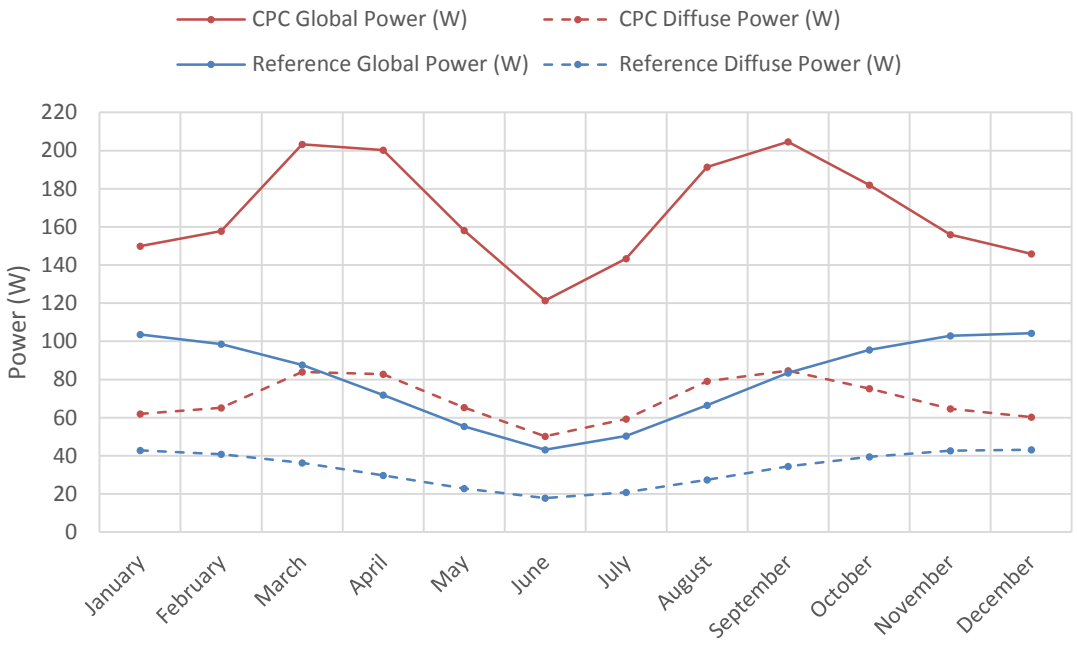

Figure 4. 20 Simulated Annual performance for the CPC and Reference systems under global and diffuse radiation for Ferrara

Figure 4.21 shows the solar cells electrical efficiency of the solar cells in both the CPC and Reference systems. It showed that the efficiency for the CPC system fluctuated between 24 % and 41 % throughout the year, while the Reference system's efficiency ranged from 9 % to 21 %. This might have seemed surprising, given that the solar cell had a nominal efficiency of 22 %. However, it was essential to understand that the efficiency of a solar cell could be influenced by various factors such as temperature, solar radiation intensity, and the angle of incidence of sunlight. In the case of the CPC system, the concentrator design effectively focused the solar radiation onto the solar cells, which led to an increase in the solar cell efficiency beyond its nominal value. This increase was due to the concentration effect resulting from the CPC, which enhanced the overall performance of the solar cells.

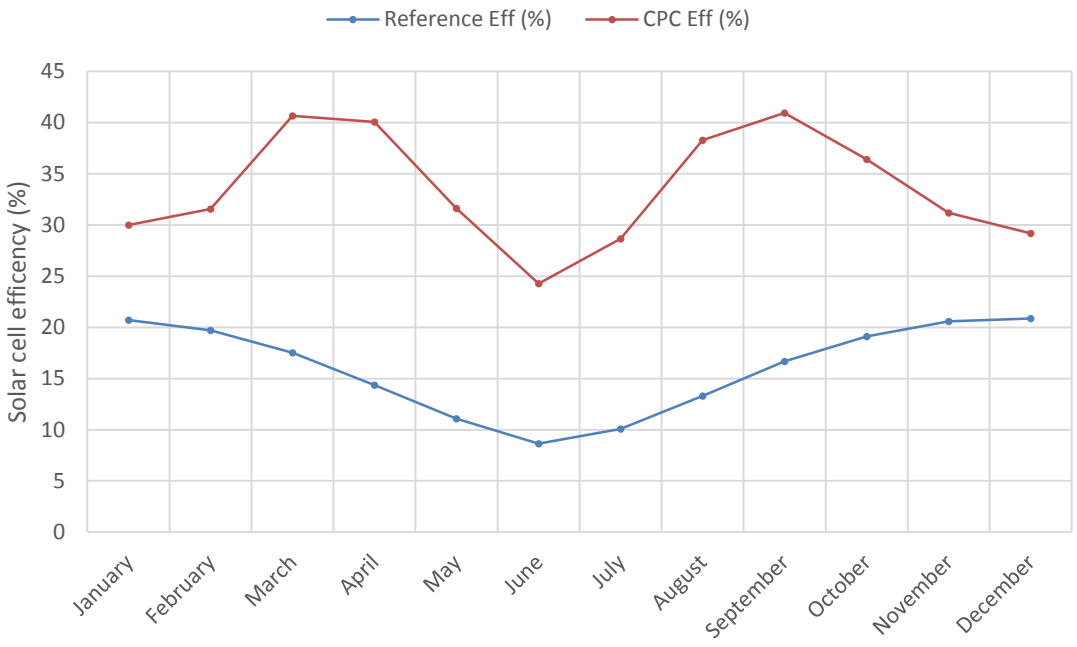

Figure 4. 21 Simulated annual solar cells electrical efficiency for CPC and Reference systems for Ferrara

The CPC power ratio was stable at ~ 2.80 from February to September with the lowest value shown in December and January of 1.42 and 1.52 respectively as it shown figure 4.22. During February to September, solar radiation intensity was generally higher, and the angle of incidence of sunlight was from 40 º - 70º, resulting in the CPC system being more efficient in capturing and concentrating the sunlight onto the solar cells. This led to a higher power ratio during these months. In contrast, during December and January, solar radiation intensity was generally lower due to the winter season, and the angle of incidence of ray lights was from 20º - 30º. These factors made it more challenging for the CPC system to capture and concentrate sunlight effectively, leading to a lower power ratio during these months.

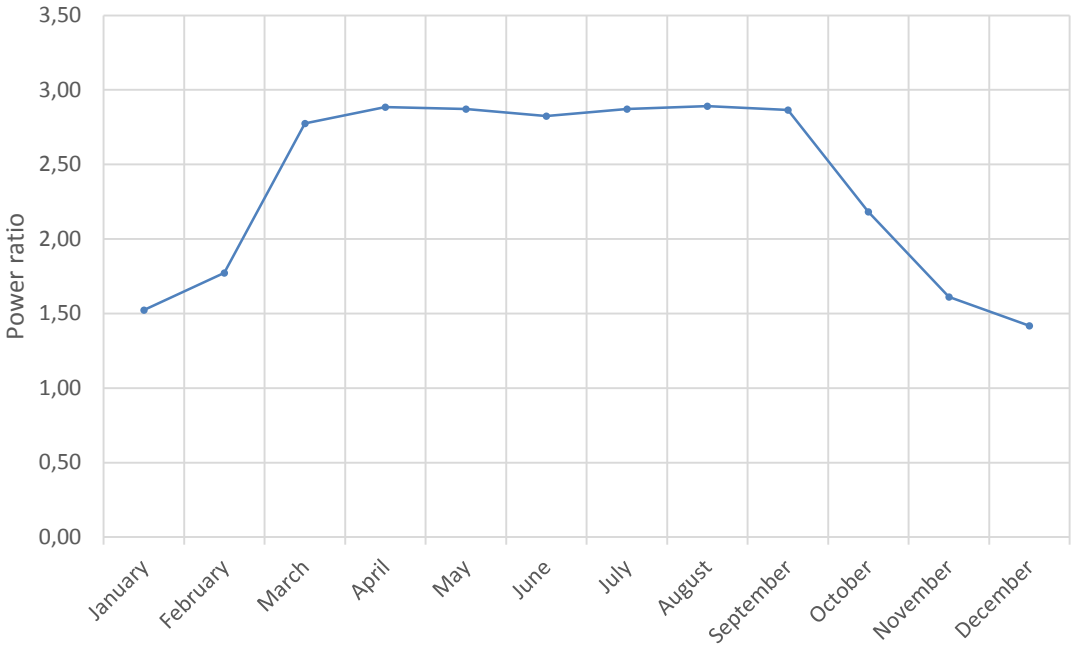

Figure 4. 22 Simulated annual power ratio for the CPC system for Ferrara

Figure 4.23 shows the yearly variation of the optical efficiency, ranging from 28 % to 74 %, with the lowest value occurring in June (summer) and the highest value in April (spring and September). Figure 4.24 illustrates how the optical efficiency reaches its maximum peak of 96 % when the solar incident angles range between 50º and 70º. As anticipated, the optical efficiency was lower outside the acceptance half-angle range (22º - 68º), specifically between 10º and 20º, as well as between 80º and 90º.

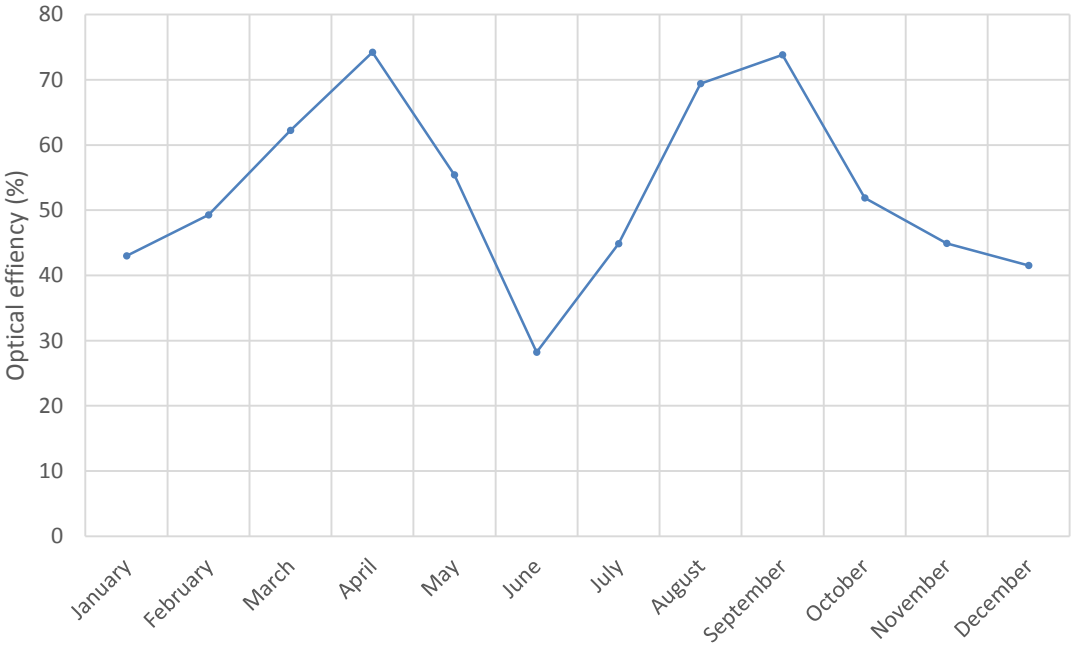

Figure 4. 23 Simulated annual optical efficiency for the CPC system Ferrara

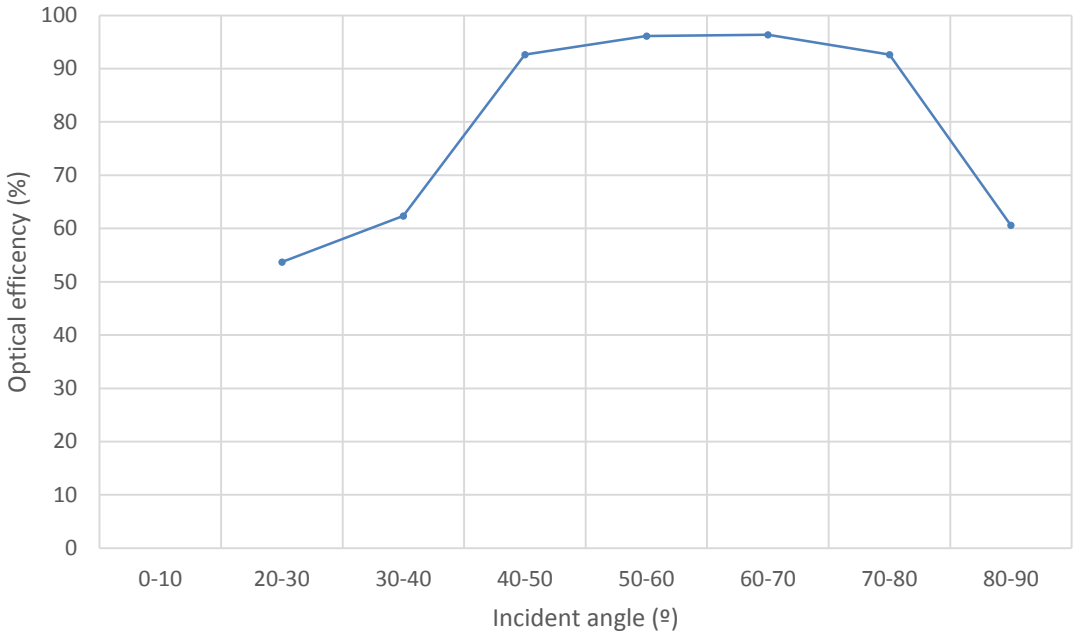

Figure 4. 24 Simulated optical efficiency for the CPC system with incident angle for Ferrara

Figure 4.25 present the annual flux distribution, providing a detailed representation of the concentration of solar radiation, or 'flux', on the solar cells over the year. The flux distribution offered a picture of how sunlight, converted into energy flux, was dispersed across the solar cells in the system as was explained in details in section 4.1.4. It was noted from this figure that during the months from October to February, a significant proportion of direct radiation - sunlight that was not reflected but directly reached the solar cells - was observed. This observation was in consonance with the data shown in Figure 4.20, where these months showed lower electricity production. In the months of May, June, July, and August, the presence of the focal line associated with the second parabola, or the bottom reflector, was prominently visible. This visibility confirmed that during these months, the reflector was functioning as designed, concentrating the sunrays onto the focal line located 10 mm from the edge of the solar cells. The period from March to May and again from September to November highlighted the importance of the top reflector in the overall performance of the Compound Parabolic Concentrator (CPC) system. In these months, the top reflector served to focus additional sunlight onto the solar cells, enhancing the system's performance. This augmented concentration of sunlight led to an increase in electricity production, signifying the advantages of the combined CPC design, which effectively utilized both the top and bottom reflectors.

The observed non-uniformity in the flux distribution at various Y-positions, as seen in these figures, was a direct result of the system's asymmetrical design. The inherent asymmetry of the CPC system led to an uneven concentration of solar radiation across the solar cells, with certain areas receiving a more substantial proportion of the flux. Despite these disparities,

the system was found to function effectively, and the performance trends and flux distribution patterns provided valuable insights into the complex dynamics of the CPC design.

As alluded to in Section 4.1.4, the diagrams were generated with a lower pixel quality, due to the limitations of the laptop's processing capabilities that was used for the simulation. Regardless of these computational restrictions, these visual representations provided crucial insights into the functional behavior and performance characteristics of the CPC system.

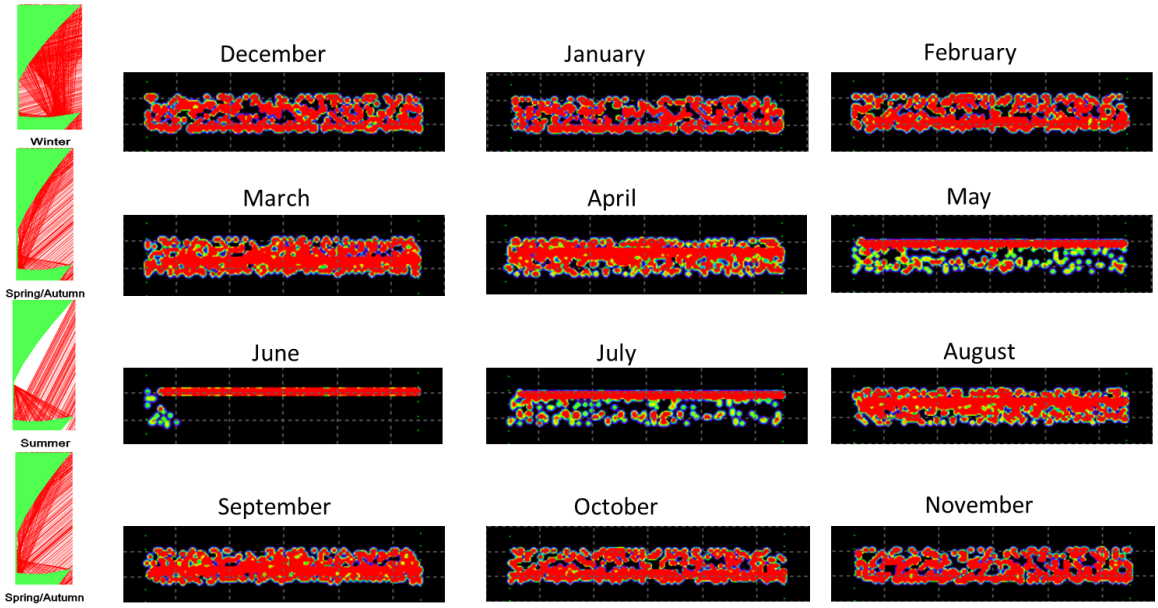

Figure 4. 25 Flux distribution obtained from simulation in a string of eight solar cells on the 21st of each month for Ferrara CPC system

As was mentioned in section 4.1.4, high-intensity peaks of solar radiation have considerable implications for the electrical performance of solar cells. Intense peaks may generate more electricity due to enhanced photon absorption, which, in turn, leads to increased electron-hole pair creation, subsequently resulting in a higher current. Nonetheless, overly intense peaks could provoke overheating, inducing thermal stress and efficiency losses due to the temperature-sensitive nature of solar cell performance.

Regrettably, due to software limitations during the simulation of the CPC system, the effects of high-intensity peaks were not incorporated into the model. The software did not provide functionalities for integrating thermal impacts or for simulating the influences of temperature fluctuations on solar cells. Therefore, the model primarily focused on solar radiation collection and absorption, without taking potential thermal effects and stress induced by high-intensity peaks into account. Despite yielding valuable insights into the fundamental operations and expected performance of the CPC system under idealized conditions, it is important to recognize the divergence between these simulations and real-world conditions.

4.3 Conclusion

A comprehensive analysis of the optical performance and acceptance half-angle for two CPC system in Mayo, Ireland and Ferrara, Italy led to the following conclusions summarized in table 4.7.

Table 4. 7 Summary of simulation conclusions

Parameter	Mayo, Ireland	Ferrara, Italy
Acceptance half angle	12° - 63°	22° - 68°
Concentration ratio	3	3
Solar cells	24	32
Target power (100 W) achieved	Yes	Yes
Maximum summer electrical output (CPC)	126 W	121 W
Maximum summer electrical output (Ref)	45 W	43 W
Solar cell efficiency (CPC)	28% - 49%	24% - 41%
Solar cell efficiency (Ref)	12% - 22%	9% - 21%
Stable CPC power ratio	2.82 (Feb - Sep)	~2.80 (Feb - Sep)
Lowest CPC power ratio	1.29 (Dec) & 1.40 (Jan)	1.42 (Dec) & 1.52 (Jan)
Optical efficiency (CPC)	34 % - 70 %	28 % - 74 %

The findings from the simulation for the two CPC systems served as a foundation for the development of a small-prototype in the next chapter. The insights gained from this analysis was used to optimize the design, materials and manufacturing process for the prototype. Additionally, the performance data was employed to create a set of criteria for assessing prototypes efficiency.

Chapter 5 Small scale prototype

Following the optical analysis of the CPC system described in Chapter 4, small scale prototype CPC systems for Ferrara and Mayo with Reference systems were designed, manufactured and characterized in order to compare the results prior to the large-scale manufacture of 100 W. The operating parameters used for the investigation of this test were: power, power ratio, solar cell temperature and efficiencies as defined in section 2.1. The manufacturing process and outdoor characterization were carried out at Civil Engineering department at Trinity College Dublin, Ireland. The CPCs were composed of a solar cell, reflector, reflector supports, thermocouples, aperture cover and frame. The materials selection, design and fabrication for each component of the CPC system are described in section 5.1 and the outdoor characterization are presented in section 5.2.

5.1 Design and manufacturing of small prototype CPC system

Two small prototypes with 3 solar cells were designed, built and assembled in order to carry out a preliminary-test before their 100 W system was manufactured. All the parts were manufactured in the workshop of the Civil Engineering department at Trinity College Dublin. The final design for the small CPC prototype for Ferrara and Mayo are shown in figures 5.1 (a) and (b) respectively with each component explained in the following subsections.

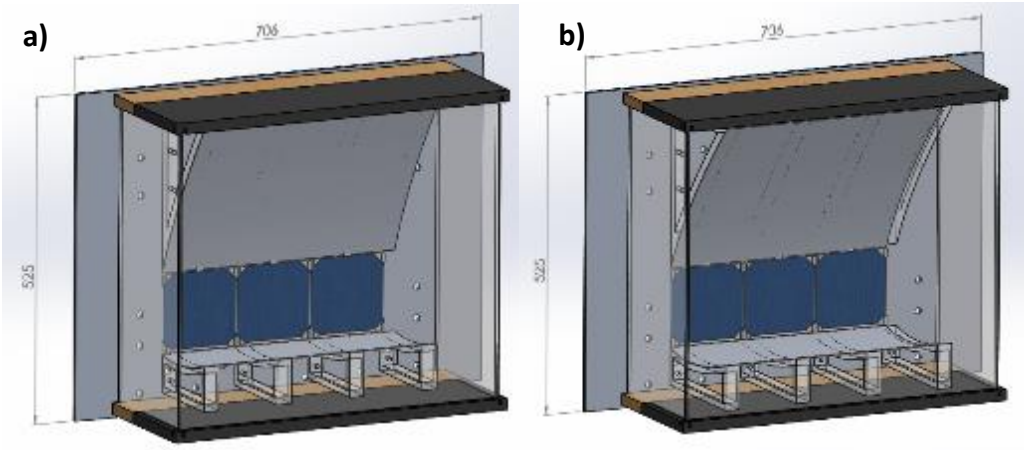

Figure 5. 1 Design CPC system small prototypes (a) CPC system Ferrara (b) CPC system Mayo

A Reference system was also designed as a crucial component for the comparative analysis of the CPC systems. It had the same area as the respective CPC system, but crucially, it lacked the concentrator elements. It was composed of the same type and arrangement of solar cells used in the CPC system, which were directly exposed to incident solar radiation without any concentration. The purpose of the Reference system was to offer a baseline performance, or a benchmark, against which the performance enhancement achieved by the CPC systems could be accurately assessed. This system provided a 'control' scenario, representing the performance of the solar cells under direct sun exposure, without any solar concentration (also explained in Chapter 4). The design, manufacturing, and characterization of the Reference system followed procedures similar to those for the CPC systems, ensuring a

consistent and fair basis for the comparative analysis. This approach enabled an accurate evaluation of the additional benefits offered by the CPC design, such as increased solar radiation concentration and, consequently, higher power output.

5.1.1 Reflective material employed for CPC system

Five different reflectors were tested to select the one with the highest reflectivity. The mirror reflectors were an aluminum foil (Easygrow), Miro 7 & Miro Sun (Alanod), self-adhesive Spectacular Film DF2000MA (3M), and Optical Lighting Film 2405 (OLF) (3M). For the reflectivity measurements, a Labsphere integrated sphere was used with ocean optics light source as was described in section 3.4. The five samples are shown in figure 5.2 (a-e). Their reflectivity is shown in figure 5.3 (a-e).

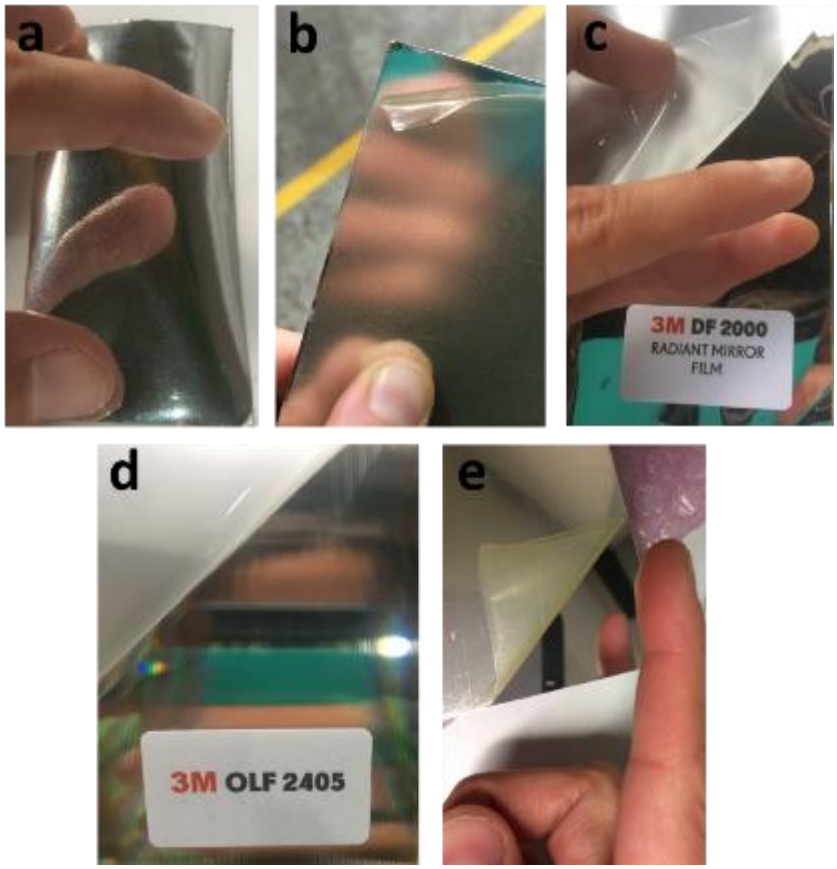

Figure 5. 2 Pieces tested for reflectivity
(a)Aluminium foil (b) Miro 7 (c) 3M DF 2000 (d) 3M OLF 2405 (e) Miro Sun

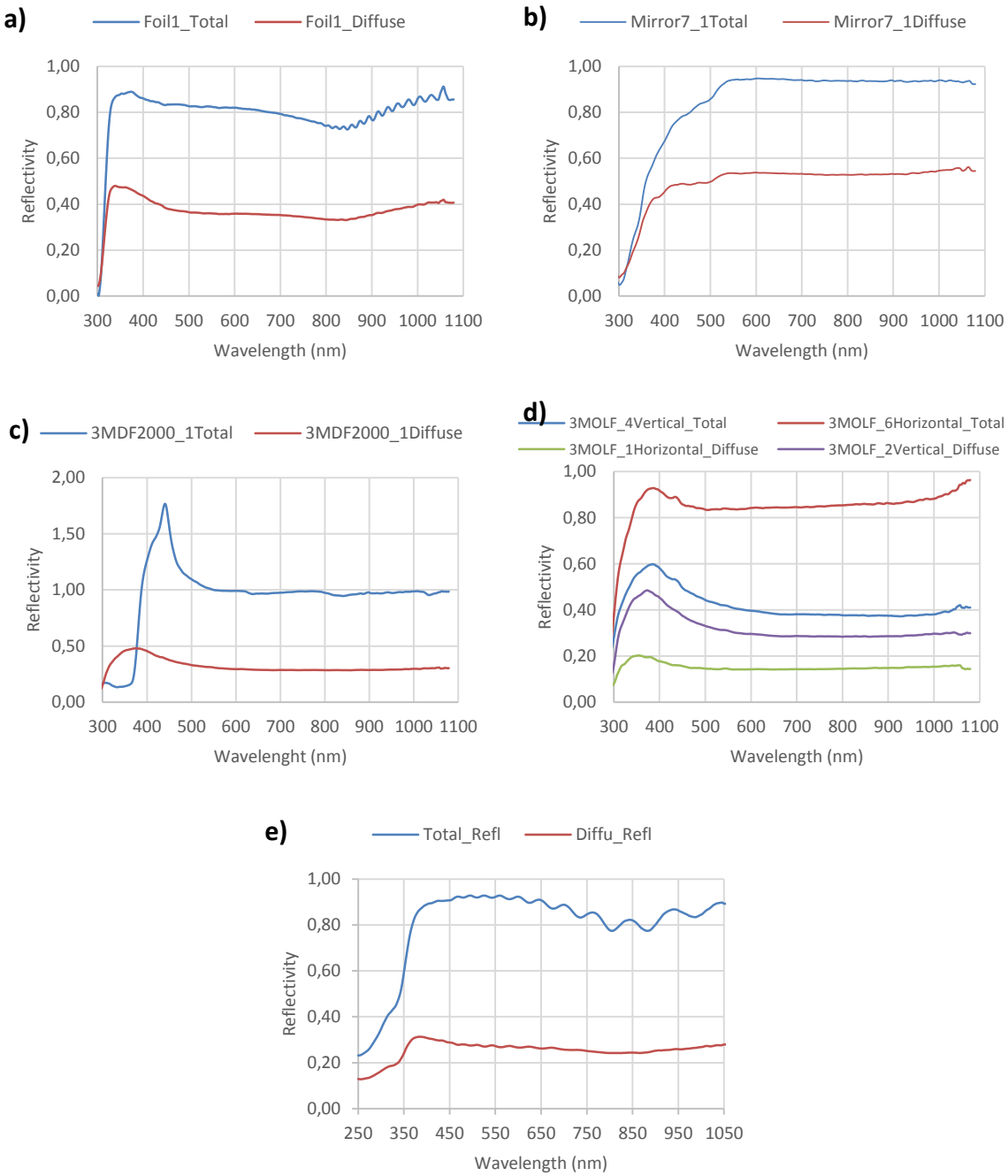

Figure 5. 3 Reflectivity results
(a) Aluminum Foil (b) Miro 7 (c) 3M DF 2000 (d) 3M OLF 2405 (e) Miro Sun

After comparing the results of reflectivity for each material, Miro Sun weather proof sheet (Alanod) with an average reflectivity of 0.98 and 0.5mm thickness was chosen as the reflector for the CPC system.

5.1.2 Design and material selection for reflector support and solar cell holders

The material selected for the backplate was aluminum due to its low weight, good thermal conductivity and low cost. The thermal conductivity for the aluminum and copper are 202

W/mk (at 0 ºC) and 206 W/mk (100 ºC) (Wu,2009), and this provided heat dissipation to reduce the solar cell temperature and helped to improve the electrical output.

Two reflector supports for the top and bottom reflector were designed and manufactured using 3D printers and PLA (Polylactic acid) filament of Ø1.74 mm. The supports were 25 mm thickness to provide strength to the bond and bending surface. For each reflector, four pieces were designed using Solidworks and those designs were transferred to the four 3D printers as described in section 3. For ease of assembly, each reflector was fixed to the back plate using two screws (M6XØ11mm). Figure 5.4 presents a 3D printed top reflector.

Figure 5. 4 A 3D printed Top reflector for Ferrara prototype

In order to attach solar cells in the CPC systems, a holder was designed and printed using 3D printers. ABS (Acrylonitrile Butadiene Styrene) was selected for its good thermal resistance and softening temperature as was described in section 3.6. The external dimensions of the solar cell holder were 126 X 120 mm and 1 mm thickness and each holder contained small slots so that the solar cell could be easily installed. The base frame is 20 mm wide so that the holder does not completely cover the back of the solar cell, providing sufficient insulation to avoid short circuits with the backplate but at the same time giving sufficient space to provide heat transfer and avoid overheating of the cells. Two holes of Ø7 mm were added in order to fix the solar cell holder to the backplate using screws. The detailed design of the solar cell holder is shown in figure 5.5.

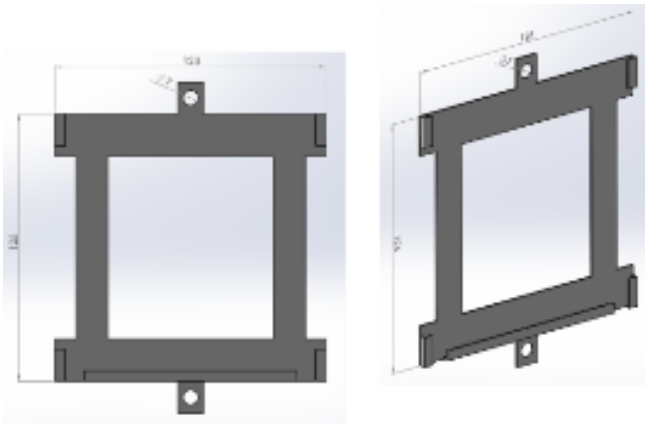

Figure 5. 5 Detail design of the solar cell holder in Solidworks

5.1.3 Design and material selection for backplate

In order to provide the base for the solar cell, a back plate was designed from aluminum with 6mm thickness. The dimensions of the back plate were 706 X 525 mm and forty-six holes of Ø11 mm were machined to fix the support reflectors and frame. The detailed design of the aluminum back plate is shown in figure 5.6. The final assembly of the reflectors and solar cell holders on the backplate is shown in figure 5.7.

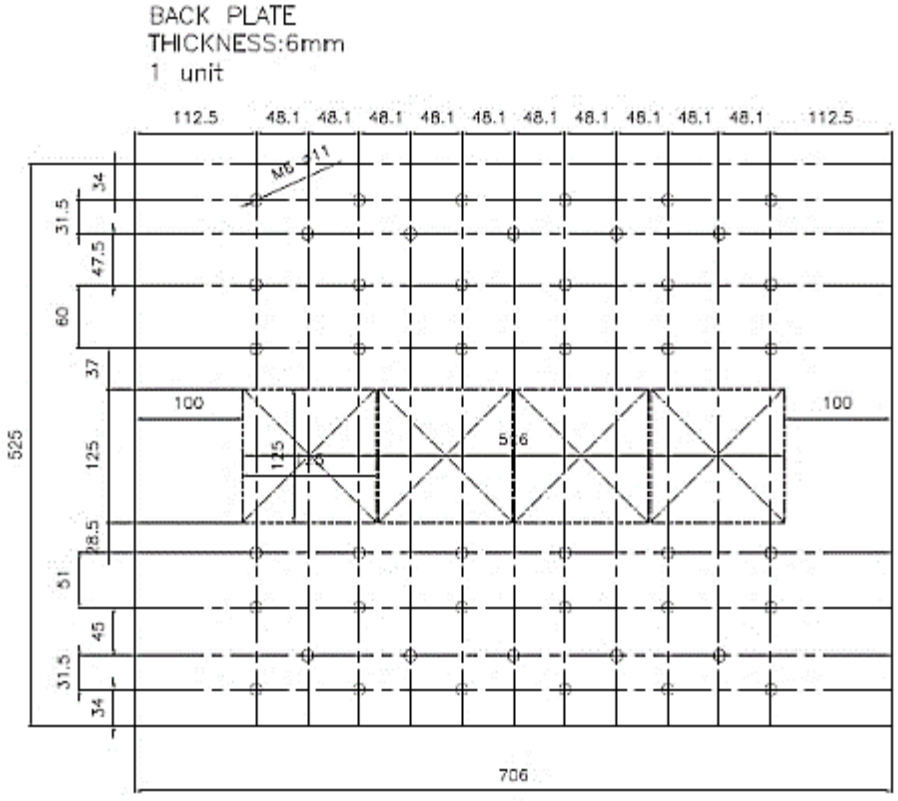

Figure 5. 6 Detail design of aluminium back plate in Autocad

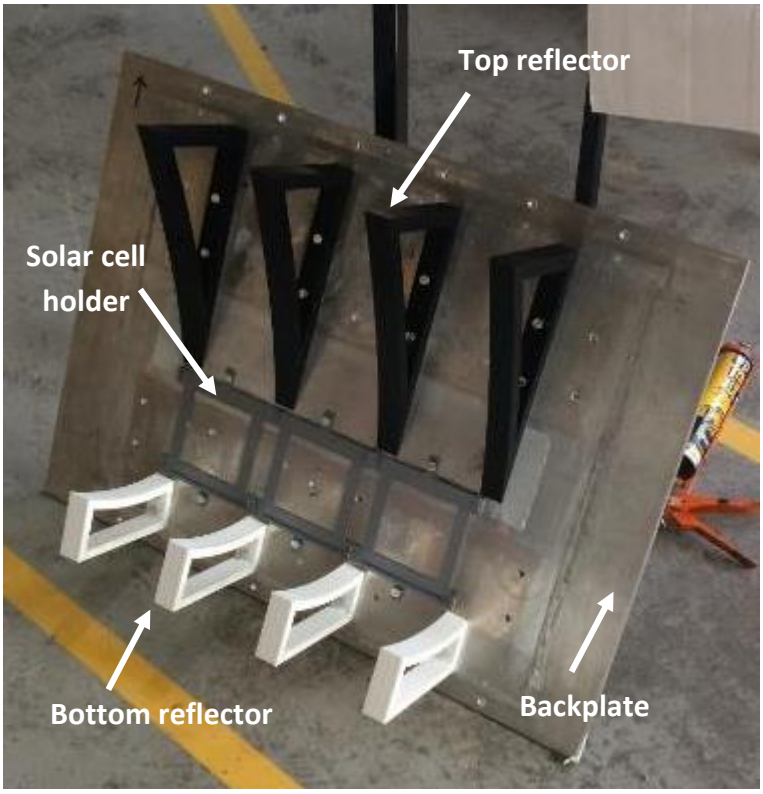

Figure 5. 7 Assembly of the reflectors and solar cell holders on the backplate

5.1.4 Reflector fabrication process

In order to achieve the desired parabolic shape for the reflectors, the 1.5 mm thick aluminum sheets were first cut into two pieces, ensuring the appropriate dimensions for forming the parabolic shape. Each piece was then compressed and rolled using a roller machine (as shown in figure 5.8) to gradually bend and shape the aluminum into the required parabolic curve. To test whether the aluminum pieces had achieved the perfect parabolic shape, the curved pieces were placed onto the printed support reflectors. The aluminum sheets should conform to the same parabolic shape as the support reflectors. This was verified by visually inspecting the fit between the aluminum sheets and the support reflector, ensuring that there were no gaps or deviations from the desired parabolic profile. If any inconsistencies were identified during the testing phase, adjustments could be made by carefully rolling the aluminum pieces again using the roller machine until the desired parabolic shape was achieved. Once the aluminum sheets match the parabolic shape of the support reflectors they could be secured in place using screws. Figure 5.8 shows the aluminum pieces of the required parabolic shapes and the roller used.

Figure 5. 8 Roller used for parabolic shape and parabolic bent pieces

After the location and fixation of the reflector supports, wood screws Ø 5 mm and 15 mm long were used. Countersink holes were made in each plate so that the head of each screw was at the root of the auxiliary plate, achieving a perfect smooth surface for the further location of the reflector. The protective sheet was removed from the auxiliary plate and was cleaned of steel debris produced during the drilling process. Figure 5.9 shows the final installation of the reflector supports with the auxiliary plate.

Figure 5. 9 Auxiliary plates installed on the reflector support

Each reflector support block with auxiliary plate was deeply sanded and cleaned before the Alanod reflector was glued. Due to the high temperatures being expected in the reflector (80 ºC), Fast-Fix High Temperature 120 ºC was used as it is an exceptionally strong aerosol spray adhesive specially formulated to withstand exposure to high temperatures (more than 100 ºC). First, the auxiliary sheet and the back of the Alanod reflector were sprayed with Fast-Fix super glue spray, then it was allowed to dry for approximately 2 minutes. After drying, the Alanod reflector was placed on the auxiliary plate and strong pressure was applied. Finally, traces of glue were removed from the block and left to dry for future final installation. The gluing process is shown in figure 5.10 and the reflector blocks corresponding to a CPC System are shown in figure 5.11.

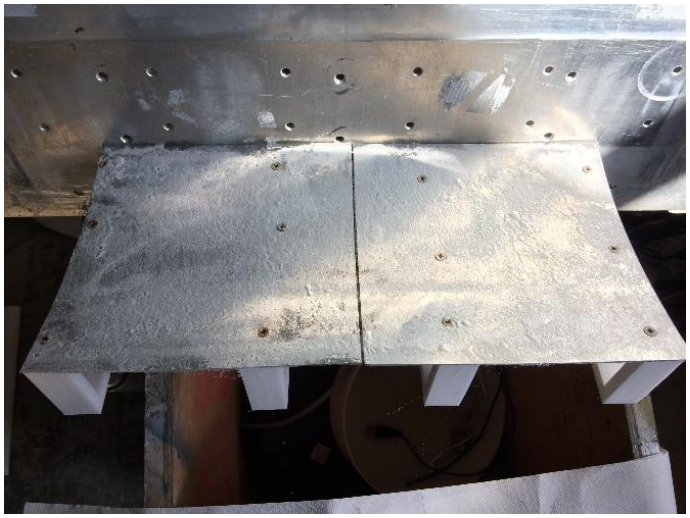

Figure 5. 10 Gluing process for small CPC systems

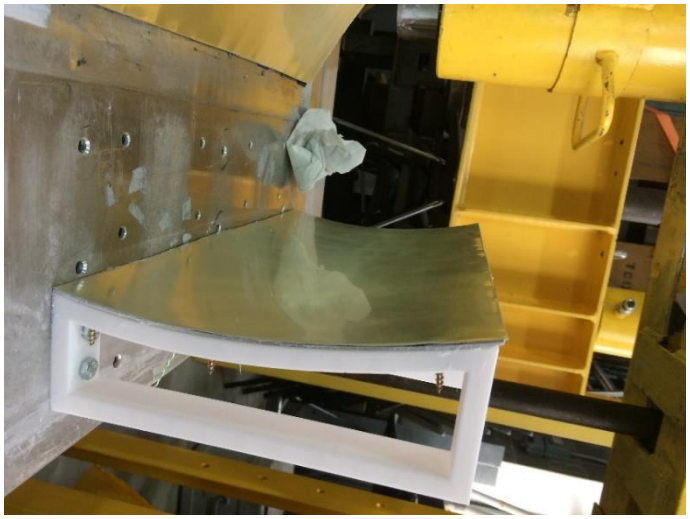

Figure 5. 11 A full reflector support, auxiliary plate and Alanod reflector assembled

5.1.5 Design and material selection for the cover and frame

Table 5.1 provides an overview of different material options and their advantages and disadvantages for the designs criteria of aperture cover, side cover and frame structure. The final decision on material was based on the specific requirements and constraints of the project, as well as a balance between performance, durability, cost and ease fabrication.

Table 5. 1 Material options for cover and frame for CPC system

Design Criteria	Material Option	Advantages	Disadvantages
Aperture Cover	Low Iron Glass	High solar transmittance, low absorption, increased efficiency	Fragile, heavy, higher cost
	Perspex	Lightweight, durable, lower cost	Lower solar transmittance, potential shading of solar cells
Side Cover	Perspex	Lightweight, durable, lower cost	Lower solar transmittance
	Glass	High solar transmittance, increased efficiency	Fragile, heavy, higher cost, potential shading of solar cells
Frame Structure	Wood	Easy to work with, good insulation, affordable	Susceptible to moisture, less durable
	Metal	Durable, strong, can provide structural support	Conducts heat, may be heavier, higher cost
	Plastic	Lightweight, affordable, resistant to moisture	Less strong, may deform under high temperatures

Low iron glass (NSG Group) of 4 mm thickness, dimensions of 457 X 556 mm, solar transmittance of 0.91, normal emissivity of 0.89 was used as a protective aperture cover for the CPC. Low iron glass is commonly used in solar applications as it absorbs less incident solar energy. This means that low iron glass allows a higher percentage of the incoming solar radiation to pass through it, instead of being absorbed by the glass material. This property makes low iron glass an ideal choice for solar applications, as it maximizes the amount of solar radiation reaching the solar cells, thereby increasing their efficiency.

For the side cover, two Perspex sheets of 5 mm thickness and dimensions of 140 X 457 mm was used in order to avoid shading the solar cells. The decision to use low iron glass for the protective cover and Perspex sheets for the side cover was based on a balance of material properties and practical considerations. Low iron glass offers higher solar transmittance and lower absorption, but it is generally heavier and more fragile than Perspex. On the other hand, Perspex is lighter and more durable, but it may have a lower solar transmittance compared to low iron glass. Using Perspex for the side covers helped to reduce the overall weight and improve the durability of the system while avoiding shading of the solar cells. However, the use of Perspex could potentially have influenced the thermal performance of the system. Specifically, the material characteristics of Perspex could potentially contribute to a

greenhouse effect within the CPC system. Perspex, being a type of acrylic plastic, can potentially trap heat within the system, leading to an increase in temperature. This phenomenon, similar to the greenhouse effect observed in the Earth's atmosphere, could potentially cause the CPC system to warm up more than it would have with a different type of material used for the side covers. Such warming could potentially have implications for the performance of the solar cells within the CPC system. Solar cells are known to have a negative temperature coefficient, meaning their efficiency tends to decrease as their temperature increases. If the Perspex side covers led to a significant increase in the temperature within the CPC system, this could potentially have caused a decrease in the overall performance of the solar cells.

Wood was chosen as the frame structure for its ease of workability, availability and affordability. Wood can be easy machined, cut and drilled to create the necessary slots and structure for the CPC. Additionally, wood provides good insulation and does not conduct heat, which can help in maintaining the temperature stability of the system. Two pieces of wood of 18 mm thickness were selected. The dimensions of the frame structure were 154 X 576 mm. Two slots of 9 mm and 4 mm were machined in order to allow the Perspex sheets and the low iron glass to be easily removed and assembled. The detailed design of the frame structure is shown in figure 5.12.

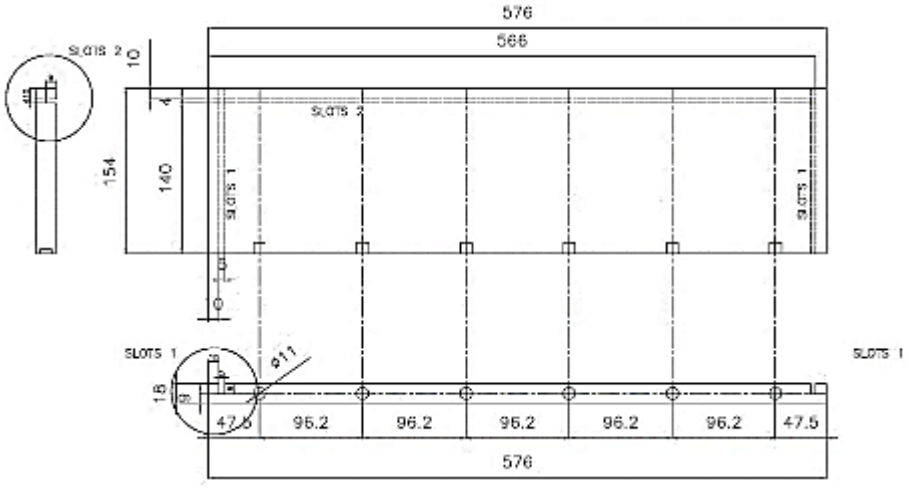

Figure 5. 12 Detailed design of the frame structure in Autocad

5.1.6 Solar cell selection and interconnection

Back contact monocrystalline silicon solar cells (SunPower), 125 mm^2 were selected for the prototypes and the details were presented in section 3.7.

This solar cells were selected for the CPC for several reasons:

- With an efficiency of 22 %, these solar cell can convert a significant portion of the incident solar radiation into electricity. This high efficiency leads to more power output per unit area compared to other solar cell technologies.
- The back contact solar cells have both positive and negative contacts on the rear side of the cell. This design eliminates the need for front gridlines reducing shading losses and improving the aesthetics of the solar panel.

- Monocrystalline silicon solar cells are known for their high efficiency, long term stability and reliable performance.
- The size 125 x125 mm make them suitable for integration with CPC system.
- Easy interconnection using dog bones. These connectors streamline the assembly by simplifying the interconnection between the solar cell.

The interconnection process of the solar cells followed the same procedure described in section 3.6. An experimental test for SunPower solar cells was undertaken using a ORIEL Sol3A Class AAA Solar Simulator. Solar module analyzer was used to determine IV from the test and pyranometer connected to voltmeter was used to measure the solar radiation. The details of devices used were presented in section 3.5. Figure 5.13 shows a schematic diagram for the experiment and figure 5.14 presents the view of the SunPower solar cell under test conditions.

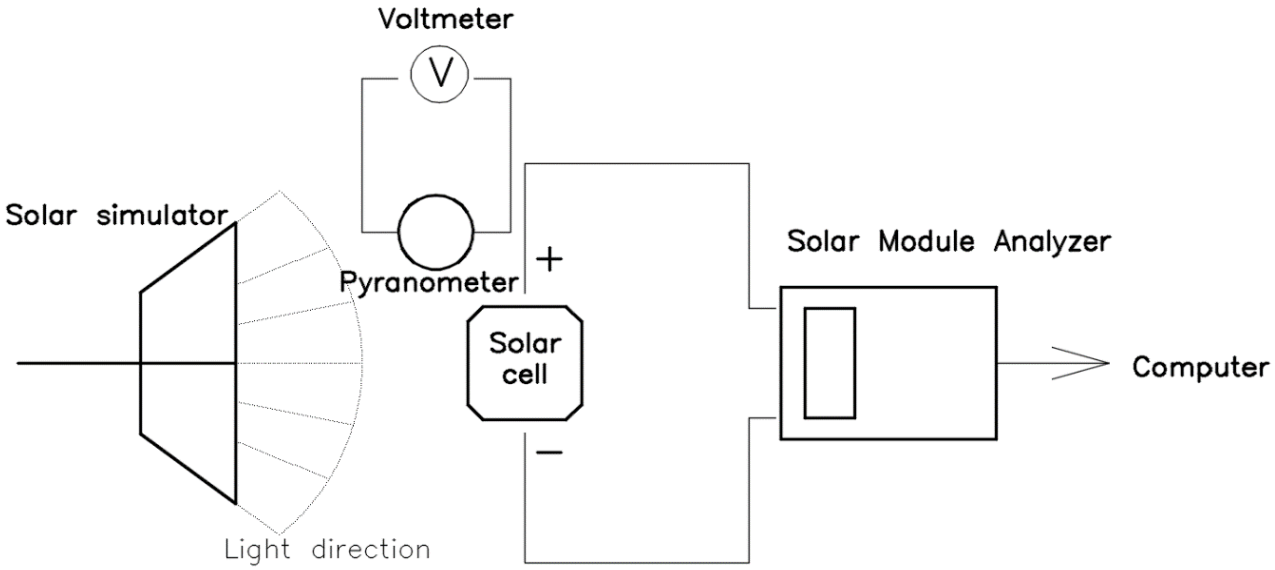

Figure 5. 13 Schematic diagram for SunPower characterization

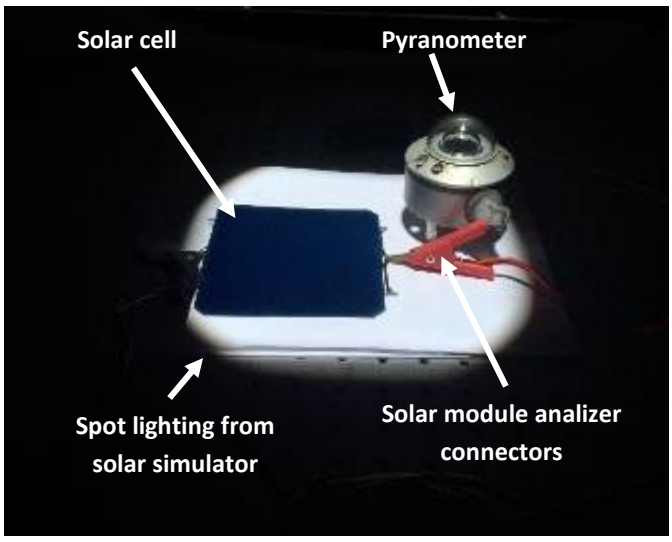

Figure 5. 14 Experimental characterization of a full size SunPower solar cell

The test was carried out for one full size SunPower solar cell at a solar radiation intensity of 900 W/m^2 and ambient room temperature of 21 ºC. The radiation was perpendicular to the solar cell. Measured solar cell I-V is presented in figure 5.15 where it is shown that at 900 W/m^2, the short circuit current and open circuit voltage were 5.81 A and 6.76 V respectively. Maximum power achieved was 3.03 W and 22 % efficiency. Experiment test results showed that the SunPower solar cells performance very close to the manufacturers specifications, with only slight deviations in open circuit voltage and short circuit current. This indicated that the solar cell should deliver the expected performance in the CPC system, making it a suitable choice for the application.

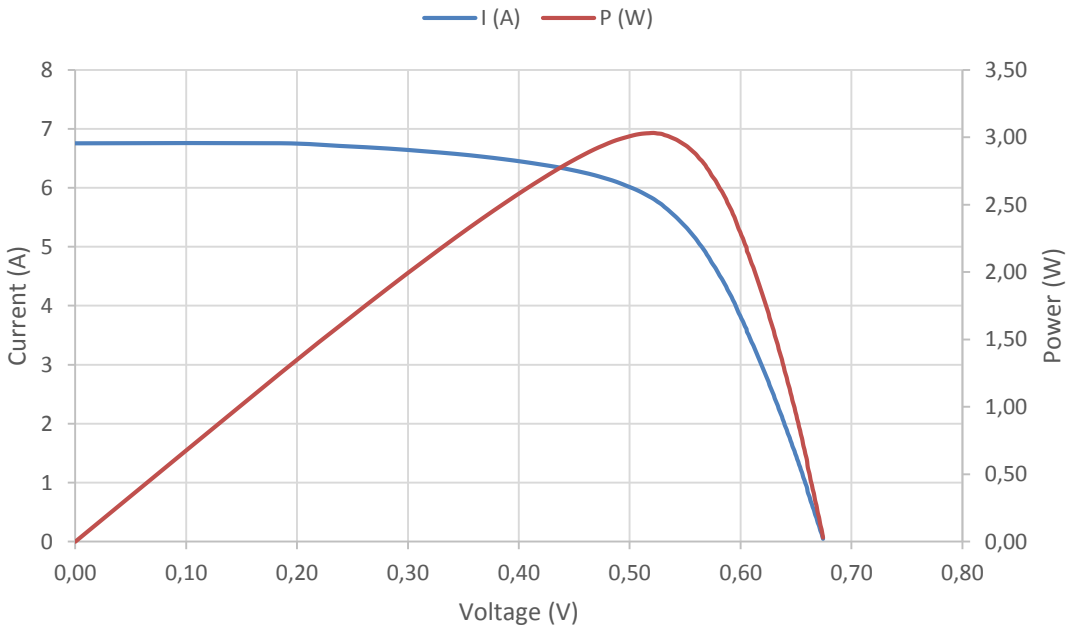

Figure 5. 15 IV Curve for a SunPower solar cell under 900 W/m^2

This test was instrumental in establishing several important conclusions:

- Manufacturer's Specifications Verification: The results demonstrated that the SunPower solar cells performed very closely to the manufacturer's specifications, validating the manufacturer's stated efficiency of 22%, open circuit voltage of 0.582 V, and short circuit current of 6 A under specific conditions. Slight deviations in open circuit voltage and short circuit current are typically due to real-world factors and are generally expected.

- Performance Under Standardized Conditions: With a solar radiation intensity of 900 W/m^2 and ambient room temperature of 21 °C, the test provided important data on the cell's performance under a set of specific conditions that may be similar to certain real-world scenarios. The 22% efficiency achieved confirmed that the solar cell could deliver the expected performance under these conditions.

- Suitability of the Solar Cell for the CPC System: The results indicated that the solar cell should deliver the expected performance in the CPC system. This is crucial because it confirmed the cell's suitability for integration within a CPC system, which could improve the overall solar energy capture and conversion process.

- Baseline Performance Metrics: The test results also serve as a baseline for comparison against future tests under varying conditions, such as different solar radiation intensities, angles of incidence, or operating temperatures.

In essence, this test provided a crucial validation of the manufacturer's specifications under certain conditions, and it confirmed the solar cell's suitability for use in the CPC system.

5.1.7 Thermocouple selection and characterization

Twenty “K” type thermocouples were used for thermal analysis of the CPC and Reference systems. All thermocouples were previously tested using the Column Heater Beckman. The thermocouples and their characterization was described in section 3.5. Results showed a maximum measured deviation of ±0.4 °C compared with a Thermometer HD 2307.0 RTD. The thermocouple distribution in each system is presented in table 5.2.

Table 5. 2 Thermocouples location

System	String Solar Cell	Back plate	System Internal	Reflectors	Total
CPC	3	3	1	6	13
PV	3	3	1	-	7

5.1.8 Electric circuit, solar sensor and data collection

An electric circuit was designed for the 3-string solar cells for outdoor characterization. Two electric circuits with the same characteristics were used to collect current and voltage for the CPC and Reference systems independently. A resistor of 0.5 ohms with maximum power of 15 W was used for each circuit. In order to avoid high current, a RS 257-408 shunt with a conversion factor of 20 A - 200 mV was connected in series and from this connected to data logger. The final circuit is represented in figure 5.16.

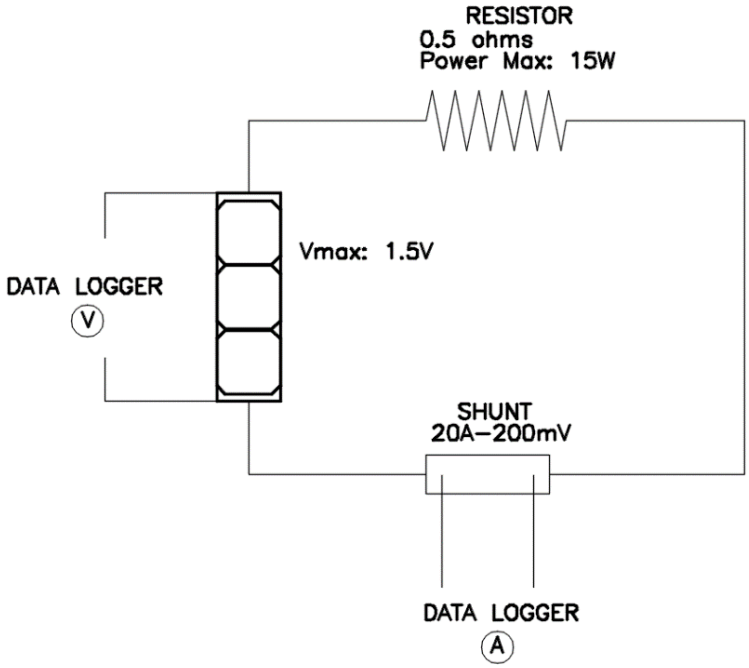

Figure 5. 16 Electric circuit forming the monitoring system

Solar radiation was measured using a pyranometer (Kipp & Zonen) and recorded on a data logger (Agilent 3472A LXI) as described in section 3.4.

5.1.9 Laser verification experiment

To verify the reliability of the optical performance, a laser verification test was performed. The experiment mainly included two laser transmitters (purple and green), an angle regulator, and a smoke machine. The angle regulator is a device used to adjust the angle of incident of the lasers to specific values, ensuring that the lasers are directed accurately towards the reflectors during the experiments. The open Ferrara CPC system is shown in figure 5.17 (a) and the experiment with lasers in figure 5.17 (b). The green laser was calibrated at 57 º (for the top reflector) and 61 º (for the bottom reflector). To calibrate the lasers at these angles, the angle regulator was adjusted to the desired angle for each laser. Both incident angles correspond to spring in Italy. The smoke machine made the direction of the lasers visible which enabled the reflection and the final point in the absorber to be seen. From the green laser (top reflector), the point of impact on the reflector was at A and on the absorber at A1. From the purple laser (bottom reflector), the point of impact on the reflector was B and on the absorber B1. Point B1 corresponds to the focal line of the bottom reflector (~>10 mm from the edge of the solar cells).

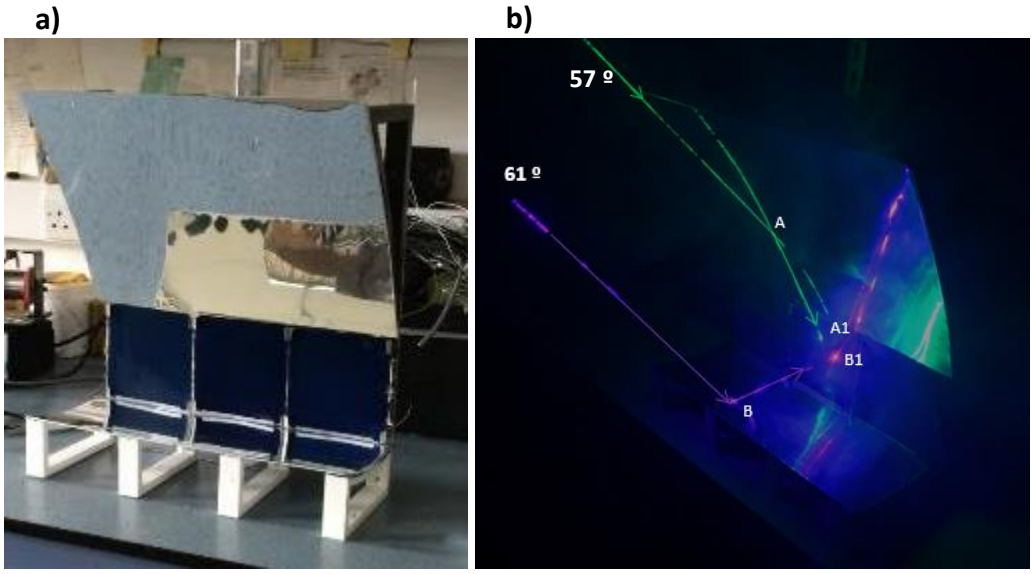

Figure 5. 17 Laser reflection experiment
(a) Small prototype CPC system Ferrara (b) Laser reflection

Comparing the end points of the laser experiment in the solar cell (A1 and B1) and flux distribution describe in section 4.2.3, it was possible to conclude that there was an acceptable result corresponding to the reflection angles.

5.1.10 Final CPC small prototype for Ferrara, Italy and Mayo, Ireland

In order to develop the CPC system for Ferrara and Mayo, the system components were assembled as shown in figure 5.18.

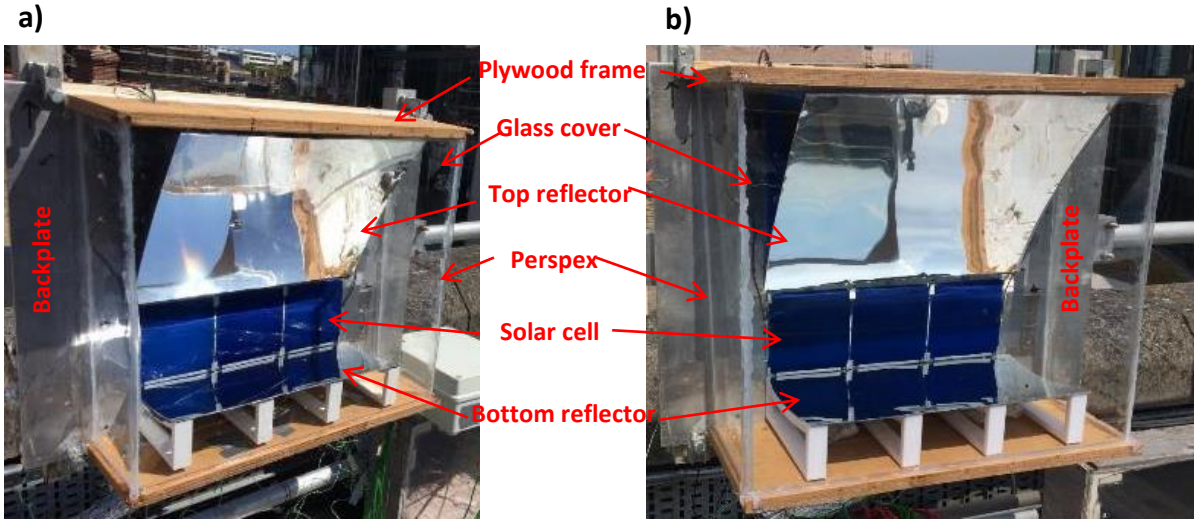

Figure 5. 18 Final assembly small prototypes CPC systems
(a) Ferrara CPC system (b) Mayo CPC system

5.2 Outdoor characterization for small prototype CPC and Reference systems for Ferrara, Italy and Mayo, Ireland

Outdoor characterization of the two systems was undertaken from 12th May to 2st June 2021 under different solar radiation intensities on the roof of Simon Perry building at Trinity College Dublin, Ireland (53.344295, -6.252416). The first step was to determine the power generation, efficiency and temperature of both systems and compare the results. The days chosen for testing were characterized by abundant sunshine and dry conditions, representative of the optimal operational conditions for the solar systems. This approach facilitated a robust baseline for assessing the performance of the systems and served as a validation check for the design and predictive simulations from Chapter 4. This testing phase was, in essence, preliminary. The days selected for testing were most conducive to the solar systems' operation and offered an accurate representation of their performance under ideal conditions. The decision to limit the testing to a single day for each system was primarily influenced by the project's time constraints, particularly the impending deadline for the Ideas Project's large-scale manufacturing phase (Chapter 1). The valuable insights gathered from these initial tests informed crucial design and manufacturing decisions, subsequently guiding the project toward the larger-scale manufacturing phase. It was understood that while these tests provided an immediate understanding of the systems' operation, future testing under a variety of environmental and operational conditions would be crucial for a comprehensive evaluation of the CPC systems' real-world performance and reliability.

In these preliminary tests, the decision to incorporate a resistor into the circuit with the systems was not solely procedural but also driven by the limitations in available resources at the time. There were not enough solar module analyzers available to carry out the detailed performance measurements such as maximum power, short circuit current, and open circuit voltage. Hence, the use of a resistor was a practical solution to ensure the continuity of the testing process. The resistor provided a means to facilitate a continuous and consistent flow of electrical current during the testing period. However, it must be reiterated that the resultant data from these tests, due to the resistor's inherent properties, did not provide absolute performance values. The focus was exclusively on facilitating a comparison between the Compound Parabolic Concentrators (CPCs) and their corresponding Reference systems. Moreover, the choice to proceed with the resistor was also influenced by the pressing timeline of the Ideas Project. The deadline for transitioning to the large-scale manufacturing phase necessitated a swift execution of these tests, limiting the scope for potential changes in the setup, including replacement or removal of the resistor. Despite these constraints, the preliminary tests yielded valuable comparative data for the CPCs and Reference systems. However, for future tests and in the lead-up to the large-scale manufacturing, it would be ideal to secure the required number of solar module analyzers for a more comprehensive assessment of the systems' performance parameters.

5.2.1 Outdoor installation for CPC system for Ferrara, Italy

The installation process for both the CPC Ferrara and the Reference systems involved careful considerations for stability, orientation, data acquisition, and protection from weather elements. The Reference system used for this investigation serves as a control, enabling direct comparison with the CPC Ferrara system. This system consisted of a bare, standalone solar cell, identical to the one used in the CPC system, but without the accompanying concentrators or reflectors. The configuration of the Reference system allowed for the evaluation of the solar cell performance under ambient conditions without any enhancement from light concentration or reflection mechanisms. Both the CPC Ferrara and the Reference systems were mounted on sub-frame rails and fastened securely with bolts on the rooftop to prevent any movement due to wind gusts, ensuring a stable and reliable experimental setup, as depicted in Figure 5.19. The systems were oriented towards the south, an orientation chosen based on its ability to capture maximum sunlight over the course of the day in the Northern Hemisphere. The accurate alignment was confirmed using an electronic compass. The incident solar radiation on the systems was measured using a pyranometer, a device that gauges the solar irradiance from all directions in the hemisphere. This data provided a critical benchmark to quantify the intensity of solar radiation during the experiment. An insulated box from Campbell Scientific Ltd. was installed nearby to house the electrical circuit, a data logger, and two 220 V plugs. The data logger was programmed to acquire data from a total of 25 channels, thereby ensuring detailed, multichannel monitoring of the system performance. The data logger and pyranometer were explain in details in section 3.5. Lastly, to protect the systems from potential rainwater infiltration, Silicone Acetate Standard Grade (saBesto) was applied in the slots and frame of each system. This ensured the longevity and operational stability of the systems in various weather conditions.

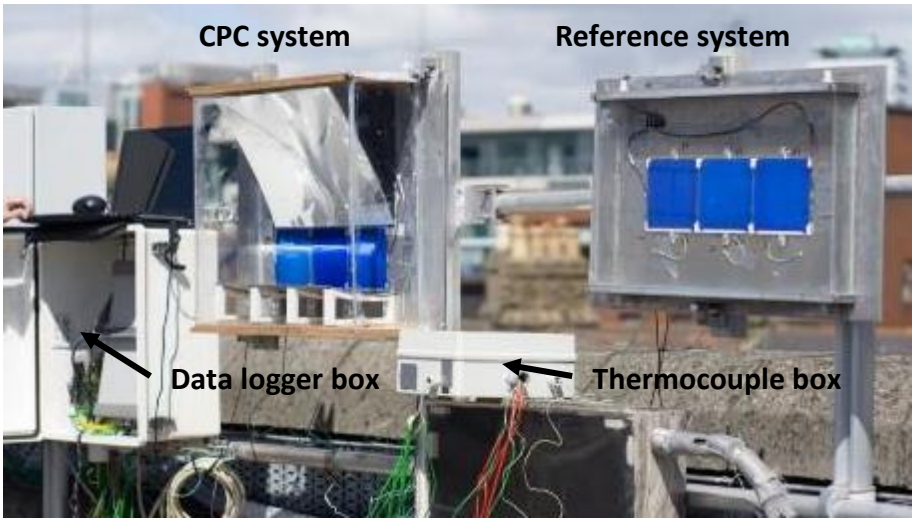

Figure 5. 19 Small Ferrara prototype CPC system and Reference system installed on the roof

The reflection of the bottom reflector formed the focal line on the solar cells which was clearly visible at the time of installation and can be seen in figure 5.20. This illustrates that system

has been manufactured correctly according to the design described in Chapter 4 and solar radiation is not lost at the edge of the solar cells. However, one possible problem for the solar cells is the occurrence of hot spots. Hot spots refer to areas on the solar cell that receive excessive sunlight, causing localized overheating and potential damage to the cell. In a CPC system, hot spots can occur if the concentration of solar radiation is not distributed evenly over the surface of the absorber and instead a significant proportion of radiation is concentrated on small area. This can reduce the efficiency of the solar cell and potentially damage it over the time. Therefore, a well-designed focus line is essential for ensuring uniform distribution of solar radiation on the surface of the absorber and avoiding the occurrence of hot spots. On the other hand, utilizing additional material to achieve optimal solar radiation distribution can increase the cost of the CPC systems. In addition, a more complex design may also increase the probability of errors during installation and manufacturing.

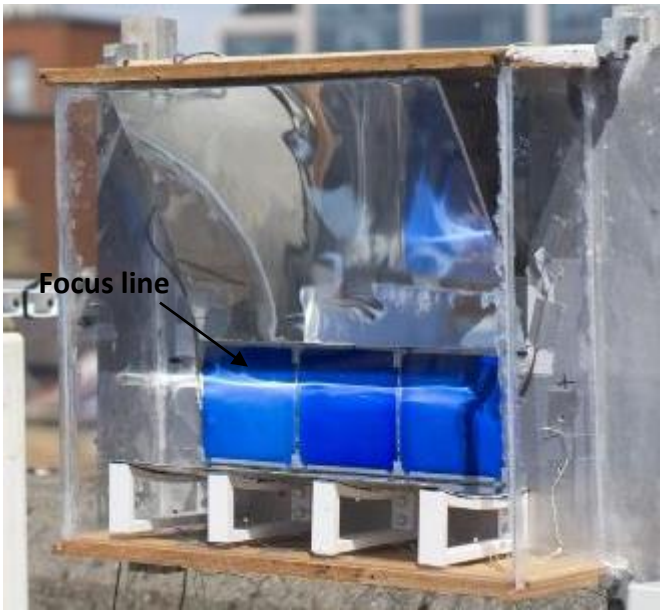

Figure 5. 20 Focus line on solar cells for small Ferrara prototype CPC system

5.2.2 Electrical analysis for CPC and Reference systems for Ferrara, Italy

The power, temperature, power ratio and efficiencies of CPC and Reference systems were measured from 12th of May 2021 from 6:00 to 21:00 with intermittent cloud cover. The variation of solar radiation and power over the day are shown in figures 5.30. As expected power and efficiencies varied along with solar radiation. Throughout the day, the CPC system showed power outputs greater than Reference system. The value of the maximum solar radiation reported that day was 842 W/m^2 at 13:18. At that time, the power output for CPC and Reference systems were 4.38 W and 3.26 W respectively. This represents an improvement of around 34 % in power output for the CPC system compared to the Reference system. An almost flat line between 13:00 and 15:00 was observed in the power output of the CPC system, this was because the resistor limited the power production of the CPC system. At the same time, it should be clarified that the CPC system was designed to operate

under the climatic conditions and location of Ferrara. This means that the observed performance improvement is particularly significant for the location. The systems design might not yield the same level of improvement in other regions with different weather patterns or solar radiations levels.

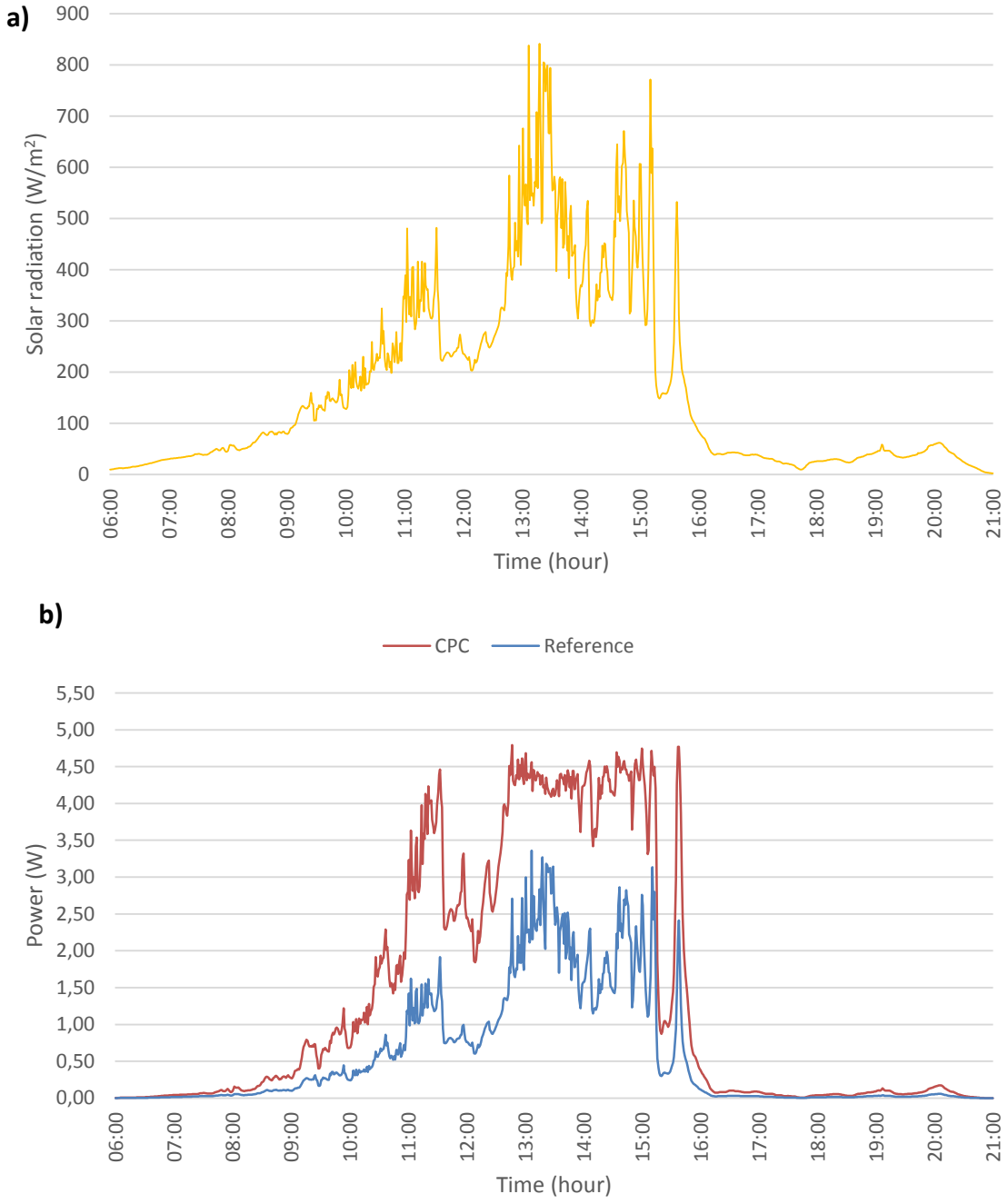

Figure 5. 21 (a) Variation of solar radiation (b) Power output for small Ferrara CPC prototype and Reference systems on the 12th of May 2021

The temperature in the solar cells of the CPC system was higher than the Reference system throughout the day as shown in figure 5.22. The highest solar cell temperature of 81 ºC was measured in the CPC system at 799 W/m^2 solar radiation, 42 º C more than the Reference system. This represents an increase of approximately 93 % in the solar cell temperature

compared to the Reference system. At maximum solar radiation (842 W/m^2), the temperatures in solar cell in the CPC and Reference systems were 69 ºC and 37 ºC respectively, representing an 86 % increase in temperature for the CPC system.

The higher temperature in the solar cells of the CPC system was attributed to the increased concentration of the solar radiation on the cells due to the parabolic reflectors. The reflector focus and direct more solar radiation onto the solar cells, resulting in higher energy absorption and consequently higher temperatures. This leads to higher energy efficiency conversion and higher power outputs, but also results in higher solar cell temperature. Higher solar cell temperature can have negative effects on the performance and efficiency of the cells, as the efficiency typically decreases with increasing temperature. Therefore, it is essential to properly manage and dissipate heat in the CPC system to maintain optimal performance. Section 2.2 described some techniques in order to manage the heat from the solar cell in CPC systems.

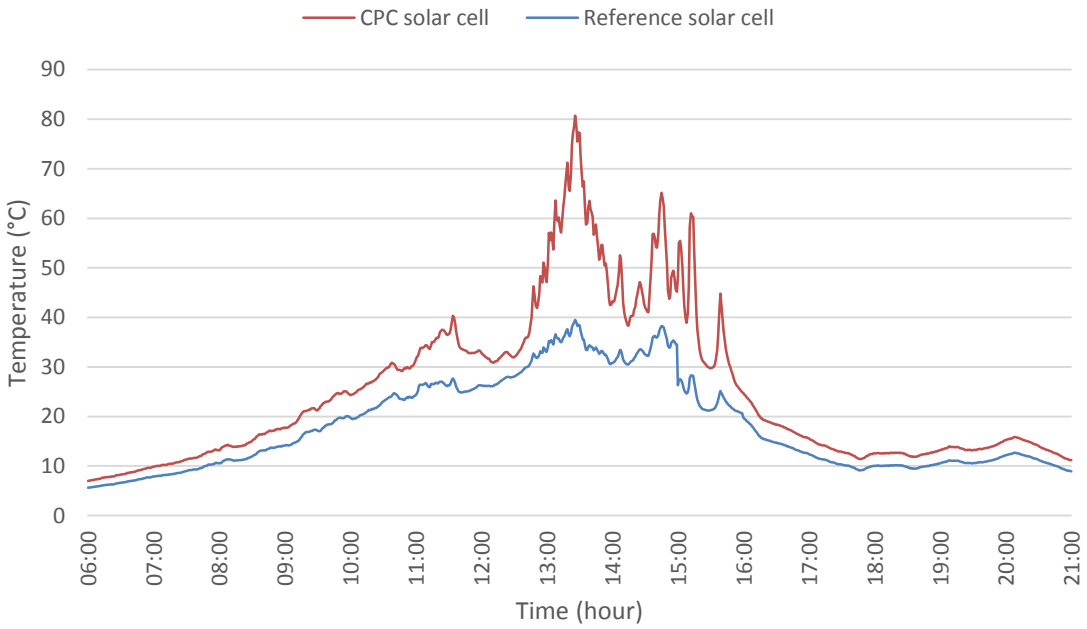

Figure 5. 22 Temperature in the solar cells for small Ferrara CPC prototype and Reference systems

Adding to the analysis, it is important to note that no thermocouples were installed to measure the outdoor temperature during the tests. This means that the precise ambient temperature, which can greatly influence the performance of the solar cells and the efficiency of the overall system, was not accounted for in this test. It is notable that higher ambient temperatures can cause a decrease in the efficiency of solar cells due to increased thermal losses. In turn, the lack of specific temperature data creates an additional uncertainty when comparing the test results with the simulated data, further explaining potential discrepancies. Future experiments might benefit from the inclusion of thermocouples or other temperature monitoring devices to provide a more accurate account of environmental conditions during testing. The decision to not install thermocouples during the tests was influenced by a number

of factors. One principal reason was the goal of the testing phase. The main focus was on assessing the relative performance between the CPC and the Reference systems under the same environmental conditions, then the exact ambient temperature was considered less critical, as both systems would be equally affected. Additionally, it was a matter of practicality or resource allocation. Installing, calibrating, and monitoring thermocouples can add complexity and cost to a test. This includes not just the direct cost of the equipment itself, but also the additional time and effort required for installation, data collection, and analysis. However, the lack of specific temperature data can be seen as a limitation of this experiment, as it leaves out an important factor that can significantly affect the performance of solar cells.

Power ratio for the CPC system during the day is shown in figure 5.33. The average value of the power ratio during the day was 2.80 and fluctuated from 1.34 to 3.43. It could be observed that the power ratio values decreased between 13:00 and 15:00 as a consequence of the resistor that limits the maximum power production of the CPC system at high solar radiation. At the maximum solar radiation (842 W/m^2) the power ratio was 1.34. When solar radiation was high, the solar cell generated more current, which leads to higher power output. The 0.5 ohms' resistor restricted the flow current and consequently, the power output was limited. As a result, during periods of high solar radiation, the system was not operating at its maximum potential efficiency, as some of the available solar energy was being dissipated as heat by the resistor. This is why the power ratio values decreased between 13:00 and 15:00 when solar radiation peaked. The power ratio of the CPC to the reference systems can be reduced due to a variety of loss mechanisms. Some of these include:

- Resistor Limitations: As stated in the provided information, a resistor was in place which limited the flow of current and, therefore, the power output. This resistor dissipated a portion of the available energy as heat, particularly during periods of high solar radiation. This directly reduces the power ratio of the CPC system compared to the reference system.

- Optical Losses: These can occur due to the imperfect focusing of sunlight by the CPC. Some sunlight can be reflected off the surfaces of the concentrator without hitting the solar cell, or can miss the cell entirely due to errors in the alignment or shape of the concentrator.

- Thermal Losses: Solar cells convert sunlight into electricity less efficiently at higher temperatures, so if the CPC system is operating at a higher temperature than the reference system, this could reduce its power ratio. The concentrator can cause the cell to heat up, either by focusing additional sunlight onto the cell, or by trapping heat that is generated by the cell. This effect can be particularly significant in concentrator systems, which often require additional cooling compared to standard flat-panel systems.

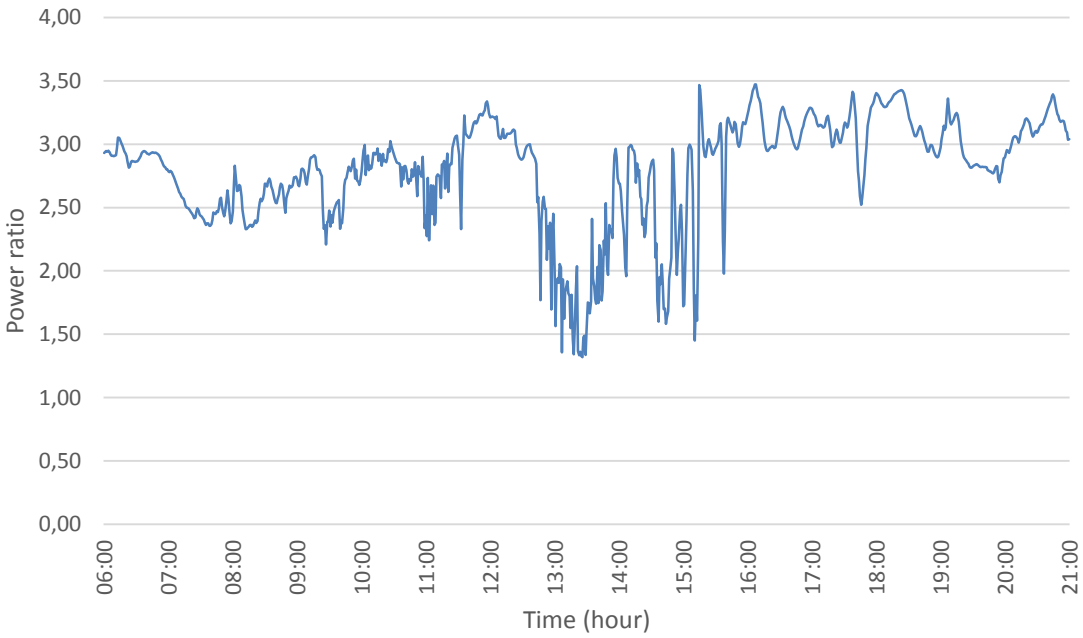

Figure 5. 23 Power ratio for small Ferrara CPC prototype

In the CPC system, the solar cell efficiency is defined as the ratio of the electrical power output of the cell to the incident solar power. This was calculated using the equation 2.3. The system efficiency of the CPC, on the other hand, is the ratio of the electrical power output of the system to the incident solar power. This includes losses due to reflection and absorption in the concentrator, losses due to electrical resistance in the wiring, and losses due to inefficiencies in the solar cell. The system efficiency was calculated using the equation 2.4. For the solar cell efficiency, the effective area used was solar cell area (0.047 m^2) and for system efficiency, the effective area used was the aperture area (0.139 m^2).

The exactly same procedure was applied to the Reference system for comparison. The use of the same aperture area for the system efficiency calculation, in this case, provides a better representation of the performance of the systems. Adding more cells to the effective aperture area of the Reference system might be limited by the available facade area, taking into account that these systems are designed for building-integrated facades. Another significant aspect is the use of a reflector in the CPC system, which aids in maintaining the design power output throughout the year, a feat unachievable in a common flat panel. The reflector in a CPC system captures and focuses sunlight onto the solar cell, making it particularly beneficial during periods of low sunlight intensity. In contrast, the Reference system, lacking a concentrator, relies directly on incident sunlight, resulting in lower performance during periods of reduced solar intensity. This capability of the CPC system makes it a more viable choice for year-round solar energy generation, especially in regions with variable sunlight conditions.

Both efficiencies are shown in figures 5.34 and 5.35, respectively. Solar cell efficiency and system efficiencies presented a similar behavior during the test. Both efficiencies were better in the CPC system than the Reference system. From the solar cell efficiency graph (figure 5.24) the maximum values obtained were 27 % and 9 % in the CPC and Reference system respectively at 311 W/m^2 solar radiation. At maximum solar radiation (842 W/m^2) the reported solar cell efficiency was 11 % and 8 % for the CPC and Reference systems respectively. From the system efficiencies graph (figure 5.25), the maximum values reported were 8.88 % CPC system and 2.90 % for Reference system at 311 W/m^2 solar radiation. At maximum solar radiation, the system efficiencies were 3.72 % and 2.77 % for CPC and Reference system respectively. Both, solar cell efficiency and system efficiency for the CPC system were higher than those of the Reference system. This means that the CPC system was more effective at converting incident solar energy into electricity.

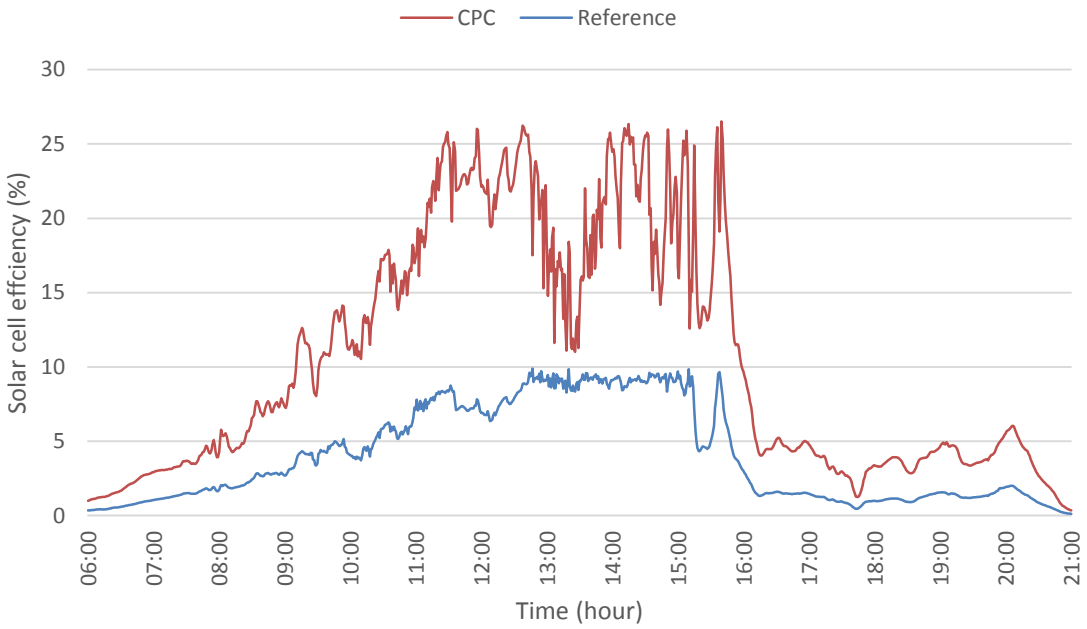

Figure 5. 24 Solar cell efficiency for small Ferrara CPC prototype and Reference systems

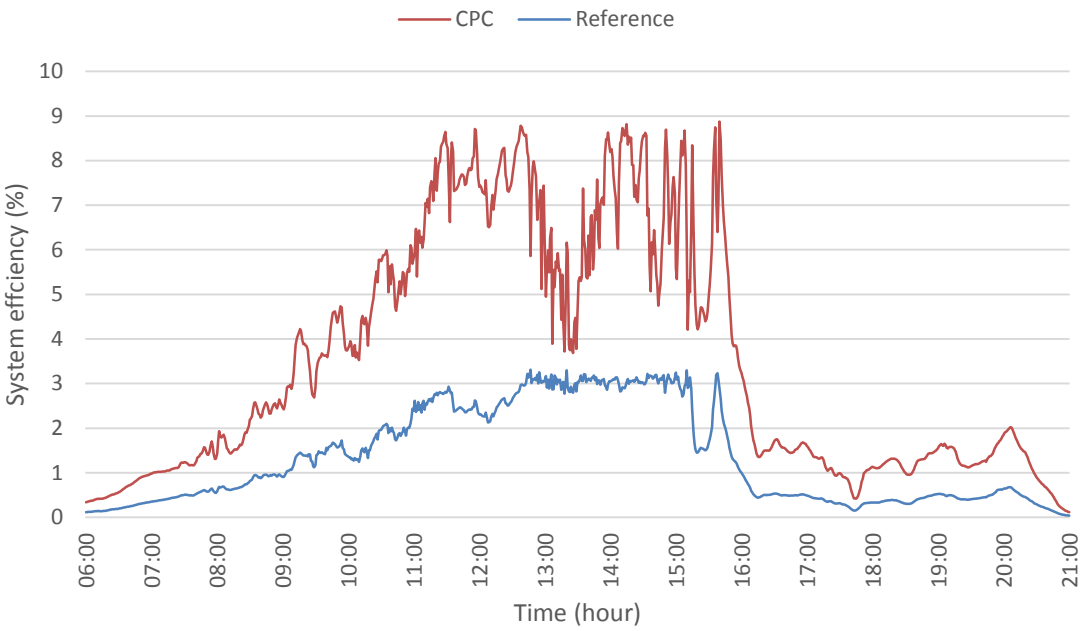

Figure 5. 25 System efficiency for small Ferrara CPC prototype and Reference systems

In the context of comparing the performance of the CPC and Reference system, the solar cell efficiency is arguably a more accurate and fair measure than system efficiency. There are several reasons behind this assertion, which are primarily centered around the equality of the solar cell area in both systems and the distinct operating principles of the two designs:

- Firstly, both the CPC and Reference systems employ solar cells of the same area. This uniformity establishes a common baseline for comparison, allowing the direct evaluation of each system's effectiveness in solar energy conversion. By focusing on solar cell efficiency, the inherent characteristics of the solar cells, including their power output and response to varying solar radiation levels, are brought to the forefront.

- Secondly, the solar cell efficiency offers an insightful look into the core performance of the systems, excluding external factors introduced by the system's design. In this case, the system efficiency could potentially mask the actual performance of the solar cells, given it incorporates elements such as reflection and absorption in the concentrator, and losses due to electrical resistance in the wiring for the CPC system. Such factors are particular to the CPC design and do not reflect the intrinsic performance of the solar cells.

- Lastly, focusing on solar cell efficiency can inform decisions about potential improvements to the systems. By isolating the performance of the solar cells from the rest of the system, it becomes easier to identify areas where the cells' efficiency could

be improved, whether through the use of different materials, changes in cell design, or enhancements in manufacturing processes.

When comparing the CPC and Reference systems, considering solar cell efficiency can provide a clearer, more accurate picture of the individual system's performance, allowing for more informed conclusions and recommendations.

While in section 5.1.8 were able to confirm that the solar cells can reach their specified efficiency of 22 % under ideal conditions (a controlled environment with a solar radiation intensity of 900 W/m^2 and an ambient room temperature of 21 ºC), there are several reasons why this level of efficiency might not be achieved in an outdoor test within the Reference system:

- Real-World Conditions: Solar radiation intensity can vary significantly throughout the day and across different seasons due to factors such as the position of the sun, cloud cover, and atmospheric conditions. If the solar radiation intensity is lower than 900 W/m^2, the solar cells may not reach their maximum efficiency.

- Temperature Effects: As per the manufacturer's specification, the solar cells suffer from temperature losses equal to 0.32 %/°C. The outdoor temperature during the efficiency tests was higher than 25 °C (the temperature at which the cells are rated). High temperatures reduce the open-circuit voltage and, therefore, the cell efficiency.

- Angle of Incidence: The efficiency of a solar cell depends on the angle at which light hits the surface. If the sunlight is not hitting the cell perpendicularly, the efficiency of the cell can decrease. In outdoor conditions, the angle of sunlight changes throughout the day, which can lead to variations in efficiency.

- Spectral Effects: The sunlight's spectrum changes based on the time of day and atmospheric conditions. The solar cell's efficiency can vary under different spectra, leading to discrepancies between real-world and specified efficiencies.

- System-Level Losses: In a real-world system, additional losses can occur, such as resistive losses in the wiring and inefficiencies in the power conversion equipment.

The difference in efficiency between the specified and measured efficiencies can be attributed to a combination of factors, all of which are part of operating in a real-world, rather than a laboratory, environment.

Figure 5.26 presents the power output for the CPC and Reference systems with solar radiation. From the results, it was evident that the CPC consistently outperformed the

Reference system in terms of power generation. The performance gap between the two systems increased as solar radiations levels rose. This indicated that the CPC was more efficient at converting ray lights into electricity. From figure 5.26 at 400 W/m^2, the power output of the CPC system tended to be constant with approximately 4.5 W. This confirmed that the resistor was limiting the power of the CPC system. As a result, the values obtained in this experiment were only for comparison with the Reference system and might not have represented the true potential of the CPC system operating without such limitations.
In some instances, the CPC produced three times greater power than the Reference system. At 58 W/m^2, the CPC generated 0.15 W, while the Reference system produced 0.05 W. This demonstrated a significant advantage of the CPC over the Reference system in terms of power generation efficiency even with the resistor limiting its power output.

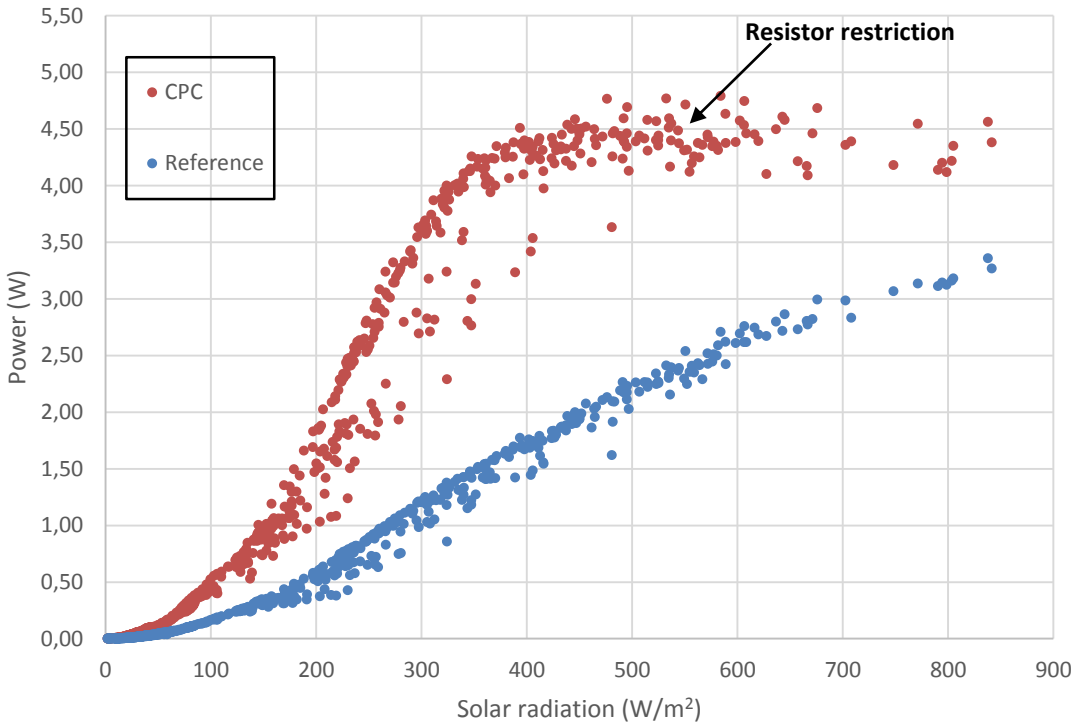

Figure 5. 26 Power with solar radiation for small Ferrara prototype CPC and Reference systems

On average, the power of the CPC system was 1.34 W and for the Reference system was 0.56 with a power ratio of 2.80. Solar cell efficiency in the CPC system was 11 %, 7 % more than the Reference system. System efficiency in the CPC system was 4 %, 3 % higher than the Reference system. Based on these results, it can be concluded that small prototype CPC system for Ferrara has a strong advantage over the Reference system in terms of power generation, solar cell efficiency and system efficiency. These results illustrated that the CPC design was promising and worth further investigation and development. If the resistor limitation was removed, the true potential of the CPC system would have been even more

impressive. Continuing with the CPC design was recommended, as it had shown potential for improved performance and efficiency compared to Reference system.

5.2.3 Outdoor installation CPC system for Mayo, Ireland

The location of CPC Mayo and Reference systems on the roof of the Simon Perry building in Trinity College Dublin is shown in figure 5.27. The Reference system utilized in this test was the same as that used for the CPC system for Ferrara test. Detailed information regarding this Reference system was provided in section 5.2.1 of this document.

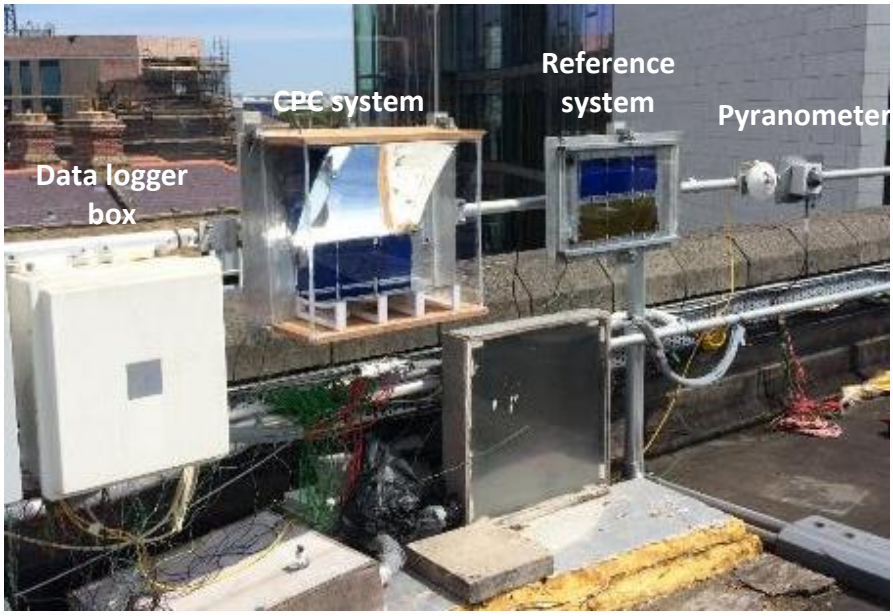

Figure 5. 27 Small Mayo prototype CPC system and Reference system installed on the roof

The reflection of the bottom reflector forming the focal line on the solar cells was clearly visible at the time of installation, and is presented in figure 5.28. Again this demonstrated that the system was constructed accurately according to the design detailed in chapter 4, ensuring that solar radiation was not lost at the edges of the solar cells. Nonetheless, hot spot overheating may be an issue in this system also which was discussed in earlier in section 5.2.1.

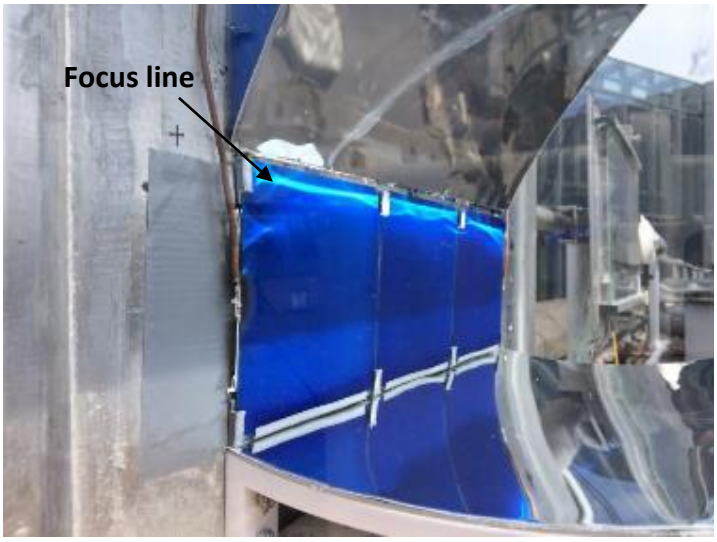

Figure 5. 28 Focus line on solar cells for small Mayo prototype CPC system

5.2.4 Electrical analysis for CPC and Reference systems for Mayo, Ireland

The power, temperature, power ratio and efficiencies of the CPC and Reference systems were measured on the 1^{sd} of June 2021 from 6:00 to 21:00. The weather during testing was generally sunny with intermittent cloud cover. The variation of solar radiation and power are shown in figures 5.29. The value of the maximum solar radiation reported this day was 761 W/m^2 at 14:13. where the power output for CPC and Reference systems were 4.67 W and 3.27 W respectively. In terms of percentage, the CPC system produced approximately 42.8 % more power than the Reference system. An almost flat line between 14:00 and 15:00 was observed in the power of the CPC system, this was because the resistor again limited the production power of the CPC system. It is important to note that the resistor was not changed during this test as it was a preliminary test conducted before large-scale manufacturing. This decision was made to ensure that the preliminary test results would be representative of the actual performance of the systems once they were manufactured on a larger scale, providing valuable insights for further development and optimization.

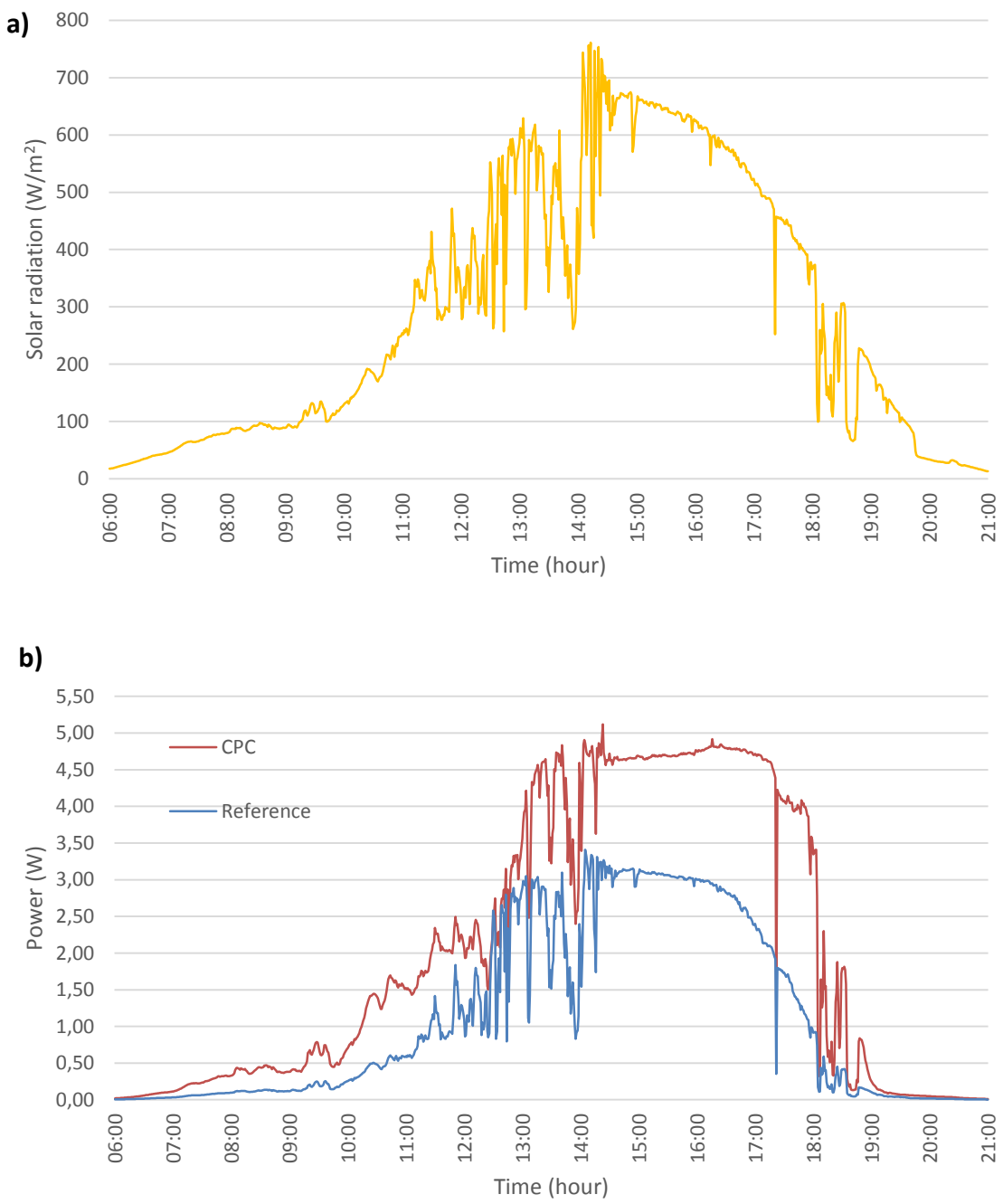

Figure 5. 29 (a) Variation of solar radiation (b) Power for Mayo CPC and Reference systems on the 1^{sd} of June 2021

The temperature of the solar cell is presented in figure 5.30 and shows similar solar cell temperatures in both systems in the morning and but higher CPC solar cell temperatures throughout the afternoon. At the beginning of the day, CPC solar cell temperature was at 15 ºC and increased to 68 ºC at 15:10. Temperature of the Reference solar cells also increased from 15 ºC to 55 ºC over the same time. The highest solar cell temperature of 68 ºC was measured in CPC system at 658 W/m^2, 13 º C more than Reference system. At maximum solar radiation (761 W/m^2), the solar cell temperatures in the CPC and Reference systems were 64 ºC and 55 ºC respectively. The temperature of the CPC solar cells was consistently higher than

those in the Reference system. This indicated that the CPC solar cells were more susceptible to heating due to the concentration of solar radiation by the reflectors. Temperature can affect the efficiency of solar cell (as discussed in section 5.2.2), so it was essential to consider the temperature differences when evaluating the performance of solar cell. Thermocouples were not installed to monitor the outdoor temperature during the tests, the explanation for this decision can be found in section 5.2.2.

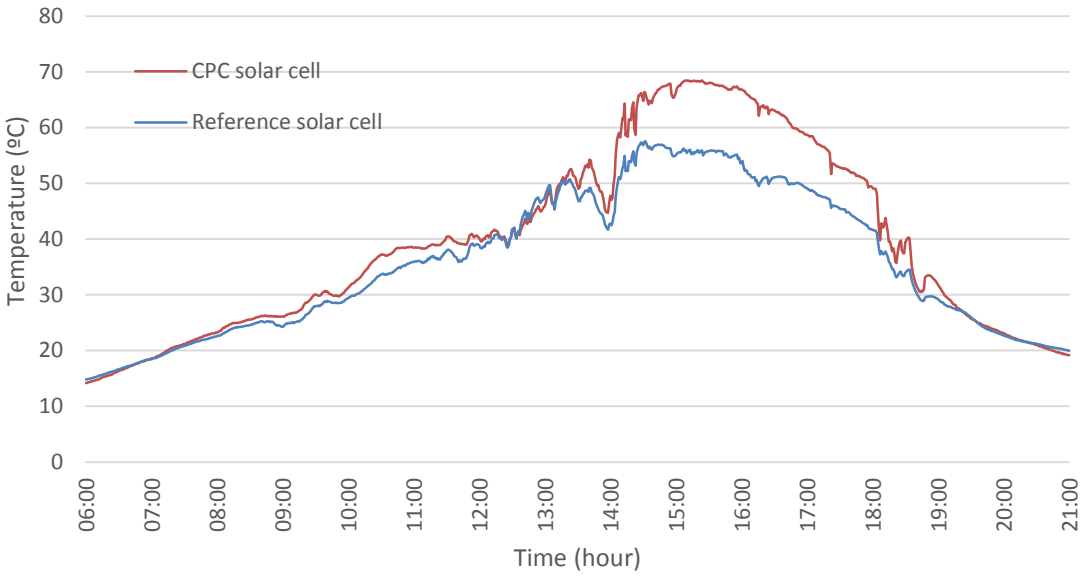

Figure 5. 30 Temperature in the solar cells for small Mayo prototype CPC and Reference systems

Power ratio for the CPC system during the day is shown in figure 5.31, where the average was 2.57 and fluctuated from 1.00 to 4.92. Power ratio decreased between 10:00 and 16:00 as a consequence of the resistor that limits the maximum power production of the CPC system at high solar radiation as discussed. At the maximum solar radiation (761 W/m^2) the power ratio reported was 1.43. The underlying causes contributing to this decrease in the power ratio were exhaustively explained in Section 5.2.2.

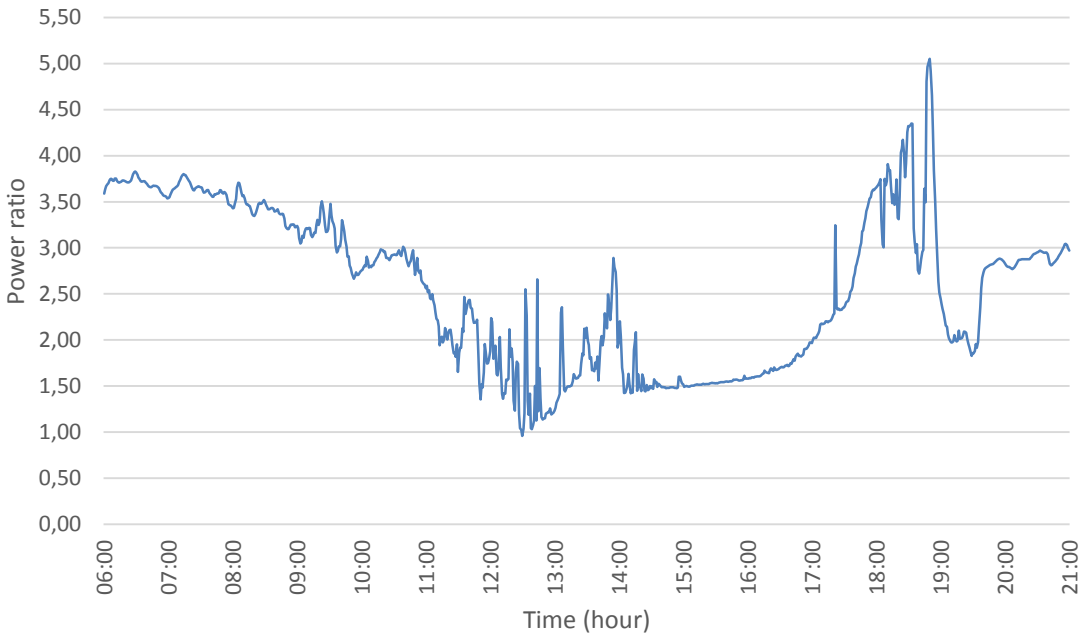

Figure 5. 31 Power ratio for small Mayo prototype CPC system

As before, for the solar cell efficiency, the effective area used was solar cell area (0.047 m^2) and for system efficiency, the effective area used was the aperture area (0.139 m^2). Both efficiencies are shown in figures 5.32 and 5.33, respectively and again solar cell efficiency and system efficiency presented a similar behavior during the test. Both efficiencies were better for the CPC system than the Reference system. The differences between these efficiencies can highlight the impact of additional components on the overall performance of the CPC system. Maximum solar cell efficiency for the CPC and Reference systems were 22 % and 14 % respectively, at 494 W/m^2. However, when considering the entire system, maximum efficiencies dropped to 7.21 % for the CPC system and 4.56 % for the Reference system at the same solar radiation. This revealed the influence of additional components on system performance and efficiency losses.

Comparing the graphs, it was possible to analyze the advantages and drawbacks of each system. The improvement in efficiency by the CPC system over the Reference system was evident, with solar cell efficiency at maximum solar (761 W/m^2) radiation being 13 % for the CPC system and 9 % for the Reference system. Similarly, the system efficiencies at maximum solar radiation were 4.28 % for the CPC system and 3 % for the Reference system, showing the benefits of using the CPC design.

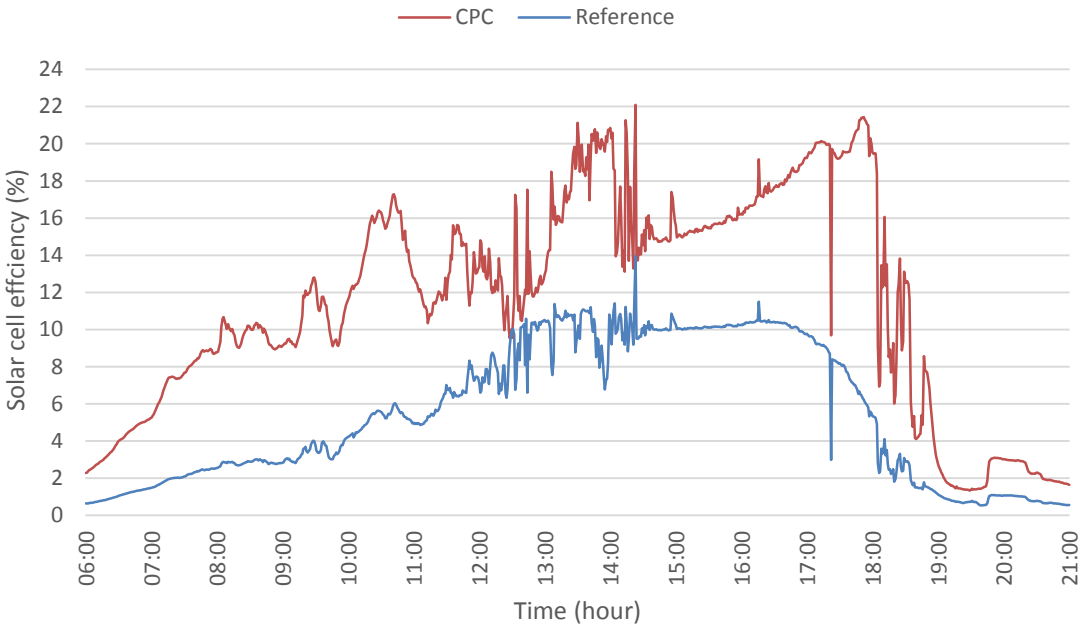

Figure 5. 32 Solar cell efficiency for small Mayo prototype CPC and Reference systems

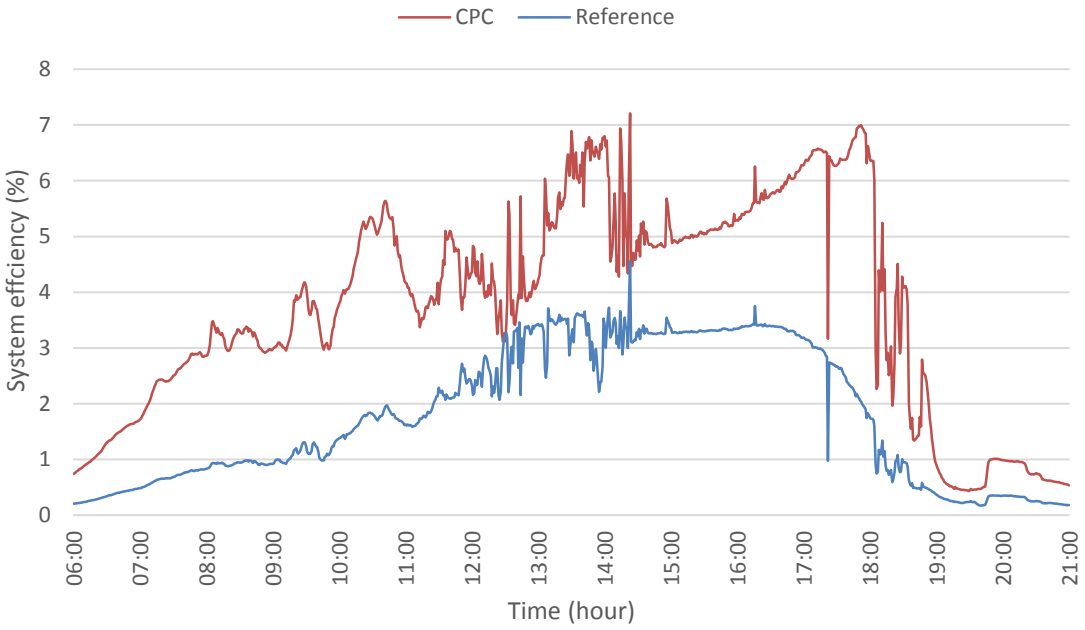

Figure 5. 33 System efficiency for small Mayo prototype CPC and Reference systems

In parallel to the test conducted for the Ferrara systems, the Reference system in the Mayo systems test only reached a solar cell efficiency of 14 %. This result significantly deviated from the manufacturer's data and the laboratory test result, which had demonstrated an efficiency of 22 %. Detailed explanations for this discrepancy were provided in section 5.2.2. It is crucial to acknowledge that laboratory conditions are typically optimized and fail to encompass the full range of environmental variables that solar cells are exposed to in real-world outdoor

settings. Therefore, efficiencies achieved under operational conditions can deviate from those measured in laboratory tests.

Figure 5.34 presents the power for CPC and Reference systems with solar radiation. From the graphs, at 500 W/m^2, the power output of the CPC system plateaued at ~ 4.84 W. This confirmed that the resistor was limiting the power of the CPC system as before. As solar radiation increased beyond 500 W/m^2, the CPC system output remained constant instead of increasing proportionally. However, it was still clear that the CPC system was more efficient at converting solar radiation into power than the Reference system.
As discussed, the resistor limitation was not addressed in this preliminary test, as it served as an initial evaluation prior to conducting more comprehensive large-scale testing.

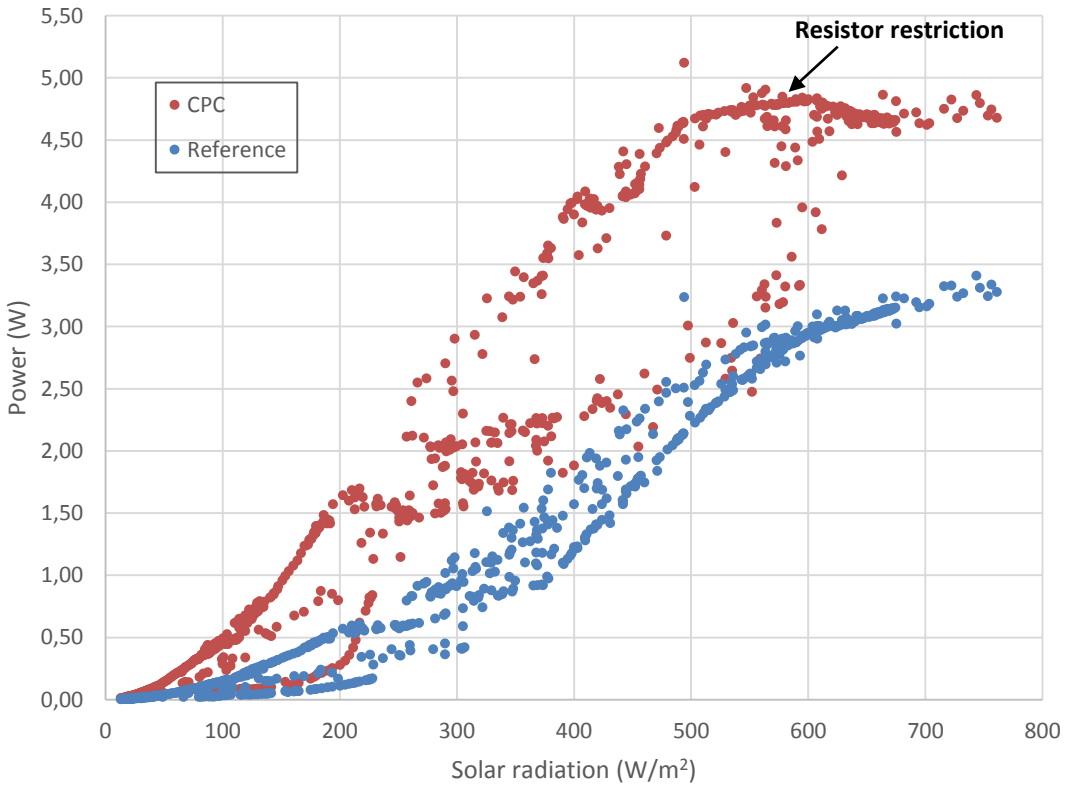

Figure 5. 34 Power with solar radiation for small Mayo prototype CPC and Reference systems

On average, the power of the CPC system was 2.01 W and the Reference system was 1.11 with a power ratio of 2.57. Solar cell efficiency of the CPC system was 11 %, 5 % higher than the Reference system. System efficiency in the CPC system was 4 %, 2 % more than the Reference system.

A phenomenon emerged when contrasting the outcomes from the Ferrara systems test figure 5.26 with those from the Mayo system tests. The graph for the Mayo systems, illustrated in

Figure 5.34, demonstrated an increased degree of scatter in the data, which contrasted with the more streamlined data presentation observed for the Ferrara systems. This heightened scatter might indicate the existence of hysteresis or it might be symptomatic of other variables tied to testing procedures or environmental factors. Hysteresis, the phenomenon where a system's response to changes is not immediate but rather lags behind, could have been present. The previous states of the system can influence its current reaction, which in the context of solar cells, could manifest as variations in the output power when the solar radiation alters.

The use of a pyranometer in these tests was another factor to consider. As an instrument designed to measure solar radiation, a pyranometer could sometimes exhibit a time delay in its data recording. In contrast, solar cells, by their nature, absorb radiation nearly instantaneously and convert it into power. This differential in response times might lead to seeming inconsistencies between the solar radiation levels as captured by the pyranometer and the power output from the solar cells. For example, if a sudden increase in solar radiation occurred, the solar cells might respond promptly, resulting in a corresponding rise in power output. However, if the pyranometer, due to its inherent delay, had not yet registered this abrupt change, the solar radiation level at that moment might appear to be lower than what the solar cells were responding to. This mismatch could lead to deviant data points, thereby contributing to the scatter seen in the graph.

Moreover, other environmental factors such as ambient temperature fluctuations, wind speed, and cloud cover could also affect both the pyranometer readings and solar cell efficiency, potentially contributing to the scatter seen. These variables could change rapidly and independently, causing deviations in the expected correlation between solar radiation and power output.

5.3 Outdoor testing versus simulation results

When comparing the simulation results from Chapter 4 with the real-life test outcomes outlined in this chapter, there were noticeable discrepancies between the two sets of data. These differences could be ascribed to several factors such as the assumption of ideal conditions in the simulations, inherent limitations of the models, weather conditions variability, manufacturing and installation imperfections, and the use of resistors in the testing setup.

A detailed comparison between the simulated and actual test results for the small prototype systems is provided in Table 5.3. Notably, both the solar cell and system efficiencies demonstrated substantial differences when compared between the simulated predictions and the results from the real-world tests. While the concentration ratios for both the Ferrara and Mayo CPC systems were quite close, there was a considerable divergence in the efficiencies.

Table 5. 3 Comparison between real test and simulation results for small prototype systems

	Concentration ratio		Solar cell effciency (%)		System efficiency (%)	
Prototype	**Simulation**	**Test**	**Simulation**	**Test**	**Simulation**	**Test**
Ferrara CPC	2.80 (Feb - Sep)	2.80 (May)	24% - 41%	11%	9% - 21%	4%
Mayo CPC	2.82 (Feb - Sep)	2.57 (June)	31% - 49%	13%	12% - 22%	4%

Specifically, the solar cell efficiency in the Ferrara CPC system ranged from 24 % to 41 % in the simulation predictions, but the real-world test only yielded a maximum of 11 %. Similarly, the solar cell efficiency in the Mayo CPC system, as predicted by the simulations, ranged from 31 % to 49 %, while the real-world test result reached only 13 %. The overall system efficiencies also demonstrated significant discrepancies, with the simulations predicting 9 % - 21 % for the Ferrara CPC and 12 % - 22 % for the Mayo CPC, while the actual test results for both systems were only around 4%.

These substantial differences can be attributed to several reasons. The simulation models, although quite effective, generally operate under ideal conditions. They may not fully incorporate real-world complexities such as fluctuations in solar radiation (i.e., the simulations assume the receipt of a full 1000 W/m^2, which might not always be the case), changes in temperature that could affect solar cell efficiency (via heat effects), or the influence of other environmental factors like wind speed and cloud cover.

Furthermore, the simulations may not account for potential imperfections that can arise during the manufacturing or the installation process of the CPC systems, which could affect their performance. The impact of using a resistor in the test setup, which can also influence the system's efficiency, may not be fully captured in the simulation models.

The discrepancies between simulation and real-life testing results in solar cell system performance can be summarized as follow:

1. **Ideal Conditions in Simulations:** Simulations are usually performed under standard test conditions (STC), which typically assume a light spectrum of AM1.5, an incident power density of 1000 W/m², and a cell temperature of 25°C. However, real-life environmental conditions often deviate from these assumptions, leading to discrepancies.

2. **Solar Irradiance Variability:** Simulations often assume constant solar irradiance, but the actual irradiance can fluctuate due to changes in weather, time of day, and seasons. This includes the effect of partial shading (from clouds, nearby buildings, or trees), which is not usually considered in simulations.

3. **Temperature Effects:** Certainly, temperature is a vital factor that significantly affects the performance of solar cells. As the temperature increases, the efficiency of solar cells decreases, a fact that is often not adequately taken into account in simulation models. This oversight can lead to overestimation of solar cell performance when extrapolating simulation results to real-world scenarios. This thermal effect on solar cell efficiency is particularly pronounced in warmer climates or during the hotter parts of the day. High ambient temperature can cause the cells to heat up, thereby reducing their operational efficiency. Each type of solar cell has a specific temperature coefficient that quantifies the decrease in efficiency for each degree increase in temperature above the Standard Test Condition of 25 °C. For instance, the SunPower solar cells used in the IDEAS project have a temperature coefficient of -0.32 %/ºC (section 3.7). This means that for each degree Celsius rise in temperature above 25 °C, the efficiency of these solar cells decreases by 0.32 %. This could lead to substantial performance loss in hot weather conditions, thereby causing notable discrepancies between simulation results and real-world performance. Therefore, when designing and evaluating solar energy systems, it is crucial to take into account the local climate, the specific temperature coefficients of the chosen solar cells, and the thermal management of the solar installation. To get more accurate simulation results, temperature effects should be incorporated into the simulation models. Similarly, for interpreting test results, the prevailing temperature conditions during testing should be considered.

4. **Imperfections in Manufacturing and Installation:** Variations in the manufacturing process can lead to differences in the performance of individual solar cells. Similarly, the installation process can impact system performance, particularly if there are issues with alignment, cleanliness, or aging of the system.

5. **Spectral Effects:** The performance of solar cells can vary based on the spectrum of the incident light, which can change due to atmospheric conditions, time of day, and location. Simulations often use a standard AM1.5 spectrum, which may not always match the actual spectrum of the incident light.

6. **System Losses:** These can include resistive losses in wiring, inverters, and batteries, losses due to dust or soiling on the solar cell surface, and losses due to imperfect angle of incidence or light concentration, among others. These factors are often not included in simulation models.

7. **Resistive Losses:** Resistance in the wiring, connectors, and other electrical components can cause energy losses. These losses increase with the square of the current, so they can be substantial in high-current systems. In real-world conditions,

the quality of the wiring, the integrity of the connections, and the length of the wire runs all contribute to these losses. However, these factors are often simplified or ignored in simulation models.

8. **Losses Due to Dust or Soiling:** Over time, dust, bird droppings, leaves, and other debris can accumulate on the surface of the solar cells, reducing the amount of sunlight that reaches the cells. Rain, wind, and maintenance activities can clean the cells, but the timing and effectiveness of these cleaning actions are difficult to predict and often not included in simulations.

9. **Angle of Incidence and Light Concentration:** The amount of sunlight that a solar cell can convert into electricity depends on the angle at which the sunlight strikes the cell. In the real world, this angle changes throughout the day and the year, and can be affected by shading from nearby objects. Moreover, the concentration of sunlight can be affected by atmospheric conditions, such as clouds or haze. Simulation models often use simplifying assumptions about these factors.

10. **Model Limitations:** No model can perfectly represent reality. Some physical phenomena might not be fully captured or may be simplified in the model to make the simulation feasible.

11. **Use of Resistors in Testing Setup:** The use of resistors in the testing setup can influence the system's overall efficiency by limiting the power output of the solar cell system. This may not be fully captured in the simulation models.

12. **Condensation on Front Glass:** Solar cells are typically encapsulated behind a glass cover to protect them from the environment. However, in certain atmospheric conditions (typically when there are high levels of humidity and large temperature variations), condensation can form on the inside of the front glass cover. This layer of condensation can scatter incoming light and reduce the amount of sunlight reaching the solar cells, thereby lowering their output. Furthermore, if condensation persists, it could lead to long-term damage such as corrosion or mould growth, which might further degrade the performance and lifespan of the solar cells. Simulation models often do not account for these transient environmental effects and long-term degradation mechanisms. It is difficult to accurately predict when and to what extent condensation will form, as it depends on a range of environmental factors including temperature, humidity, wind speed, and the design and materials of the solar module itself.

The difference between simulation and real-world results arises from a complex interplay of multiple factors, some of which are challenging to predict or control. Understanding these

discrepancies is crucial for improving both the accuracy of simulations and the performance of actual solar cell systems. In spite of these discrepancies, it is important to note that both the simulation data and the real-life test results offer valuable insights. The simulation results can provide an estimate of the system's performance under ideal conditions and give an indication of what might be achieved, while the real-world test results offer a practical perspective on how the system may perform under typical operational conditions, highlighting areas that might need improvement or adjustment.

5.4 Conclusion

Small prototype CPC systems for Ferrara, Italy and Mayo, Ireland were manufactured and tested in outdoor conditions in Dublin, Ireland and were compared with a Reference system with the same solar cell area and characteristics. Experimental results showed that for both CPC system configurations power output, power ratio and efficiencies were higher than the Reference system. Solar cell temperatures were higher in both CPC systems than the Reference system. The heat generated by these systems can be used and stored as thermal energy for a potential building application which will be incorporated into the large scale designs. The high temperatures in the solar cell affected the power production in the concentrators as show in table 5.4. All the concentrator systems tested reported power production limitation caused by the resistor. Table 5.4 summaries the results reported from small prototype test. To optimize the performance of solar cell systems, it is crucial to continually refine the simulation models and the testing methodologies to ensure closer alignment between the theoretical expectations and practical outcomes. This involves a deep understanding and thorough examination of the observed discrepancies, and the development of strategies to minimize these in future iterations.

Table 5. 4 Summary of performance data of small scale Ferrara and Mayo prototypes

Small Prototype	**Maximum Solar Radiation (W/m^2)**	**Maximum Power (W)**	**Solar Cell Efficiency (%)**	**System Efficiency (%)**	**Solar Cell Temperature (ºC)**
Ferrara	842	CPC: 4.38, Reference: 3.26	CPC: 11% Reference: 8%	CPC: 3.72% Reference: 2.77%	CPC: 69, Reference: 37
	Average	CPC: 1.34, Reference: 0.56	CPC: 11% Reference: 4%	CPC: 4% Reference: 1%	CPC: 25, Reference: 18
Mayo	761	CPC: 4.67, Reference: 3.27	CPC: 11% Reference: 9%	CPC: 4.28% Reference: 3%	CPC: 64, Reference: 55
	Average	CPC: 2.01, Reference: 1.11	CPC: 11% Reference: 5%	CPC: 4% Reference: 2%	CPC: 39, Reference: 36

Chapter 6 Manufacturing process for largescale CPC systems

Using the designs described in chapter 5, largescale systems were manufactured and assembled for the two demonstration sites in Ferrara and Mayo. They are described in table 6.1.

Table 6. 1 Systems manufactured for Large-scale demo-sites Ferrara and Mayo

Location	Sun Altitude	System Type	Solar Cells	Features
Ferrara, Italy	Max: 68° Min: 22°	CPC System	32	Compound parabolic concentrator with Luminescent down shifting layer coating
		CPC/PCM System	32	Compound parabolic concentrator with Luminescent down shifting layer coating and Phase change material containers behind backplate
		Reference System	32	Flat non-concentrating panel
Mayo, Ireland	Max: 60° Min: 12°	CPC System	24	Compound parabolic concentrator
		CPC/PCM System	24	Compound parabolic concentrator with Phase change material containers behind solar cells
		Reference System	8	Flat non-concentrating panel

The components of the systems include the solar cells, reflectors, reflector supports, PCM containers, aperture cover and support frame. Most parts of all systems were fabricated and fully assembled at Simon Perry Building (Civil Engineering Department) at Trinity College Dublin. The material selection for the different components, and the individual component design and fabrication of the systems are described in the following sections.

6.1 Design details for CPC systems for Ferrara, Italy

6.1.1 Design and material selection for reflector support and backplate

The reflector supports and back plate were designed for the CPC structure. Table 6.2 illustrates the material options for the reflector supports and backplate for the CPC structure, comparing plywood with other potential materials such 3D printed plastic, aluminum and steel.

Table 6. 2 Material selection for reflector support and backplate for CPC system; advantages and disadvantages

Material	Advantages	Disadvantages
Plywood	- Easy to work with - Ease of manufacturing at large scale with external company - Lightweight - Cost-effective	- Susceptible to moisture and weather damage - Less durable compared to metal - Can warp or deform over time
3D Printed Plastic	- Customizable and design precision - Rapid prototyping	- Limited structural strength - Expensive for large-scale production
Aluminum	- Good thermal conductivity - Lightweight - Durable and resistant to weather	- Potential for warping or deformation - Higher cost compared to plywood - More difficult to work with for fabrication
Steel	- Good thermal conductivity - High strength and durability - Resistant to weather	- Requires specialized equipment for manufacturing - Heavy in weight - Higher cost compared to plywood - Requires specialized equipment for manufacturing

Plywood was chosen for the reflector supports sections due to its ease of use, light weight, cost-effective and compatibility with large-scale manufacturing. While aluminum and steel offer better durability and weather resistance, they come with higher costs, increasing weight (especially steel), and a more complex fabrication process. 3D printed plastic can be customized and allows for rapid prototyping, but may not have the structural strength required for large scale production and can also be expensive and prone deformation. For the backplate, the material selected was aluminum due to its good thermal conductivity, which helps with heat dissipation to maintain the system efficiency. Plywood and aluminum for the CPC structural sections have advantages such as ease of use, low weight, cost-effectiveness and manufacturing compatibility. Three plywood reflector supports, corresponding to the

top, middle and bottom reflector (figure 6.1) were designed. These supports had a thickness of 25 mm to ensure sufficient strength and rigidity for the bonding and bending surfaces. To provide the base for the solar cell, a back plate was designed using aluminum of 5 mm thickness. Dimensions of the back plate were 1693 X 1123 mm and the detailed design of the aluminum back plate is shown in figure 6.2.

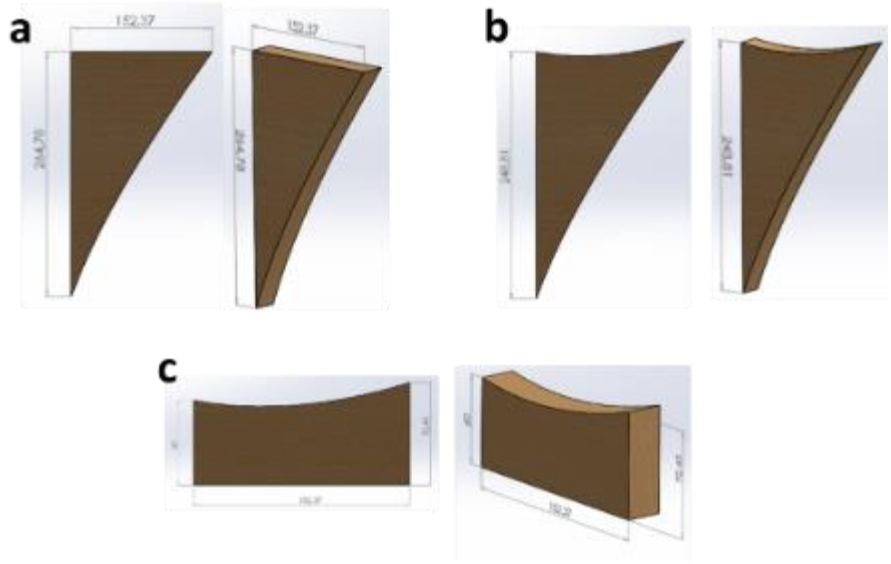

Figure 6. 1 Detail design for top, middle and low reflector support in Solidworks
(a) Top Reflector Support, (b) Middle Reflector Support, (c) Bottom Reflector Support

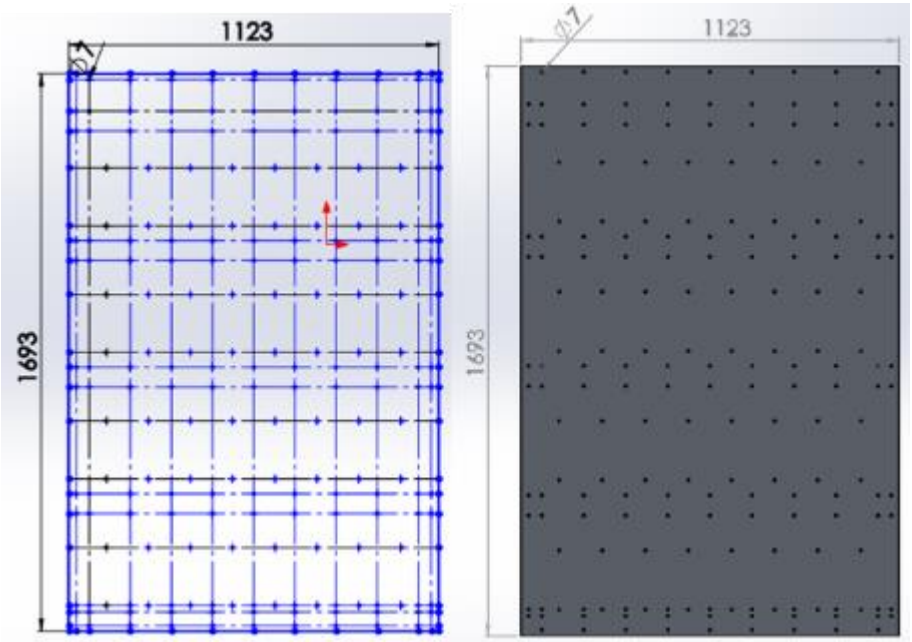

Figure 6. 2 Detail design of aluminium back plate in SolidWorks

6.1.2 Design and material selection for the cover and frame

The method used for this section was the same as that employed for the small scale prototype described in section 5.1. Low iron glass (1659 X 1077 mm) was used along with Perspex for the side elements of the frame with 15 mm and 20 mm thickness to provide strength and secure the glass in the system. The detailed design of the frame structure is shown in figure 6.3.

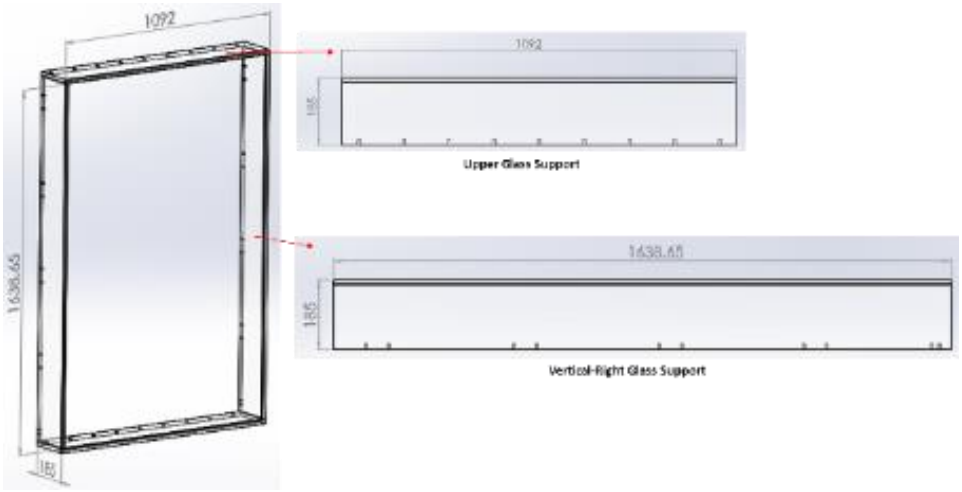

Figure 6. 3 Detailed design of the frame structure in SolidWorks

6.1.3 Final design for CPC systems for Ferrara, Italy

Design of the CPC Systems to be manufactured for Ferrara are shown in figure 6.4 and the reference system used for the comparison is shown in figure 6.5.

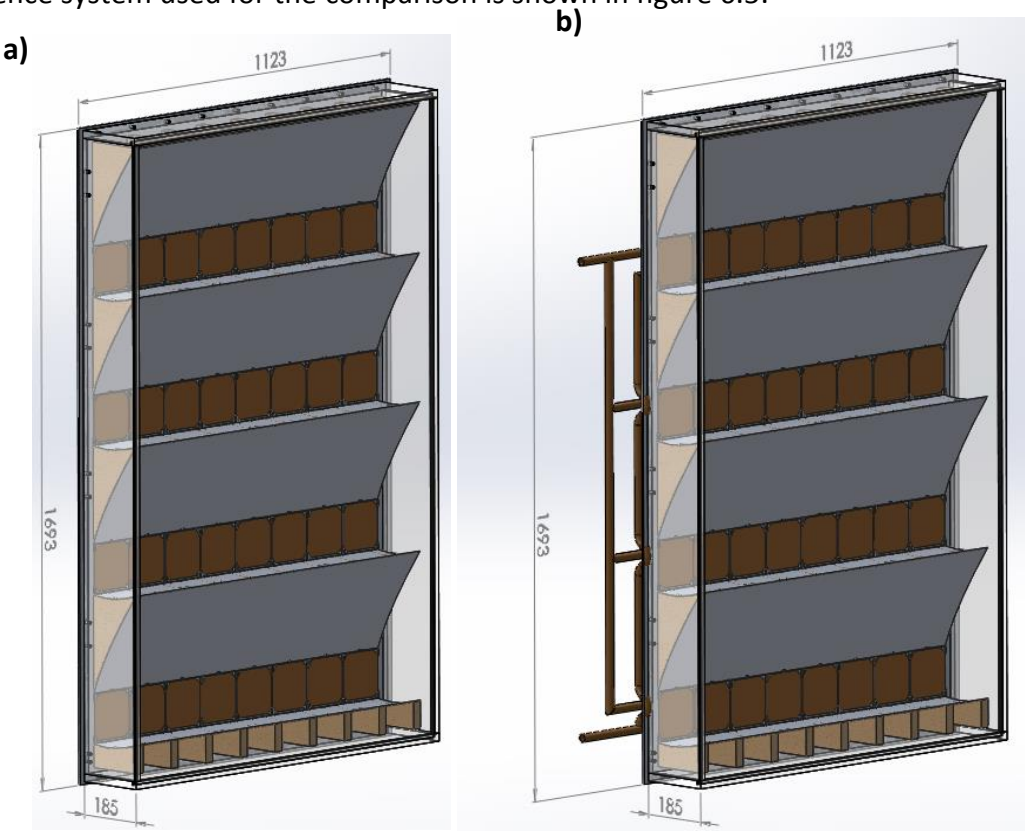

Figure 6. 4 CPC Systems designs for Ferrara

(a) CPC system (b) CPC/PCM system

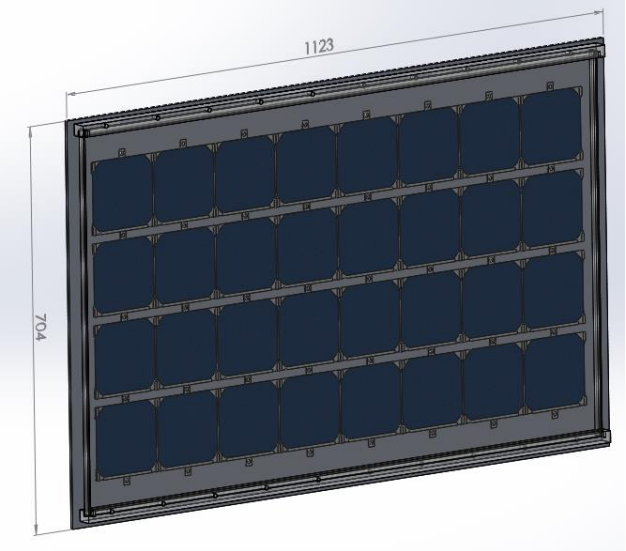

Figure 6. 5 Reference design for Ferrara

6.2 Manufacturing process for CPC system for Ferrara, Italy

6.2.1 Manufacturing for solar cell holders

One hundred and six solar cell holders were printed using 3D printers described in section 5.1.2. The total printing time was 160 hours distributed in 10 hours each day for 16 days. 3.5 Kg of ABS printing filament was used in total. A full string of eight solar cell holders is shown in figure 6.6.

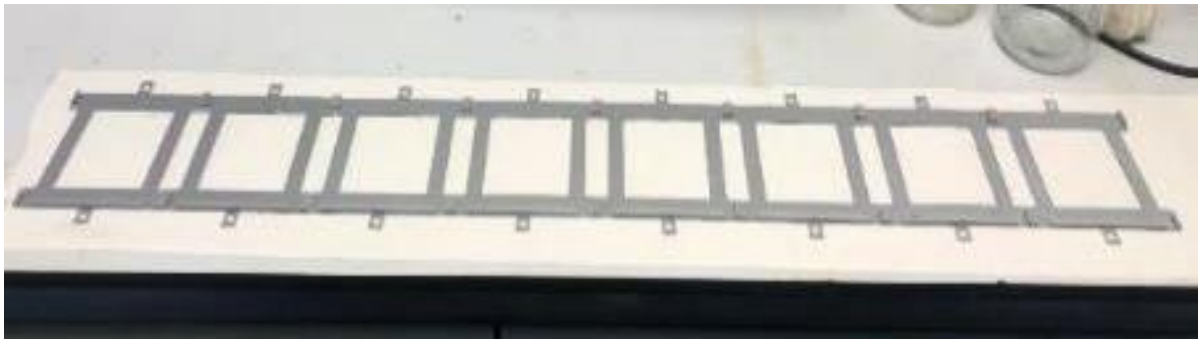

Figure 6. 6 Full string of eight solar cells holders

6.2.2 Reflective material selection

Alanod Miro Sun reflect material as described in section 5.1.1 was used. The reflector section dimensions are presented in table 6.3.

Table 6. 3 System reflector dimensions

CPC System	Reflector dimension	Quantities	Reflector Area
Top Reflector	308 X 1024 mm	1	0.32 m^2
Middle Reflector	463 X 1024 mm	3	1.42 m^2
Low Reflector	155 X 1024 mm	1	0.15 m^2
		TOTAL	**1.89 m^2**

6.2.3 External manufacturing

After designing the systems components as previously described, the wooden reflector supports, aluminium backplate, Perspex frame sections and reflector sections were produced by external companies

For the reflector supports and backplate, the pieces were designed using Autocad and Solidworks and produced by Aqua Design (Kerry, Ireland). For the top, middle and lower reflector supports, 9, 27 and 9 pieces respectively were manufactured in total for each CPC system. The dimensions of the back plate were 1693 X 1123 mm and 192 holes of Ø 7 mm were machined to fix the support reflectors, solar cell holders and frame. Figures 6.7 and 6.8 show the backplate and reflector supports.

Figure 6. 7 Aluminum backplate from Aqua Design Company

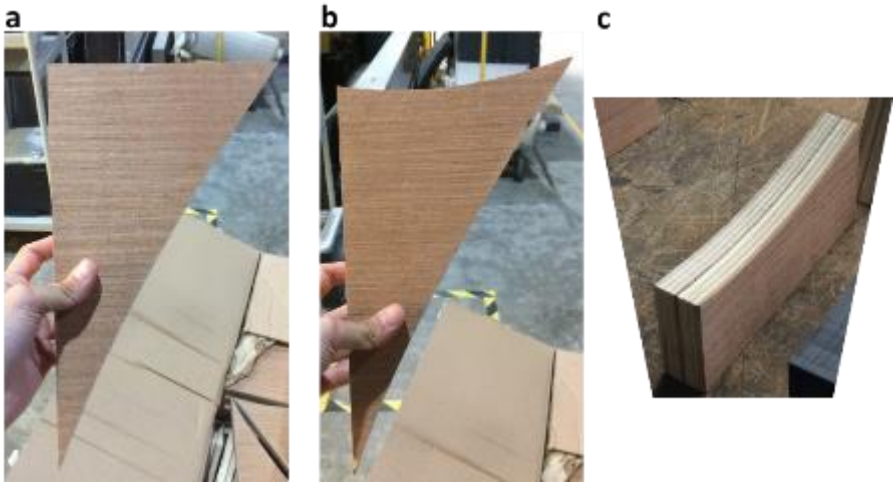

Figure 6. 8 Plywood reflector supports from Aqua Design

Clear Polycarbonate sheets of 15 and 20 mm thickness were used for the frame of the CPC system (Plastic 365) (Dublin, Ireland). Each individual reflector sheet dimension of 1250 X 2000 mm was cut using a 1250 mm wide guillotine. The cuts were made according to the dimensions of the required reflectors as in table 6.3. The guillotine is shown in figure 6.9.

Figure 6. 9 Guillotine used for cutting Alanod reflectors

6.2.4 Parabolic reflectors

The same process as described in section 5.1.4 was used. The dimensions are shown in table 6.4.

Table 6. 4 Pieces dimension for the reflector shape

CPC System	Reflector dimension	Quantities
Top Reflector	308 X 262 mm	8
Top Reflector	308 X 250 mm	8
Low Reflector	154 X 262 mm	8
Low Reflector	154 X 250 mm	8

6.2.5 Solar cells interconnection and pre test

The solar cell interconnection process was used as presented in section 3.7. Four strings of eight solar cells with LDS coatings were used for each Ferrara system. Details of the LDS manufacturing process was explained in section 3.2.

A voltmeter was used to measure voltage of each connected string. A summary of the voltage values taken during connection for the Reference, CPC and CPC/PCM system are shown in the figures 6.10, 6.11 and 6.12 respectively.

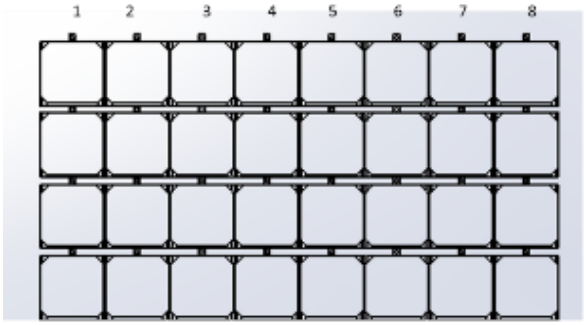

Voltage checking for REFERENCE SYSTEM (V)	
String	Voltage (V)
1	4.91
2	4.93
3	4.92
4	4.87
	19.63

Figure 6. 10 Voltage control during solar cell connection. Reference System

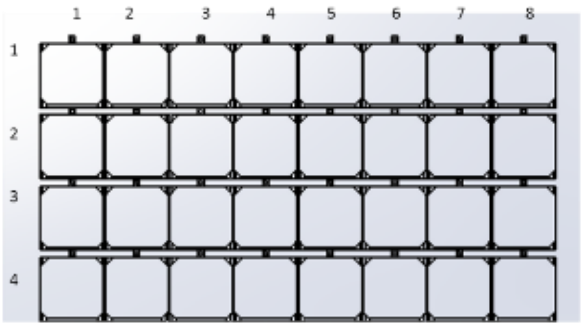

Voltage checking for ALPHA SYSTEM (V)	
String	Voltage (V)
1	4.91
2	5.37
3	5.40
4	5.38
	21.06

Figure 6. 11 Voltage control during solar cell connection. CPC System

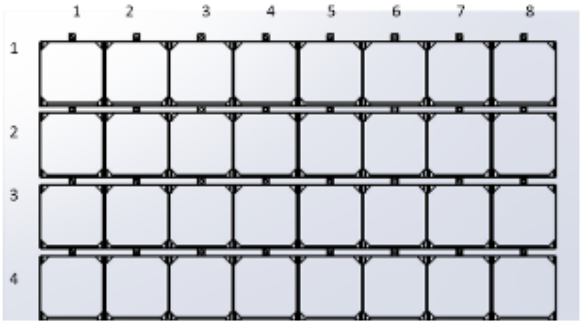

Voltage checking for OMEGA SYSTEM (V)	
String	Voltage (V)
1	5.34
2	5.36
3	5.38
4	5.37
	21.45

Figure 6. 12 Voltage control during solar cell connection. CPC/PCM System

6.3 Assembly process for CPC, CPC/PCM and Reference systems for Ferrara, Italy

Figure 6.13 presents a process flow chart to provide an overview of the assembly process for the systems designed and manufactured for Ferrara, Italy. The chart outlines the sequential steps involved in creating and integrating the various components of the systems, ensuring that they function effectively and efficiently. The assembly process begins with the creation of solar cell strings and progresses through to the addition of reflector supports and auxiliary plates, gluing of Alanod reflectors, frame assembly, electrical connections, and PCM container

integration. The final step in the process was packaging and shipping the completed systems to their destination in Ferrara. Each step is described in this section.

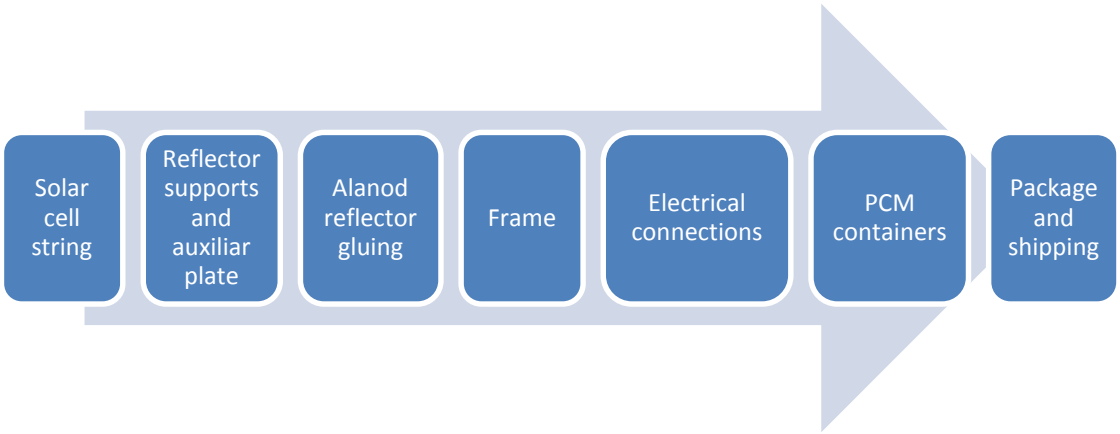

Figure 6. 13 Assembly process flow chart for Ferrara systems

For the solar cell string assembly, insulating tape was placed on the backplate in the dog bone section to avoid any contact between the connectors and the backplate. Strings of solar cells and LDS coatings were placed in solar cell holders and were installed on the backplate using screws. White paper was used and placed on top of the solar cells in order to protect them from dust or other debris during the assembly process. Figure 6.14 shows the final location of each string on the backplate.

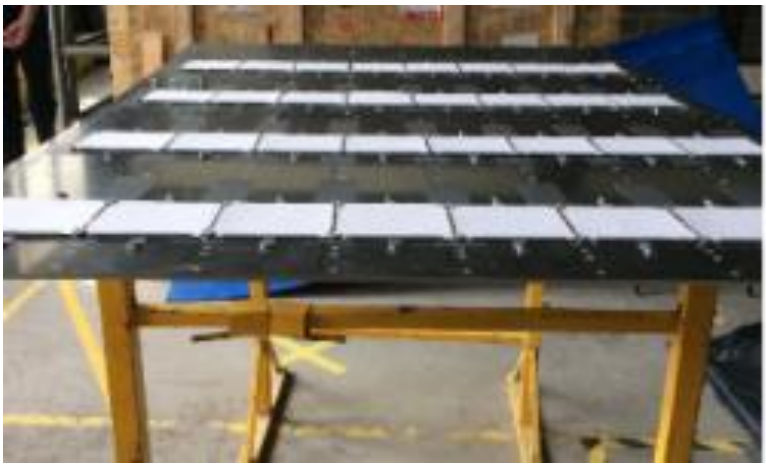

Figure 6. 14 Final location of the four strings of solar cells on the backplate

Each reflector support was attached to the backplate using Ø7mm, 30mm long wood screws. In order to avoid short circuit, the blocks were placed leaving 2mm distance from the strings of solar cells. Figure 6.15 shows the installed reflector supports.

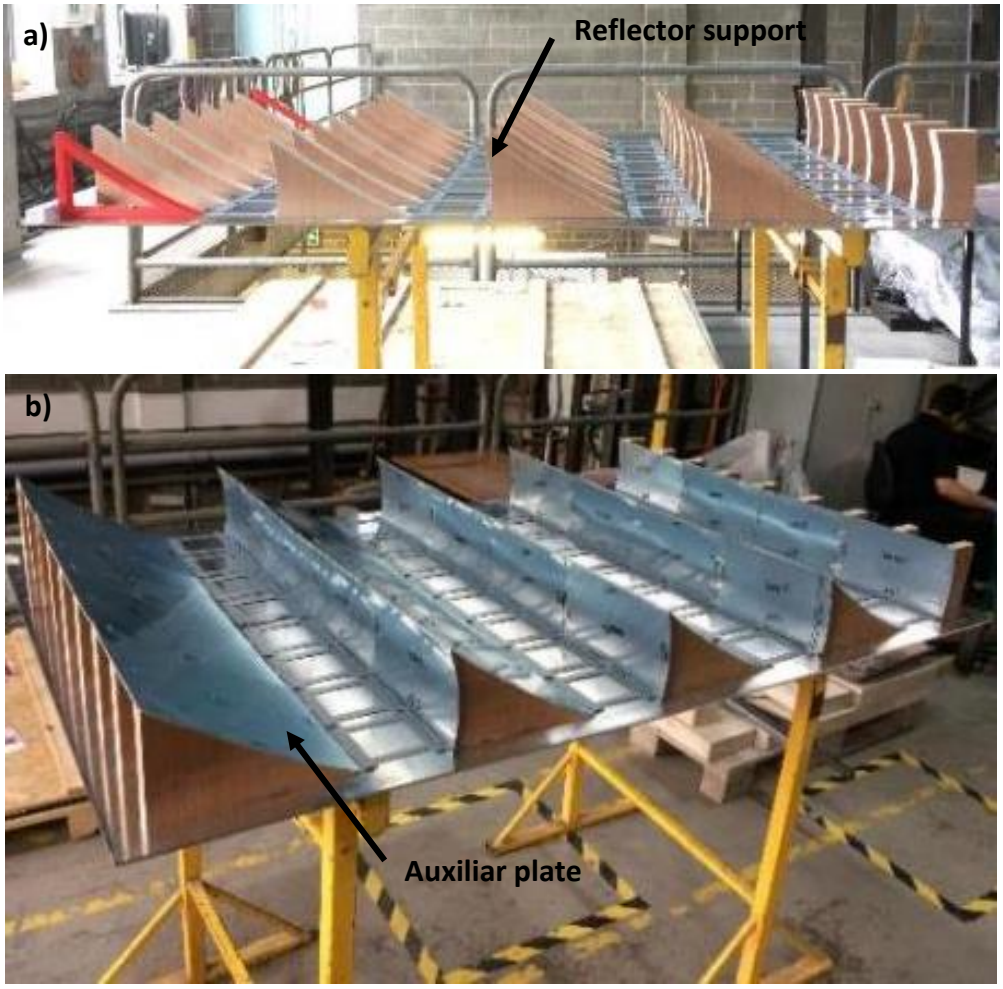

Figure 6. 15 (a) Reflector supports installed on the backplate (b) Final installation of the reflector supports with the auxiliary plate

The same procedure outlined in section 5.1.4 was used for the gluing process. Figure 6.16 shows (a) the auxiliary plate cleaned, (b) super glue sprayed on the auxiliary plate, (c) Alanod reflector installed. The reflector blocks were carefully placed on the backplate. Extreme care was taken so as not to damage any solar cells during the process. After that, the reflective blocks, solar cell strings, and backplate were left ready for the next step of the assembly process. Figure 6.16 shows the three installations carried out.

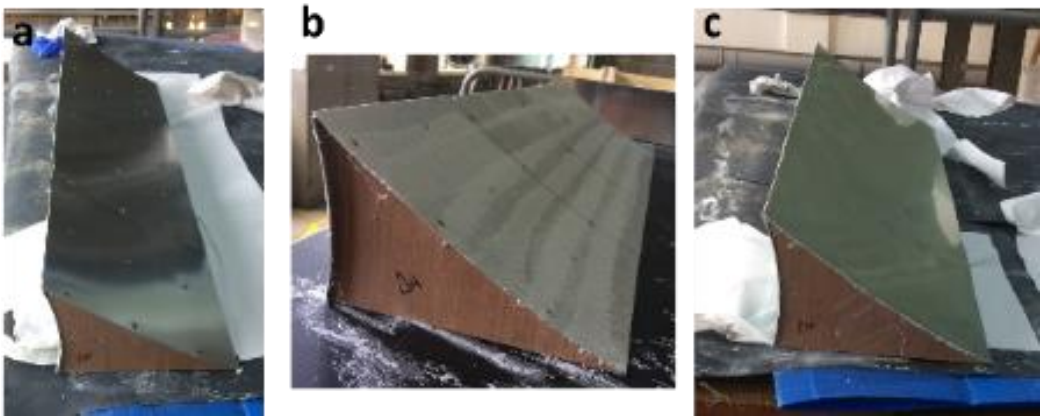

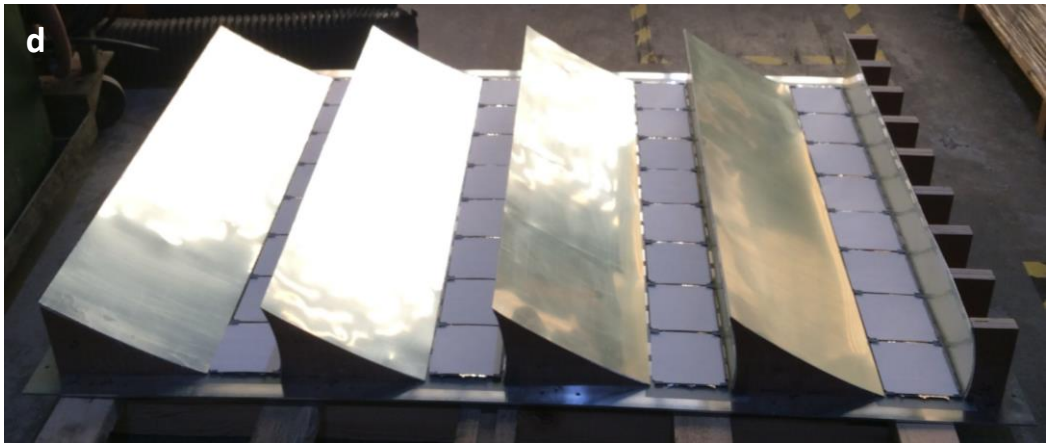

Figure 6. 16 Alanod reflector gluing process
(a) Cleaning process (b) Super glue sprayed (c) Alanod reflector installed (d)Reflector blocks, solar cells strings and backplate, full assembled

The CPC system frame was secured to the backplate using screws with a diameter of 7 mm and a length of 30 mm. The horizontal frames were first positioned and fastened to the backplate, followed by the vertical frames, which were attached to both the backplate and the horizontal frame to enhanced stability. Figure 6.17 illustrates the fully installed framework within the CPC system.

Figure 6. 17 Frame installed in the CPC System

The connection between the solar cell strings was done in series. For this, 2 mm^2 of electric cable was used in order to handle the 6 A of current. Two cables, one positive and one negative remained for testing purposes. The final cables were connected to a terminal block, in order to give security to the cables when the external connection is produced. In order to protect the solar cells from hot-spot phenomena (described in section 5.2), a PV solar junction box IP65 with 3 diodes for solar panel 100 W - 180 W was installed on top of one of the frames of the CPC System. Two pairs of 3 m solar cable 4 mm^2 were connected to the bypass diode

box. At the end of each solar cable, MC4 male and female connectors were installed for final testing. Figure 6.18 (a) shows the internal connections between the solar cell strings and terminal block and (b) shows the bypass diode box along with the solar cables installed.

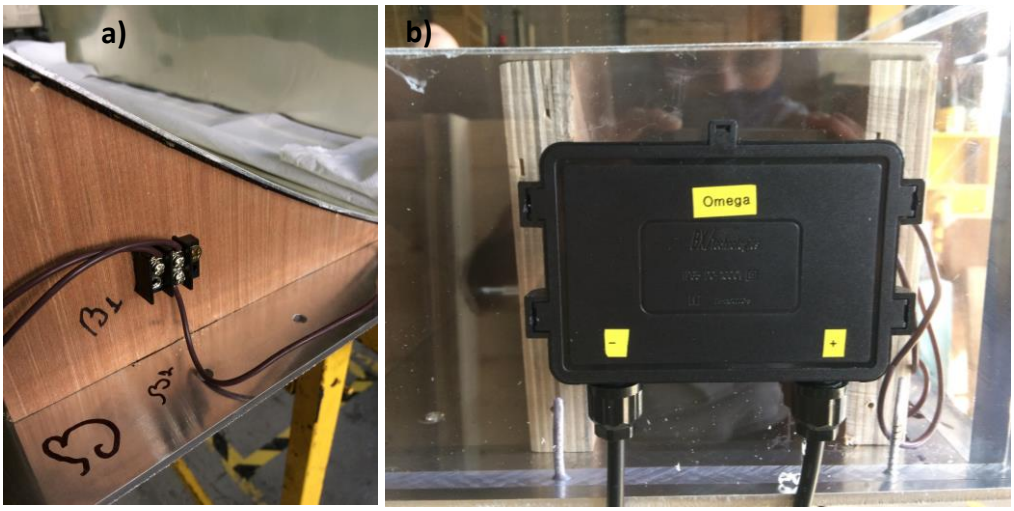

Figure 6. 18 (a) Internal connections between the solar cell strings and terminal block (b) Bypass diode box

The PCM containers were provided by the Ulster University as part of IDEAS Project. Details of the PCM containers were described in section 3.2. The set of containers was placed exactly at the location of the solar cells on the backplate. A perfect contact without air gap is necessary between the PCM containers and the backplate in order to ensure good heat transfer. For this, two square bars of 25 X 25 mm and 4 mm thick were placed in the back of the containers, leaving the containers in the middle between the backplate and the bars. Five round threaded rods Ø 7 mm and 100 mm long were inserted into each square bar and passing through the backplate, so that the end of these parts is inside the CPC system. Two nuts were placed between the inside of the backplate and the rear of the bars. Each nut was turned so that they exert pressure on the bars, using a clamp in order to press the containers against the backplate. The system of square bars installed with the PCM containers for CPC/PCM for Ferrara is shown in figure 6.19.

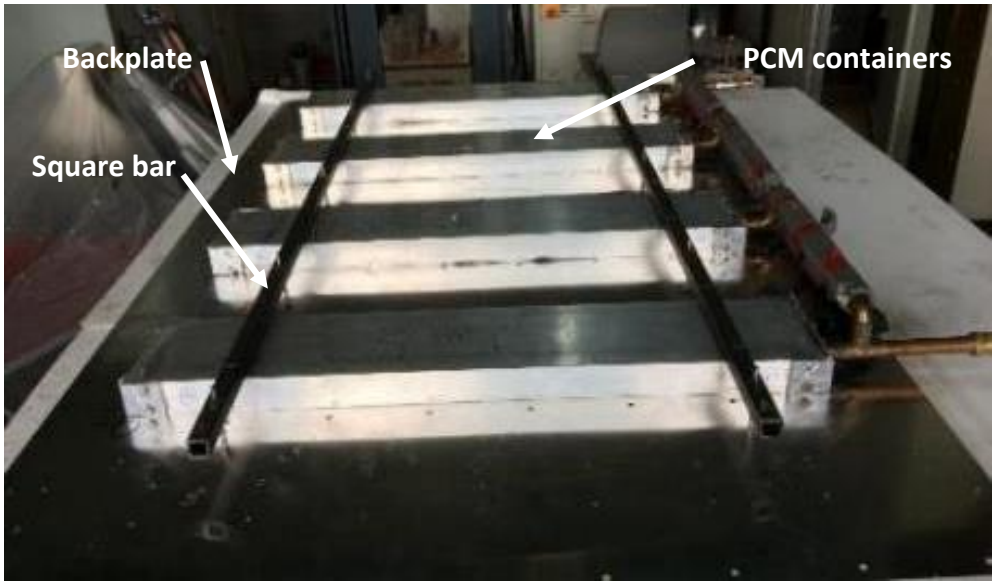

Figure 6. 19 PCM containers installed in the backplate

In order to complete the assembly of the CPC System, the last piece to be installed was the glass. The left vertical frame was removed from the backplate and the low iron glass was carefully slid through the slots made in the frames. Then the vertical section was replaced. To avoid condensation within the systems, four packets of desiccant were placed at the bottom of each CPC System. Figure 6.20 show the final assembly of a CPC System.

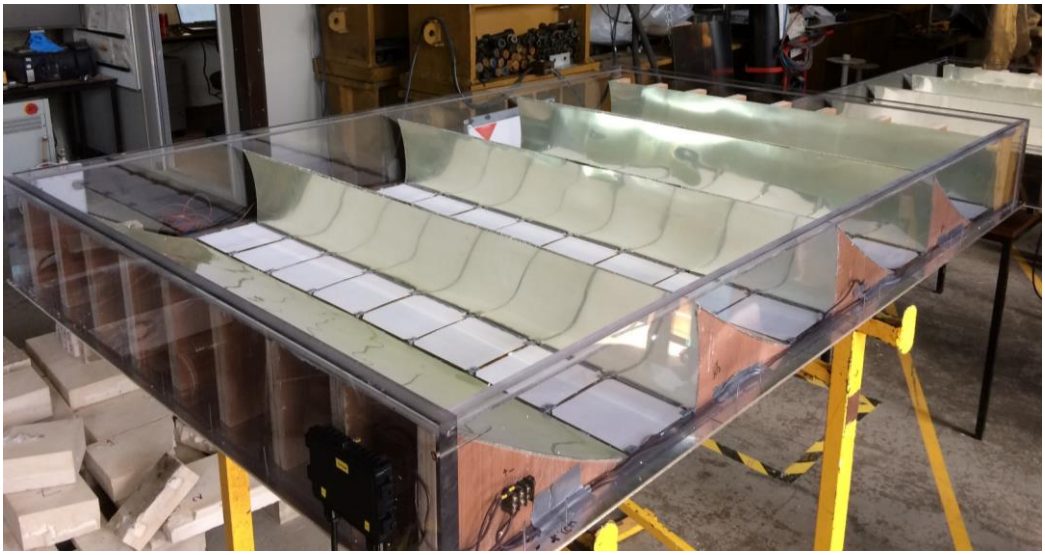

Figure 6. 20 Final assembly of one CPC System for Ferrara

For the CPC/PCM system, in order to prevent heat dissipation from the containers, insulating foam was placed on the exposed edges of the PCM containers. Polyiso under floor insulation of 40 mm thick was used for this process as shown in figure 6.21.

Figure 6. 21 Insulation installed in the PCM containers

A similar assembly process was performed for the PV reference system with the difference that reflectors were not used. The size of the pieces such as backplate (704 X 1126 mm), low iron glass (665 X 1072) and frames (20 X 25 X 1092 mm and 4 X 11 X 665 mm) were reduced. The electrical connection process was the same as described in section 3.7, and the same number of solar cells were used as in the CPC systems in order to make a fair comparison of the electrical behavior. The finished reference is shown in figure 6.22.

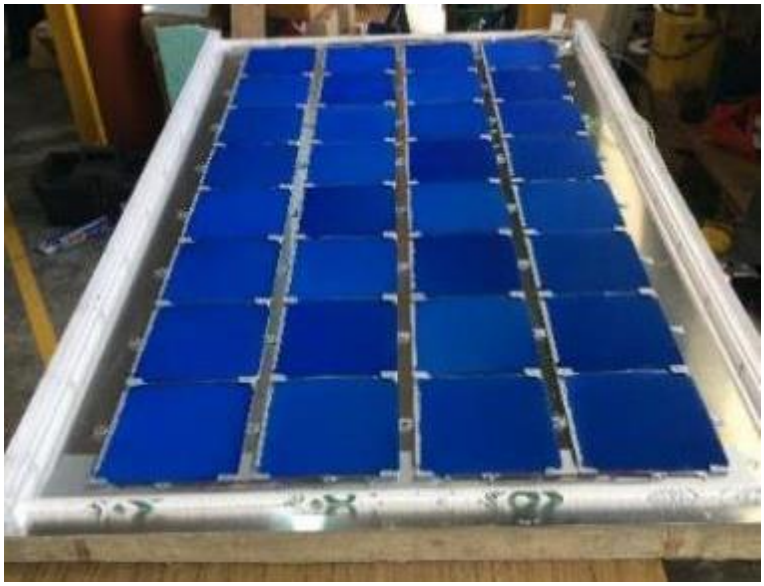

Figure 6. 22 PV Reference System fully assembled

The manufactured systems were shipped to Ferrara in crates manufactured and supplied by Precision Box with the following dimensions:

- 1 Crate for CPC: 1693 X 1123 X 190 mm

- 1 Crate for CPC / PCM: 1693 X 1126 X 245 mm
- 1 Crate for Reference: 704 X 1123 X 30 mm
- 1 Crate for Glasses: 2 Glasses of 1658 X 1077 X 4mm & 1 Glass of 665 X 1072 X 4mm

Each system was carefully placed inside a crate using a crane. The crates were sealed and placed inside the truck for transportation to Italy as shown in 6.23 (a and b)

Figure 6. 23 (a) Crates used for transportation to Ferrara (b) Truck in charge of transportation containing all systems

6.4 Design details for CPC systems for Mayo, Ireland

Using the same methodology as for the Ferrara systems, components for the Mayo systems were designed. New designs were required for the reflector support (as explained in section 4.1.3), the cover and frame were manufactured as in sections 6.2.2 - 6.2.5. In order to improve the performance of the Mayo systems, design changes were made:

1. Removal of 3D printed solar cell holders and addition of encapsulation: The 3D printed solar cell holders were removed because they began to warp under high temperatures, leading to the breakage of some solar cells. Encapsulation was added to provide better protection and stability for the solar cells in high-temperature concentrating conditions.

2. Improved surface contact between solar cells and PCM containers: A hole was created in the backplate of the CPC/PCM system, with dimensions matching those of the PCM containers. This allowed the solar cells to be placed directly on top of the PCM containers, improving thermal contact and heat transfer.

3. Vents for condensation prevention: Vents were added to the system to prevent condensation on the front glass of the systems, as the bags of desiccants were insufficient for this purpose. These vents allowed for better air circulation and moisture control within the system, reducing the likelihood of condensation-related issues.

4. Addition of thermocouples: Thermocouples were integrated into the three systems to gather more information about temperature variations within the systems. This data can be used to optimize the performance of the solar cells and the PCM materials, as well as to identify potential areas for further improvements.

5. Solar cells without LDS: Solar cells without luminescent down-shifting (LDS) layers were used due to the rapid degradation observed in the LDS layers. A separate PhD study is being conducted to improve the technology and address the degradation issues, with the aim of eventually reintroducing LDS layers into the systems for enhanced performance.

The dimensions of the aluminum back plate were 1321 x 1123 mm with 5 mm thickness and 102 holes of Ø7 mm were machined to fix the support reflectors and frame. Three holes were machined in the backplate with the dimensions corresponding to the PCM containers, in order to fit the containers in the backplate and thus encapsulate the string cells on them. Figure 6.24 shows the schematic manufacturing design of the new backplate for the CPC/PCM system. First, the PCM containers were placed on the backplate at the height of the solder cells, then the size and shape of the containers were drawn in Autocad and sent to Aqua design so that they could manufacture the backplate.

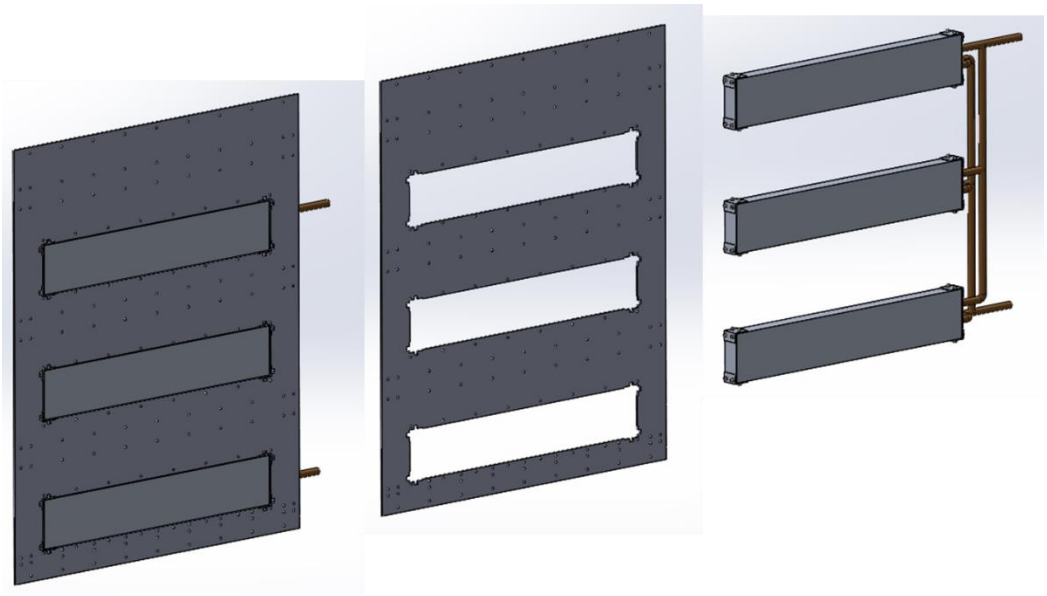

Figure 6. 24 Schematic design of the backplate corresponding to CPC/PCM system for Mayo

The design of the CPC Systems to be manufactured for Mayo are shown in figure 6.25 (a-c).

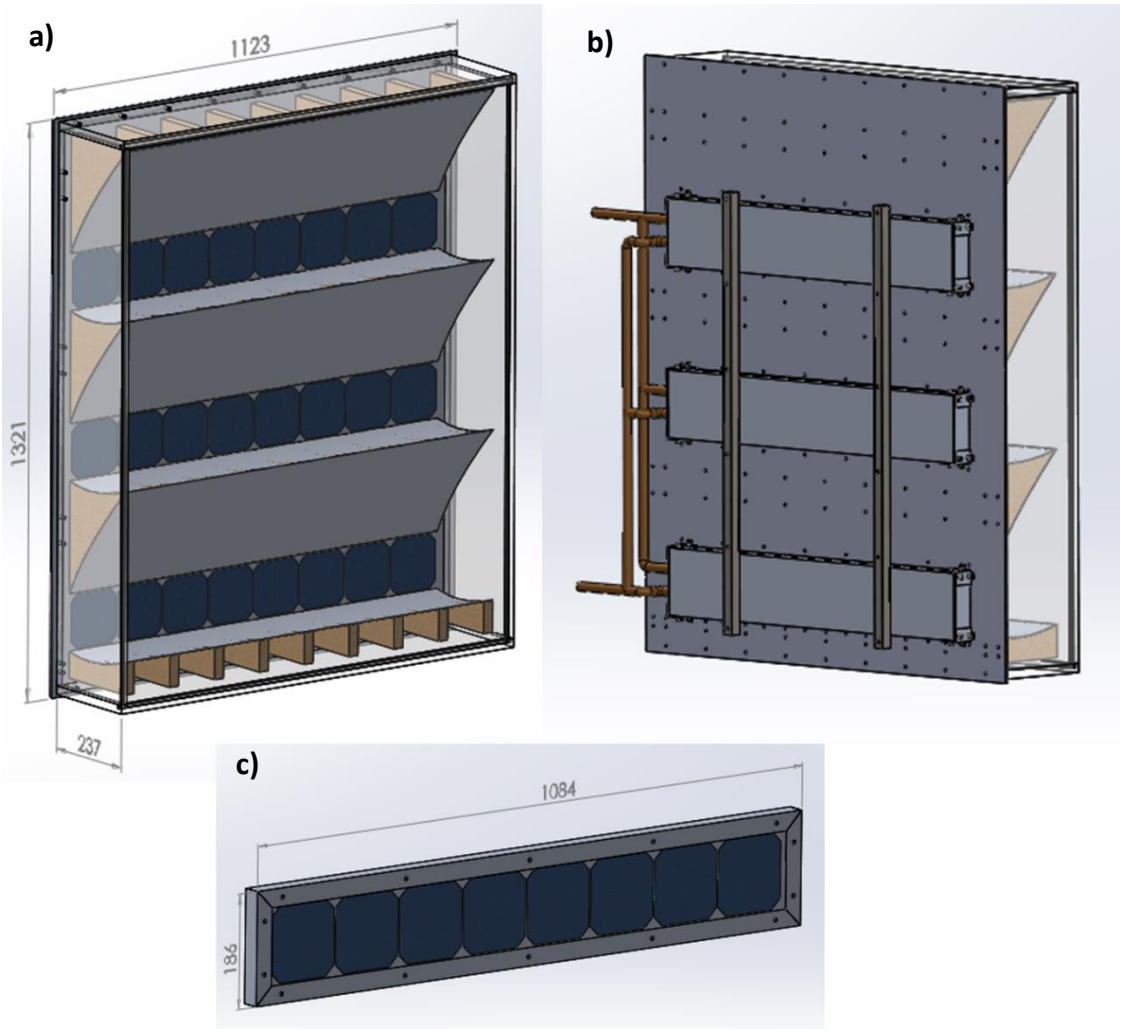

Figure 6. 25 CPC systems designs for Mayo
(a) CPC system (b) CPC/PCM system (c) Reference system designs for Mayo

6.5 Manufacturing process for CPC system for Mayo, Ireland

The same methodology was used for the Ferrara systems; the different parts of the Mayo systems were manufactured as described in sections 6.2.2 to 6.2.5. To attach the solar cells in the CPC systems for Mayo the encapsulation process described in section 3.7 was used. The complete backplate corresponding to the CPC system encapsulated with three solar cells strings is shown in figure 6.26.

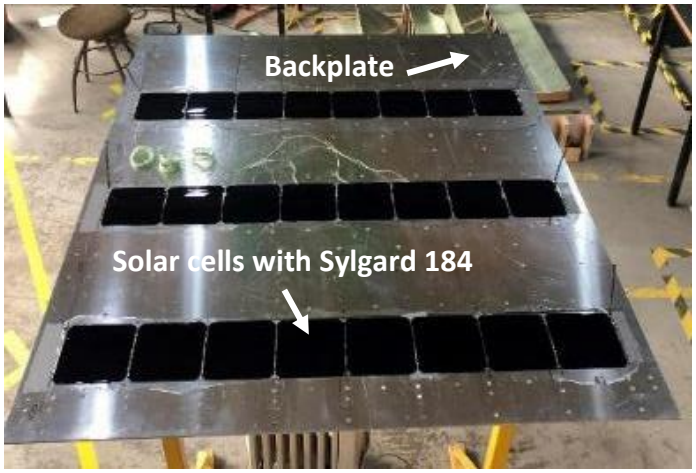

Figure 6. 26 Solar cell encapsulation process and CPC system with solar cells encapsulated

The process of fitting the PCM containers and the backplate corresponding to the CPC/PCM system is shown in figure 6.27. The PCM containers were installed in the backplate holes and carefully levelled so that the top of the containers met the backplate to form one single piece. Then the same fixing process as described in section 6.3 was used. Silicone was added to the edges in order to avoid air gaps and the introduction of water into the system. It was left to dry for 24 hours and then was ready for the encapsulation process.

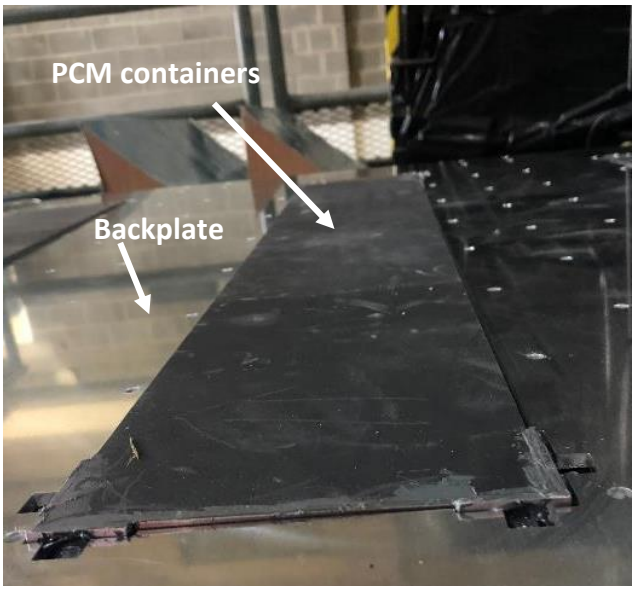

Figure 6. 27 CPC/PCM backplate with PCM containers fitting process

The complete encapsulation of the solar cells in the backplate of the CPC/PCM system can be seen in figure 6.28. The distinction between Figure 6.26 and 6.28 lay in the fact that Figure 6.26 displayed the solar cells encapsulated in the backplate, whereas Figure 6.26 illustrated the solar cells encapsulated in the PCM containers, which were affixed to the backplate. The containers were situated behind the solar cells. Figure 6.29 shows the Reference system with the encapsulated solar cells.

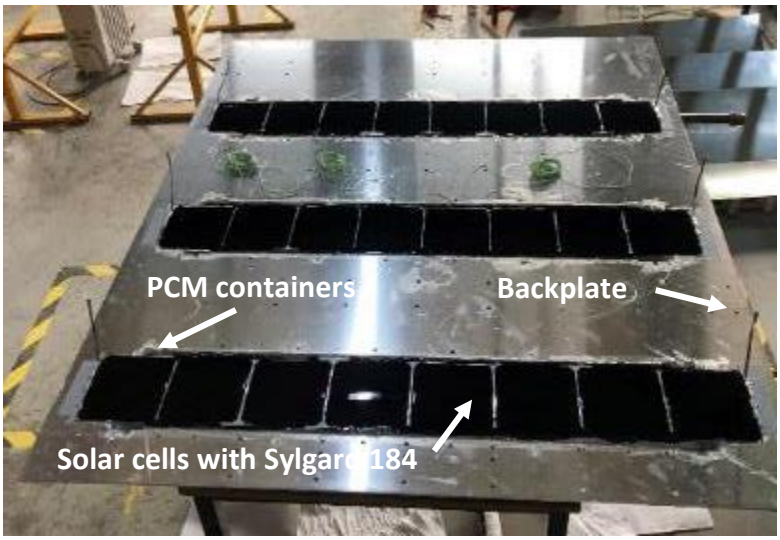

Figure 6. 28 CPC/PCM system with solar cells encapsulated

Figure 6. 29 Reference system with solar cells encapsulated

Twenty-eight "K" type thermocouples (chromel-alumel) were used for thermal analysis of the CPC, CPC/PCM and Reference systems for Mayo. The same approach as described in section 3.5 was used. The thermocouple distribution in each system is presented in table 6.5. Figure 6.30 (a) and (b) show the thermocouple location in the back of the solar cells, back of the reflector (left) and the location in the backplate (right) for the CPC and CPC/PCM systems respectively. Figure 6.30 (c) shows the thermocouple locations in the back of the solar cells (top) and the location in the backplate (bottom) for the Reference system.

Table 6. 5 Thermocouples distribution in systems for Mayo

System	Solar cell	Back plate	Top Refl.	Bottom Refl.	Back PCM Container	Pipe Top	Pipe Bottom	Total
CPC	3	3	2	2	-	-	-	10
CPC/PCM	3	-	2	-	3	1	1	12
Reference	3	3	-	-	-	1	1	6

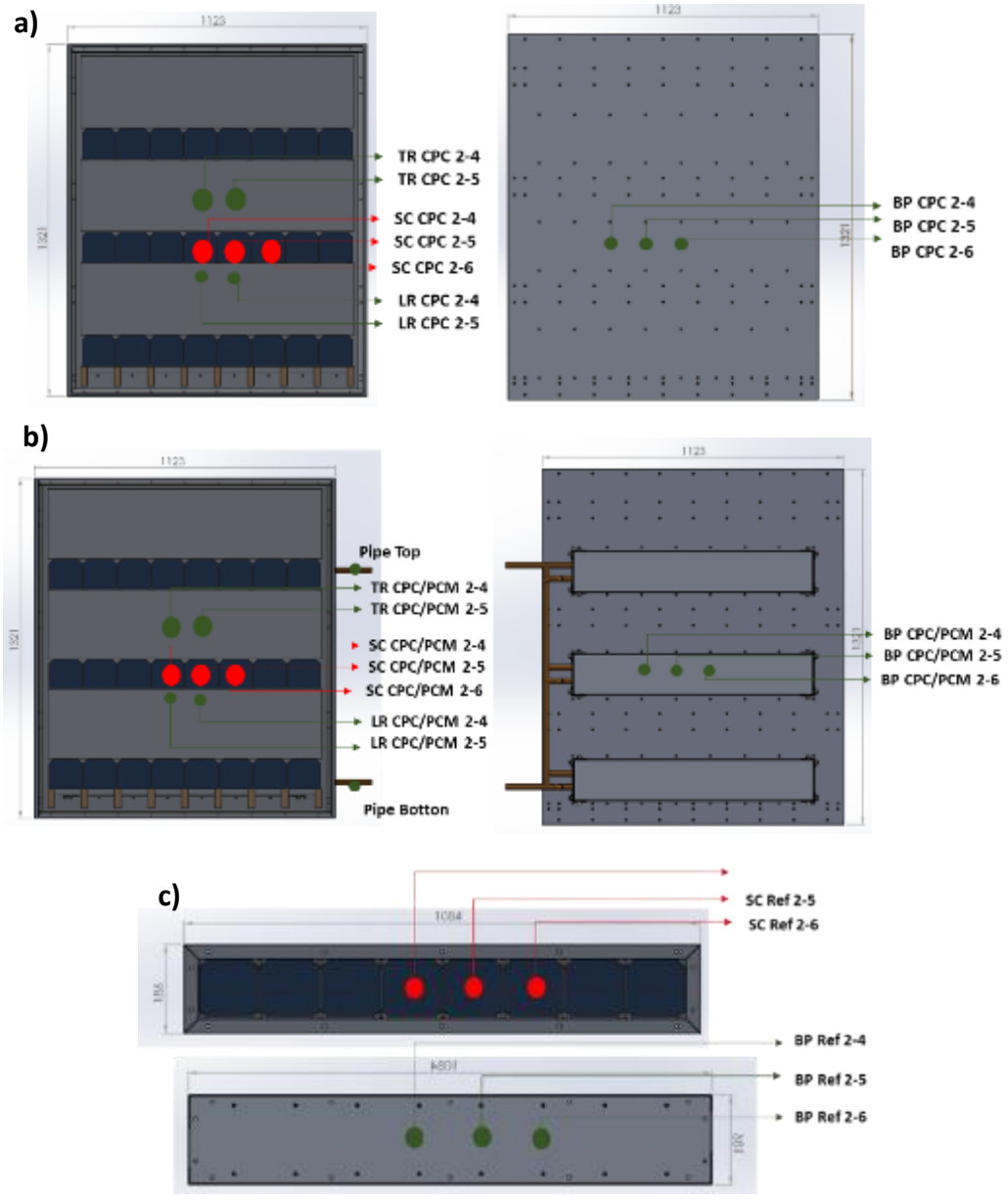

Figure 6. 30 (a) Thermocouples location for CPC system (b) CPC/PCM system (c) Reference system

6.6 Assembly process for CPC, CPC/PCM and Reference systems for Mayo, Ireland

The assembly process of the CPC, CPC/PCM and Reference systems for Mayo follows the same methodology described in section 6.3. The fully assembled CPC, CPC/PCM and reference systems are shown in figures 6.31 (a-c) respectively.

Figure 6. 31 Mayo Final system assembly
(a) CPC system (b) CPC/PCM system (c) Reference system

Table 6.6 delineates a detailed comparison of the weights associated with various solar systems implemented in Ferrara and Mayo. Weighing in at 73 Kg, the Ferrara CPC system tipped the scales slightly heavier than its Mayo counterpart which came in at 65 Kg. When PCM containers were integrated into the system, resulting in a CPC/PCM setup, an increase

in the overall weight was observed, amounting to 88 Kg for the Ferrara system and 76 Kg for the Mayo system. This weight increase can be attributed to the PCM containers, contributing an additional 15 Kg and 11 Kg respectively. Conversely, the reference systems were significantly lighter, weighing 19 Kg in Ferrara and a mere 3.7 Kg in Mayo, a reflection of their simpler design and fewer components.

The weight reduction, through the use of alternative materials should not be overlooked. The selected materials for the current design was dictated by specific properties required for research and testing, and for their ease of manipulation in a laboratory setting. In a commercial context, lighter weight materials could be explored to balance system performance with efficiency and effectiveness, potentially leading to improvements in areas such as transportability and ease of installation. This could open up wider application possibilities for these systems.

Table 6. 6 Resume of weight for Ferrara and Mayo systems

System	System weight (Kg)	
	Ferrara	Mayo
CPC	73	65
CPC/PCM	88	76
PCM Containers	15	11
Reference	19	3.7

Table 6.7 outlines the cost associated with the construction of the CPC systems in Ferrara and Mayo. The cost for constructing a CPC system was higher in Ferrara, amounting to 1254 euros, compared to Mayo, where the cost was 1116 euros. These costs reflect the expenses associated with materials, manufacturing, and assembly of the systems. The discrepancy in cost between the two locations was attributable to the variations in the system designs that. It is also worth noting that these costs represent the expenses in a research setting, and could potentially be reduced in a commercial or industrial scenario with larger-scale production.

Table 6. 7 Resume of cost for Ferrara and Mayo CPC system

System	Cost (€)/system	
	Ferrara	Mayo
CPC	1254	1116

6.7 Conclusion

A tailored design and fabrication method was developed to produce two groups of systems for two different locations: Ferrara, Italy and Mayo, Ireland. The following table 6.8 presents the systems designed and manufactured for each location, along with the manufacturing techniques and design changes:

Table 6. 8 Final large scale systems designed and manufactured for Ferrara and Mayo

Location	System Type	Description	Manufacturing Techniques & Changes
Ferrara, Italy	CPC System	Concentrating compound parabolic concentrator with 32 solar cells in series	- Standard manufacturing techniques - Use of LDS coating
	CPC/PCM System	CPC with PCM containers at the back of the solar cells; 32 solar cells	- Addition of PCM containers - Use of LDS coating
	Reference System	Flat non-concentrating panel with 32 solar cells in series	- Non-concentrating configuration - Solar cells without LDS
Mayo, Ireland	CPC System	Concentrating compound parabolic concentrator with 24 solar cells in series	- Reduced number of solar cells - Removal of 3D printed solar cell holders - Addition of encapsulation - Vents for condensation prevention - Addition of thermocouples - Solar cells without LDS
	CPC/PCM System	CPC with PCM containers at the back of the solar cells; 24 solar cells	- Reduced number of solar cells - Addition of PCM containers - Improved surface contact with PCM containers - Removal of 3D printed solar cell holders - Addition of encapsulation - Vents for condensation prevention - Addition of thermocouples - Solar cells without LDS
	Reference System	Flat non-concentrating panel with 8 solar cells in series	- Non-concentrating configuration - Reduced number of solar cells - Removal of 3D printed solar cell holders - Addition of encapsulation - Vents for condensation prevention - Addition of thermocouples - Solar cells without LDS

Chapter 7 Experimental characterization of CPC systems for Ferrara and Mayo

The concentrators and Reference systems as presented in table 6.6 were characterised in outdoor conditions in two different locations: Ferrara, Italy and Mayo, Ireland over a period of 4 – 5 months to determine the performance. For Ferrara, the systems were characterized from August to December 2021 and for Mayo from July to October 2022.
The results were analyzed in terms of the following parameters described in Chapter 2:

- Power output
- Solar cell temperatures
- Power ratio
- Fill factor
- Solar cell efficiency
- Optical efficiency
- System efficiency

7.1 Performance for CPC, CPC/PCM and References systems for Ferrara, Italy

The outdoor experimental performance of the systems was monitored using the devices described in section 3.5.

The CPC and CPC/PCM systems had been fitted with LDS layers, with the manufacturing procedures having been detailed in Section 3.2, and the installation process depicted in Section 3.7. Regrettably, upon exposure to the environmental elements, the LDS layers underwent rapid degradation. In fact, the color of these layers had faded merely two days post the systems' installation in Ferrara. Due to this accelerated deterioration, the test results were primarily analyzed in terms of the impact of the reflectors on the concentrators. Furthermore, the PCM containers had been equipped with water circulated through their pipes, following the methodology outlined in Section 3.2. The aim had been to extract heat from the PCM and store it in a water tank. The integration of the LDS layers and PCM containers was realized as a part of a cooperative initiative under the Ideas Project, detailed in Chapter 1.

Due to the global repercussions of the COVID-19 pandemic, the Trinity College team was unable to travel for the systems' installation. Hence, the installation task in Ferrara was carried out by the University of Ferrara (UNIFE) team, acting as a part of the collaborative endeavor under the Ideas Project. Concurrently, the responsibility of conducting the tests and gathering the needed data for the subsequent analysis, conducted by the author and detailed

in this thesis, fell on the shoulders of the UNIFE team. Regrettably, the UNIFE team was equipped with only two solar analysis equipment, which were to conduct tests on the CPC, CPC/PCM, and Reference systems. This limitation resulted in paired testing results from Ferrara. Specifically, comparisons were made between the CPC and CPC/PCM systems in August, and subsequently between the CPC/PCM and Reference systems from September to December.

Figure 7.1 shows the installed systems at the Ferrara demo-site University of Ferrara (UNIFE). All systems were installed vertically, facing south. The electrical characterization data of the systems was measured at 1-minute interval.

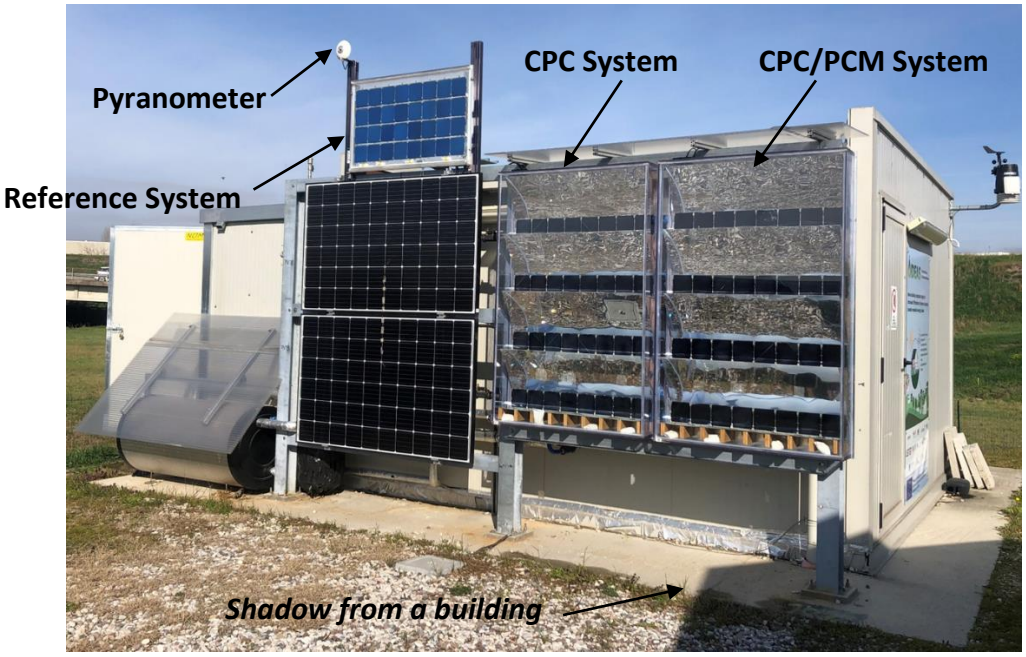

Figure 7. 1 CPC, CPC/PCM and Reference systems installed in Ferrara

7.1.1 Overall performance for CPC, CPC/PCM and Reference systems

Power production and efficiency of CPC, CPC/CPM and Reference systems were characterised in different seasons. Data were analyzed for typical days of sunny, cloudy, and overcast conditions. It should be noted that the values represented in the power outputs graphs are indicative of the peak outputs achieved during each respective month.

Power production of the CPC/PCM system shown in figure 7.2, was highest in September, at 113 W, and the second highest was in November at 95 W. Maximum power was achieved in September, of 113 W at an incident solar radiation of 823 W/m^2 and in November, it reached 95 W at 989 W/m^2. For August, October, and December, the power production fluctuated between 80 - 85 W and produced more electrical power than the Reference system. CPC/PCM and CPC systems reached 80 W and 72 W, respectively, at 653 W/m^2 (August).

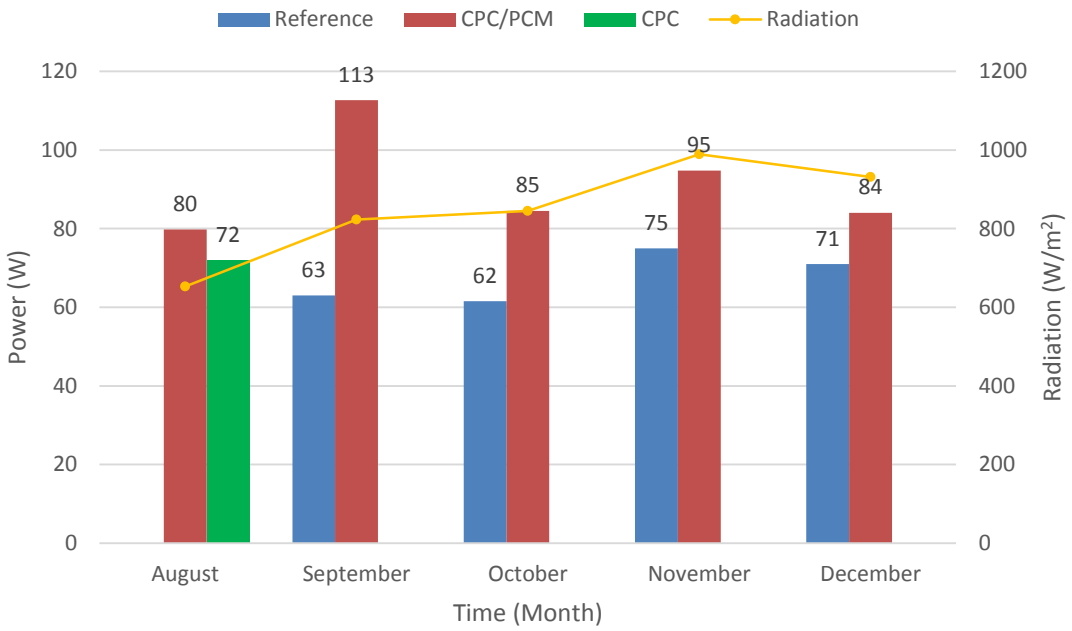

Figure 7. 2 Peak power output for CPC/PCM, CPC, and Reference systems in Ferrara

Solar cell efficiency and power ratio are presented in figure 7.3 and 7.4 respectively. The solar cell efficiency of the CPC/PCM system was stable throughout the day but seasonally it decreased from 27 % in September to 18 % in December. The change in solar cell efficiency may be due to cloudy, overcast, and rainy days that occurred during these months where diffuse solar radiation was dominant, which was captured in the CPC systems. The solar cells efficiency of the Reference system remained stable with 15 % from September to December. The CPC system reached an efficiency of 22 % in the month of August, (2 % less than system CPC/PCM). The results show that the CPC/PCM system can effectively improve electrical production and efficiency compared with the Reference system, with an average power ratio of 1.79.

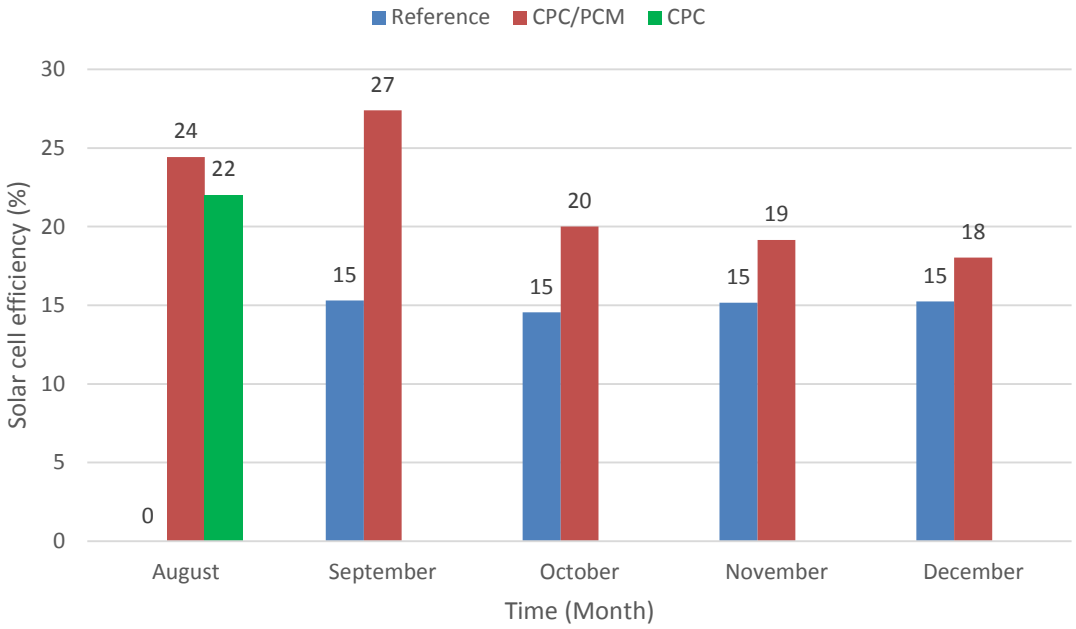

Figure 7. 3 Efficiency for CPC/PCM, CPC, and Reference systems in Ferrara

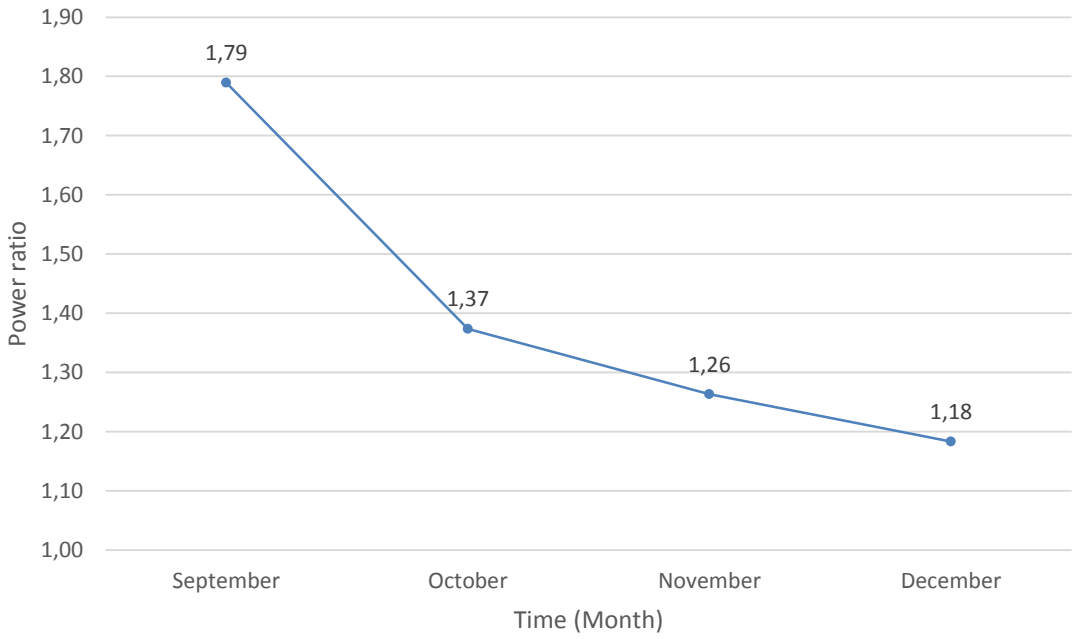

Figure 7. 4 Power ratio for CPC/PCM system in Ferrara

The performance of the CPC/PCM and CPC systems compared to the simulation results could be analyzed as follows:

- Solar cell efficiency: The observed solar cell efficiency for the CPC/PCM system ranged from 18 % in December to 24 % in August, while the CPC system reached 22 % efficiency in August. These values did not fall exactly within the range predicted by the simulation (24 % to 41 %), but they were close, indicating that the observed

efficiencies were reasonably close to expectations. The actual range of 18 % to 24 % was narrower than the predicted range, but still provided valuable insights into the system's performance.

- Power ratio: The average power ratio for the CPC/PCM system was 1.79, which was lower than the simulated value of 2.8 for the summer months (Feb - Sep) but higher than the simulated values of 1.42 (Dec) and 1.52 (Jan). This suggested that the observed power ratio was generally lower than expected during the summer months but higher during the winter months.

- Power output: Maximum power output for the CPC/PCM system under summer conditions (1000 W/m² and 25 ºC) was 113 W at 823 W/m² solar radiation in September, which was slightly lower than the simulated value of 121 W. The difference could be attributed to the lower solar radiation experienced during the testing period.

Several factors could have contributed to these discrepancies, including:

- Ideal Conditions in Simulations: Simulations often assume ideal conditions for operation, such as a perfectly uniform light spectrum, stable temperatures, and a continuous, high-intensity light source. In contrast, real-world conditions fluctuate substantially, which can result in deviations from the expected performance.

- Model Limitations: Simulations often simplify complex processes to make calculations tractable. While useful for providing a rough estimate of performance, these simplifications may overlook key factors that affect real-world performance, leading to discrepancies between simulation and experimental results.

- Weather Variations: Weather conditions during the outdoor test might not have aligned with the assumptions used in the simulations. For example, the simulations assumed a higher level of solar radiation (1000 W/m^2) than was present during testing, leading to discrepancies in performance data.

- Manufacturing and Installation Imperfections: In real-world settings, variations in production quality and installation can impact the system performance. Imperfections in the manufacturing process or issues during the installation can degrade the system's efficiency.

- Temperature Effects: Solar cell efficiency decreases as temperature increases. This impact of temperature, often overlooked in simulations, can significantly affect real-world system performance.

- System Losses: These can include resistive losses in wiring, losses due to dust or soiling on the solar cell surface, and losses due to imperfect angle of incidence or light concentration, among others. These factors may not have been adequately accounted for in simulation models.

- Condensation on Front Glass: Condensation on the front glass of the solar panel can significantly affect the system's performance. It can reduce the amount of light reaching the solar cells, which in turn reduces their output. Furthermore, if left unchecked, prolonged moisture exposure may lead to degradation of the panel components, leading to a further decrease in efficiency. This effect is generally not considered in simulation models, contributing to the observed discrepancies between the simulated and experimental results.

7.1.2 August performance for CPC/PCM and CPC systems

CPC/PCM and CPC systems were tested, and their results were compared in August for three days, (20^{th}, 21^{st}, and 22^{nd} August). The electrical power generated together with the solar radiation corresponding to the three days is shown in figure 7.5. The average solar radiation for those days ranged from 517 W/m^2 on the first day to 653 W/m^2 on the last day.

During the testing period in August, the CPC/PCM system demonstrated superior electrical power production compared to the CPC system. On August 22^{nd}, the CPC/PCM system reached an electrical power production of 80 W at 653 W/m^2, which was 8 W more than the CPC system. This indicates a 12.5 % improvement in power output for the CPC/PCM system over the CPC system without PCM. The electrical gain of 1.12 for the CPC/PCM system signified that it is 12 % more efficient in producing electrical power compared to the CPC system without PCM containers. This demonstrates the effectiveness of integrating PCM containers into the system to enhance the performance of the concentrator, resulting in a more efficient and productive solar energy system.

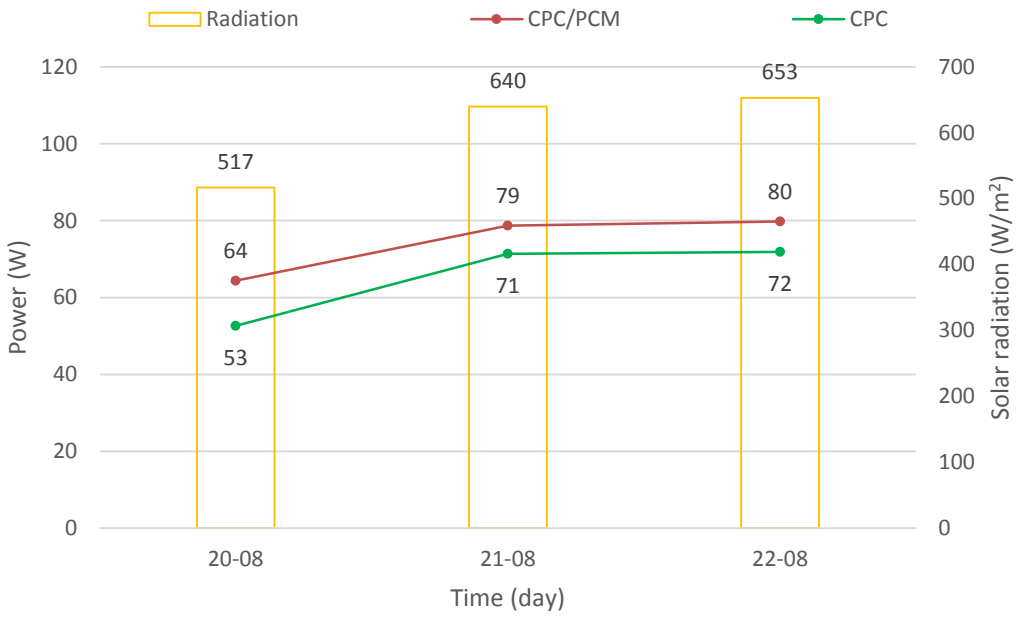

Figure 7. 5 Peak power output and solar radiation for CPC/PCM and CPC systems in August in Ferrara

Figures 7.6 and 7.7 show the solar radiation and the electrical power generated on August 22nd (the day of the highest electrical power). The maximum intensity of the radiation on a sunny day was 653 W/m^2 at noon. There was a decreased in the power due to the shadow generated by the nearby building on the CPC/PCM system between 06:00 and 11:00. Between 12:00 and 14:00, the CPC/PCM system reached a maximum of power between 78 W and 80 W at 653 W/m^2, compared to the CPC system which generates between 68 W and 72 W. The average solar cells efficiency of the systems on this day was 19 % and 17 %, for CPC/PCM and CPC systems, respectively.

In the CPC/PCM system, the heat exchanger is an important element as it aids the extraction of excess heat from the solar cells by 2 %.

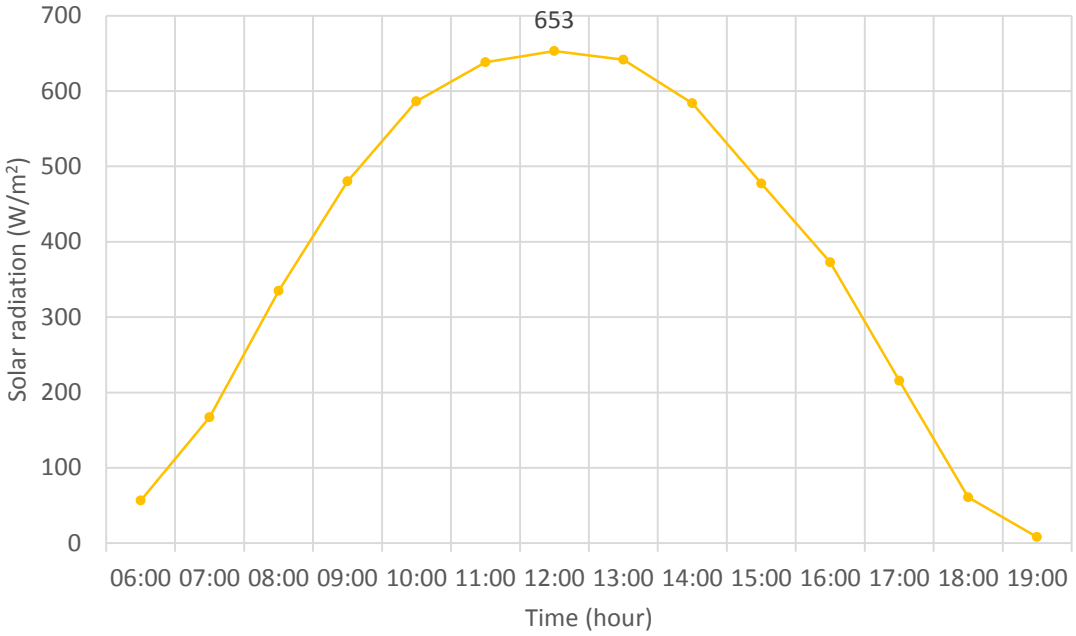

Figure 7. 6 Variation of solar radiation on the 22nd of August 2021 in Ferrara

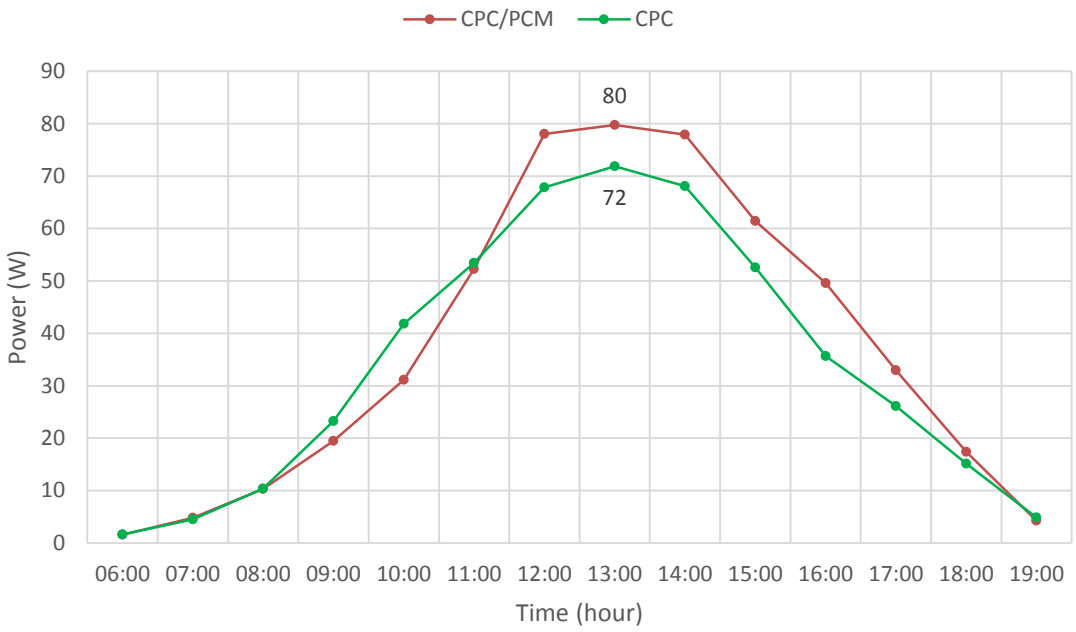

Figure 7. 7 Peak power output for CPC/PCM and CPC systems on the 22nd of August in Ferrara

Table 7.1 presents a comparison between the experimental results and the simulation results for both the CPC/PCM and CPC systems in terms of solar cell efficiency and maximum power output. Experimental test results showed that the CPC/PCM system had a solar cell efficiency of 17 %, while the CPC system had a solar cell efficiency of 15 %. In comparison, the simulation results predicted that the solar cell efficiency for both systems would range between 24 % and 41 %.

It is important to note that the maximum efficiency of silicon solar cells is typically around 30%. The 41% efficiency predicted by the simulation might seem unrealistic at first glance. However, this value was likely obtained due to the concentration effect provided by the CPC system, which focuses solar radiation onto the solar cells, leading to increased efficiency. It is worth mentioning that the simulation results represent an ideal scenario, and the actual efficiency in real-world conditions might be lower due to various factors such as temperature, dust accumulation, and manufacturing tolerances. Therefore, the discrepancy between the predicted and observed efficiencies can be attributed to these factors, as well as the inherent limitations of the simulation model.

This indicates that the experimental test results demonstrated lower efficiencies than the simulation results. In the experimental test results, the CPC/PCM system produced a maximum power output of 80 W at a solar radiation intensity of 653 W/m². The CPC system, on the other hand, produced a maximum power output of 72 W at the same solar radiation intensity. The simulation results predicted a maximum power output of 121 W for both systems at a higher solar radiation intensity of 1000 W/m² and a temperature of 25 ºC. This means that the experimental test results showed lower maximum power output values than the simulation results, possibly due to the difference in solar radiation intensity and temperature conditions during the tests.

Table 7. 1 Comparison between experimental test and simulation results for CPC and CPC/PCM system in August at Ferrara

Parameter	**Experimental Test Results**		**Simulation Results**
	CPC/PCM	**CPC**	
Solar Cell Efficiency (%)	17%	15%	24 % - 41 %
Max Power Output (W)	80 W (at 653 W/m²)	72 W (at 653 W/m²)	121 W (at 1000W/m^2 - 25 ºC)

The PCM containers, situated at the back of the backplate for the CPC/PCM system, had a total weight of 15 Kg as was explained in section 6.6. This contributed to the overall weight of the CPC/PCM system, which was 88 Kg. The cost for constructing these systems approximated to 1254 euros (section 6.6). The process for heat removal from the PCM involved utilizing water that was directed towards the tanks, an initiative included within the scope of the Ideas Project described in chapter 1. Notably, this was a research endeavor and as such, costs were expected to be higher than in an industrial manufacturing setting. In the context of this research, the use of PCM containers offered potential advantages, primarily due to their heat storage capability which could extend the operational efficiency of the system beyond daylight hours. However, the practical implementation had to grapple with challenges such as additional weight and costs. Future research and development could explore the use of lighter and cheaper materials for the PCM containers, which could

potentially mitigate these challenges. Alternative materials or design modifications could reduce the weight of the containers without compromising their heat storage capacity. Similarly, optimizing the manufacturing process or exploring cheaper materials could potentially lower the costs. Thus, while the current implementation presented certain constraints, the concept of integrating PCM in solar concentrator systems remains promising with room for optimization.

7.1.3 September performance for CPC/PCM and Reference systems

CPC/PCM and Reference systems were compared in September for 21 days (1st-21st). Figure 7.8 shows the electrical performance of the systems with solar radiation. The weather in this period was sunny with intermittent cloud cover with an average solar radiation of 850 W/m^2. CPC/PCM system produced higher electrical power during the 21-day test period compared to the Reference system. In addition, CPC/PCM system exceeded the design target for electrical power, reaching a maximum of 113 W on September 21st. The average power production for the CPC/PCM system was 93 W and 53 W for the Reference system, with an average solar radiation of 735 W/m^2. CPC/PCM system produced 1.75 times more power than the reference system in this 21-day test period in September.

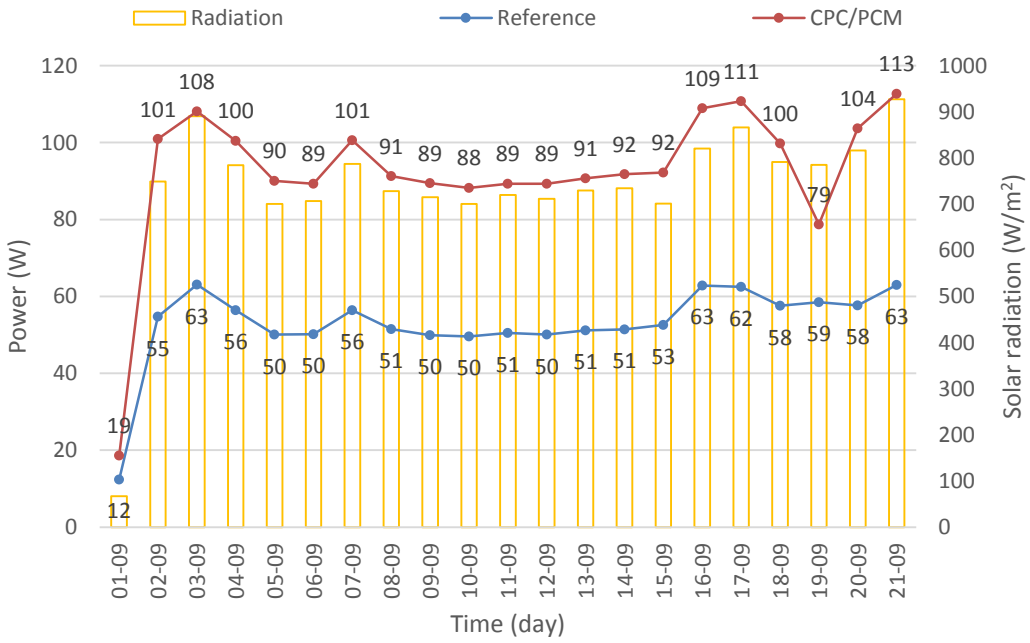

Figure 7. 8 Peak power output and solar radiation for CPC/PCM and Reference systems in September in Ferrara

Figures 7.9 – 7.11 show the solar radiation, electrical power generated, and power ratio for September 21st (the day of highest electrical power in the test period). Figure 7.9 shows the diurnal variation of solar radiation reaching a maximum of 928 W/m^2 at 10:00. Figure 7.10 shows power production for CPC/PCM and Reference systems where the CPC/PCM system

shows a higher power output throughout the day. Between 12:00 and 14:00, the CPC/PCM system reaches a maximum power of ~100 - 113 W with an average solar radiation of 800 W/m^2, compared to the Reference system that generates between 60 - 66 W. Maximum electrical production at 13:00 is reached in CPC/PCM and Reference systems of 113 W and 63 W, respectively, at 823 W/m^2. At that time, a maximum power ratio is observed of 1.80. It is expected that the CPC systems had higher temperatures, therefore even with this reduction in solar cell efficiency due to high temperatures, CPC/PCM system had a higher power production. The average solar cells efficiency of the systems on this day was 13 % and 10 %, corresponding to CPC/PCM and reference systems, respectively.

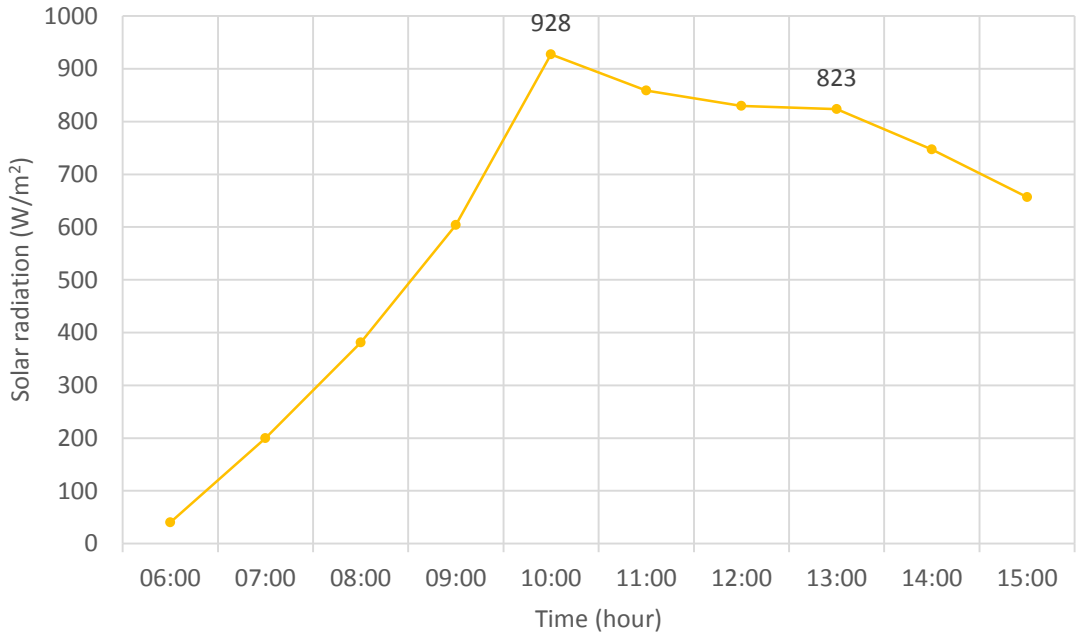

Figure 7. 9 Solar radiation on 21st September 2021 in Ferrara

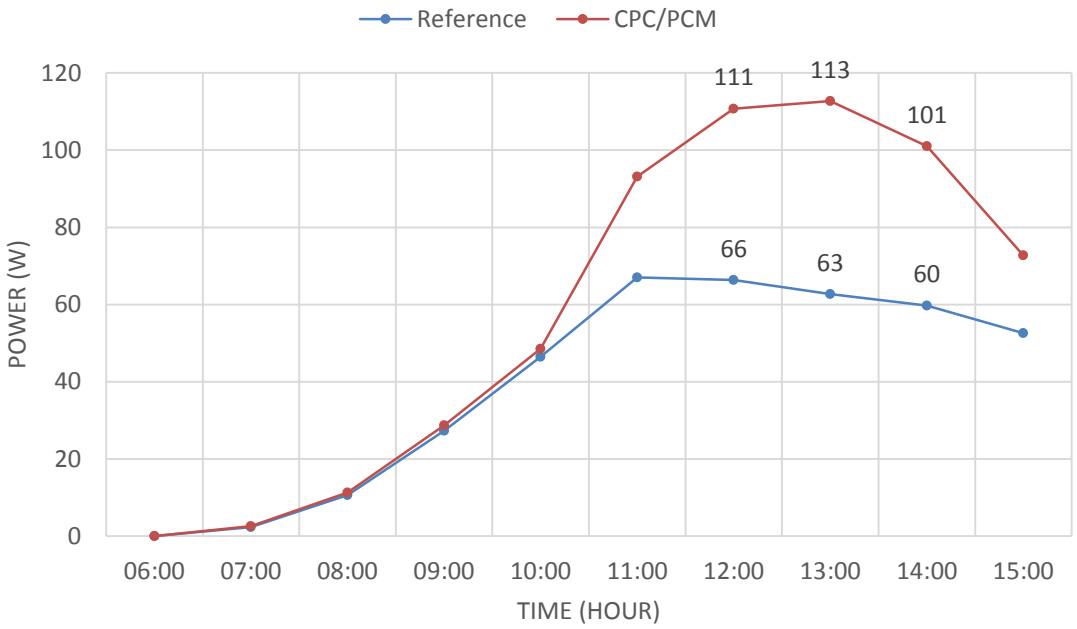

Figure 7. 10 Peak power output for CPC/PCM and Reference systems on 21st September in Ferrara

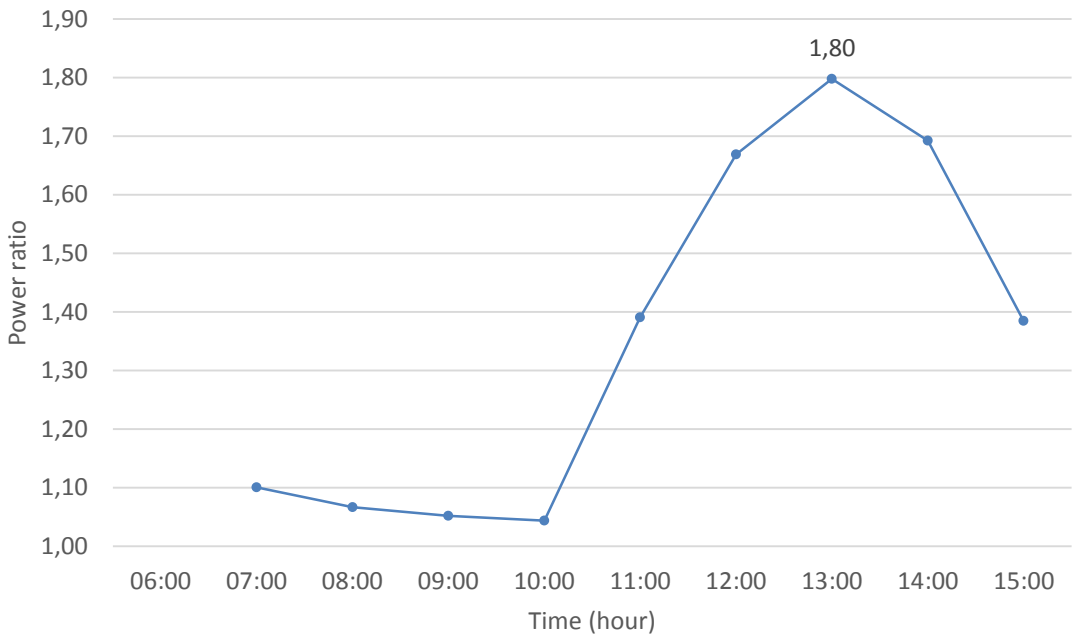

Figure 7. 11 Power ratio for CPC/PCM system on 21st September in Ferrara

The table 7.2 summarizes the results from the real experimental test comparing with the simulations results.

Table 7. 2 Comparison between experimental test and simulation results for CPC/PCM system in September at Ferrara

Parameter	Experimental Test Results	Simulation Results
Solar Cell Efficiency (%)	CPC/PCM: 13 %	24% - 41%
	Reference: 10 %	
Max Power Output (W)	CPC/PCM: 113 W (at 823 W/m²)	121 W (at 1000 W/m² - 25 ºC)
	Reference: 63 W (at 735 W/m²)	
Power Ratio	CPC/PCM: 1.80 (CPC/PCM)	2.8 (Feb-Sep)
		1.42 (Dec)
		1.52 (Jan)

When comparing the experimental test results with the simulation values, it can be observed that:

- Solar cell efficiency: The experimental test results for solar cell efficiency were lower than the simulation values for both CPC/PCM and Reference systems. The CPC/PCM system achieved an efficiency of 13 % in the experimental test, while the simulation values ranged between 24 % and 41 %. The Reference system's experimental test efficiency was 10 %.

- Maximum power output: The experimental test results for maximum power output were also lower than the simulation values. The CPC/PCM system reached a maximum power output of 113 W at 823 W/m², while the simulation value was 121 W at 1000 W/m² and 25 ºC. The Reference system achieved a maximum power output of 63 W at 735 W/m² during the experimental test.

- Power ratio: The experimental test power ratio for the CPC/PCM system was 1.80, which is lower than the simulation values of 2.8 for February-September, 1.42 for December, and 1.52 for January.

The experimental test results were lower than the simulation values. This discrepancy could be due to differences in the actual weather conditions, solar radiation intensity, and temperature during the experimental test compared to the conditions used for the simulation. Additionally, factors like manufacturing tolerances, system aging, and other real-world factors (such as dust and dirt accumulation, condensation in front glass, degradation materials, variability in solar radiation and temperature effect) might have contributed to the difference between the experimental test results and the simulation values.

7.1.4 October performance for CPC/PCM and Reference systems

In October, CPC/PCM and Reference systems were tested for four days (26^{th} – 29^{th}). Figure 7.12 shows the electrical performance of the systems with solar radiation. The average solar radiation was 822 W/m^2. Maximum electrical power was 85 W and 62 W for CPC/PCM and

Reference systems respectively at 845 W/m^2. Although the CPC/PCM system performed better than the Reference system during the 4-day testing period, with a factor of 1.37.

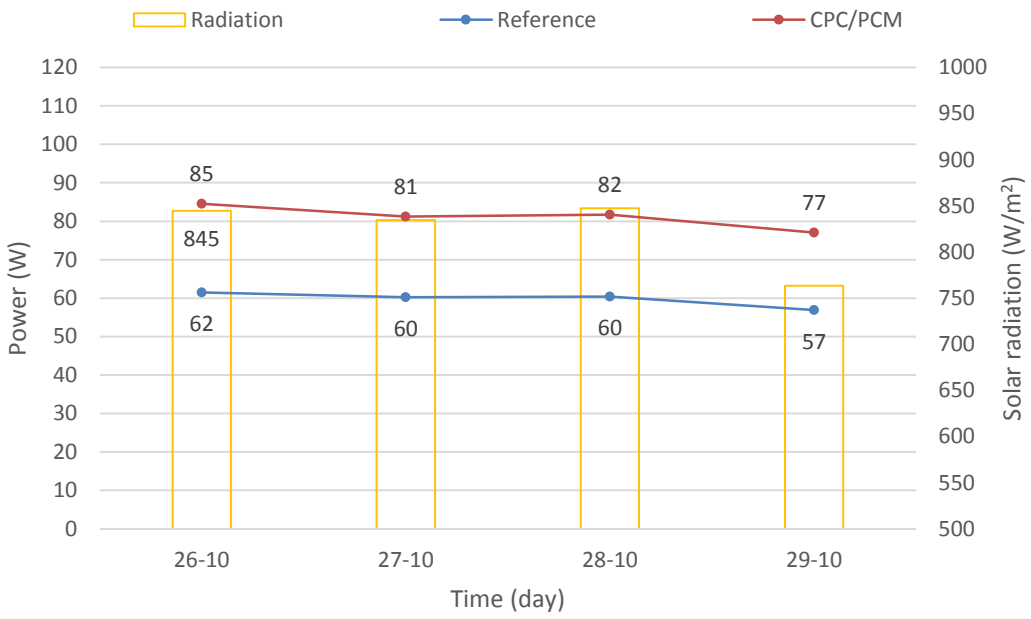

Figure 7. 12 Peak power output and solar radiation for CPC/PCM and Reference systems in October in Ferrara

Figures 7.13 – 7.15 show the solar radiation, electrical power, and power ratio for October 26th, (the day of highest generated power in October). Figure 7.13 shows the diurnal variation of solar radiation with a maximum of 845 W/m^2 at 12:00. Figure 7.14 shows the power production for CPC/PCM and Reference systems. From the graph, CPC/PCM system shows a higher power output throughout the day. At 12:00, the CPC/PCM system reaches a maximum power of 84 W with an average solar radiation of 845 W/m^2, compared to the reference system, which reached 62 W. CPC/PCM system had a factor of 1.37 higher power output than the Reference system. The average solar cell efficiency of the systems was 20 % (this discrepancy was explained in section 7.1.2) and 15 % for CPC/PCM and Reference systems respectively.

The obtained solar cell efficiency for the CPC/PCM system (20 %) appears to be higher than the range of values predicted by the modeling (9 % to 21 %). This suggests that the actual performance of the CPC/PCM system exceeded expectations, at least in terms of solar cell efficiency. This improved efficiency could be attributed to favorable weather conditions on the testing day, or a higher-than-expected optical efficiency of the CPC/PCM system.

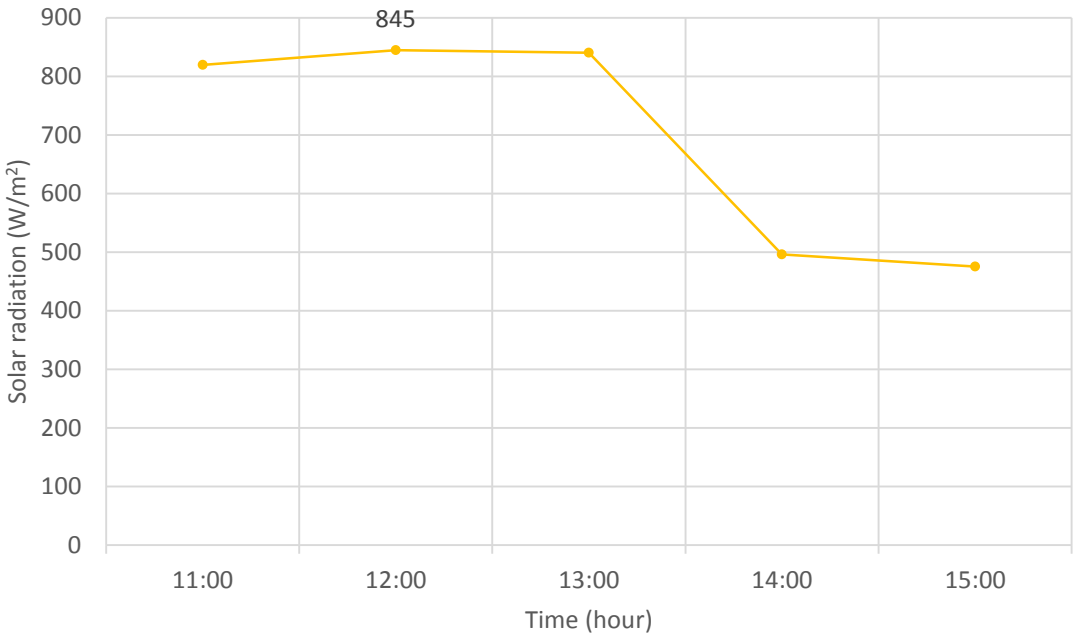

Figure 7. 13 Variation of solar radiation on the 26th of October in Ferrara

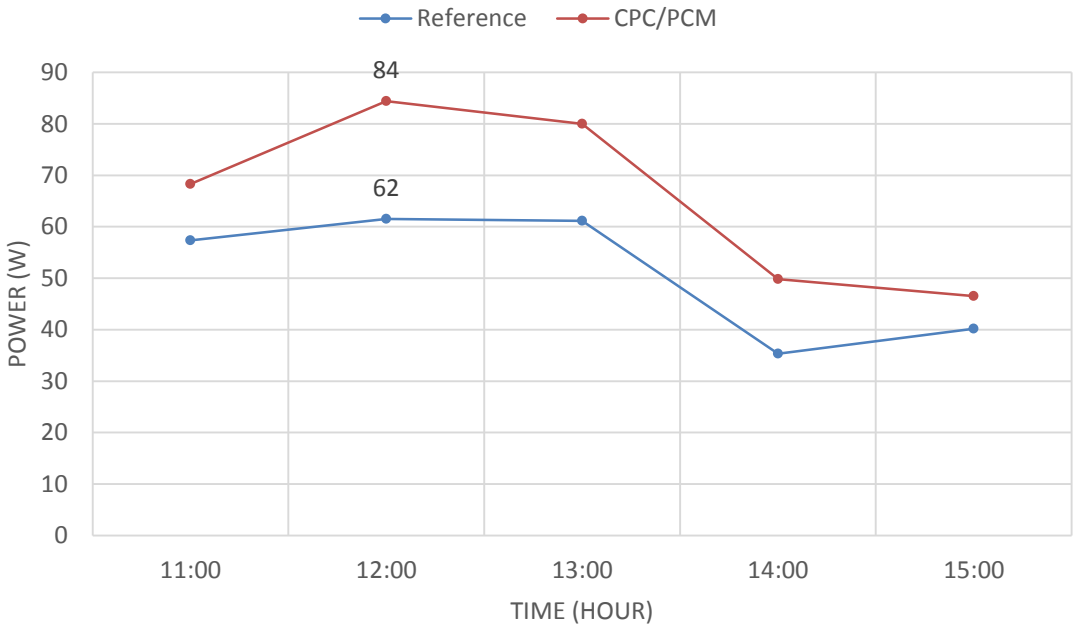

Figure 7. 14 Peak power output for CPC/PCM and Reference systems on 26th October in Ferrara

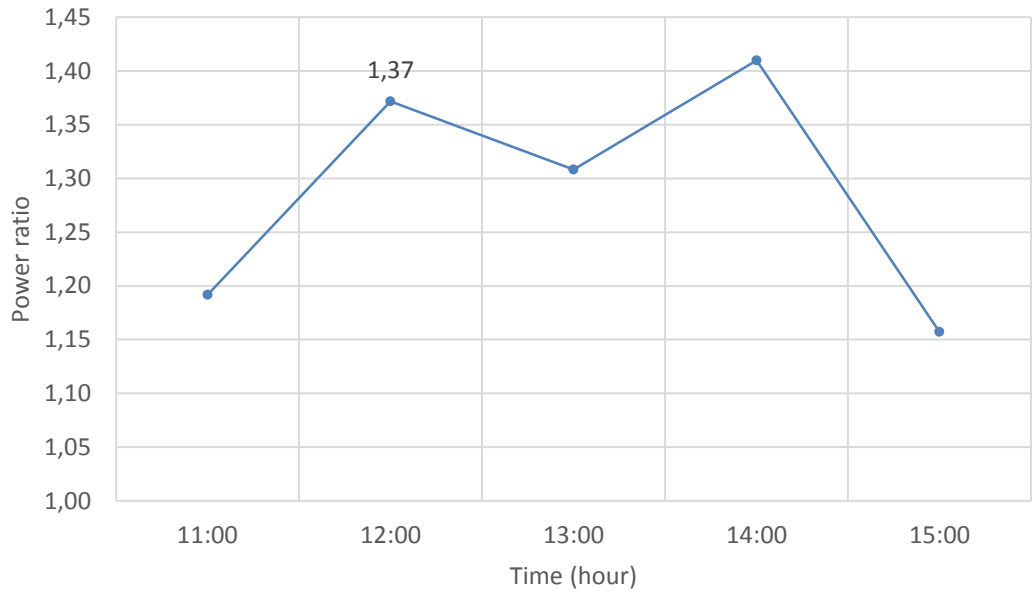

Figure 7. 15 Power ratio for CPC/PCM system on 26th October in Ferrara

Table 7.3 summarizes the results from the experimental test comparing with the simulations results.

Table 7. 3 Comparison between experimental test and simulation results for CPC/PCM system in October at Ferrara

Parameter	Experimental Test Results	Simulation Results
Solar Cell Efficiency (%)	CPC/PCM: 20%	24% - 41%
	Reference: 15%	
Max Power Output (W)	CPC/PCM: 85 W (at 845 W/m²)	121 W (at 1000 W/m² - 25 ºC)
	Reference: 62 W (at 845 W/m²)	
Power Ratio	CPC/PCM: 1.37	2.8 (Feb-Sep)
		1.42 (Dec)
		1.52 (Jan)

The comparison between the experimental test results and simulation values revealed the following observations:

- Solar Cell Efficiency: The CPC/PCM system's experimental test result for solar cell efficiency (20 %) fell within the range of values predicted by the simulation (24 % - 41 %).

- Max Power Output: The experimental test result for the CPC/PCM system's maximum power output (85 W at 845 W/m²) was lower than the simulation value (121 W at 1000 W/m² and 25 ºC).

- Power Ratio: The power ratio for the CPC/PCM system in the experimental test results (1.37) was lower than the simulation values for February - September (2.8), December (1.42), and January (1.52).

Solar cell efficiency of the CPC/PCM system in the experimental test results was within the range predicted by the simulation, while the maximum power output and power ratio were lower than the simulation values. This suggested that the actual performance of the CPC/PCM system was somewhat lower than expected, although the solar cell efficiency was still within the predicted range. There could be several reasons for this discrepancy for example:

- Variability in weather conditions can significantly impact the performance of solar systems. During the testing period, factors such as intermittent cloud cover, varying levels of solar radiation, and fluctuations in temperature might have affected the performance of the CPC/PCM system.

- Additionally, some solar cells were reported to have broken due to the warping of the solar cell holder. This mechanical issue could have resulted in a reduced number of functioning solar cells, leading to lower-than-expected power generation.

- Condensation on the front glass of the systems might have also played a role in the performance discrepancy. The presence of condensation can reduce the transmission of sunlight through the glass, subsequently decreasing the amount of solar radiation absorbed by the solar cells and, consequently, impacting the overall efficiency.

7.1.5 November and December performance for CPC/PCM and Reference systems

CPC/PCM and Reference systems characterized in November for 22 days and December for 7 days. Figure 7.16 shows the electrical performance of the systems with solar radiation for November. Very low solar radiation (50 to 64 W/m^2) can be observed on November 20th, 21^{st,} and 22nd where the average electricity production by CPC/PCM and Reference systems was only 7 W and 6 W respectively. Maximum power for November was achieved on November 4th, where CPC/PCM and Reference systems generated 95 W and 75 W, respectively, at 989 W/m^2. In general, the CPC/PCM system generated more electrical power throughout November than the Reference system. The average electrical power for November for CPC/PCM and Reference systems was 47 W and 38 W, respectively, with average solar radiation of 495 W/m^2. The average solar cells efficiency over the 22 days was 20 % and 16 % for the CPC/PCM and Reference systems respectively.

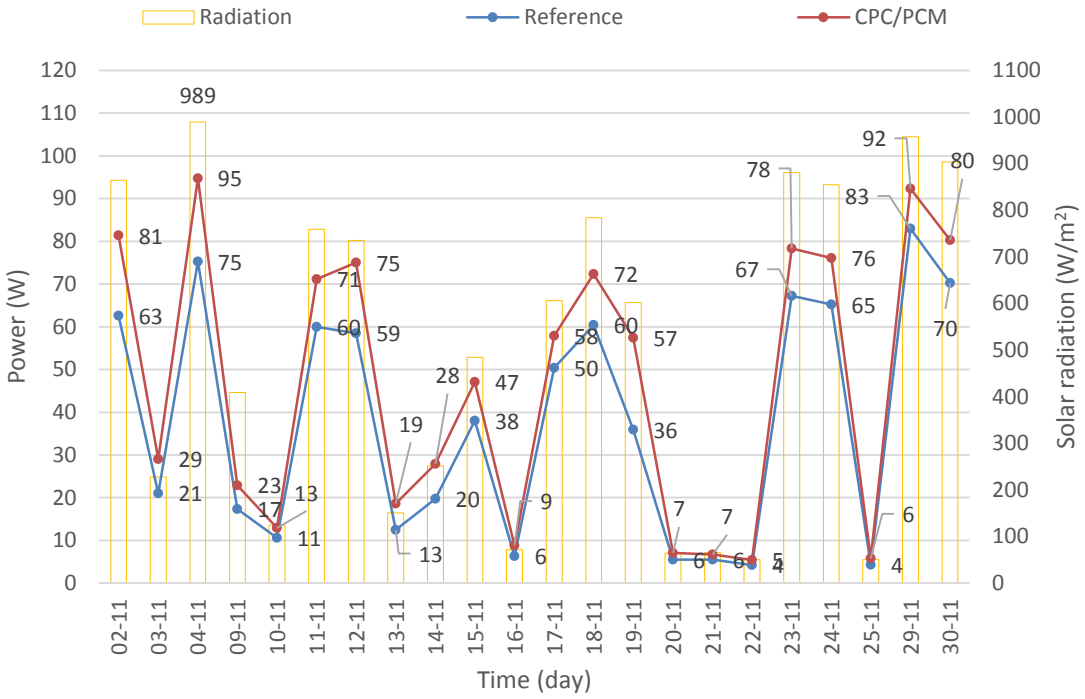

Figure 7. 16 Peak power output and solar radiation for CPC/PC, and Reference systems in November in Ferrara

Figure 7.17 shows electrical power production with solar radiation for CPC/PCM and Reference systems in December. The average solar radiation in December was 748 W/m^2. CPC/PCM and Reference systems have an average electrical power of production of 78 W and 69 W, with an average efficiency of 21 % and 19 %, respectively. Maximum power was observed on 1st December where the systems produced 84 W for CPC/PCM system and 71 W for the Reference, at 931 W/m^2. Maximum efficiency was achieved on December 12th, when CPC/PCM and Reference systems reached record values of 28 % and 26 %, respectively.

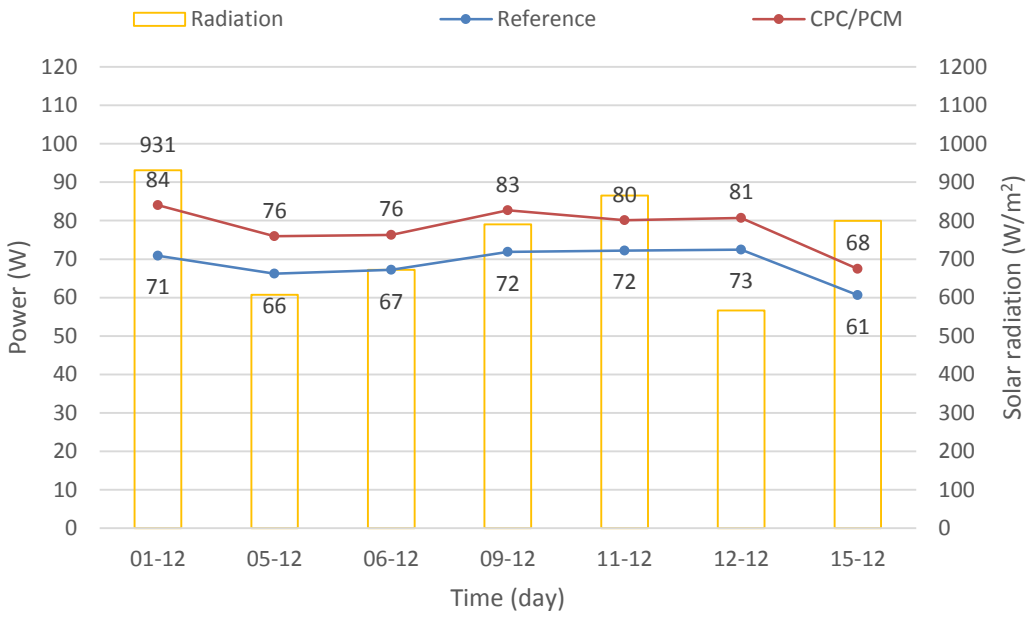

Figure 7. 17 Peak power output and solar radiation for CPC/PCM and Reference systems in December in Ferrara

The table 7.4 summarizes the results from the experimental test comparing with the simulations results.

Table 7. 4 Comparison between experimental test and simulation results for CPC/PCM system in November and December at Ferrara

Parameter	Experimental Test Results (Nov)	Real Test Results (Dec)	Simulation
Solar Cell Efficiency (%)	CPC/PCM: 20%	CPC/PCM: 21%	24% - 41%
	Reference: 16%	Reference: 19%	
Max Power Output (W)	CPC/PCM: 95 W (at 989 W/m²)	CPC/PCM: 84 W (at 931 W/m²)	121 W (at 1000 W/m² - 25 ºC)
	Reference: 75 W (at 989 W/m²)	Reference: 71 W (at 931 W/m²)	
Power ratio	CPC/PCM: 1.26	CPC/PCM: 1.18	2.8 (Feb – Sep)
			1.42 (Dec)
			1.52 (Jan)

The experimental test results for November and December for the CPC/PCM system displayed some differences compared to the simulation results.

- When examining solar cell efficiency, the CPC/PCM system in November had an efficiency of 20 %, while in December it was 21%. These values were below the range

predicted by the simulation (24% - 41%), indicating that the efficiency during these months was not as high as expected.

- Regarding maximum power output, the experimental test results for the CPC/PCM system in November showed a maximum output of 95 W at 989 W/m², while in December, it reached 84 W at 931 W/m². Both of these values were lower than the simulation result of 121 W at 1000 W/m² and 25 ºC. This indicates that the system's power generation capacity was not as high as expected during the testing period.

- The power ratio of the CPC/PCM system in the experimental test results was 1.26 in November and 1.18 in December. These values were lower than the simulation values for December (1.42) and January (1.52), and substantially lower than the range for February through September (2.8). This discrepancy suggests that the actual performance of the CPC/PCM system in terms of power output relative to the reference system was not as high as predicted by the simulation.

The experimental test results for the CPC/PCM system in November and December were lower than the simulation values in all parameters: solar cell efficiency, maximum power output, and power ratio. This indicates that the actual performance of the system during those months did not match the expectations based on the simulation. Factors such as weather conditions, system design limitations, solar cells broke, condensation or unaccounted losses in the simulation model could have contributed to the discrepancies observed between the experimental test results and the simulation values.

7.2 Performance for CPC, CPC/PCM and Reference systems for Mayo, Ireland

The systems were installed at the Mayo demo-site at Brackloon Drummin Community Centre. The first step was to determine the power generation, efficiency and temperature of both systems and compare the results. Their electrical and thermal characteristics were measured over four months (July to October 2022) for an average period of 10 hours per day.

In the case of the Mayo systems, the entirety of the installation process, data gathering, and subsequent analysis were managed by the primary researcher. Additionally, the benefit of having three Solar Module Analyzers at their disposal meant all systems could be tested concurrently. However, a considerable setback encountered during this phase was the inability to circulate water through the pipes of the PCM containers. The plumbing team, occupied with other sections and technologies pertinent to the Ideas Project, did not complete the installation of the necessary pipes connecting the PCM containers to the tanks in time for the designated testing days. This delay resulted in the absence of water circulation in the PCM containers during the tests. In addition, no LDS layers was added to these systems. The reason of this was explained in section 7.1.

The experimentally characterized systems are shown in the figure 7.18.

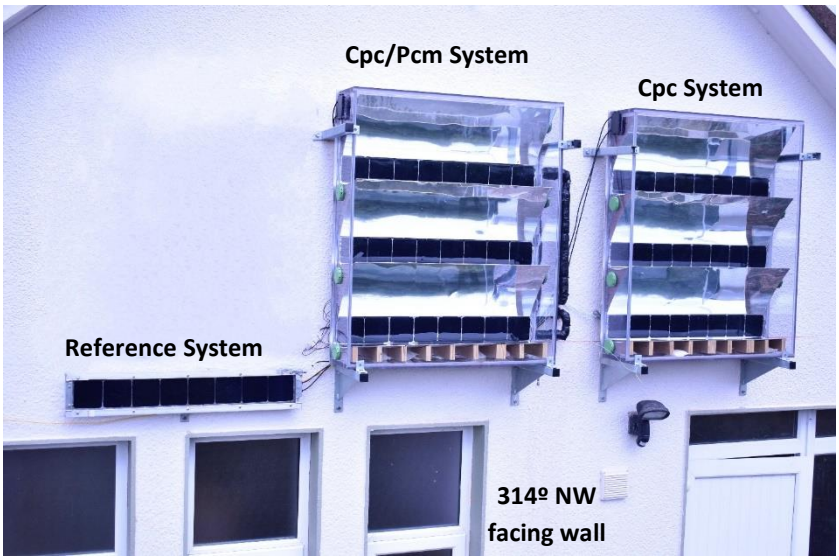

Figure 7. 18 Systems installed at Brackloon Drummin Community Centre façade in Mayo

The front wall has a deviation of 46 º with the south. The outdoor experimental performance of the systems was monitored using three independent solar module analyzer, Agilent data logger, Kipp and Zonen Sp Lite 2. The details of these devices were described in section 3.5. All the data were recorded every 2 minutes. The solar module analyzers and Agilent data logger were linked to a PC as shown in figure 7.19.

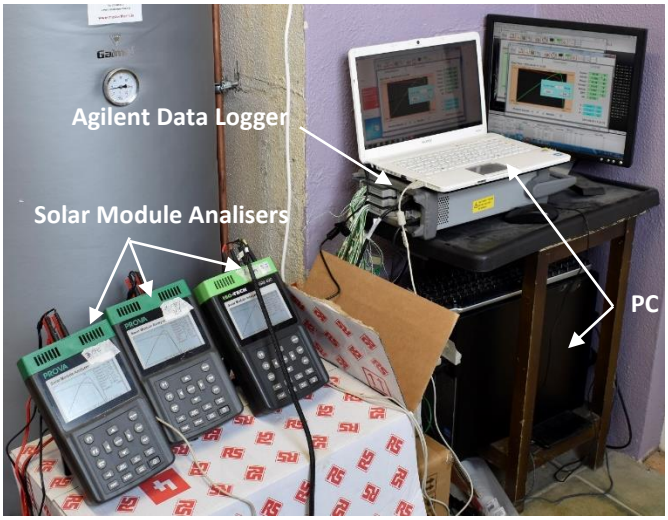

Figure 7. 19 Monitoring system used in the characterization of the CPC, CPC/PCM and Reference systems

Figure 7.20 presents the schematic design connections for the CPC, CPC/PCM and Reference systems, with pyranometer and thermocouples. The solid lines represent the positive and negative wires of each device, while the dashed lines represent the thermocouples. SMA1, 2 and 3 represent the solar module analyzers used during testing.

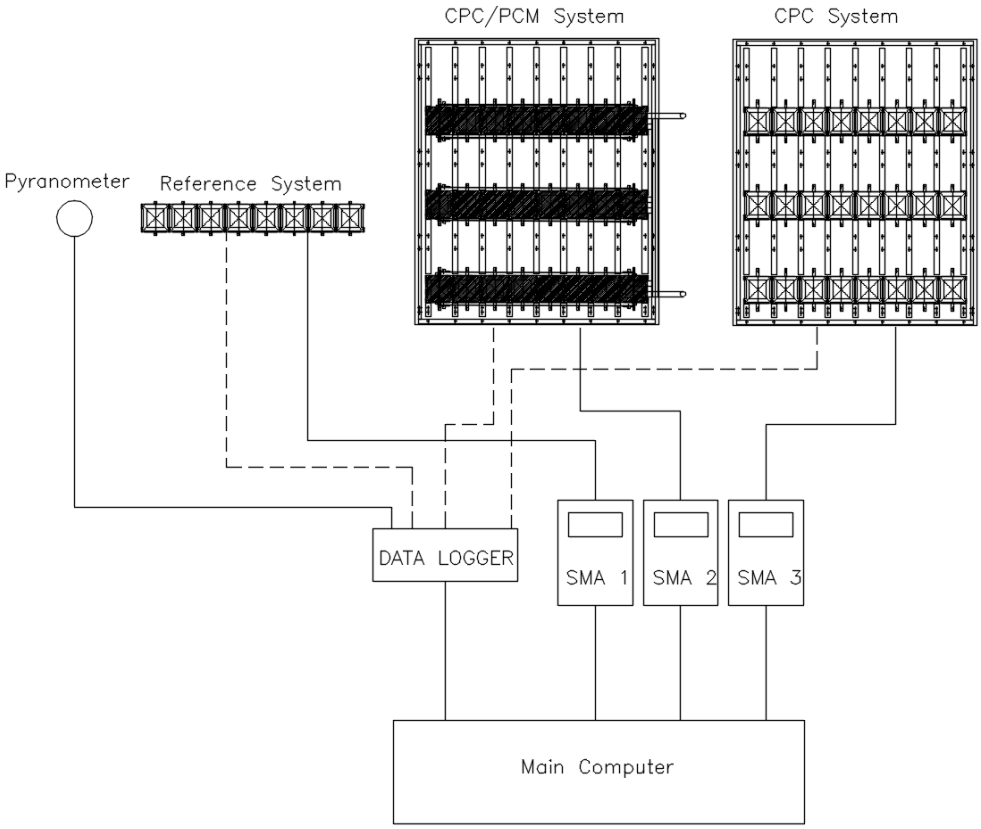

Figure 7. 20 Schematic monitoring connection for the CPC, CPC/PCM and Reference systems

7.2.1 Electrical analysis under clear sky

The results were recorded for four days on 9th, 10th, 11th and 13th of August 2022 from 08:00 to 18:00 hours, which were consistently clear days out of the four months of measurements. Figure 7.21 shows the variation of the incident solar radiation for the four days where the maximum solar radiation was 695 W/m^2. The graph displays an asymmetrical curve and a sudden drop at 15:30, which can be attributed to the 46º deviation of the wall from the south direction.

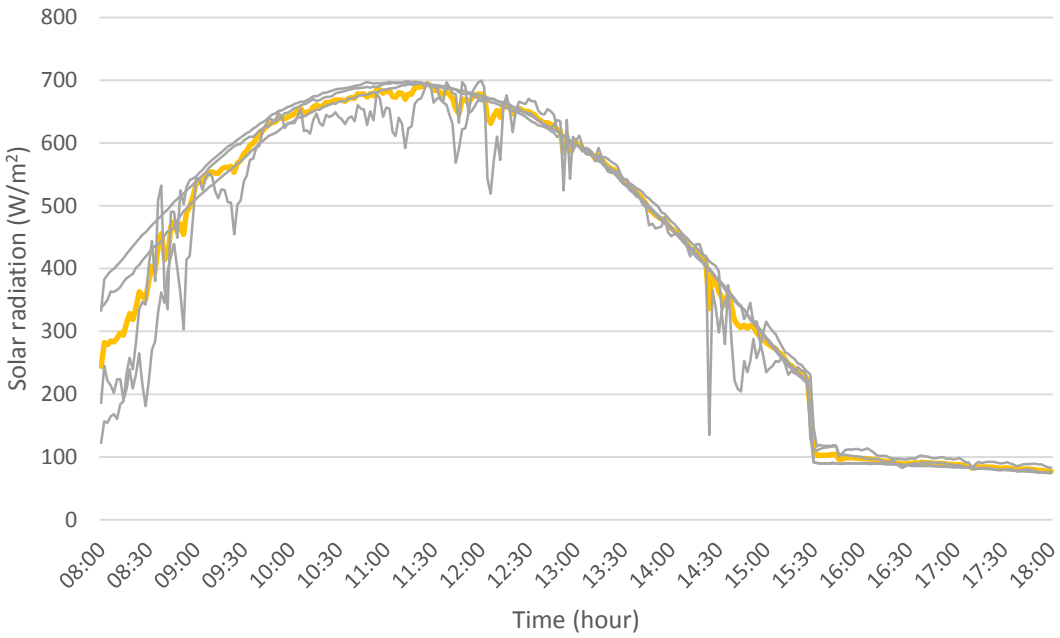

Figure 7. 21 Average variation of solar radiation under clear sky with time between the 9th, 10th, 11th and 13th of August 2022

Figure 7.22 presents the power output with time. As expected the power output for the three systems change linearly with incident solar radiation intensity with maximum values at noon. Throughout the four days, the two concentrators showed power outputs greater than the Reference system. The maximum power output for CPC, CPC/PCM and Reference systems were 71, 76 and 35 W respectively. The systems were installed side by side with a location from east to west in the following order: CPC, CPC/PCM and Reference system (as shown in figure 7.18), as a consequence of this in the morning the CPC system generated a shadow on the CPC/PCM system from 9:00 to 11:00. In the same way, the CPC/PCM system casts a shadow on the Reference system from 8:00 to 8:30. From 11:00 to 12:00 the CPC/PCM system began to cast the shadow over the CPC system. At approximately 14:30 a sudden drop in the power of the CPC/PCM system was observed due to the 46º rotation of the wall to south.

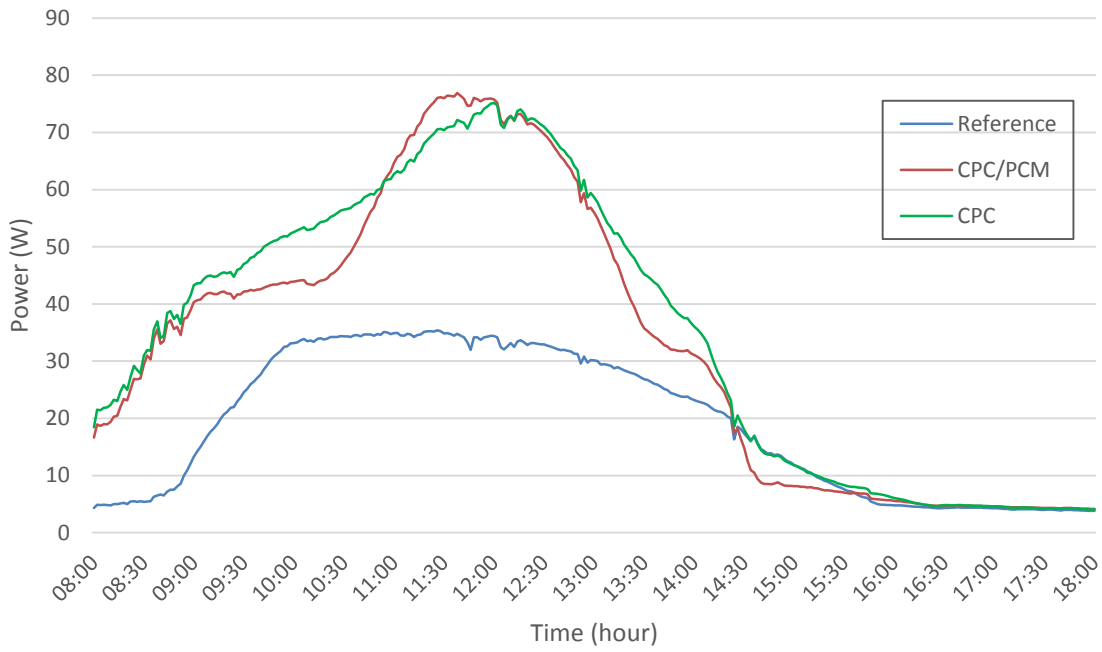

Figure 7. 22 Power output under clear sky for the CPC, CPC/PCM and Reference systems

Figure 7.23 shows the temperature of the solar cells in the three systems. CPC/PCM system reached the maximum of 109 ºC between 12:00 and 12:30, this was 85 ºC higher than the outdoor temperature (24 ºC). This occurred because the PCM stored thermal energy, and since it was not yet connected to a heat exchanger (pipes with water), the thermal energy was transferred back to the solar cells, keeping them at high temperatures, particularly during the afternoon. Between 08:00 and 09:00, the three systems showed the same temperature behavior. At maximum radiation (694 W/m^2) the reported temperatures were 75 ºC, 98 ºC and 58 ºC for the CPC, CPC/PCM and Reference system respectively, with an outdoor temperature of 23 ºC.

Theoretically, due to its thermal capacity, the CPC/PCM system should have reached its peak temperature later in the day compared to the CPC system. This anticipated pattern is typically a consequence of the PCM's property to store and gradually release heat, generating a delayed temperature peak. Nonetheless, in this specific instance, the expected behavior was not clearly observed. A plausible explanation could be an increased rate of heat loss from the solar cells in the CPC system, which resulted in a rapid decline in temperature, obscuring the expected delay. Moreover, certain conditions during the testing period might have influenced these observations. For example, shade falling on the CPC/PCM system could have impacted its capacity to effectively capture and store heat. Further, the rotation of the wall in use could have modified the angle of incident sunlight on the systems, which, in turn, might have affected the performance and temperature profiles of the systems.

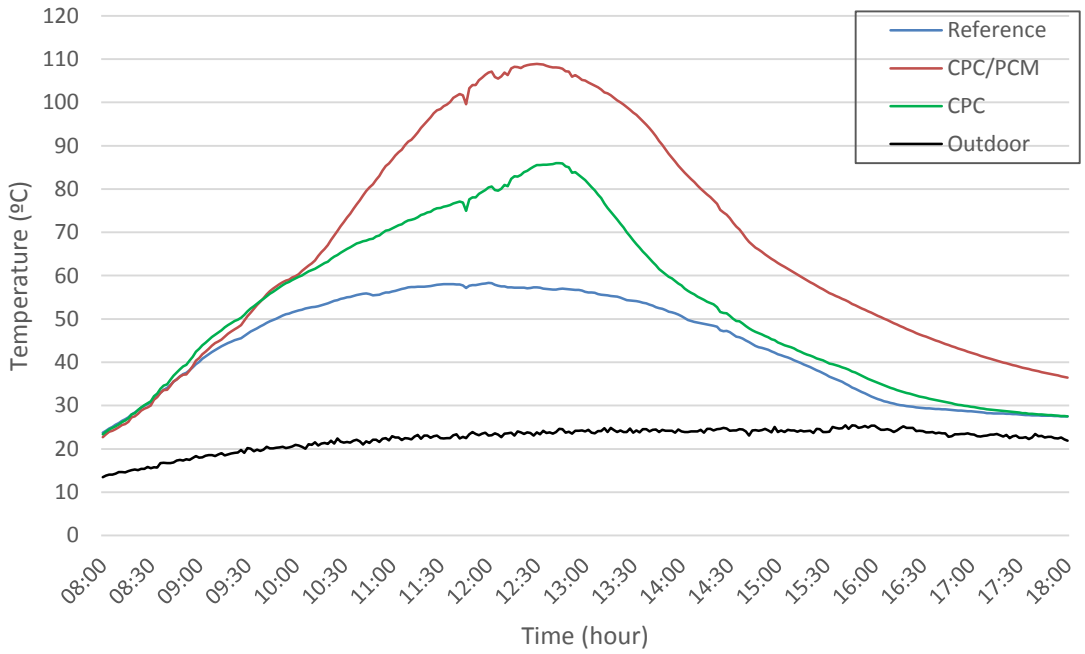

Figure 7. 23 Solar cells temperature under clear sky for the CPC, CPC/PCM and Reference systems

Power ratio is presented in figure 7.24 for both concentrators. As expected, due to the shadow generated in the Reference system, between 08:00 and 08:30 the power ratio increased, reaching a maximum peak of approximately 6. This could be attributed to the shadowing effect on the Reference system. In the morning, when the sun was at a lower angle, the concentrators could still capture and focus ray lights effectively onto the solar cells. However, the Reference system, which did not employ concentrators, was more susceptible to shadows cast by surrounding objects or even the CPC systems themselves. This shadowing effect reduces the amount of ray lights reaching the solar cells in the Reference system, decreasing the amount of power generated. As a result, the power output from the CPC/PCM system appears relatively higher when compared to the Reference system. Consequently, the power ratio (CPC/PCM power output divided by the Reference system power output) increases during this period, leading to the observed maximum peak of approximately 6.

From 09:30 to 13:00 the average power ratio for the CPC and CPC/PCM systems was 1.90 and 1.84 respectively. At the time of maximum solar radiation (694 W/m^2) the power ratio was 1.99 and 2.15 for the CPC and CPC/PCM system respectively. After 13:00 the CPC system had a better power ratio than the CPC/PCM system, this was mainly due to the high temperatures reported by the solar cells in the CPC/PCM system. At 14:30, the sudden drop in the power ratio in the CPC/PCM system was observed as a consequence of the aforementioned 46 º rotation of the wall.

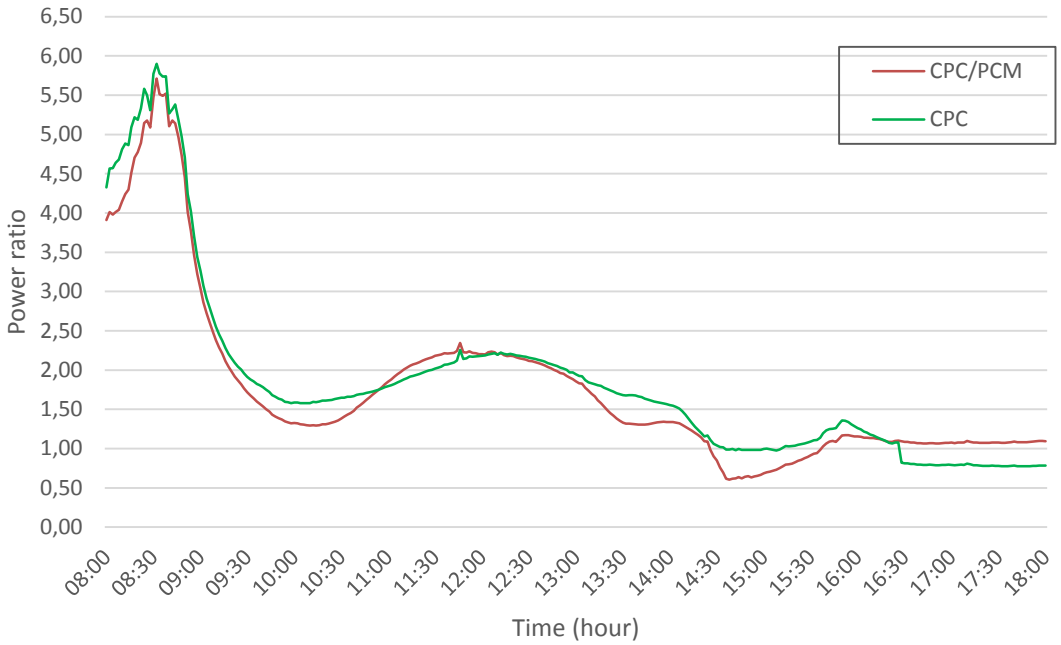

Figure 7. 24 Power ratio under clear sky for the CPC and CPC/PCM systems

Figure 7.25 reports the fill factor for CPC, CPC/PCM and Reference system. The Reference system reported a more stable fill factor than the concentrators with a value equal to 0.79 for the Reference system and 0.39 – 0.65 for the concentrators. This was mainly due to the fact that both concentrators have high ohmic losses as a result of the high currents. CPC system showed a better fill factor behavior than CPC/PCM system with 0.1 more at noon. The decrease of the fill factor was due to the temperature effect of the solar cells in the CPC/PCM system. At the time of maximum solar radiation (694 W/m^2) the fill factor reported was 0.60, 0.58 and 0.79 for the CPC and CPC/PCM system respectively.

The fill factor is an important parameter as it indicates the quality of a solar cell or photovoltaic (PV) module. It represents the effectiveness with which a solar cell converts the solar radiation received into usable electrical power. A higher fill factor implies better performance and efficiency in the conversion process.

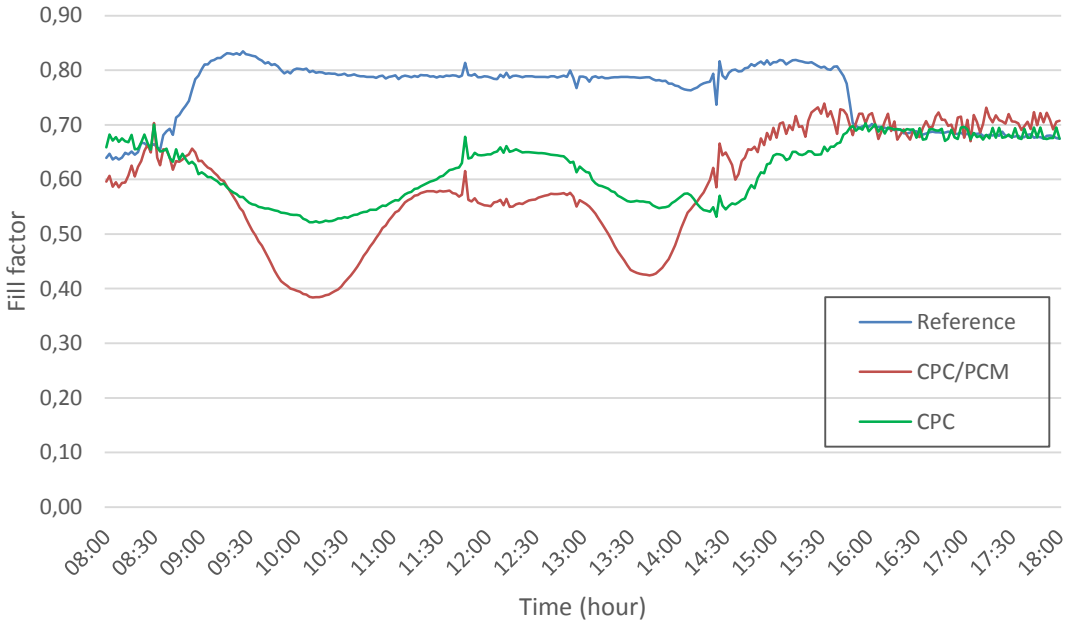

Figure 7. 25 Fill factor under clear sky for the CPC, CPC/PCM and Reference systems

Solar cell efficiency for the three systems is presented in figure 7.26. The effective solar area (0.375 m^2) was considered to calculate the solar cell efficiency of the systems. On average, the two concentrators showed better solar cell efficiency during the test. The CPC system presented better solar cell efficiency in the morning (between 8:00 to 11:00) compared to the other systems with values between 20 % to 24 %. Between 11:00 and 12:30, the CPC/PCM system presented better solar cell efficiency, reaching a maximum peak equal to 30 %. Between 12:30 and 14:30, CPC system showed better values, this is mainly due to the high temperatures of the solar cells in the CPC/PCM system. The drop in efficiency of the systems at around 14:30, extended more deeply for the CPC/PCM system (due to the deviation of 46 º with the south). A small elevation was observed at 15:30 in the three systems as a consequence of the deviation from the south, thus producing a reduction of the temperature in the solar cells. The Reference system showed a drop between 08:00 and 08:30 due to the shadow of the CPC system on the Reference system. Between 10:00 and 14:00 the Reference system presented a stable solar cell efficiency equal to 14 %. At maximum solar radiation (695 W/m^2) the reported solar cell efficiencies were 27 %, 29 % and 14 % for the CPC, CPC/PCM and Reference systems, respectively. The temperature in the solar cells was 75 ºC, 98 ºC and 58 ºC for the CPC, CPC/PCM and Reference systems respectively. This represented a difference with outdoor temperature equal to 52 ºC (CPC system), 75 ºC (CPC/PCM) and 35 ºC (Reference system).

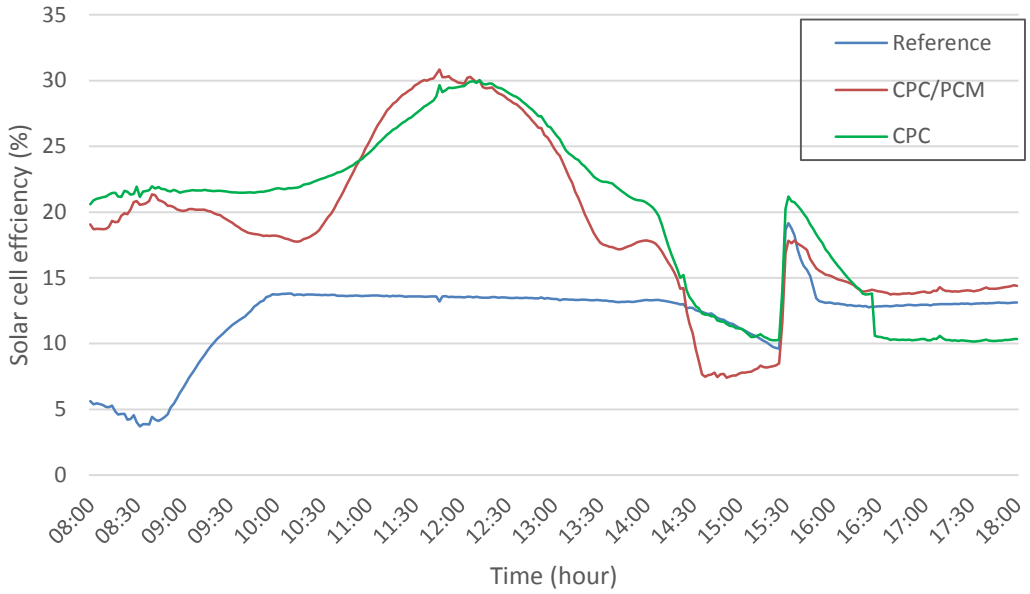

Figure 7. 26 Solar cells efficiency under clear sky for the CPC, CPC/PCM and Reference systems

Figure 7.27 reports the optical efficiency of the concentrators which correlates with the power ratio. The high value of the optical efficiency (180 %) in the morning (08:00 to 08:30) was due to the shadow produced in the Reference system. Between 09:00 and 14:00 both concentrators showed a stable solar cell efficiency with an average value equal to 79 % and 87 % for the CPC and CPC/PCM system respectively. At maximum solar radiation (695 W/m^2) the optical efficiency were 80 % and 92 % for the CPC and CPC/PCM systems, respectively.

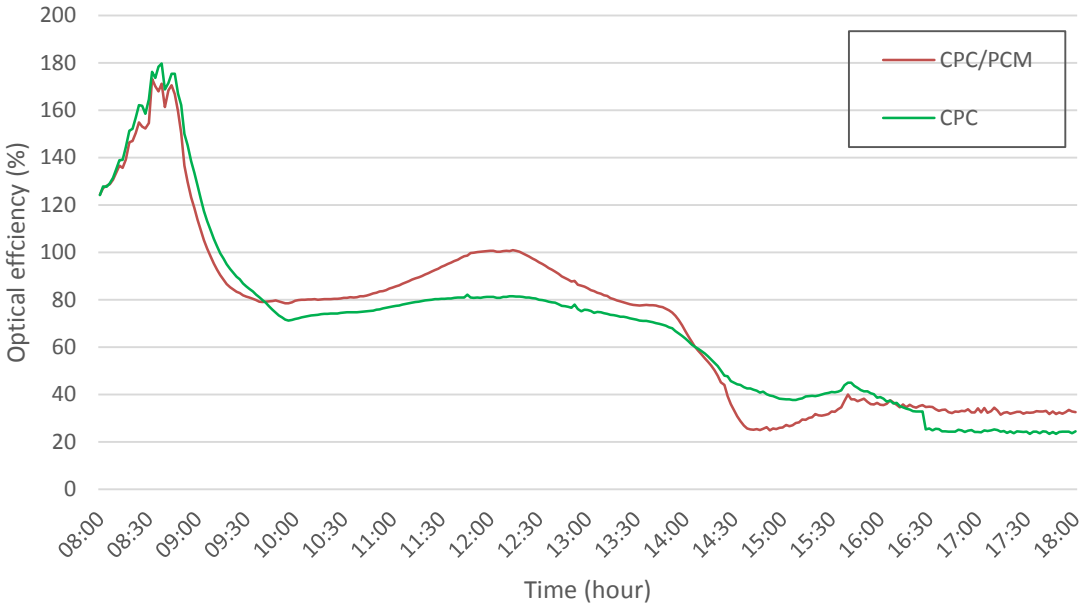

Figure 7. 27 Optical efficiency under clear sky for the CPC and CPC/PCM systems

System efficiency for the three systems is presented in figure 7.28. The effective aperture area (1.19 m^2) was considered in calculating the system efficiency of the systems. From the graph a similar behavior to the solar cell efficiency can be seen, this is because in the equations 2.3 and 2.4 presented in section 2.1 only the area was the factor of change. Between 10:00 and 14:00 the Reference system presented a stable system efficiency, approximately equal to 4 %. At maximum solar radiation (695 W/m^2) the reported efficiencies were 9 %, for the CPC and, CPC/PCM systems and 4% for the Reference system, respectively. The temperature in the solar cells was 75 ºC, 98 ºC and 58 ºC for the CPC, CPC/PCM and Reference systems respectively. This represented a difference from outdoor temperature of 52 ºC (CPC system), 75 ºC (CPC/PCM) and 35 ºC (Reference system). It was expected that the performance of solar cells generally increases with solar radiation, as more solar radiation is available to be converted into electricity. However, an important factor that negatively affects solar cell performance is the increase in solar cell temperature. As the temperature of the solar cells increases, the open-circuit voltage decreases, leading to a reduction in overall system efficiency.

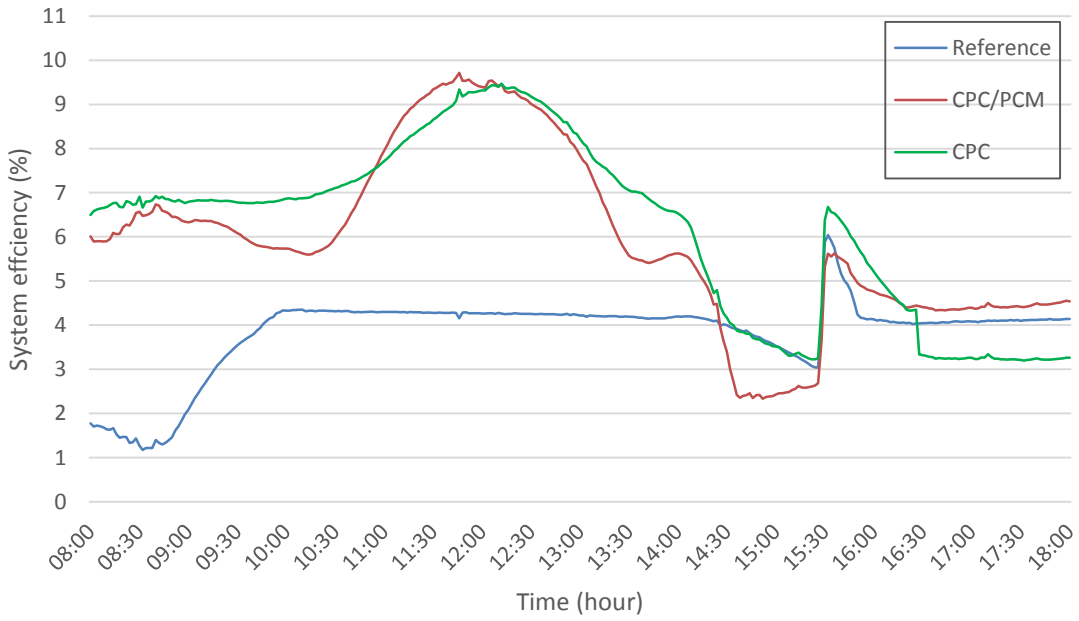

Figure 7. 28 System efficiency under clear sky for the CPC, CPC/PCM and Reference systems

Indeed, using the effective surface area of the solar cell to calculate solar cell efficiency for the Reference system might seem to put it at a disadvantage when compared with the CPC system. This is primarily because the area occupied by reflectors in the CPC system does not contain solar cells in the Reference system. As such, one might argue that an increased number of reference cells could fill the area taken up by the reflectors, thereby potentially enhancing its overall efficiency and making the comparison seem inequitable. However, this perspective may not entirely stand the test of accuracy for several key reasons:

- Efficiency of Resources: While populating the Reference system with more solar cells to equate to the CPC system's area with reflectors may appear advantageous, it is

essential to factor in the related cost and resource implications. The manufacturing of solar cells often incurs a higher expense and consumes more resources compared to reflectors. The fundamental concept behind employing a concentrator, as in the CPC system, is to amplify the efficiency of a given solar cell area, thereby enhancing cost-effectiveness and resource efficiency.

- Fundamental Design Principles: The underlying operating principles of each system are inherently different. The CPC system boosts solar capture by harnessing reflectors to concentrate light onto a more confined area of solar cells, thereby enhancing their efficiency. Conversely, the Reference system operates based on the principle of direct sunlight capture without any concentration. Thus, contrasting the two systems predicated on their unique design principles, rather than artificially expanding the cell area of the Reference system, enables a more meaningful and equitable comparison.

- Thermal Management Considerations: An increase in cells for the Reference system could potentially lead to a heightened accumulation of heat, which could conversely reduce the efficiency of the solar cells. In contrast, the CPC system, with its integrated PCM, possesses a mechanism for thermal management that improves overall efficiency.

Concentrating on solar cell efficiency utilizing their effective surface area delivers a fair and reasonable methodology for comparison, respecting the distinct design principles and constraints inherent in the two systems. More reason about this were explain in section 5.2.2.

Table 7.5 shows the average behavior of the systems under clear sky. On average among the concentrators, the CPC system reported higher power (37 W) and higher power ratio (1.86) compared to the CPC/PCM system (33 W and 1.77) this was mainly due to the elevated temperatures reported in the solar cells in the CPC/PCM system. Both concentrators reported a system efficiency equal to 6 %, which is 2 % more than the Reference system.

Table 7. 5 Systems average performance under clear sky

System	Power (W)	Power ratio	Fill factor	Solar cell efficiency (%)	Optical efficiency (%)	System efficiency (%)	Solar cell temperature (ºC)
CPC	37	1.86	0.62	20	69	6.20	53
CPC /PCM	33	1.77	0.59	19	72	5.94	67
Reference	19	-	0.76	12	-	3.82	44

The table 7.6 summarizes the results from the experimental test comparing with the simulations results.

Table 7. 6 Comparison between experimental test and simulation results for CPC and CPC/PCM systems in Mayo

Parameter	Experimental Test Results	Simulation Results
Solar Cell Efficiency	CPC: 20 % CPC/PCM: 19 %	28% - 49%
Power Ratio	CPC: 1.86 CPC/PCM: 1.77	2.82 (Feb-Sep) 1.29 (Dec) 1.4 (Jan)
Power Output	CPC: 37 W CPC/PCM: 33 W (at 420 W/m^2)	126 W (1000 W/m^2 at 25 ºC)

From the table, it can be observed that the experimental test results showed lower solar cell efficiency, power ratio, and power output compared to the simulation results.

- The experimental test results showed a solar cell efficiency of 20 % for the CPC system and 19 % for the CPC/PCM system, which was lower than the simulation range of 31 % - 49 %.

- Power ratio for the experimental test results was also lower, with 1.86 for the CPC system and 1.77 for the CPC/PCM system, as compared to the simulation results of 2.82 (Feb-Sep), 1.29 (Dec), and 1.4 (Jan).

- Furthermore, the power output recorded from experimental testing was notably lower than anticipated from simulation forecasts. The CPC system generated 37 W and the CPC/PCM system produced 33 W under conditions of 420 W/m^2 solar radiation, a significant deviation from the projected 126 W under optimal conditions of 1000 W/m^2 solar radiation and 25 ºC in the summer months.

The experimental test results for power output were measured at a solar radiation intensity of 420 W/m², which was significantly lower than the 1000 W/m² used in the simulation results. This difference in solar radiation intensity was a critical factor to consider when comparing the experimental test results with the simulation results. As the intensity of solar radiation decreased, the amount of energy available to be converted into electricity by the solar cells also decreased. This, in turn, led to lower power output values. The experimental test results obtained at a lower solar radiation intensity of 420 W/m² were therefore expected to be lower compared to the power output values predicted by the simulation at 1000 W/m². Modeling at different solar radiation intensities was not been done due to various reasons, such as computational limitations, time constraints, or the focus on the performance of the

system under standard test conditions, such as those specified by ASTM G173. ASTM G173 specifies standard spectra for solar energy applications, which includes a standard reference spectrum with a solar radiation intensity of 1000 W/m². This intensity is often referred to as Air Mass 1.5 (AM1.5) and represents a typical mid-latitude solar radiation condition. The use of 1000 W/m² as a reference intensity is common in solar energy research and testing to provide a standard baseline for comparing the performance of different solar energy systems.

It was also important to note that solar cell efficiency and power ratio may have been influenced by solar radiation intensity. The performance of solar cells could vary under different levels of solar radiation, and their efficiency might not have been constant across the entire range of solar radiation intensities. As a result, the discrepancies between the experimental test results and simulation results might have been partially attributed to the difference in solar radiation intensity during the testing period and rotation of 46º of the wall in use.

7.2.2 Average behaviour under clear sky

Variation of the average power for the three systems under clear sky is shown in figure 7.29. In both concentrators the power output increased exponentially from 250 W/m^2. At 200 W/m^2, a small increase in the power of both concentrators was observed due to the high power produced in the morning (figure 7.22). For low solar radiation (100 W/m^2 - 150 W/m^2) the three systems present similar values. The CPC system reported a higher power output from 200 W/m^2 to 700 W/m^2 compared with CPC/PCM and Reference systems.

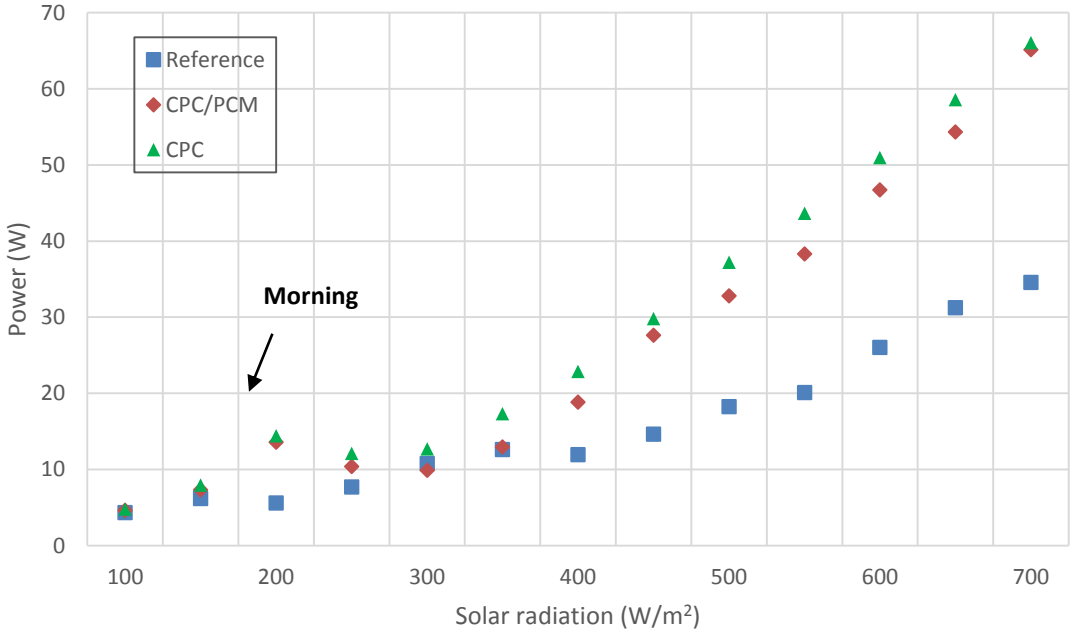

Figure 7. 29 Average power output under clear sky for CPC, CPC/PCM and Reference systems

The important aspects of this graph are the following:

- Both the CPC and CPC/PCM systems showed an exponential increase in power output as solar radiation intensity increases from 250 W/m².

- At solar radiation levels of 200 W/m², both concentrators exhibited a small increase in power, likely due to the high power generated in the morning. This was the time when the Reference system experienced shading, which contributed to the observed differences in power output.

- For low solar radiation levels (100 W/m² to 150 W/m²), the three systems showed similar performance, suggesting that the concentrators did not provide a significant advantage at these low light levels.

- The CPC system consistently demonstrated a higher power output than the CPC/PCM and Reference systems from 200 W/m² to 700 W/m², indicating its superior performance under these solar radiation conditions.

Figure 7.30 presents the temperature variation in the solar cells of the three systems with solar radiation. It is clear that the CPC/PCM system showed higher temperatures compared to the other systems and its temperature increased as the solar radiation increased. The exception can be observed at 200 W/m^2 where both concentrators presented similar temperatures and the three systems presented lower temperatures compared to the rest of the solar radiations. This was due to the fact that in the morning the three systems presented low temperatures as a result of the cooling during the night. At solar radiations 100 W/m^2 and 150 W/m^2 an increase in the temperature in the CPC/PCM system was reported due to the thermal energy stored in the PCM during the evening.

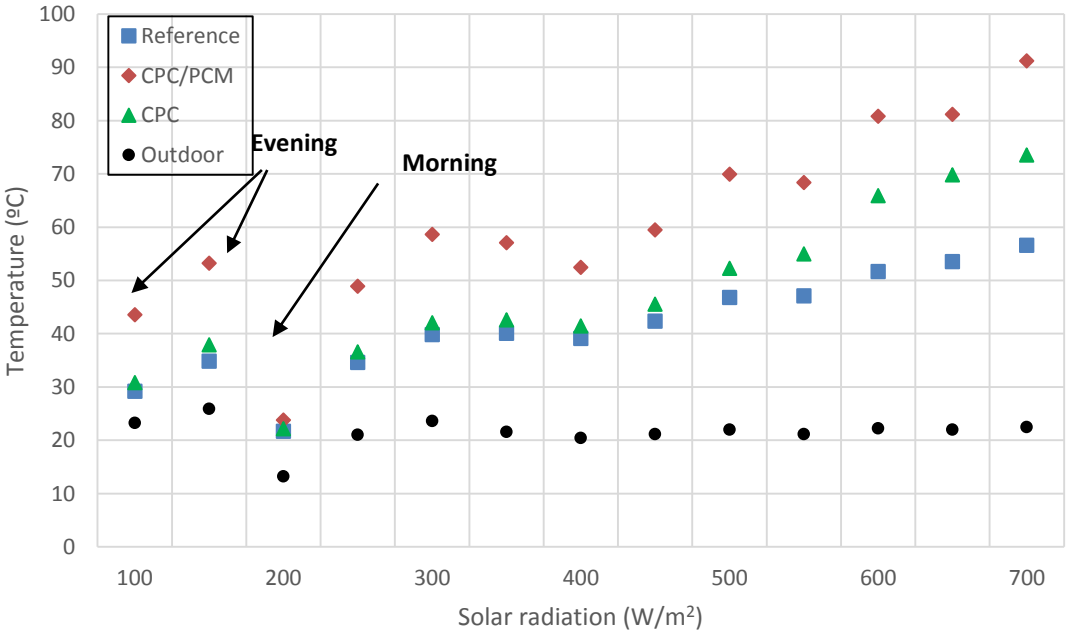

Figure 7. 30 Average solar cell temperature under clear sky for CPC, CPC/PCM and Reference systems

Specific temperature variations and the differences between the systems provided valuable insights into the performance and thermal behavior of the systems. The graph illustrated the temperature variations in the solar cells of the three systems under various solar radiation conditions. It allowed to understand how the systems reacted to different levels of solar radiation and their thermal performance.

Power ratio of the concentrators is reported in figure 7.31. At 100 W/m^2 the power ratio in both systems was low and equal to 1. The CPC system showed the lowest power ratio due to the drop after 16:30 (figure 7.24). From 150 W/m^2 the CPC system showed a better power ratio compared to the CPC/PCM System. Between 200 - 250 W/m^2 and 400 - 450 W/m^2, high power ratio values were observed in both concentrators as a consequence of the peak produced in the morning where the Reference system was covered by shadow generated by the CPC/PCM system. Power ratio at high solar radiation (600 W/m^2 - 700 W/m^2) was ~ 2.

The observed power ratios were generally lower than the simulated values of 2.82 (Feb-Sep), 1.29 (Dec), and 1.4 (Jan). However, the high power ratio values observed between 200 - 250 W/m² and 400 - 450 W/m² aligned with the expected behavior due to shading effects. The results, while not entirely matching the simulation, still provided valuable insights into the concentrators' performance in real-world conditions.

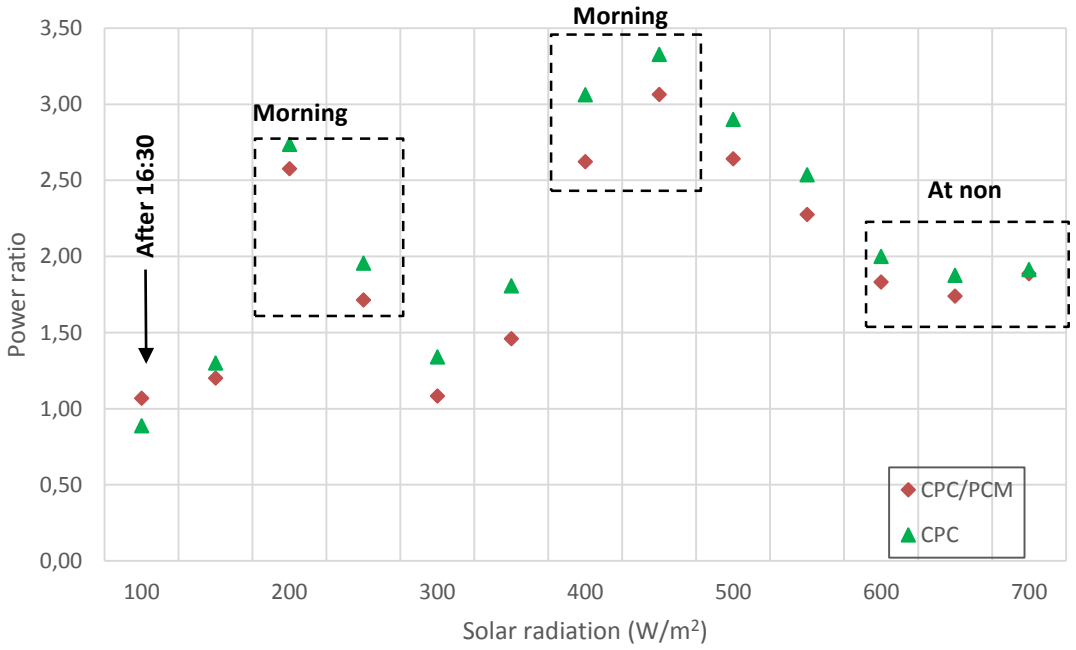

Figure 7. 31 Average power ratio under clear sky for CPC and CPC/PCM systems

Variation of the fill factor of the three systems with solar radiation is presented in figure 7.32. The Reference system maintained a fill factor close to 0.80. Contrastingly, both the CPC and

CPC/PCM systems exhibited a distinct downward trend in their fill factors with increasing solar radiation. This decrease was attributed to several key factors. One significant factor was the rise in solar cell temperature, which led to a decrease in cell performance. The escalating temperature induced by the augmented solar radiation causes increased kinetic energy of the electrons in the solar cells, leading to a higher probability of recombination and thus, a decrease in the fill factor. Moreover, the series resistance within the system contributes to the declining fill factor. As solar radiation increases, the current produced by the solar cells also increases. However, a higher current flowing through the system inevitably leads to a greater voltage drop across the internal resistances (due to Ohm's law: V = I*R), which diminishes the overall output voltage and hence, the fill factor. Lastly, defects in the soldering joints could exacerbate this decline. Soldering defects can introduce additional resistances in the system, which when combined with the increased current from the higher solar radiation, could result in a significant voltage drop, thereby reducing the fill factor.

In the CPC/PCM system, a higher drop was observed from 500 W/m^2, reaching ~0.5. In the CPC system, after 500 W/m^2 the fill factor stabilised at ~0.6.

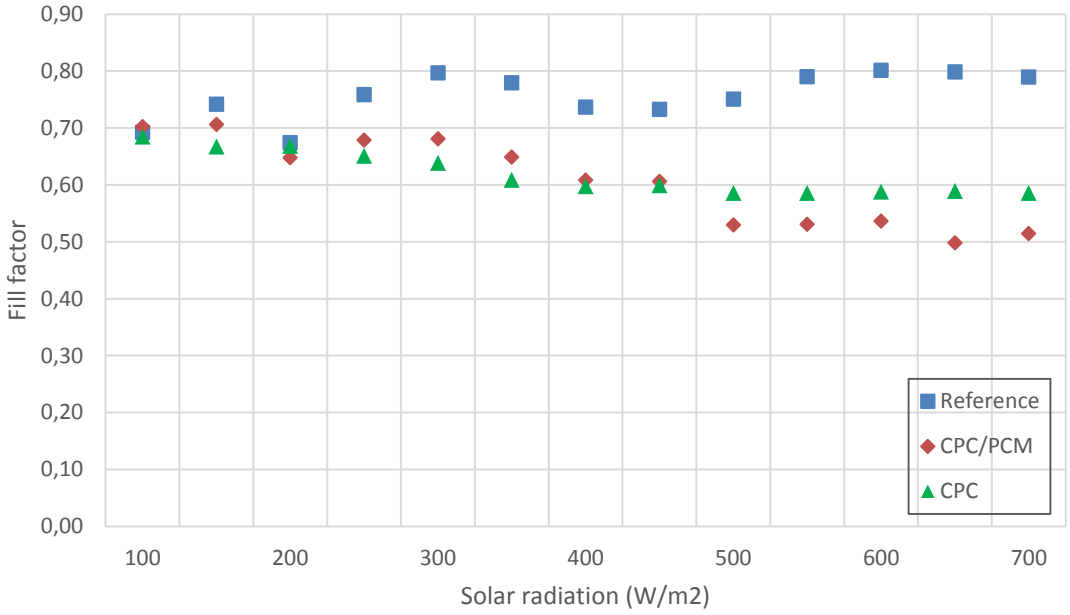

Figure 7. 32 Average fill factor under clear sky for CPC, CPC/PCM and Reference systems

Variation of solar cell efficiency of the three systems is shown in figure 7.33. The results show at low radiations (100 – 150 W/m^2) there is an increase in solar cell efficiencies due to the sudden increase in efficiency that occurs between 15:30 and 16:00. At 200 W/m^2, both concentrators had better solar cell efficiency compared to the Reference system due to the shadow that was generated on the Reference system in the early morning hours (figure 6.25). From 300 W/m^2, both concentrators show higher solar cell efficiency values compared to the reference system and the increase was linear. The CPC had an approximate increase of 2 % compared to the CPC/PCM system and 12 % compared to the Reference system at 700 W/m^2.

The rationale for considering the aperture of the Reference system as the aperture of the CPC has been thoroughly discussed and articulated in sections 5.2.2 and 7.2.1.

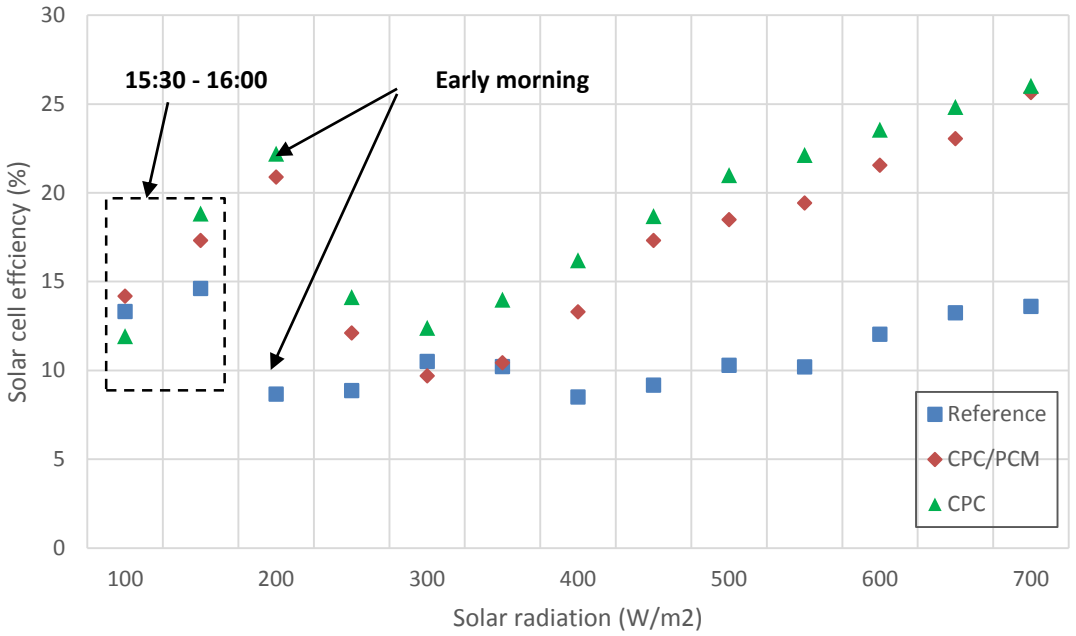

Figure 7. 33 Average solar cell efficiency under clear sky for CPC, CPC/PCM and Reference systems

Figure 7.34 illustrates the change in optical efficiency of the concentrators with respect to solar radiation. A noticeable increase in efficiency was observed between 200 and 250 W/m², which can be attributed to the shading effects on the reference system, which resulted in the concentrators, particularly the CPC system, having a relatively higher efficiency in comparison. Beyond 300 W/m², the efficiency rise, stabilizing between 400 and 550 W/m². Within this solar radiation range (300 - 550 W/m²), the CPC system displayed higher efficiency values compared to the CPC/PCM system, reaching a peak value of 98 % at 550 W/m². The efficiency values for the CPC system declined between 600 and 700 W/m², as the CPC system recorded lower values compared to the CPC/PCM system at noon.

Reaching 98 % efficiency was possible due to the optimal alignment and positioning of the concentrator components, as well as the use of appropriate materials with high reflectivity.

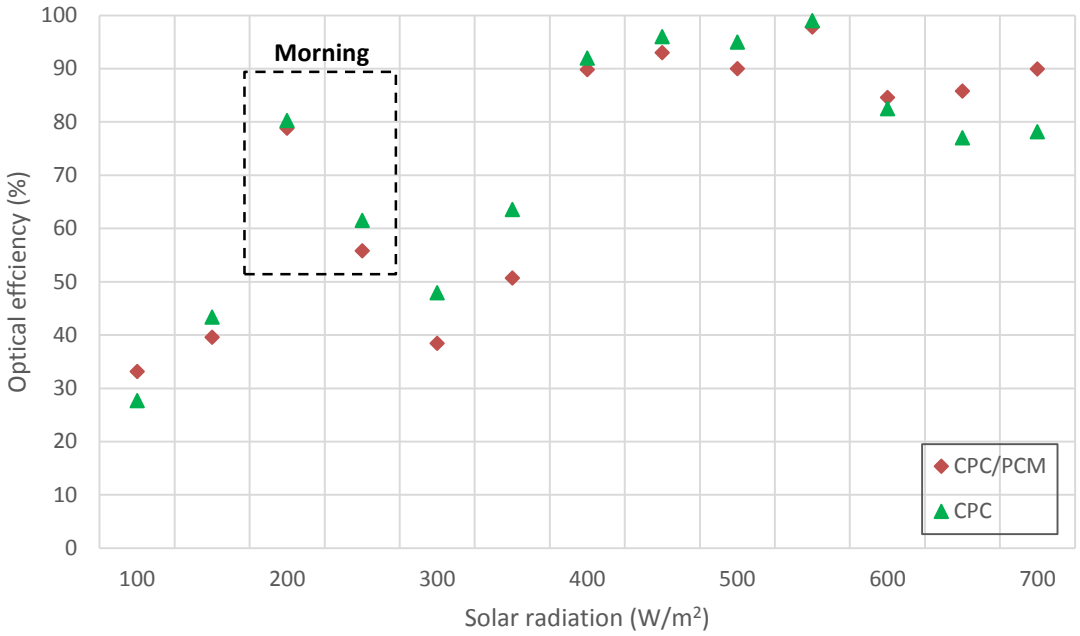

Figure 7. 34 Average optical efficiency under clear sky for CPC and CPC/PCM systems

System efficiency of the three systems is presented in figure 7.35. A behavior similar to solar cell efficiency can be observed. From 300 W/m^2, a linear increase in system efficiency was observed, with the CPC system being highest. At 700 W/m^2, both concentrators had a system efficiency equal to 8 % compared to the Reference system of 4 %. Between 100 - 150 W/m^2, the three systems reported high values due to the sudden increase in system efficiency that occurred between 15:30 - 16:00. At 200 W/m^2, both concentrators reported high values compared to the Reference system due to the shadow produced on the Reference system in the early hours of the morning.

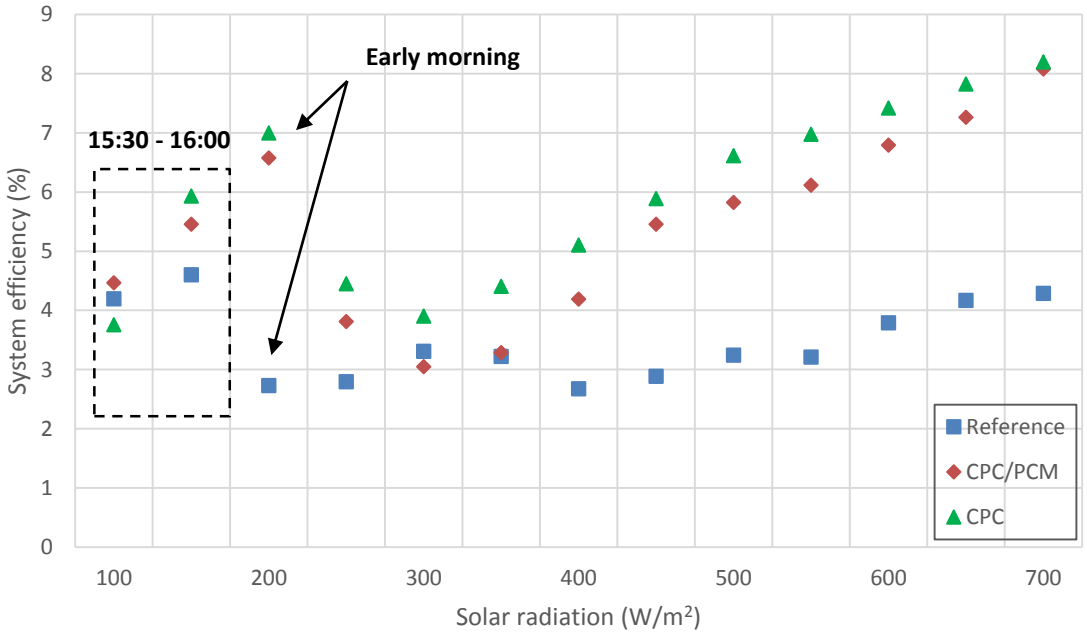

Figure 7. 35 Average system efficiency under clear sky for CPC, CPC/PCM and Reference systems

7.2.3 I-V analysis under clear sky

Figure 7.36 displays the maximum power output of the three systems across a range of incident solar radiation intensities. Variations in solar radiation were less than 1 W/m² between measurements and had no significant impact on the power output of the systems. At 700 W/m², the power outputs for the CPC, CPC/PCM, and Reference systems were 76 W, 78 W, and 35 W, respectively. Power concentration for the CPC and CPC/PCM systems was 2.17 and 2.22, respectively, which were lower compared with the simulation results of 2.82 (at 1000 W/m²). Most losses were due to temperature fluctuations, deviations from south-facing alignment, and shading effects. An approximate distribution in the radiation curve was selected for determining the maximum values presented in figure 7.36. For example, at 150 W/m², measurements were taken at 08:00, while at 450 W/m², they were taken at 14:06. At 250 W/m² and 300 W/m², readings were recorded at 15:30 and 15:04, respectively. This suggests that partial cloud cover was present during these readings, causing a decrease in solar radiation.

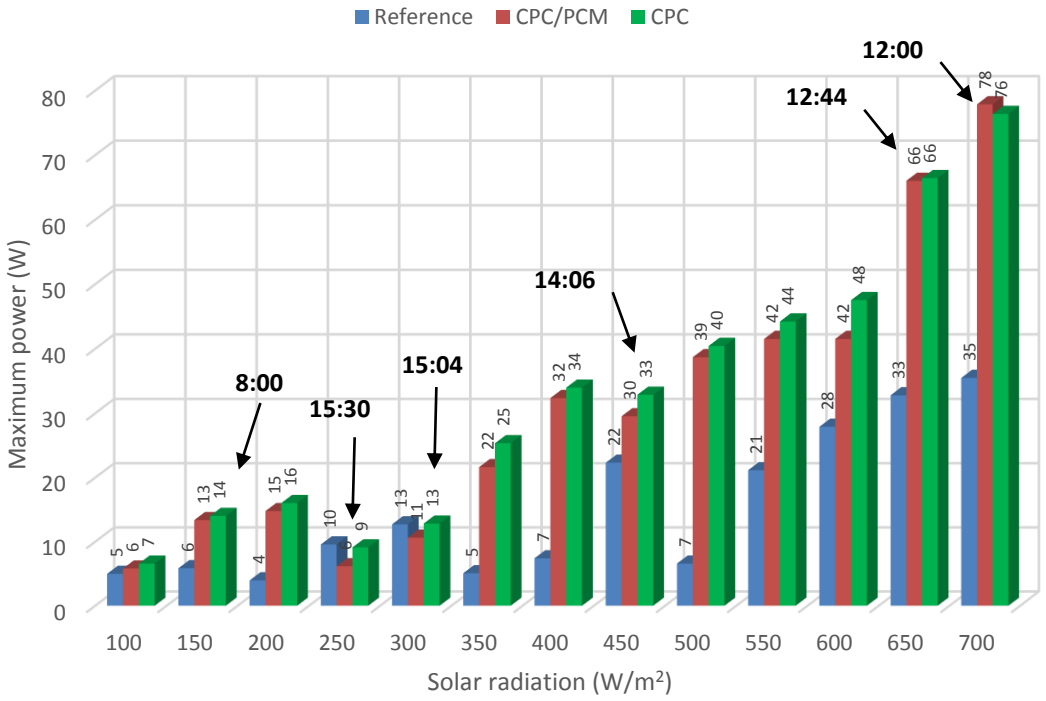

Figure 7. 36 Maximum power achieved under clear sky for CPC, CPC/PCM and Reference systems

Maximum power output and I-V curves for Reference, CPC/PCM and CPC system are shown in figures 7.37, 7.38 and 7.39 respectively. From figure 7.37 all power output curves have

similar behaviour as it was expected for the Reference system. The open circuit voltage ranged from 14 V to 15 V and the short circuit current ranged from 0.5 A to 3.2 A.

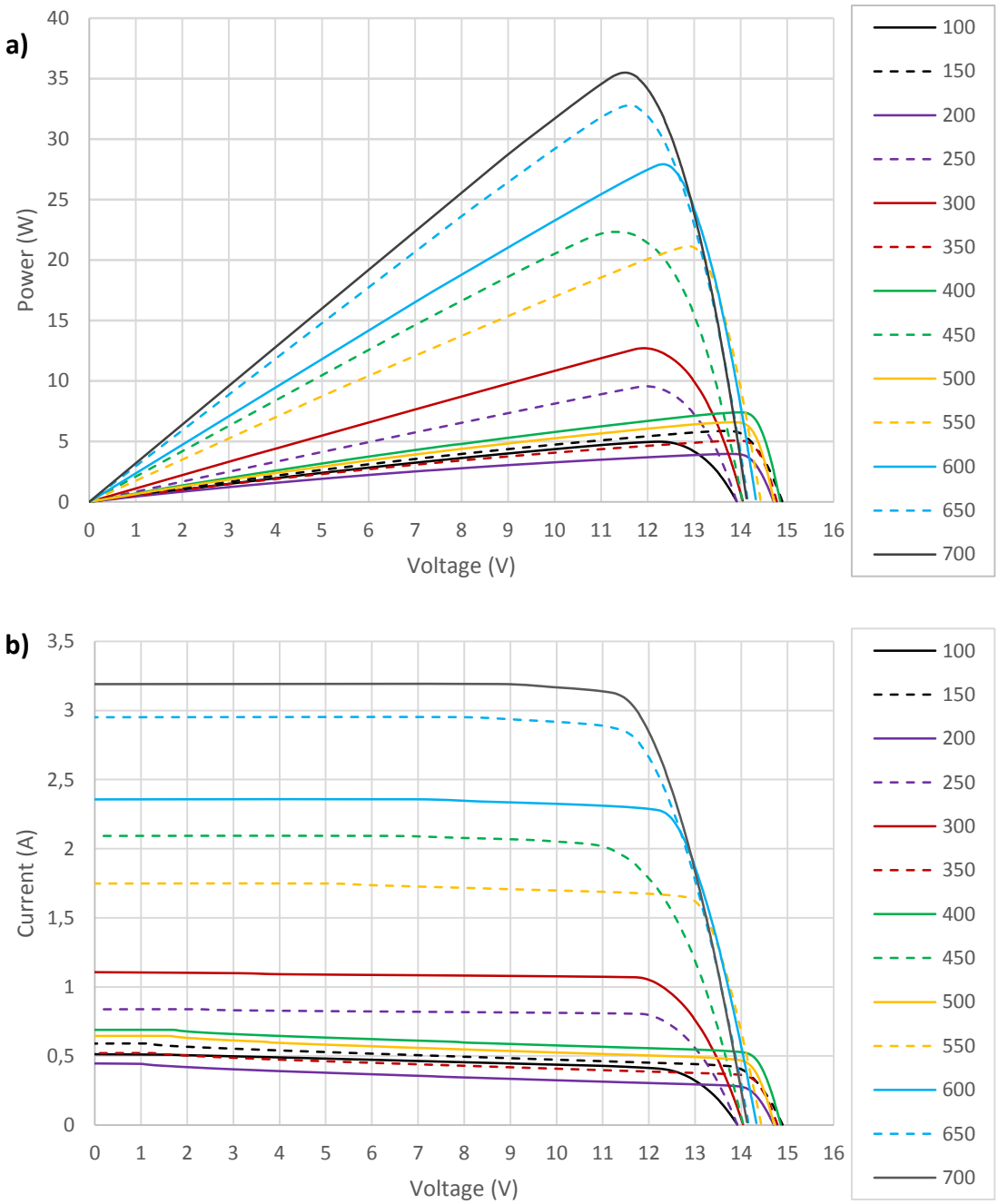

Figure 7. 37 Maximum power output and I-V curve with solar radiation under clear sky of Reference system
(a) Maximum power (b) I-V curve

From figure 7.38, the CPC/PCM system power output curves fluctuated at 600 W/m^2 and 350 W/m^2. For the IV curves the fluctuation was observed at 650, 600, 500 and 350 W/m^2. This can be explained by the extra power drop across the solar module analyzers and the resistive losses in each component due to the high current to voltage ratio. These are due this:

- Extra power drop across the solar module analyzers: The solar module analyzers are devices used to measure the performance of the solar cells. However, these analyzers themselves can contribute to some power losses in the system due to their internal resistance, leading to a reduction in the overall power output.

- Resistive losses in each component due to the high current to voltage ratio: The electrical components in the system, such as wires, connectors, and other devices, have an inherent resistance that causes power losses when current flows through them. When the current to voltage ratio is high, it means that there is a large amount of current flowing through the system relative to the voltage. This high current can lead to more significant resistive losses in the components, further reducing the system's power output.

The open circuit current in the CPC/PCM system varies between 0.5 A to 9.5 A, open circuit voltage varies from 14.5 V to 17 V approximately. It could be observed that the short circuit current and open circuit voltage in the CPC/PCM system were 6 A and 1 V more respectively compared to the reference system.
Fluctuations observed in the IV and Power curves may be due to measurement errors, which could affect the accuracy of the data collected during the testing process.

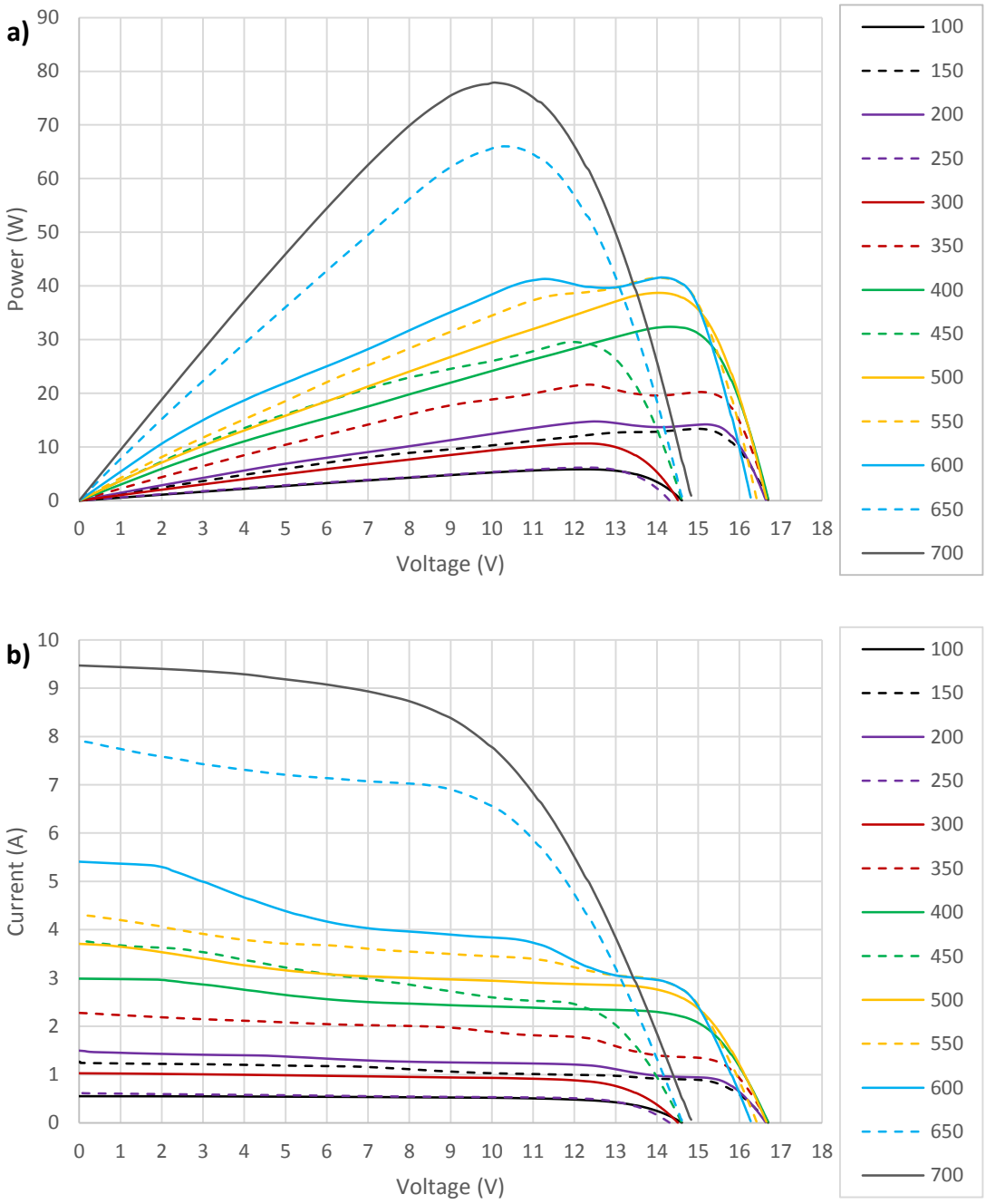

Figure 7. 38 Maximum power output and I-V curve with solar radiation under clear sky of CPC/PCM system
(a) Maximum power (b) I-V curve

From figure 7.39, it is important to note the fluctuations in the power output curves of the CPC system at 600, 550, and 400 W/m². These fluctuations can provide insights into the system's performance under varying solar radiation conditions. Additionally, the open circuit voltage varied between 15 V to 17 V, and the short circuit current ranged from 0.5 A to 7.8 A. It is also significant that the short circuit current and open circuit voltage in the CPC system were 4 A and 1 V higher, respectively, compared to the Reference system. This information

highlights the superior performance of the CPC system in comparison to the Reference system.

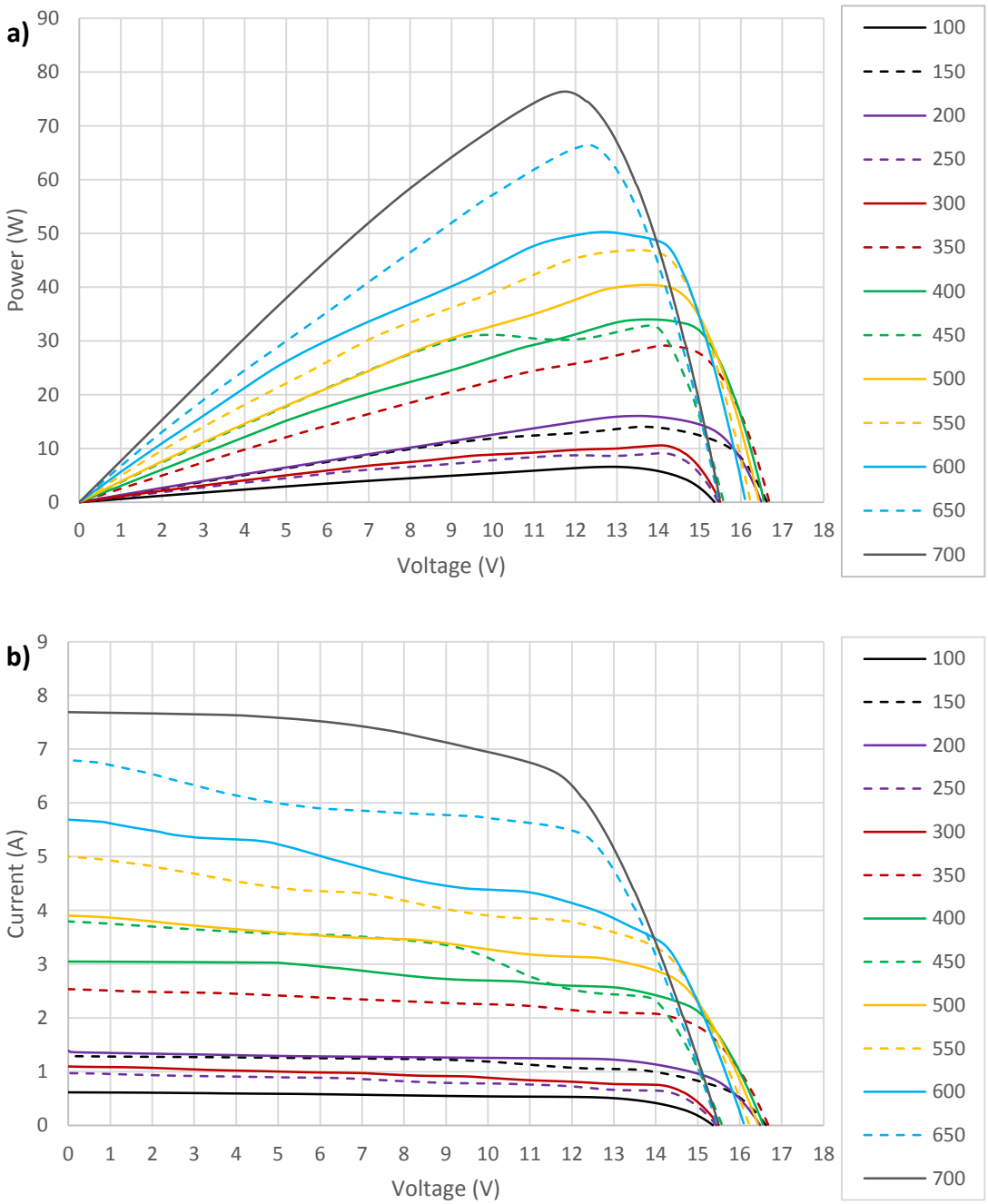

Figure 7. 39 Maximum power output and I-V curve with solar radiation under clear sky of CPC system
(a) Maximum power (b) I-V curve

7.2.4 Thermal analysis under clear sky

Average temperatures in the solar cells and backplate in the reference system are shown in figure 7.40. Maximum temperature of the solar cells and backplate was 58 ºC and 50 ºC with an outdoor temperature of 23 ºC at 11:00. It was observed that heat was absorbed by the

backplate from the solar cells and dissipated to the external environment which reduced the temperature by 8 ºC in the backplate at that moment and the solar cell was 35 ºC more than outdoor temperature. From 16:00 the solar cells and backplate were the same temperature of 27 ºC, 4 ºC more than the outdoor temperature.

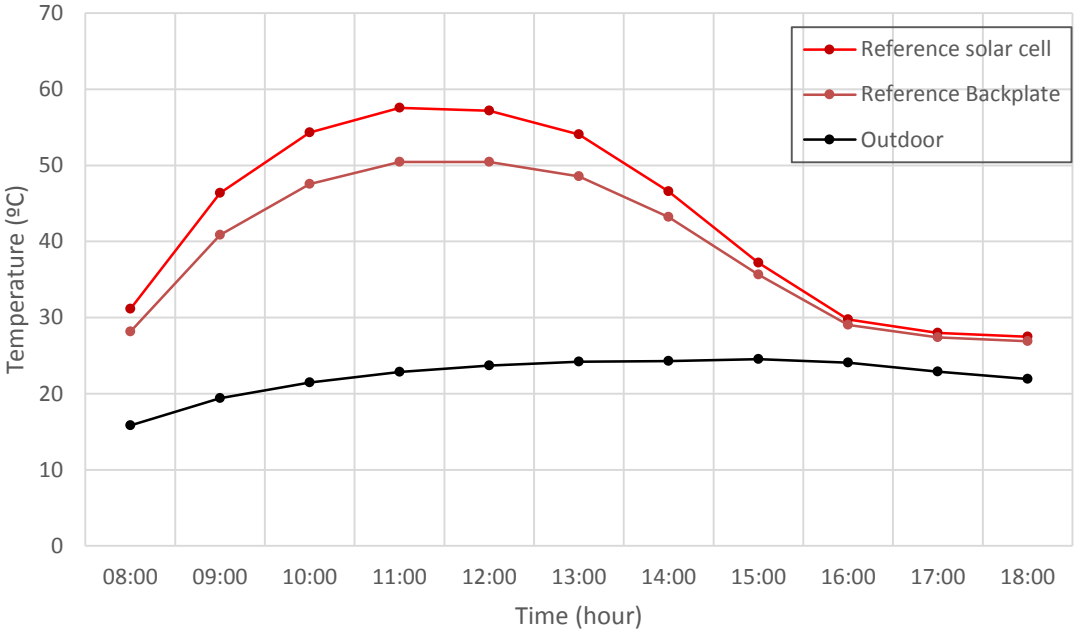

Figure 7. 40 Average temperature under clear sky on Reference system

Figure 7.41 shows the average temperatures in various components of the CPC/PCM system. Solar cells exhibited the highest temperatures, with a maximum value of 107 ºC at 12:00, which was 83 ºC higher than the external temperature. This significant temperature difference can be attributed to the combined effect of the concentrated solar radiation in the CPC system and the thermal energy stored and released by the PCM. The concentration of solar radiation increases the amount of energy absorbed by the solar cells, which in turn raises their temperature. Additionally, the PCM absorbs and releases thermal energy, further contributing to the elevated solar cell temperatures.

The backplate in the CPC/PCM system exhibited the second-highest temperature during the test, reaching a maximum value of 79 ºC at 13:00. This elevated temperature can be attributed to the proximity of the backplate to the solar cells and the PCM. As the solar cells and PCM experienced increased temperatures due to the concentrated solar radiation and the thermal energy storage/release process, the backplate absorbed some of the excess heat from these components. The close positioning of the backplate to the heated components allows for heat transfer to occur, resulting in an increased temperature for the backplate as well.

After 14:00, the solar cells and backplates exhibited the same temperature until 18:00, indicating as equilibrium heat transfer between these components. The temperatures of both

reflectors (top and bottom) remained approximately the same throughout the test, reaching a maximum value of 64 ºC at 13:00. This uniform temperature profile confirms the high reflectivity of the reflectors because it suggests that the reflectors were able to effectively redirect the incident solar radiation towards the solar cells without absorbing a significant amount of heat themselves. If the reflectors had poor reflectivity, they would have absorbed more solar radiation, leading to a more noticeable increase in temperature. The relatively stable and similar temperatures of both reflectors demonstrate their efficient performance in concentrating the ray lights onto the solar cells.

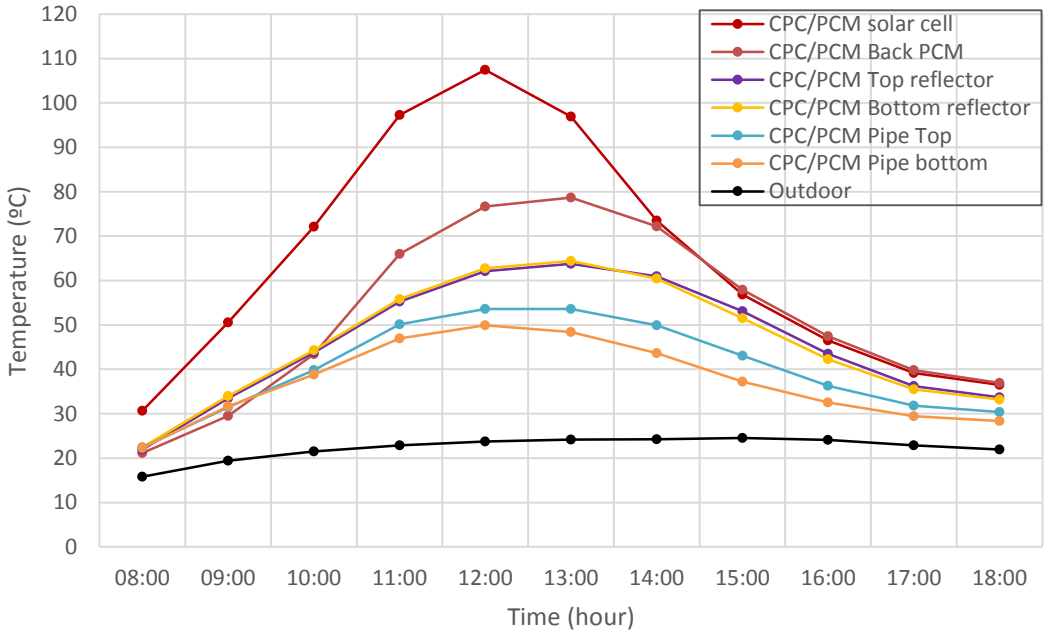

Figure 7. 41 Average temperature under clear sky on CPC/PCM system

Figure 7.42 presents the temperature difference between the solar cells and the backplate in the CPC/PCM system. This temperature variation is an indication of the heat transfer between the solar cells and the backplate. The temperature difference suggests that there is potential for future energy storage with heat exchanger, as the excess heat generated by the solar cells could be captured and stored in a thermal storage medium to eventually heat water as a heat exchanger. In such a system with heat exchanger, the stored thermal energy could be used to maintain the solar cells' performance during periods of low solar radiation or to supply heat for other applications. This would improve the overall efficiency and utilization of the solar energy system by harnessing the otherwise wasted heat generated by the solar cells.

The variation in temperature between the solar cells and the backplate ranging from 10 ºC to 31 ºC from 08:00 to 12:00 can be understood as "charging the PCM." This means that during this time period, the excess heat generated by the solar cells is being transferred to the PCM, causing it to change its phase (typically from solid to liquid).

As the PCM changes phase and stores the thermal energy, it helps maintain the solar cells' temperature within a more optimal range, improving their efficiency and performance. The stored thermal energy in the PCM can later be released and utilized when needed, for example, during periods of low solar radiation or to provide heat for other applications.

From noon, the PCM discharge process occurred. The temperature variation decreases from 31 ºC to 1 ºC at 14:00. From 14:00 to 17:00 the temperature variation is reduced from 1 ºC to -1 ºC, which means that the backplate was 1 ºC more than the solar cells. While this appears to be a real difference, it is essential to consider the measurement or experimental error associated with the temperature measurements. Factors such as sensor accuracy, calibration, and environmental influences could contribute to potential discrepancies in the temperature data.

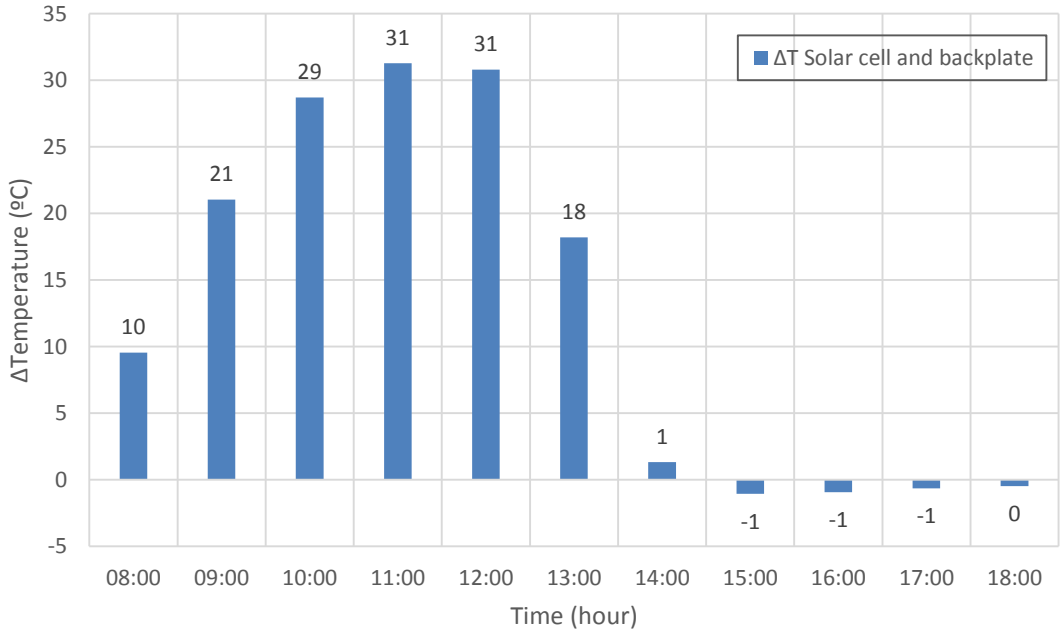

Figure 7. 42 Temperature difference between solar cell and backplate on CPC/PCM system under clear sky

Average temperatures of the CPC system are shown in figure 7.43. The solar cells had the highest temperatures from 08:00 to 14:00 with a maximum value at 12:00 of 84 ºC. Both reflectors (top and bottom) were the same temperature from 08:00 to 13:00. After that time, the top reflector was 2 ºC more than the bottom reflector. The backplate had the lowest temperature in the system, which demonstrates the cooling process through the backplate and distributed through the entire system. This is the reason why between 13:00 and 14:00 the solar cells and reflectors began to decrease in temperature during the afternoon until late at night. The maximum temperature on the backplate was 49 ºC at 12:00, 25 ºC higher than the external temperature.

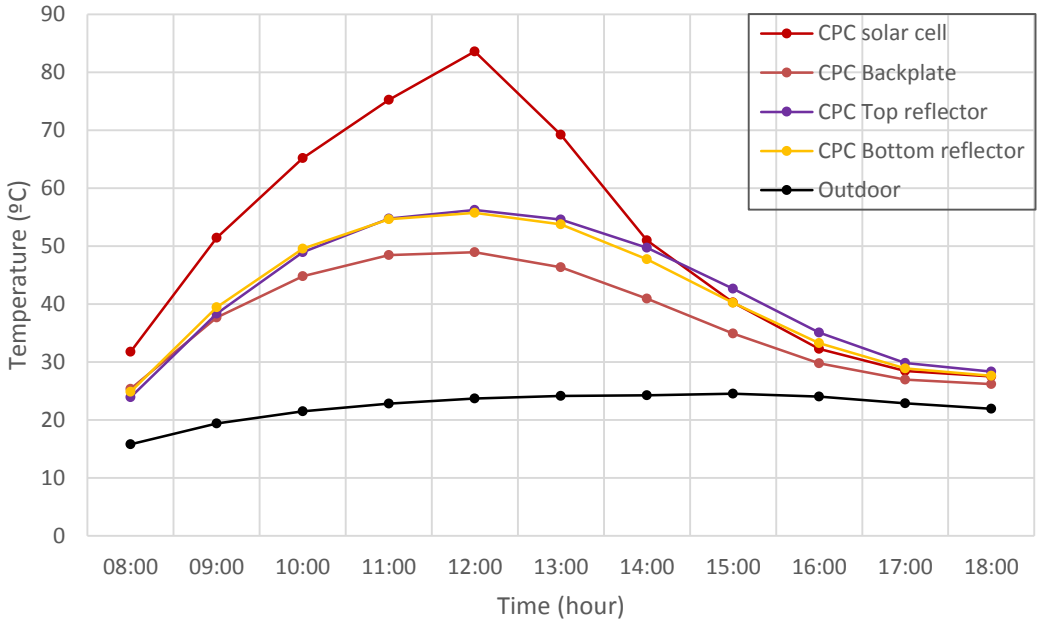

Figure 7. 43 Average temperature under clear sky on CPC system

The percentage of power losses due to temperature in the solar cells of the three systems is shown in figure 7.44 which was calculated by taking into account the temperature difference between the solar cells and the standard temperature of 25 ºC. To determine these losses, data provided by the manufacturer, as mentioned in section 3.7, were used. According to the manufacturer, the power loss due to temperature in the solar cells is equal to 0.32 % per degree Celsius above 25 ºC. In order to calculate these losses, the temperature difference between the solar cell's operating temperature and the standard temperature of 25 ºC was determined. This temperature difference was then multiplied by the power loss coefficient of 0.32 %/ºC. The result gives the percentage of power losses experienced by the solar cells due to the increased temperature. By understanding and quantifying these losses, measures can be taken to improve the overall efficiency and performance of the solar cell system, such as implementing better cooling mechanisms or using materials with lower temperature coefficients.

The results reported that the maximum losses due to temperatures occur at noon with values equal to 11 %, 19 % and 27 % in the Reference, CPC and CPC/PCM systems. The CPC/PCM system had the highest losses throughout the day, this is due to the process of discharging the thermal energy of the PCM in the solar cells. Average losses were 7 %, 9 % and 13 % for the reference, CPC and CPC/PCM systems respectively.

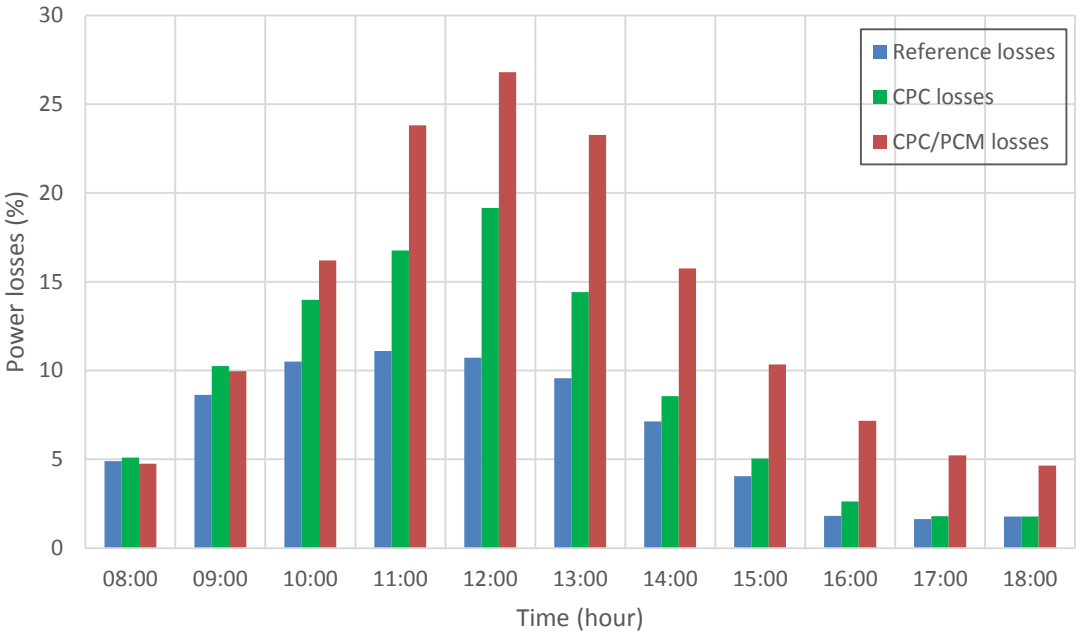

Figure 7. 44 Percentage power losses due to temperatures in the CPC, CPC/PCM and Reference systems under clear sky

Figure 7.45 shows the power of the three systems without the losses due to temperature. Once the percentage of power losses due to temperature for each system was determined, the power output without these losses could be calculated. To do this, the original power output of each system (as measured during the tests) was taken and adjusted by adding the percentage of power losses due to temperature. This provided the power output of each system without the influence of temperature-related losses.

An improvement of 17 W occurred in the CPC/PCM system at 11:00 and 13 W in the CPC system. The reference reported having 4 W and 3 W more at 11:00 and 12:00 respectively. A significant improvement could be observed in the power output if the temperature in the solar cells is controlled.

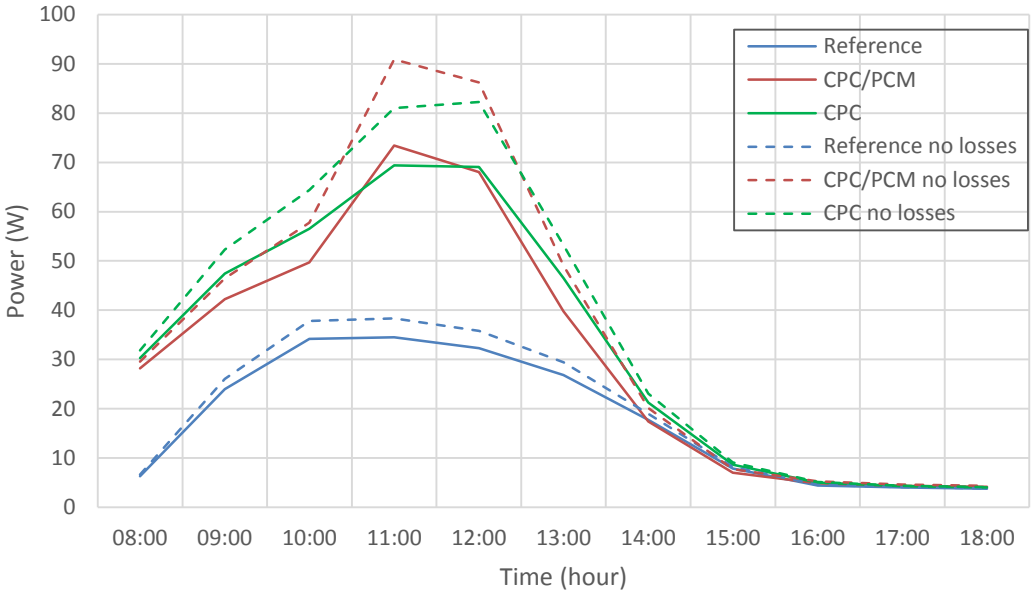

Figure 7. 45 Power experimental test and with no temperature losses in the CPC, CPC/PCM and Reference system under clear sky

Considering that this investigation was fundamentally a research project, it is essential to note that the primary objective was to explore and understand the potential benefits and challenges of integrating Phase Change Materials (PCMs) into CPC systems, rather than achieving immediate cost-effectiveness or commercial viability.

The research setting allowed for extensive experimentation and analysis, providing valuable insights into how PCMs interact with these systems, how they can enhance performance, and the potential drawbacks to their integration. As such, the costs and complexities encountered during this project should be viewed within this context - as part of an iterative research and development process, aimed at enhancing knowledge and understanding, and potentially informing future design improvements and cost reduction strategies.

In research projects, initial prototypes often bear higher costs and less efficiency due to the exploratory nature of the project and the need for custom, small-scale manufacturing. However, as the design is optimized and production is scaled up, costs can be significantly reduced, and performance further improved. Moreover, the experience and knowledge gained during the project can inform future initiatives, potentially leading to more efficient and cost-effective PCM-integrated solar systems.

Furthermore, it is worth mentioning that the research's value extends beyond the immediate project outcomes. The findings could contribute to the broader scientific community's understanding, potentially informing other research and development efforts in the area of solar energy technology. It is this collective advancement of knowledge that propels the field

forward and brings us closer to developing more efficient, sustainable, and cost-effective energy solutions.

7.2.5 Electrical analysis under diffuse radiation

Electrical results were recorded for four days on 11th and 27th of September 2022 and 3rd and 6th of October 2022 from 10:00 to 17:00 hours. These days were mostly consisting of diffuse solar radiation. The average of the data obtained in the four days was calculated and represented in each set of graphs. Figure 7.46 shows the variation of the incident solar radiation for the four days tested. Under diffuse radiation conditions, there was not sudden drop at 15:30, a phenomenon typically observed under direct radiation as a result of the 46º deviation from the wall to the south. The maximum solar radiation in the four days was only 83 W/m^2 approximately.

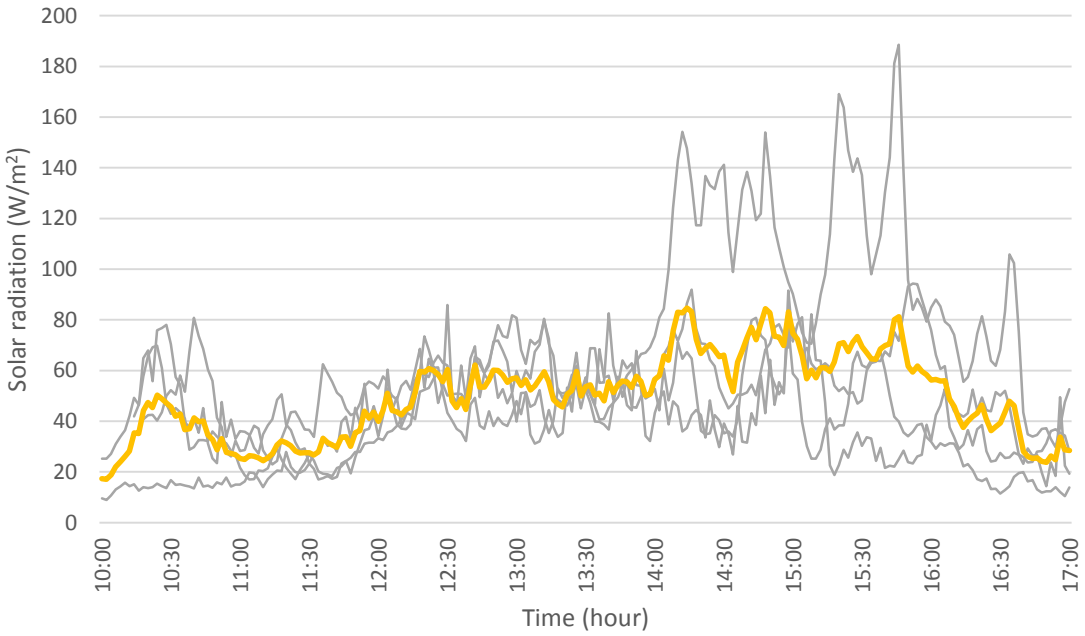

Figure 7. 46 Average variation of diffuse solar radiation with time between the 11th and 27th September, 3rd and 6th of October 2022

Power output for CPC, CPC/PCM and Reference systems are shown in figure 7.47 which changes linearly with incident solar radiation intensity as expected, with maxima at 14:30. Throughout the four days, the two concentrators showed power outputs greater than the Reference system. The maximum power output for CPC, CPC/PCM and Reference systems were 9, 9 and 4 W respectively at 85 W/m^2 solar radiation.

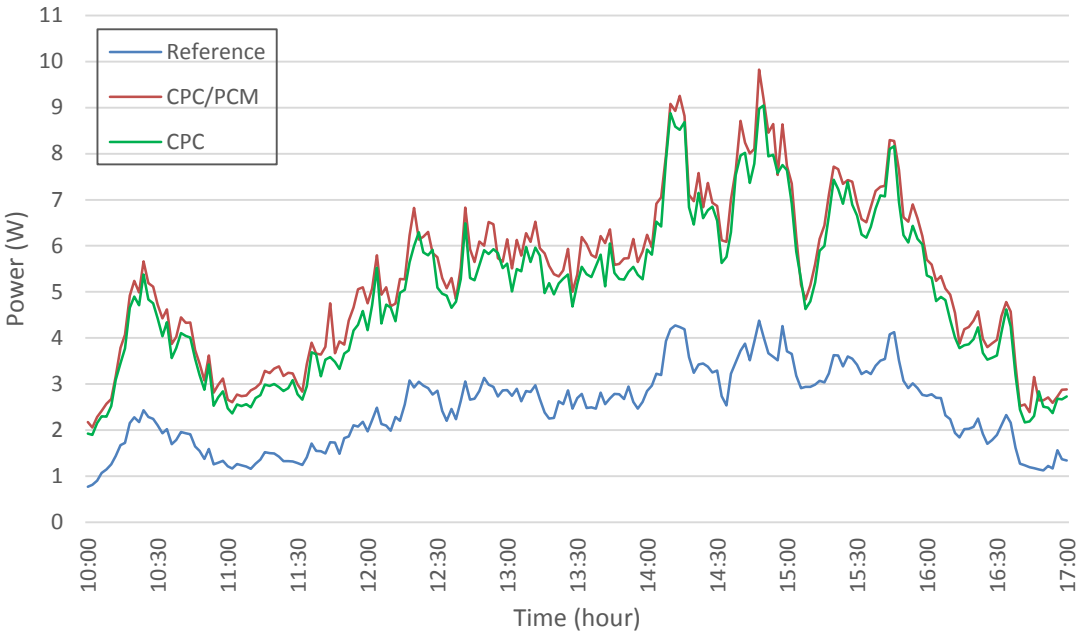

Figure 7. 47 Power output under diffuse radiation for the CPC, CPC/PCM and Reference systems

Figure 7.48 shows the temperature in the solar cells in the three systems. From 10:00 to 11:00 the three systems presented the same temperatures in the solar cells equal to 15 ºC. At the moment of maximum radiation (85 W/m^2) the reported temperatures were 19 ºC, 20 ºC and 18 ºC for the CPC, CPC/PCM and Reference system respectively, with an outdoor temperature of 14 ºC.

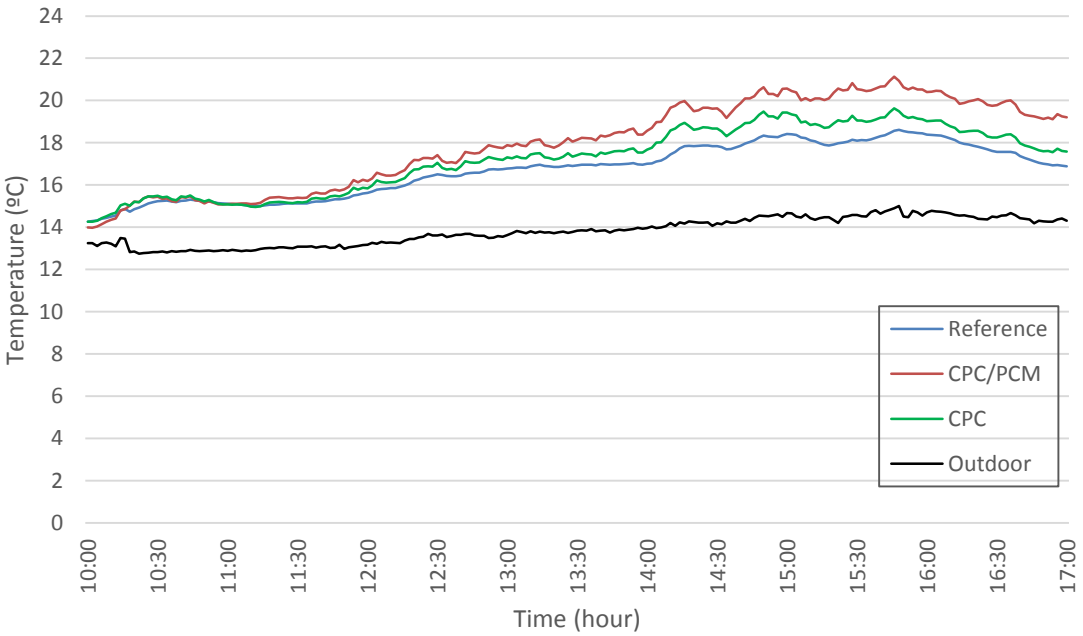

Figure 7. 48 Solar cells temperature under diffuse radiation for the CPC, CPC/PCM and Reference systems

Power ratio is presented in figure 7.49 for both concentrators, which fluctuates between 2 to 2.7 during the day with CPC/PCM system being slightly better than CPC system of 2.11 and 2.07 respectively (in average).

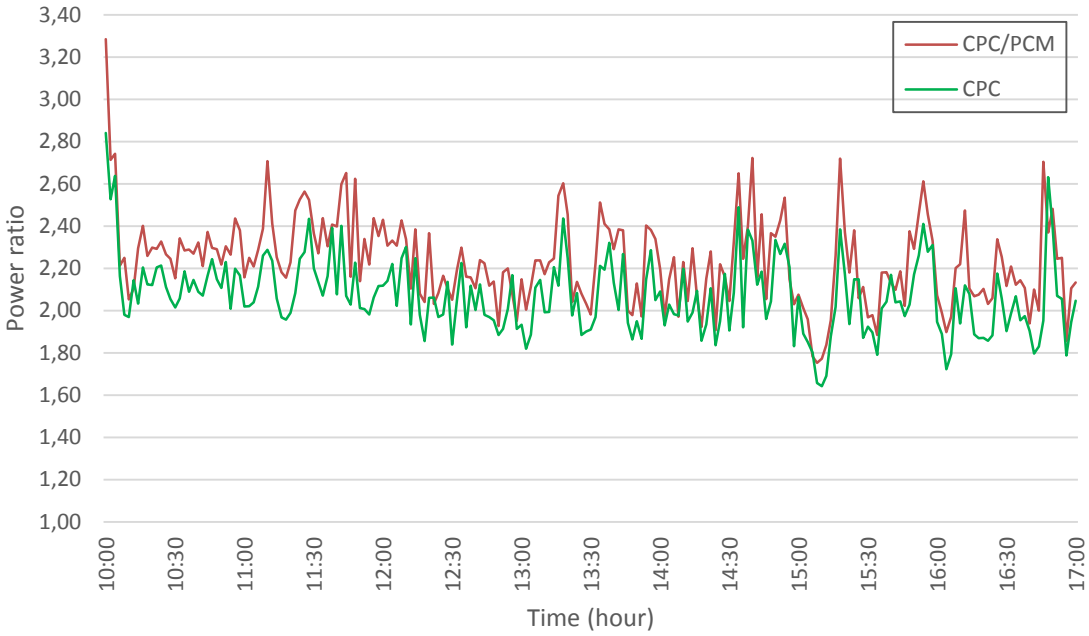

Figure 7. 49 Power ratio under diffuse radiation for the CPC and CPC/PCM systems

Figure 7.50 displays the fill factor for the CPC, CPC/PCM, and Reference systems. The Reference system showed a slight improvement in the fill factor between 14:30 and 15:00. Throughout the day, the average fill factor was 0.69, 0.73, and 0.70 for the CPC, CPC/PCM, and Reference systems, respectively.

In this case, the fill factor differences between the systems were not extremely large, but they did suggest that the CPC/PCM system had a slightly better performance in terms of power conversion under the tested conditions.

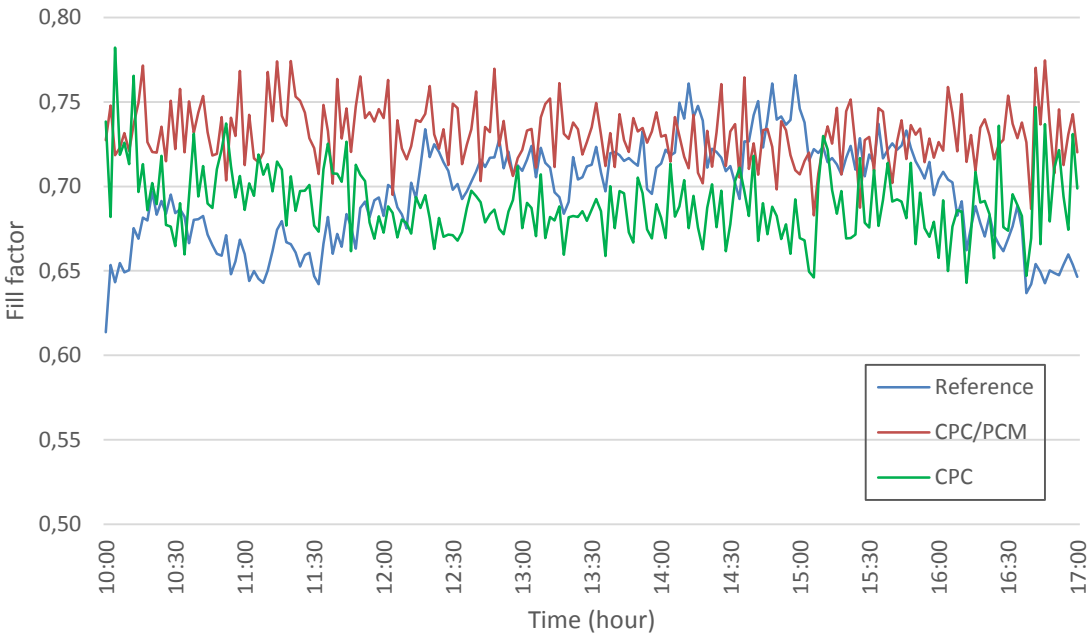

Figure 7. 50 Fill factor under diffuse radiation for the CPC, CPC/PCM and Reference systems

Solar cell efficiency for the three systems is presented in figure 7.51. The effective solar cell area (0.375 m^2) was considered to calculate the solar cell efficiency of the systems. On average, the two concentrators showed better solar cell efficiency compared with Reference system. The reference system was a stable but low solar cell efficiency with an average of 13 %. For the CPC/PCM and CPC systems the values were 29 % and 27 % on average, respectively. It is important to note that the concentration effect contributed to the higher efficiency values observed in the CPC/PCM and CPC systems. Due to this effect, the efficiency of the solar cells in these systems exceeded the nominal 22% efficiency, demonstrating the benefits of incorporating concentrating technologies like CPCs in solar energy systems. The concentration effect effectively focuses the solar radiation onto the solar cells, which can lead to an increase in solar cell efficiency beyond its nominal value. This enhancement in performance showcases the potential of utilizing CPCs to improve solar energy capture and conversion.

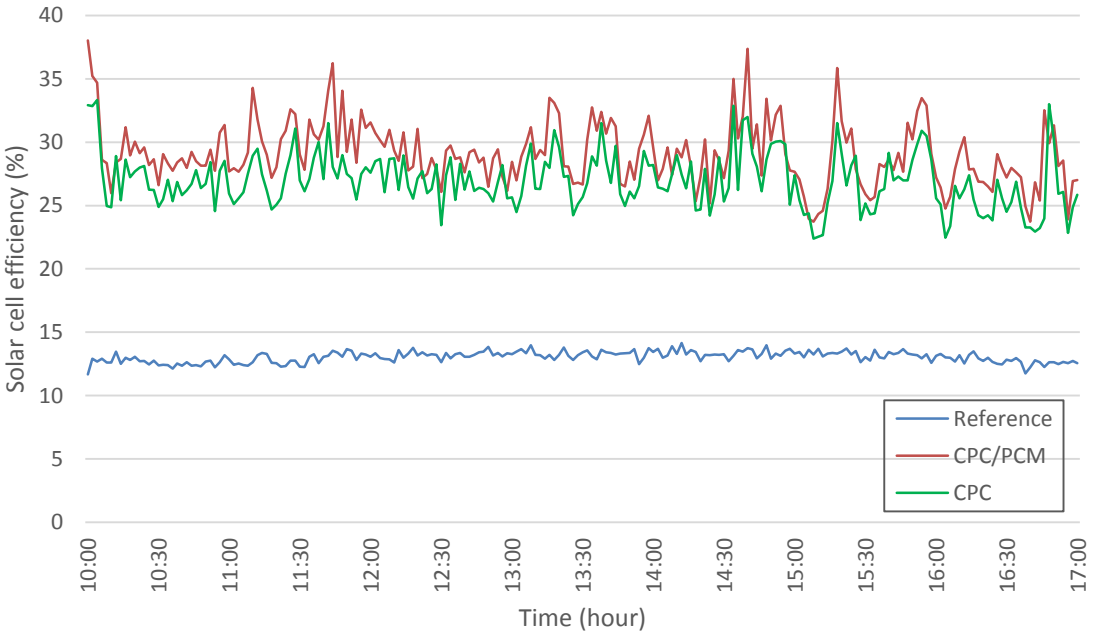

Figure 7. 51 Solar cells efficiency under diffuse radiation for the CPC, CPC/PCM and Reference systems

Figure 7.52 presents the optical efficiency of the concentrators which are closely aligned. On average, the CPC and CPC/PCM systems exhibited the same optical efficiency of 63%.

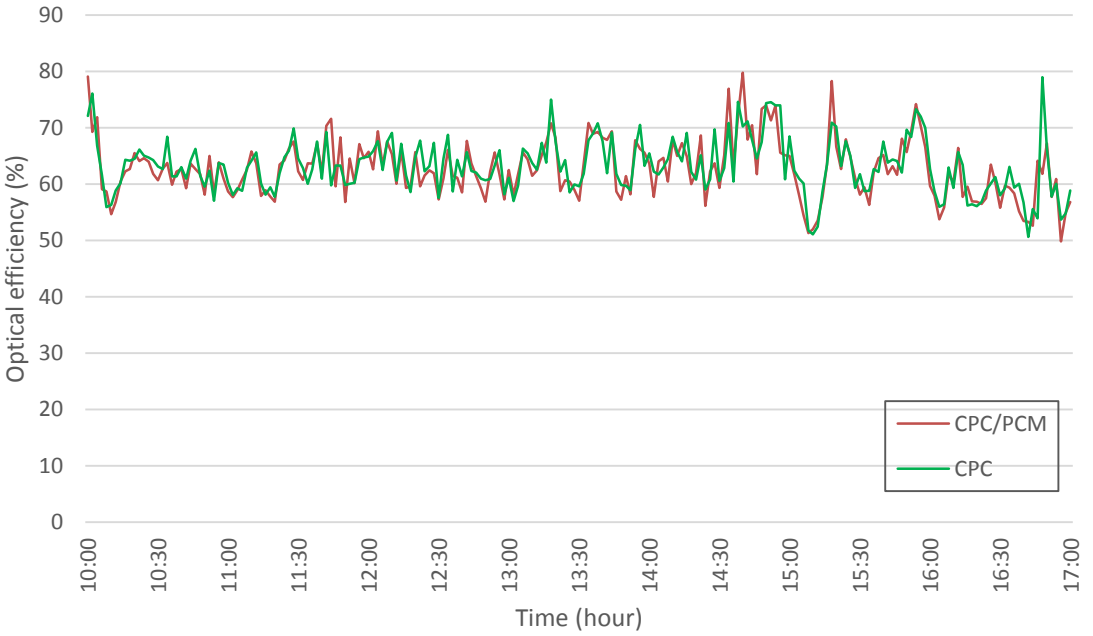

Figure 7. 52 Optical efficiency under diffuse radiation for the CPC and CPC/PCM systems

System efficiency for the three systems is presented in figure 7.53. The effective aperture area (1.19 m^2) was considered to calculate the system efficiency of the systems. From the graph a similar behaviour to the solar cell efficiency is seen, this is because in the equation only the area was the factor of change. The Reference system showed a stable system

efficiency throughout the day with small fluctuations between 3.68 % and 4.17 % with an average value equal to 4 %. Both concentrators presented fluctuations during testing but the CPC/PCM system was reported to have better system efficiency than the CPC system. The average values obtained were 9 % and 8 % for the CPC/PCM system and CPC system respectively.

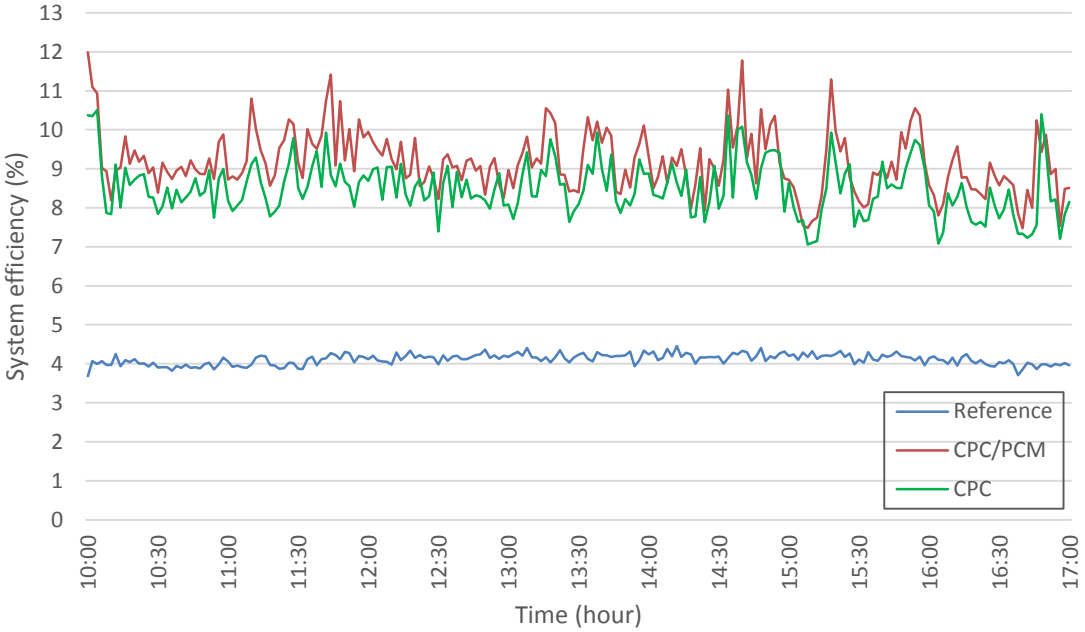

Figure 7. 53 System efficiency under diffuse radiation for the CPC, CPC/PCM and Reference systems

Table 7.7 shows the average performance of the systems under diffuse solar radiation. The temperature in the solar cell of the CPC system was the same as the Reference system at 17 ºC. However, the CPC/PCM system showed a temperature increase of 1 ºC. When exposed to diffuse radiation, CPC/PCM system outperformed the CPC system in terms of power ratio, fill factor, solar cell efficiency and system efficiency.

Table 7. 7 Systems average performance under diffuse radiation

System	Power (W)	Power ratio	Fill factor	Solar cell efficiency (%)	Optical efficiency (%)	System efficiency (%)	Solar cell temperature (ºC)
CPC	5	2.07	0.69	27	63	8.49	17
CPC /PCM	5	2.23	0.73	29	63	9.16	18
Reference	2	-	0.70	13	-	4.11	17

From the table, it can be observed that both the CPC and CPC/PCM systems outperform the Reference system in terms of power output, power ratio, solar cell efficiency, and system efficiency. The higher power ratio and solar cell efficiency for the CPC and CPC/PCM systems

indicated an improvement in capturing and converting diffuse radiation. The similar optical efficiency values for the CPC and CPC/PCM systems, at 63 %, demonstrated their comparable abilities to capture and transmit diffuse light to the solar cells. The fill factor values for all systems were relatively close, reflecting the similar capabilities of efficiently converting the absorbed solar energy.

7.2.6 Average behaviour with diffuse radiation

Maximum power for the three systems with diffuse solar radiation is shown in figure 7.54. For both concentrator systems the maximum power point varies linearly with incident solar radiation intensity. At 200 W/m^2 the power output for the CPC and CPC/PCM system were 19 W and 18 W respectively, this was double the power generated for the Reference system.

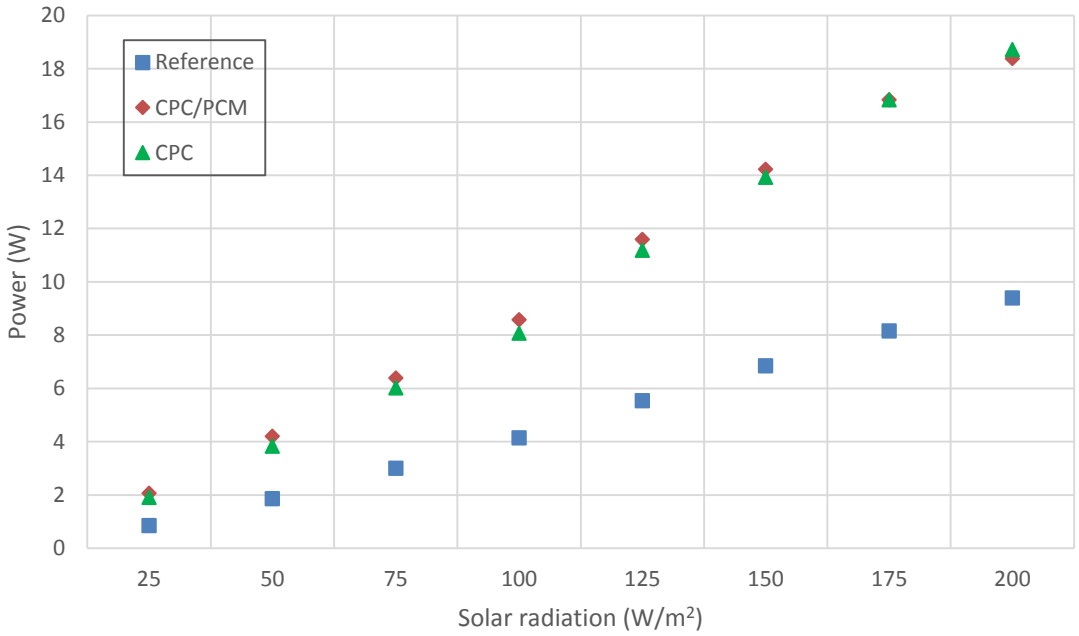

Figure 7. 54 Average power output under with diffuse solar radiation for CPC, CPC/PCM and Reference systems

Figure 7.55 presents the variation of temperature as a function of solar radiation. The outdoor temperature showed a small variation between 13 ºC to 17 ºC when the solar radiation varied between 25 W/m^2 to 200 W/m^2. The CPC/PCM system consistently reported the highest temperature throughout the entire radiation range. At 200 W/m^2, the CPC/PCM system reported an average temperature of 27 ºC, while the CPC system had 26 ºC, both 3 ºC higher than the Reference system.

This temperature variation indicates that the CPC/PCM system was more effective in capturing and retaining heat compared to the other two systems. The higher temperatures in the CPC/PCM system could be attributed to the additional thermal storage provided by the PCM, which allowed for better heat absorption and retention. This behavior aligned with expectations, as the CPC/PCM system was designed to enhance the performance of solar energy capture and conversion through the use of a concentrator and thermal storage.

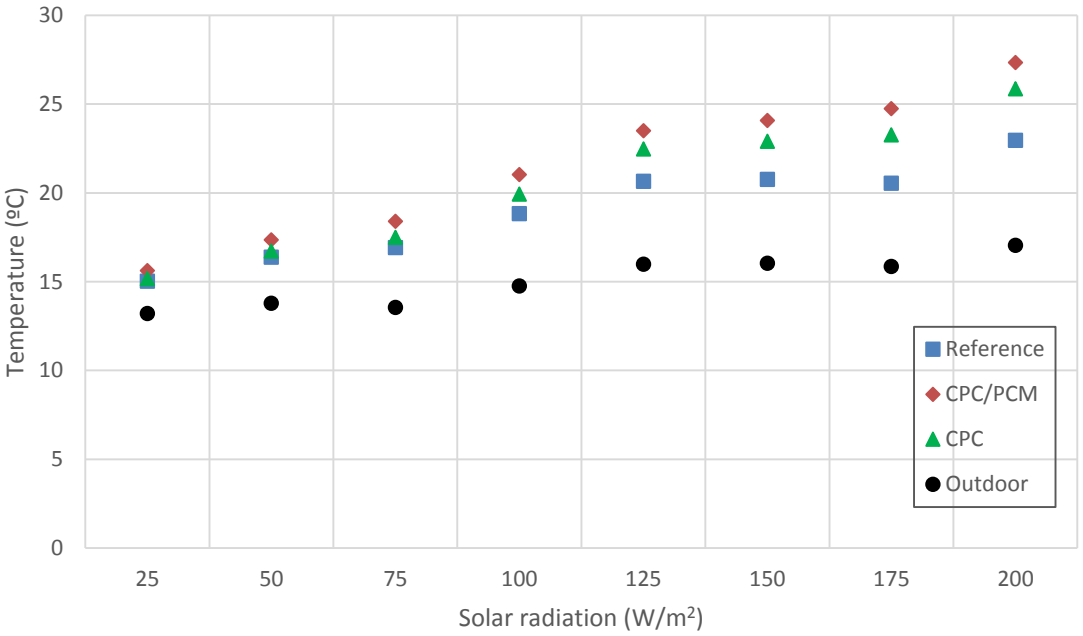

Figure 7. 55 Average solar cell temperature with diffuse solar radiation for CPC, CPC/PCM and Reference systems

Change of power ratio with incident solar radiation intensity is shown in figure 7.56. Average maximum power point ratio between the Reference system and the concentrators was 2. The power ratio for both concentrators tended to decrease for diffuse radiation ranges between 25 W/m^2 to 200 W/m^2. The CPC/PCM system demonstrated better power ratios between 25 W/m^2 to 150 W/m^2. There were significant additional losses for the concentrators when compared with the reference system as a consequence of condensation in the front glass.

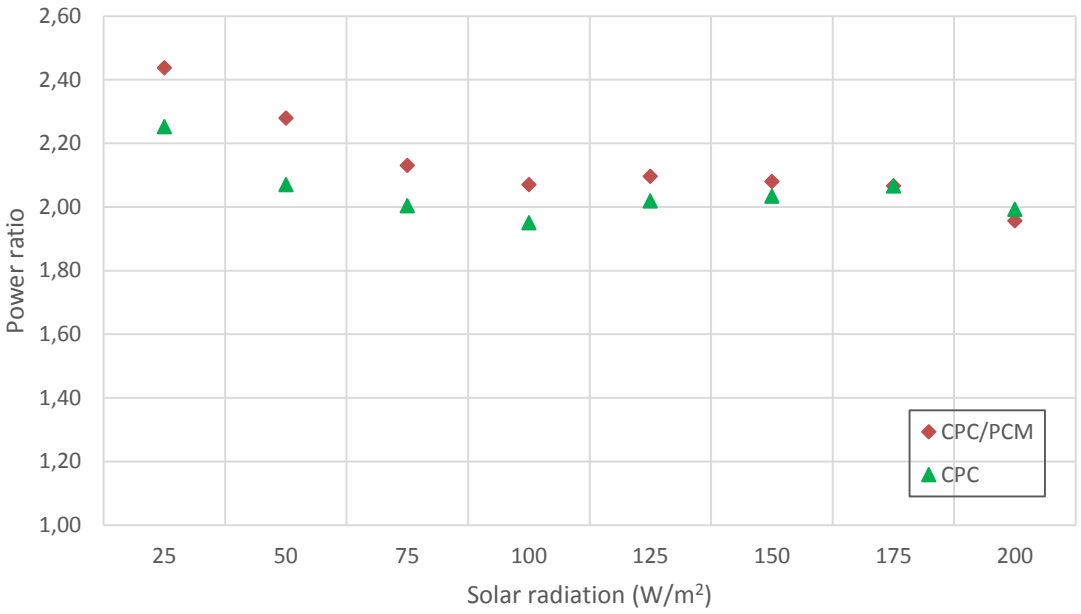

Figure 7. 56 Average power ratio with diffuse solar radiation for CPC and CPC/PCM systems

Average fill factor for each system is presented in figure 7.57. From the figure is clear the Reference system reported better fill factor than the concentrator systems from 75 W/m^2 to 200 W/m^2. Between the concentrators, CPC/PCM system showed better performance, with values from 0.70 – 0.73 for the CPC/PCM system and 0.70 – 0.71 for the CPC system. However, at 200 W/m^2, CPC system had a fill factor of 0.69 and 0.68 for CPC/PCM system. The fill factor for the Reference system was 0.79 at the high solar radiation.

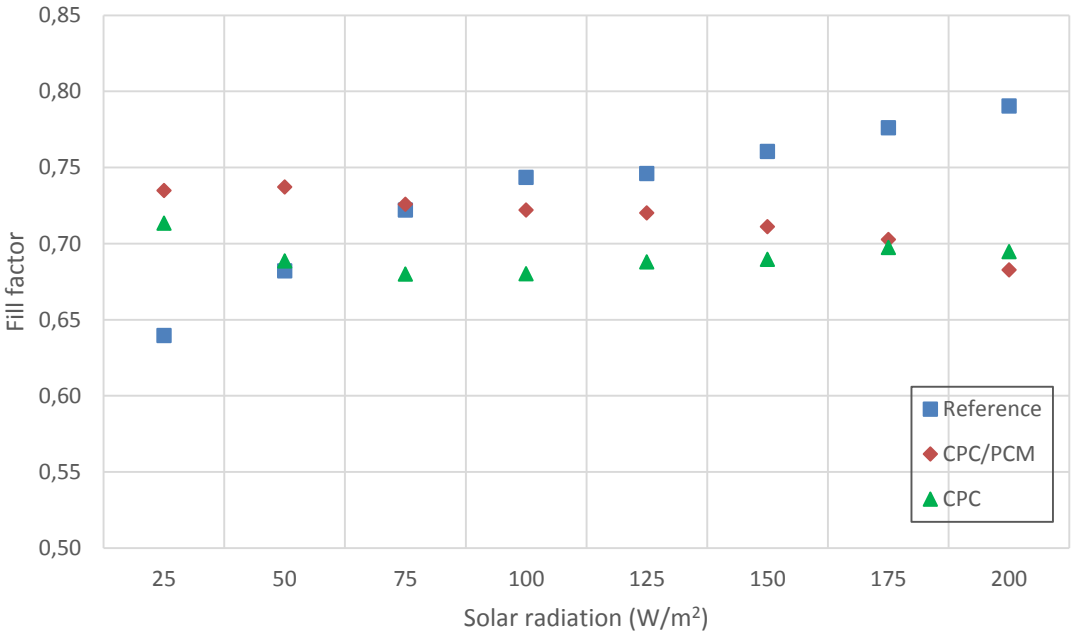

Figure 7. 57 Average fill factor with diffuse solar radiation for CPC, CPC/PCM and Reference systems

Figure 7.58 presented the solar cell efficiency of the different systems. At 200 W/m^2 solar cell efficiency was 27 % for both concentrators and 14 % for the Reference system. This result indicated that the concentrators were more effective at converting solar energy into electrical power compared to the Reference system. The enhanced performance of the concentrator systems demonstrated their potential for improving solar energy harvesting and conversion.

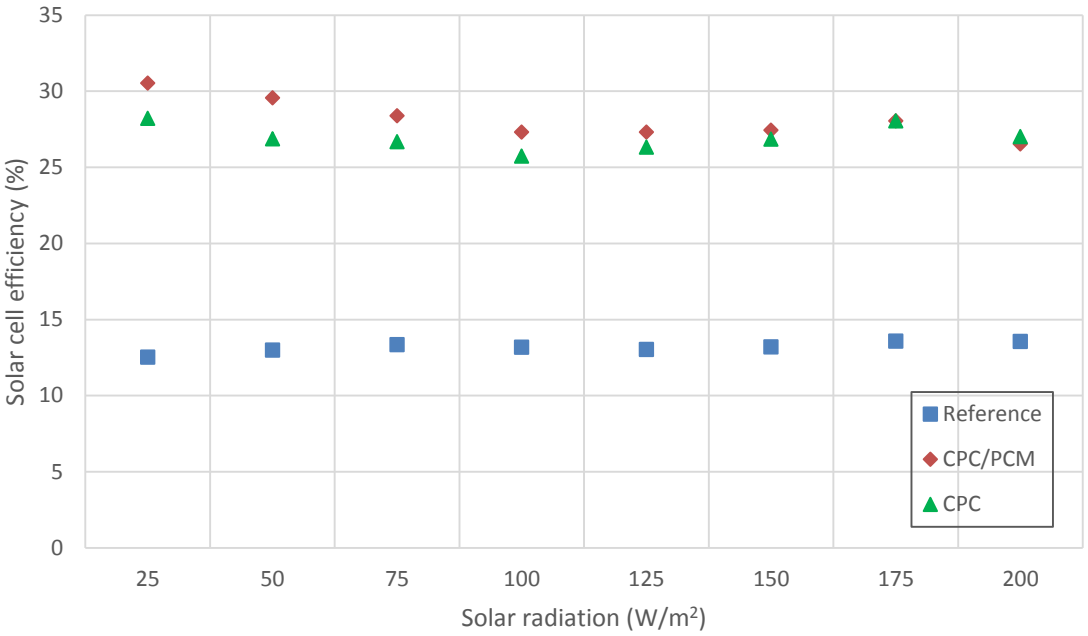

Figure 7. 58 Average solar cell efficiency with diffuse solar radiation for CPC, CPC/PCM and Reference systems

Figure 7.59 showed the optical efficiency for the concentrators, which was approximately the same and increased over the range of solar radiation. Between 25 - 200 W/m², the optical efficiency for the concentrators increased from 6 % to 68 %. This increase demonstrated the concentrators' improved ability to capture and transmit light as solar radiation increased, highlighting their advantage in harnessing available solar energy more effectively.

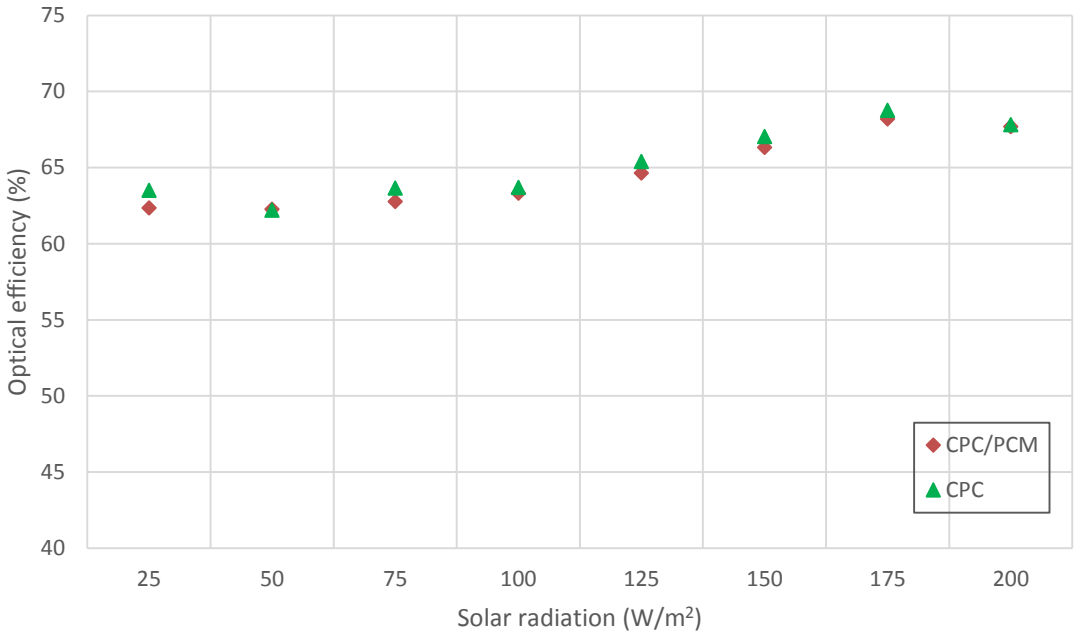

Figure 7. 59 Average optical efficiency with diffuse solar radiation for CPC and CPC/PCM

Figure 7.60 displayed the average system efficiency achieved for the different systems. The Reference system reached a maximum of 4 % compared to 9 % for the CPC system and 8 % for the CPC/PCM system. These figures emphasized the superior overall performance of the concentrator systems in capturing solar energy and converting it into useful power. The higher system efficiency of the concentrator systems underlined the importance of utilizing such technologies for enhanced solar energy harvesting and improved overall performance.

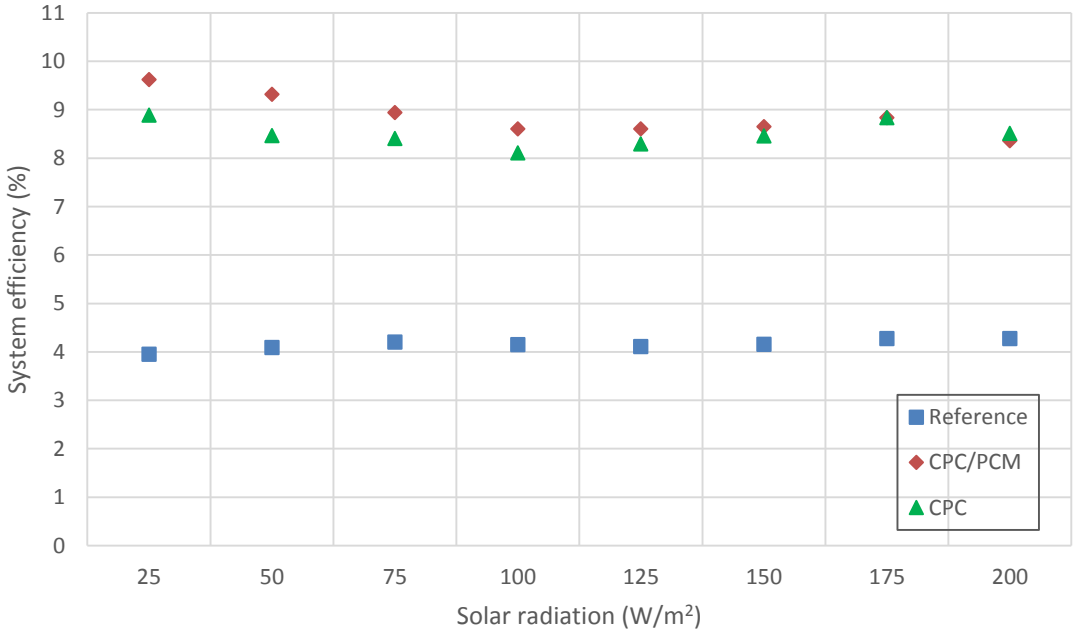

Figure 7. 60 Average system efficiency with diffuse solar radiation for CPC, CPC/PCM and Reference systems

7.2.7 I-V analysis under diffuse radiation

Maximum power output of the three systems for a range incident diffuse solar radiation range are shown in figure 7.61. The solar radiation fluctuations were less that 1 W/m^2 between the measurements which does not have any significant impact on the power output of the systems. Power output for the CPC, CPC/PCM and Reference systems were 19 W, 19 W and 9 W respectively at incident solar radiation of 200 W/m^2. This shows that the power concentration ratio of the concentrators was 2 and 1.96 for the CPC and CPC/PCM system respectively in contrast to the results from simulation equal to 2.82.

Most of the losses under diffuse radiation occur due to the heavy rains that occurred during testing. Condensation was observed on the glass cover which leads to reduced performance. An approximate distribution in the radiation curve was chosen for the selection of the maximum values represented in figure 7.61. At 200 W/m^2 data were collected at 15:46 and 50 W/m^2 were collected at 13:58. The maximum power for concentrators tends to increase with diffuse radiation and is approximately double compared to the reference system.

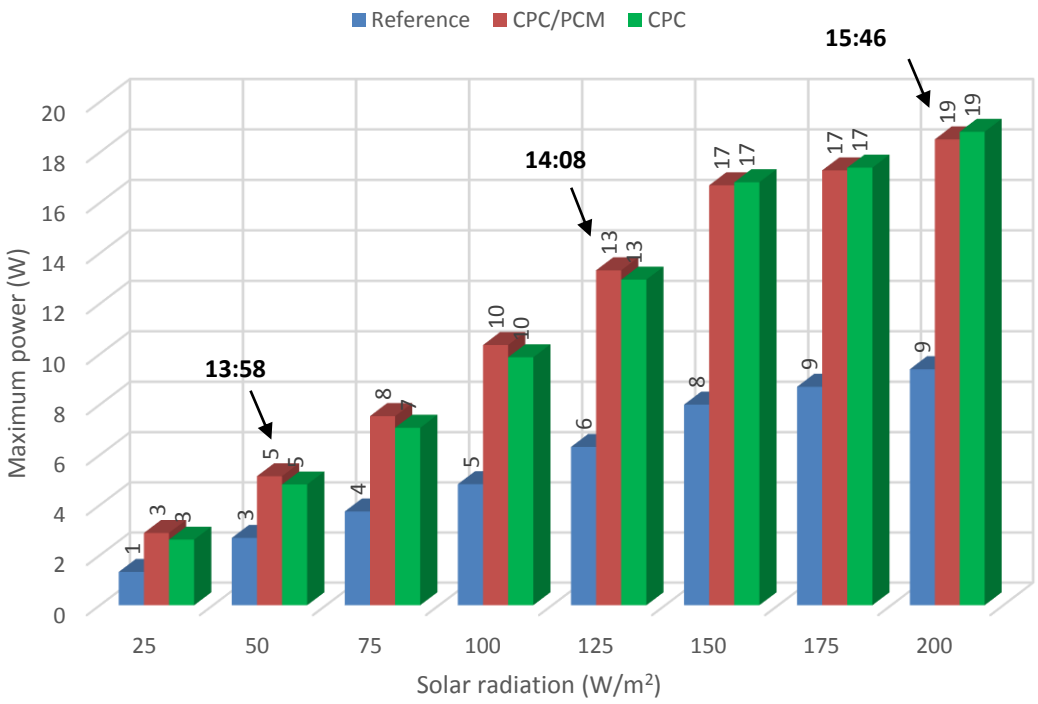

Figure 7. 61 Maximum power achieved with diffuse solar radiation for CPC, CPC/PCM and Reference systems

Maximum power output and I-V curves for Reference, CPC/PCM and CPC system are shown in figures 7.62, 7.63 and 7.64 respectively. From figure 7.62 all power output has a similar behaviour for the range of solar radiation tested in the Reference system. It is important to note that while the output was not identical, their similar behavior indicated consistent performance characteristics of the Reference system under varying solar radiation levels. The open circuit voltage ranged from 13.5 V to 14.71 V and the short circuit current ranged from

0.14 A to 0.81 A (25 – 200 W/m^2). Those values allowed for a comparison with the values obtained from the concentrator systems. This comparison enabled a better understanding of the improvements and enhancements provided by the concentrators in terms of their performance and efficiency.

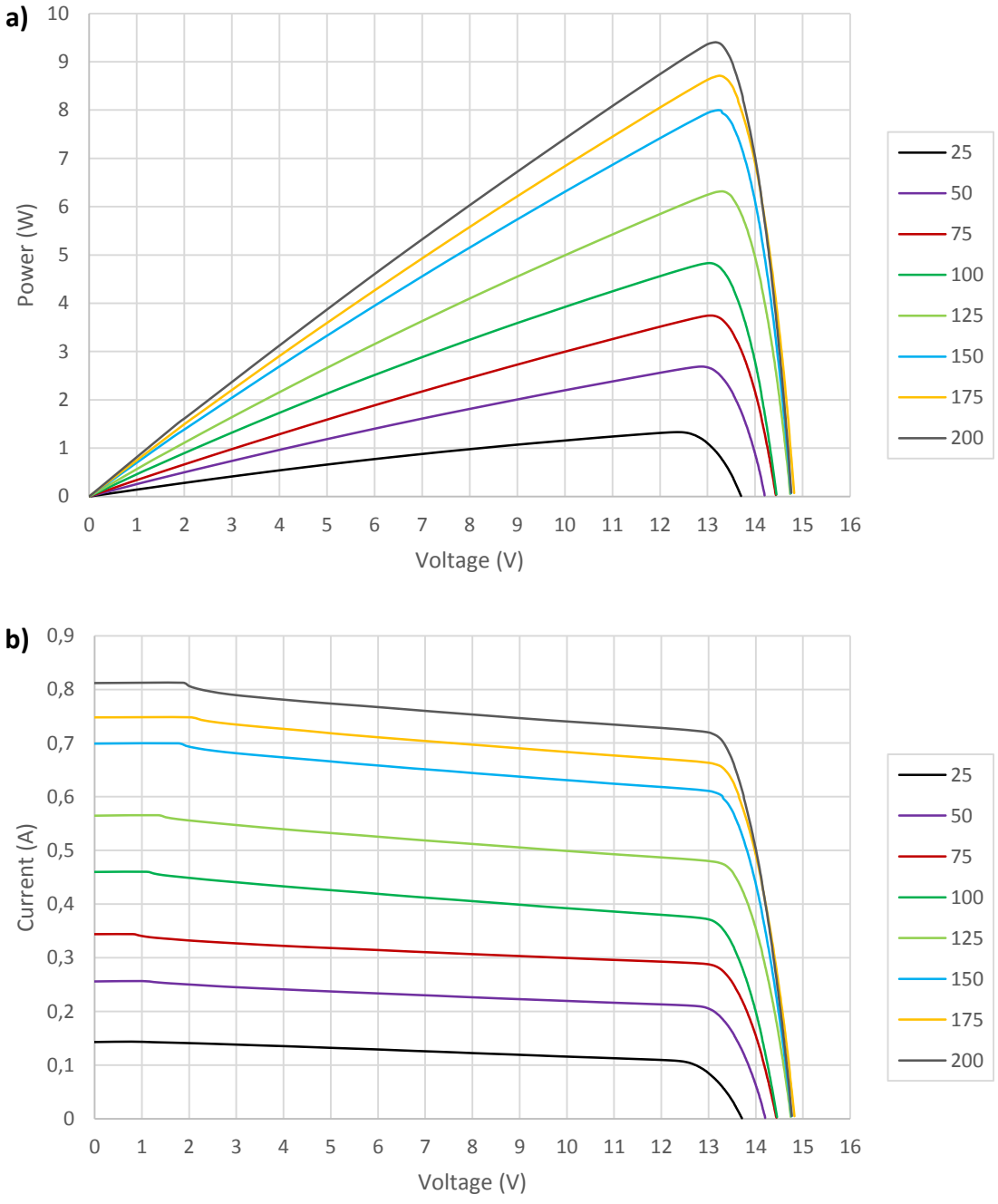

Figure 7. 62 Maximum power output and I-V curve with diffuse solar radiation of Reference system
(a) Maximum power (b) I-V curve

In Figure 7.63, for the CPC/PCM system, the open circuit voltage ranged from 15.44 V to 16.48 V, while the short circuit current varied between 0.21 A and 1.66 A. Maximum open circuit

voltage and maximum short circuit current in the CPC/PCM system were, respectively, 1.77 V and 0.85 A higher compared to the Reference system values.

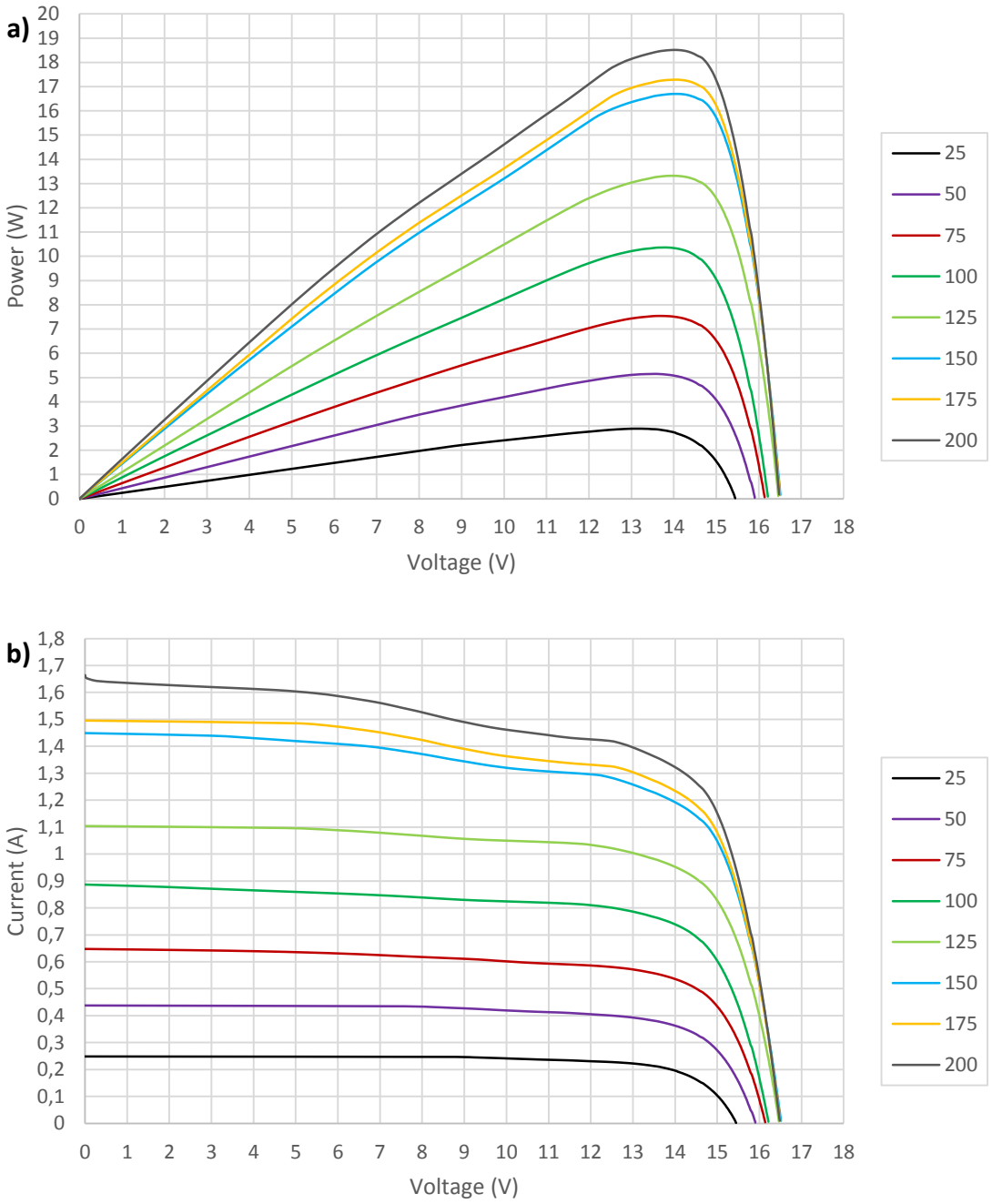

Figure 7. 63 Maximum power output and I-V curve with diffuse solar radiation of CPC/PCM system
(a) Maximum power (b) I-V curve

In Figure 7.64, for the CPC system, the open circuit voltage ranged from 14.77 V to 16.46 V, while the short circuit current varied between 0.24 A and 1.66 A. Maximum open circuit

voltage and maximum short circuit current in the CPC system were, respectively, 1.77 V and 0.85 A higher compared to the Reference system values.

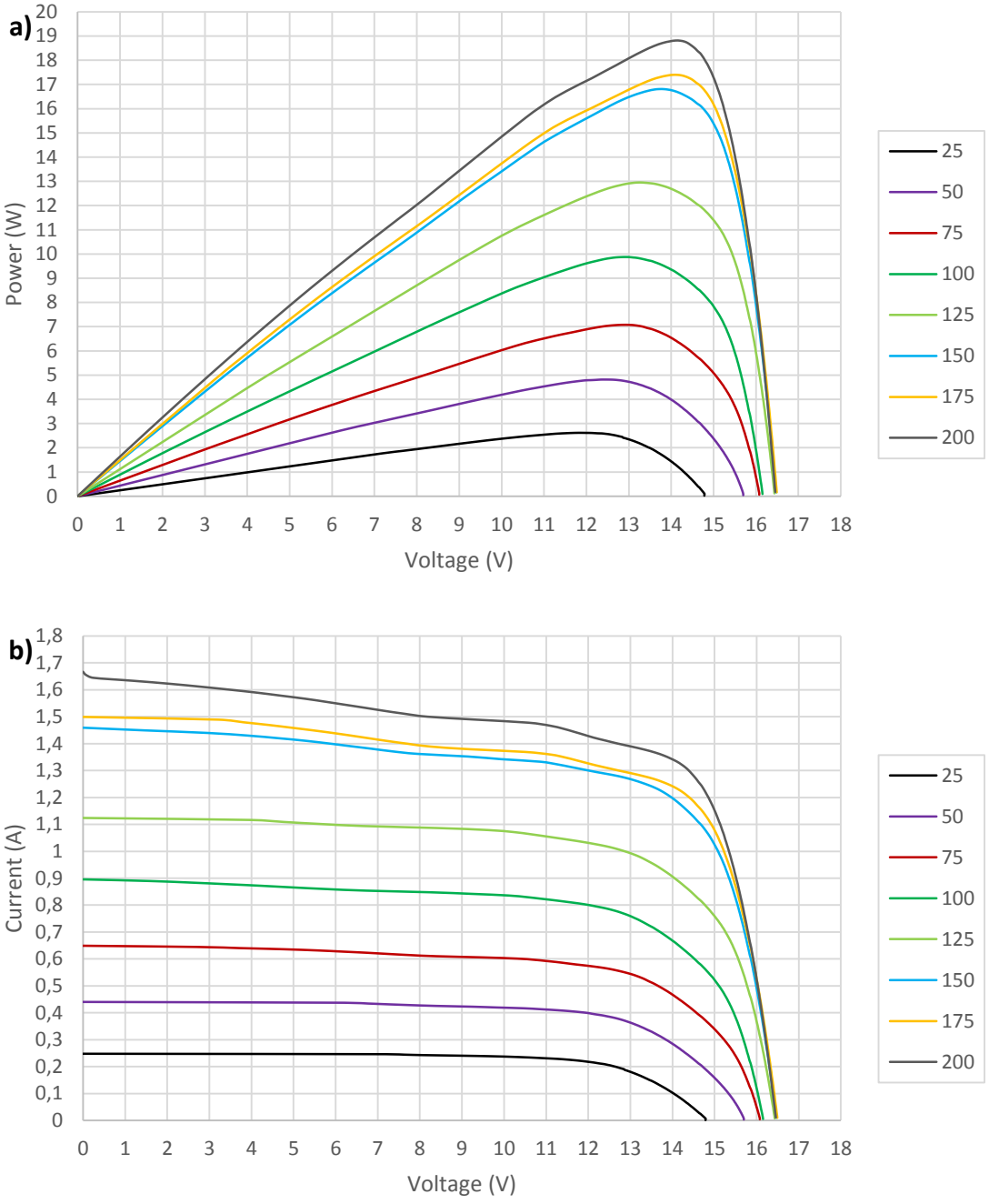

Figure 7. 64 Maximum power output and I-V curve with diffuse solar radiation of CPC system
(a) Maximum power (b) I-V curve

The concentrators (CPC and CPC/PCM) did not exhibit significant differences in open circuit voltage and short circuit current under diffuse radiation because diffuse radiation consisted of scattered sunlight, rather than direct solar radiation. This type of solar radiation had a

lower intensity. Although the reflectors in the concentrators were still functioning under diffuse radiation, their ability to concentrate and enhance the open circuit voltage and short circuit current was limited due to the lower intensity of the diffuse radiation.

7.2.8 Thermal analysis under diffuse radiation

Average temperatures in the solar cells and backplate in the reference system are shown in figure 7.65. Maximum temperature reported in the solar cells and backplate was 18 ºC and 17 ºC with an outdoor temperature of 15 ºC at 15:00.

It was observed that heat was absorbed which reduced the temperature by 1 ºC in the backplate at that moment and the solar cell presented only 3 ºC more than outdoor temperature. This relatively small temperature difference between the solar cell, backplate, and outdoor temperature could be attributed to the lower intensity of the diffuse radiation. Under diffuse solar radiation conditions, the amount of energy absorbed by the solar cell was lower, resulting in less heat being generated in the solar cell and consequently a smaller temperature difference between the solar cell, backplate, and outdoor temperature.

Given that the thermocouples used had a measured deviation of ±0.4 °C (section 5.1.7), the observed 1 ºC difference between the solar cell, backplate, and outdoor temperature can be considered measurable and significant. The accuracy and precision of the temperature sensors were greater than the observed temperature difference, indicating that the difference was not within the error of the measurement.

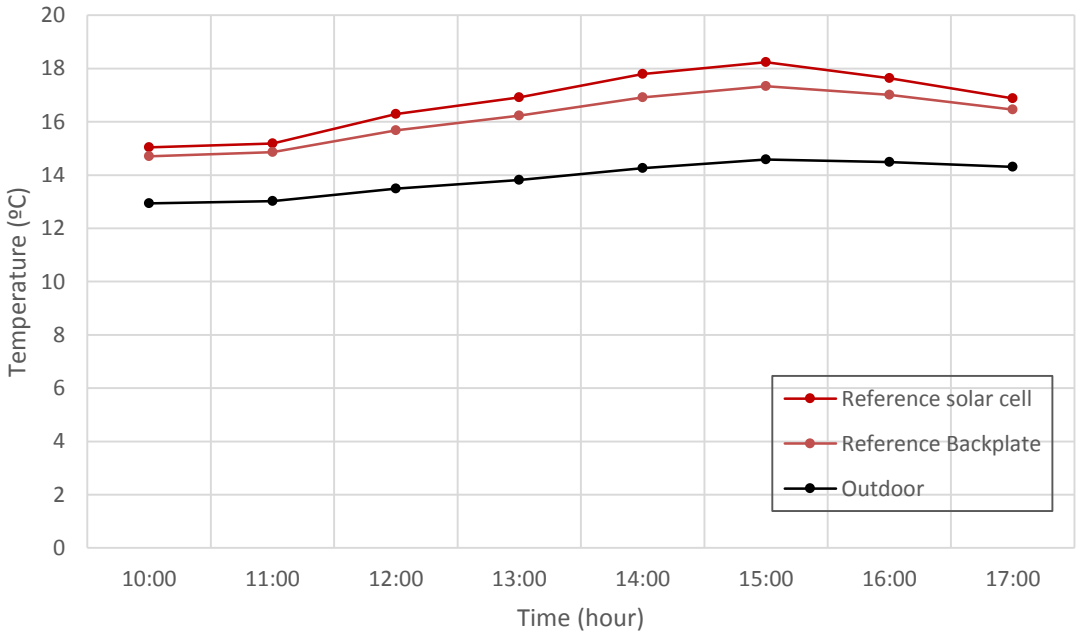

Figure 7. 65 Average temperature under diffuse solar radiation on Reference system

Average temperatures in the different components of the CPC/PCM system are presented in figure 7.66. Solar cells reported the highest temperatures during the testing period, with a

maximum value at 15:00 of 20 ºC, this was 5 ºC more than the outdoor temperature. The backplate was next with a maximum of 19 ºC at 15:00. Temperatures in both reflectors (top and bottom) had approximately the same temperature throughout the test with a maximum value at 15:00 of 17 ºC, this confirms the good diffuse reflectivity of the Alanod reflectors.

The similar temperatures observed in both reflectors, as well as the relatively small temperature differences between the solar cell, backplate, and outdoor temperature, suggest that the Alanod reflectors were effective in reflecting and distributing diffuse radiation. Good diffuse reflectivity means that the reflectors were able to capture and redirect a considerable amount of the available diffuse radiation towards the solar cells, enabling them to perform more effectively under diffuse radiation conditions.

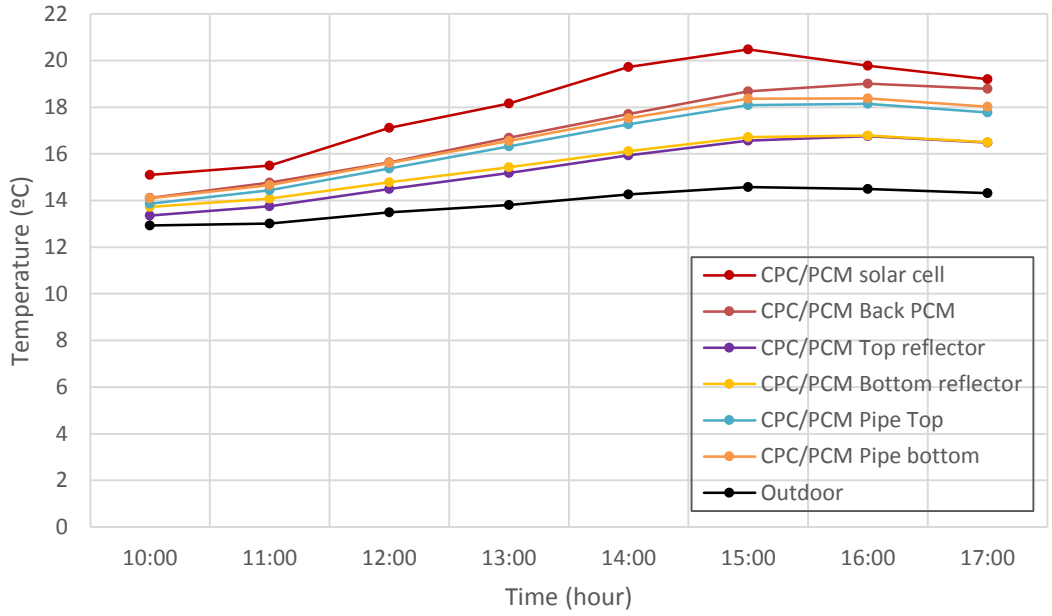

Figure 7. 66 Average temperature under diffuse solar radiation on CPC/PCM system

The temperature difference between the solar cells and the backplate in the CPC/PCM system was found to be around 1 to 2 ºC. This small temperature difference is not significant enough to be utilized for energy storage purposes.

Average temperatures of the CPC system are shown in figure 7.67. The solar cells exhibited the highest temperatures from 10:00 to 16:00, peaking at 19 ºC at 15:00. Both the top and bottom reflectors maintained similar temperatures ranging from 14 ºC to 18 ºC. The backplate exhibited the lowest temperature within the system, illustrating the cooling process that occurred through the backplate and distributed heat throughout the entire system. This was why, from 16:00 to 17:00, the solar cells and reflectors began to display similar temperatures until the end of the day. The backplate's maximum temperature was 17 ºC at 15:00, which was 2 ºC higher than the external temperature.

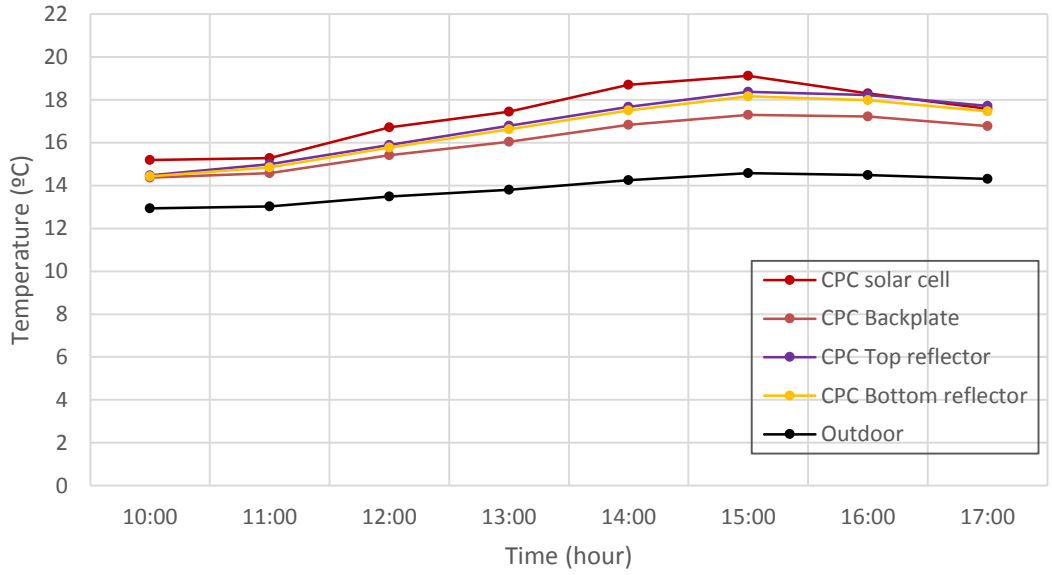

Figure 7. 67 Average temperature under diffuse solar radiation on CPC system

The percentage of power loss due to temperature in the solar cells of the three systems is shown in figure 7.68. The power losses were calculated as explained in section 7.2.4. Maximum losses due to temperature occur at 15:00 with values equal to 1.17 %, 1.89 % and 1.45 % in the Reference, CPC and CPC/PCM systems. At the beginning of the day, the CPC system reported more losses than the other systems, this showed that the PCM stored thermal energy in the CPC/PCM system during the early hours of the morning. The average losses were 0.92 %, 1.1 % and 1.37 % for the Reference, CPC and CPC/PCM systems respectively.

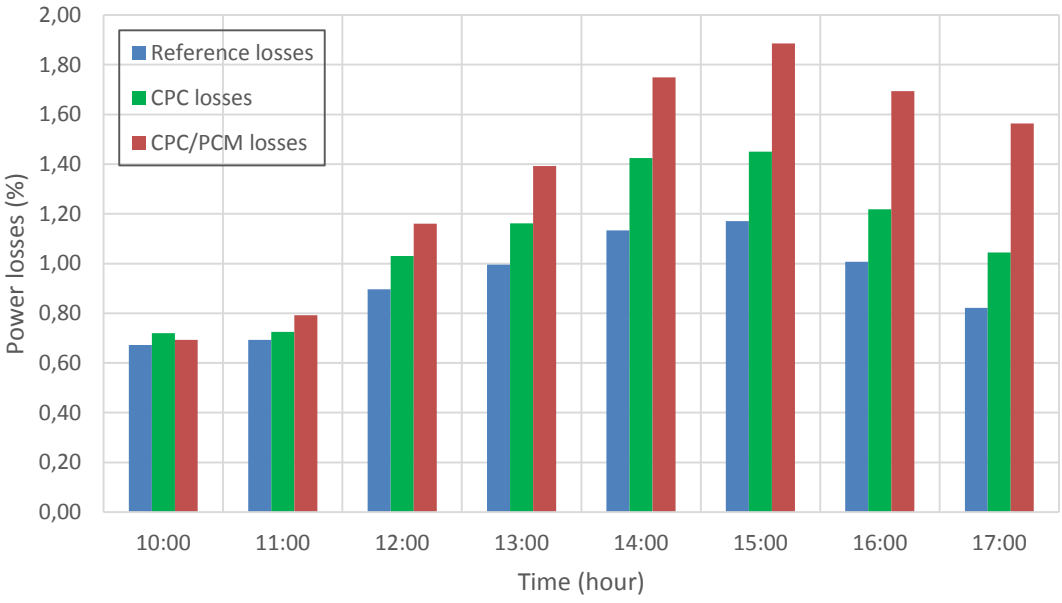

Figure 7. 68 Percentage power losses due to temperatures in the CPC, CPC/PCM and Reference systems under diffuse radiation

Figure 7.69 shows the power of the three systems without the losses due to temperatures. This was calculated as was mentioned in section 7.2.4. A difference of 0.13 W occurred in the CPC/PCM system at 15:00 and 0.1 W in the CPC system at 11:00. No significant improvement could be observed in the power output when the temperature of the solar cells was low under diffuse solar radiation.

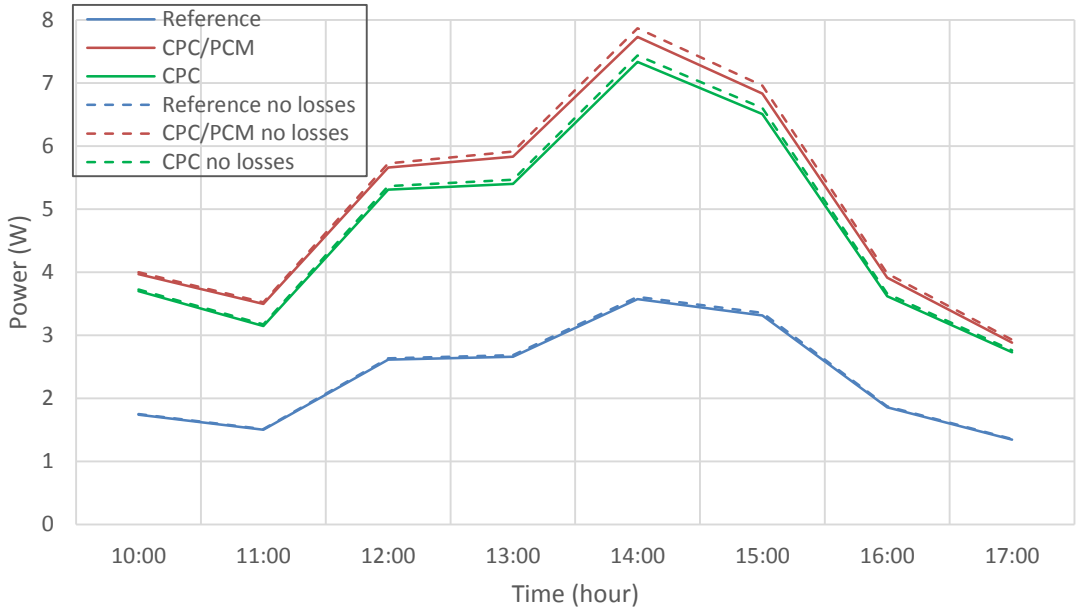

Figure 7. 69 Power experimental test and with no temperature losses in the CPC, CPC/PCM and Reference system under diffuse radiation

7.2.9 Four-month system performance analysis

The following graphs show the average of the three systems in the four-month test period (July – October 2022) in terms of power, solar cell temperature, fill factor and the efficiencies (solar cell, optical and system). Figure 7.70 shows the average power for each month of the three systems along with solar radiation. Both concentrators had 8 W higher power than the Reference system. In July, the CPC system performed better, producing 0.5 W more power than the CPC/PCM system. From August to October, both concentrators exhibited similar power output values ranging between 12 and 17 W. The highest power output for all three systems was observed in August, with average values of 17 W for both concentrators and 9 W for the Reference system, corresponding to a solar radiation intensity of 185 W/m².

The fact that both concentrators display the same average power output in August, September, and October could be due to a number of factors. One possibility is that the PCM in the CPC/PCM system may not be providing significant additional thermal regulation during these months. This could be due to the PCM was fully charged/melted and it does not effectively store or release thermal energy. Additionally, it is important to note that the PCM containers were not connected to water tanks during this period, which could further affect the performance of the CPC/PCM system.

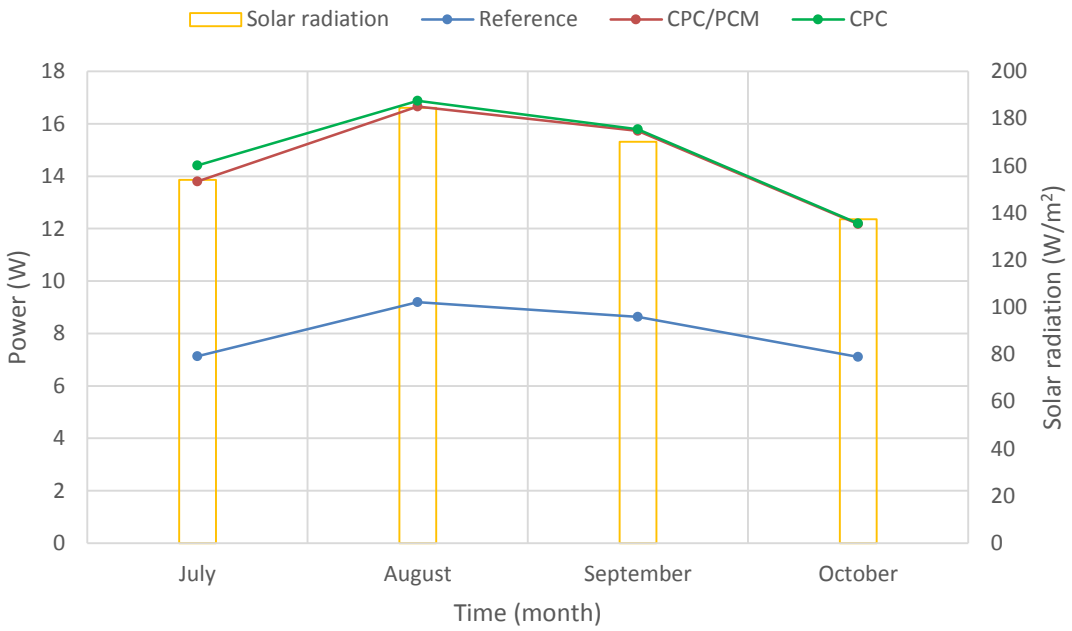

Figure 7. 70 Average power output and solar radiation for four months for CPC, CPC/PCM and Reference systems

Temperatures in the solar cells were higher in the CPC/PCM system in the four months with values between 26 ºC – 38 ºC, reaching a maximum value of 38 ºC in August as shown in figure 7.71. In that month the temperatures in the CPC and Reference systems were 30 ºC and 28 ºC with an outdoor temperature of 17 ºC. The higher temperatures in the solar cells provide insights into the performance and efficiency of the solar cells, as elevated temperatures tend to decrease photovoltaic cell efficiency.

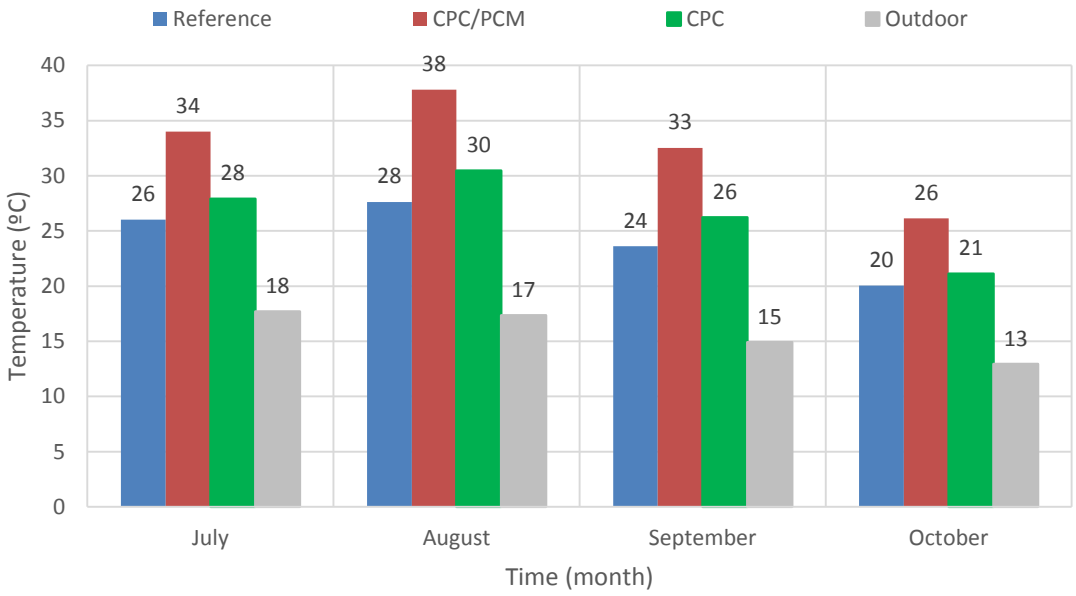

Figure 7. 71 Average power solar cell temperature for four months for CPC, CPC/PCM and Reference systems

The CPC/PCM system had the maximum average power ratio equal to 1.99 compared to 1.96 for the CPC/PCM system in the month of July (summer) as seen in figure 7.72. In August, the month with the highest solar radiation and temperature the power ratio was 1.88 for both concentrators and significant losses due to temperatures could happen this month. In October the CPC system had an average power ratio of 1.83 and 1.89 for the CPC/PCM system, losses due to condensation on the glass cover could be affect the performance in this month.

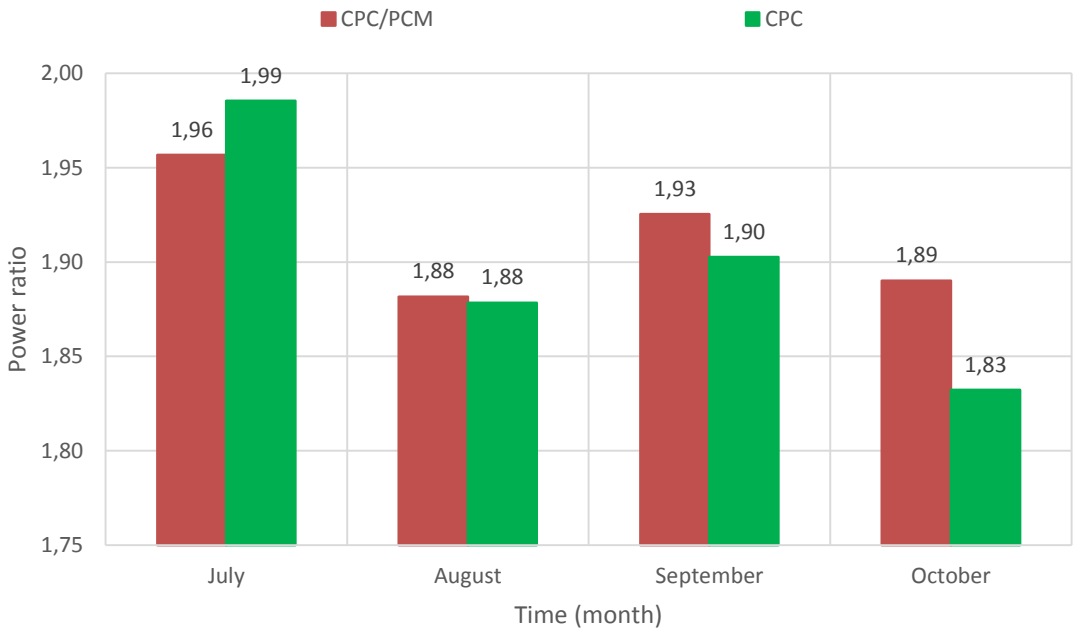

Figure 7. 72 Average power ratio for four months for CPC and CPC/PCM systems

Fill factor is presented in figure 7.73 where the Reference system had the best fill factor with a maximum value of 0.73 in October. The CPC/PCM system fill factor varied between 0.68 to 0.70 and CPC system between 0.68 to 0.67 (from July-August).

A fill factor value within the range of 0.68 to 0.73 is generally regarded as an acceptable level for solar cell performance, indicating that the solar cell is operating efficiently within its expected parameters. While the Reference system had the best fill factor with a maximum value of 0.73, the CPC and CPC/PCM systems still demonstrated reasonable performance with values between 0.67 to 0.70. However, a higher fill factor alone does not necessarily mean the best overall performance, as the other parameters also play a crucial role.

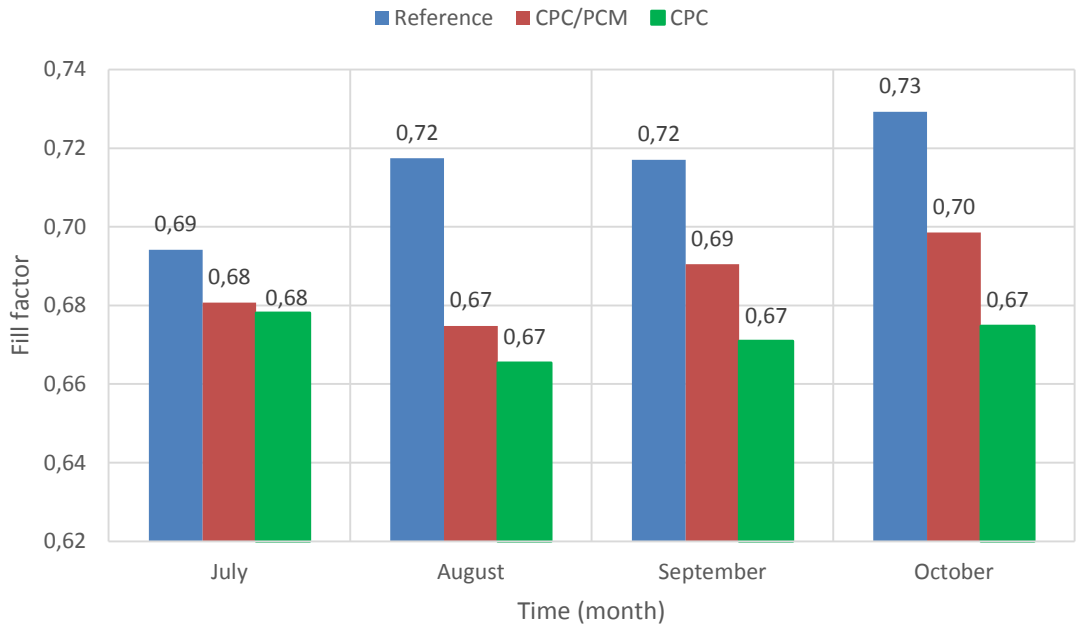

Figure 7. 73 Average fill factor for four months for CPC, CPC/PCM and Reference systems

Solar cell, optical and system average efficiencies are presented in figures 7.74, 7.75 and 7.76 respectively.

Solar cell efficiency for the concentrators ranged between 25 % to 26 % during the four months while the Reference only reported 13 % to 14 %. A factor of 2 was observed in favour of the concentrators during the four months. The system efficiency for the concentrators were 8 %, this was twice the system efficiency of the Reference. The optical efficiency presented the maximum value of 66 % for the CPC system and 65 % for the CPC/PCM in July. In August where both concentrators reported 63 % in optical efficiency. This reduction was most likely due to the losses caused for high temperature in the solar cell and shadows generated between the systems, in addition to the deviation from the south of the wall in use for testing. The lowest optical efficiency was observed in October of 61 % in the CPC system, this was due to excess condensation formed on the protection glass. There was condensation presents in the front glass at this time due to rains and may have been the cause of this lower optical efficiency

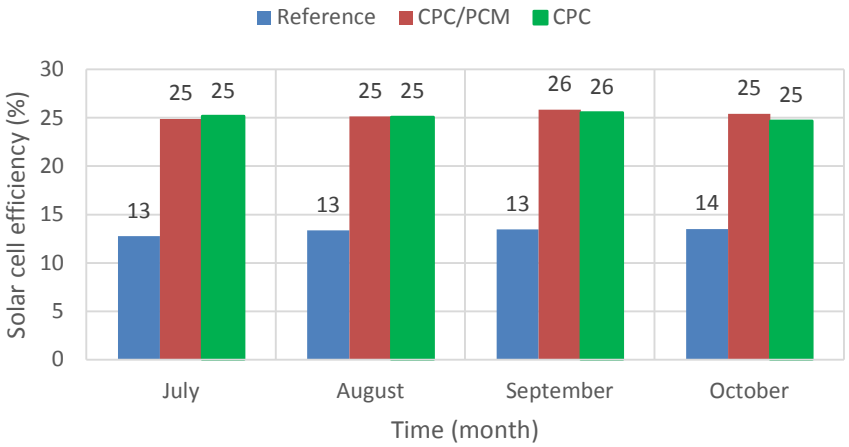

Figure 7. 74 Average solar cell efficiency for four months for CPC, CPC/PCM and Reference systems

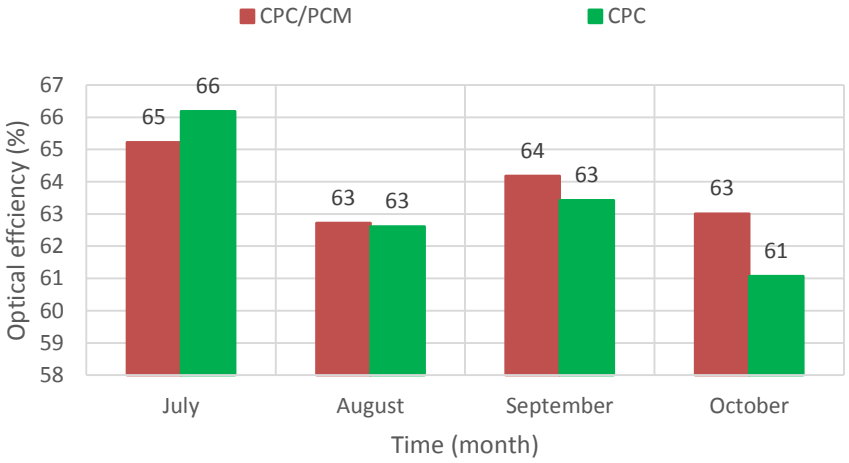

Figure 7. 75 Average optical efficiency for four months for CPC and CPC/PCM systems

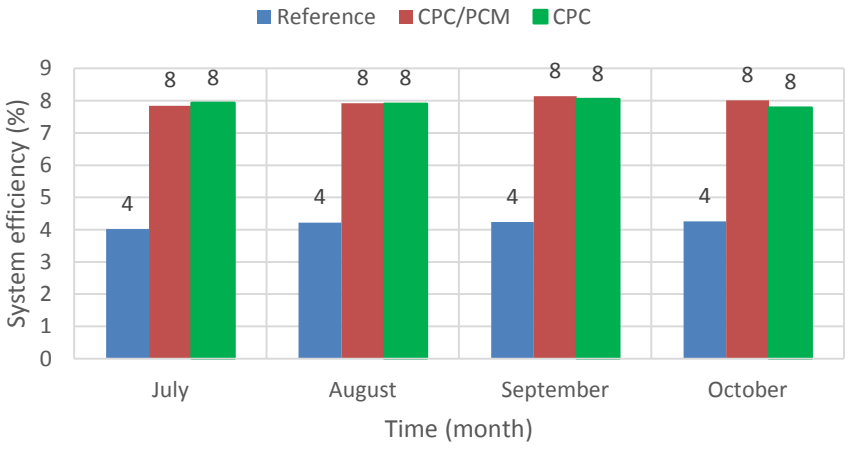

Figure 7. 76 Average system efficiency for four months for CPC, CPC/PCM and Reference systems

Average values of the results are summarized in table 7.8. In summary, the results reported power values of 15 W and 8 W for the Reference system. The power ratio was on average 0.90 and 9.91 for the CPC and CPC/PCM system respectively. Fill factor was slightly better in the reference at 0.71. between the concentrators it was 0.69 and 0.67 for the CPC/PCM and CPC system respectively. System efficiency was double for concentrators and equal to 8 % compared to Reference. The highest temperature in the solar cells was recorded in the CPC/PCM system due to the discharge of thermal energy from the PCM in the solar cells.

Table 7. 8 Systems average performance for four month tested

System	Power (W)	Power ratio	Fill factor	Solar cell efficiency (%)	Optical efficiency (%)	System efficiency (%)	Solar cell temperature (ºC)
CPC	15	1.90	0.67	25	63	8	26
CPC /PCM	15	1.91	0.69	25	64	8	33
Reference	8	-	0.71	13	-	4	24

When the experimental test results were compared to the simulation results, it was evident that there were differences in the values obtained for both solar cell efficiency and power ratio. The solar cell efficiency from the experimental test results (25% for both CPC and CPC/PCM systems) was lower than the values obtained from the simulations (31% - 49%) (discrepancy explained in 7.1.2). This discrepancy might have been due to factors such as temperature, dust, condensation during rainy seasons, or other real-world conditions (explained in section 7.1.5) that could have affected the performance of the solar cells.

The power ratio also showed some differences between the experimental test results and the simulation results. The experimental test results for the CPC and CPC/PCM systems showed power ratios of 1.90 and 1.91, respectively. In comparison, the simulation results showed a higher power ratio of 2.82 for February to September, and lower power ratios of 1.29 and 1.4 for December and January. This difference might have been due to seasonal variations in solar radiation and weather conditions, including the presence of condensation during rainy seasons, as well as other factors not accounted for in the simulations.

The power generated during the four months in total is presented in figure 7.77. The CPC system proved to produce a total of 344 KW while the CPC/PCM system produced 339 KW. The reference reported a total of 190 KW during testing. This was an improvement in production power in factor of 1.81 and 1.78 for the CPC and CPC/PCM systems respectively.

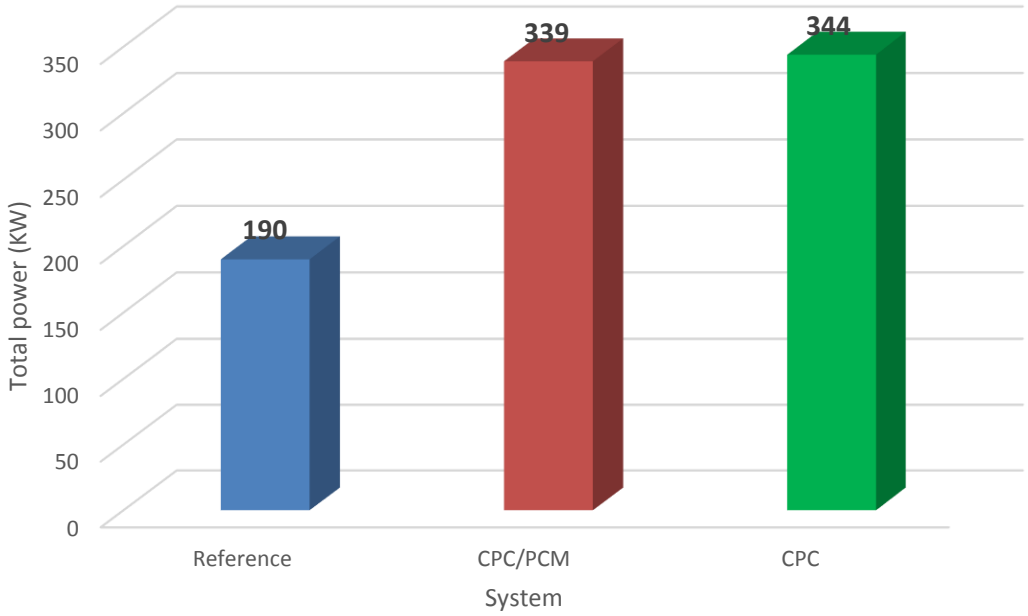

Figure 7. 77 Total power generated for four month tested for CPC, CPC/PCM and Reference systems

7.2.10 Analysis of CPC and CPC/PCM systems at 100 W power production

The characteristics of the systems at 100 W production are summarized in tables 7.9 for the CPC/PCM system and table 7.10 for the CPC system.

The concentrators were designed to produce 100 W at noon under ideal conditions, which refer to 1000 W/m^2 solar radiation with 25 ºC temperature in solar cells, throughout the year. During the four-month test period from July to October, it was reported that the CPC/PCM reached the target 100 W power 14 times and the CPC system 29 times. Both concentrators reached 100 W or more in August and September between 11:00 and 12:30. For the CPC/PCM system, the average solar radiation was 824 W/m^2, which produced an average of 103 W with a power ratio equal to 2.79. The fill factor was 0.61, with a system efficiency equal to 11 %. The temperature in the solar cells was 53 ºC, which was 35 ºC more than the outdoor temperature. For the CPC system, in the 29 times of 100 W or more power production, the average power was 104 W with a solar radiation equal to 832 W/m^2 and a power ratio of 2.65. The fill factor was 0.63, with a system efficiency equal to 11 %. The temperature in the solar cell was 50 ºC, which was 33 ºC more than the outdoor temperature. It was evident that high temperatures were one of the main reason that affected the target production power in the CPC/PCM system, resulting in fewer instances of reaching the target power compared to the CPC system.

Based on the results from this four-month test, the concentrators partially met the design criteria. They achieved a power output of 100 W at noon during specific months but not consistently throughout the year. The concentration ratio was higher than 2, which was in

line with the design criteria. The novel solar technology, efficiency improvement, and building integration aspects of the design criteria were addressed, with the development of large-scale CPCs and incorporation of phase change materials for heat collection.

However, it is essential to consider that the systems were tested under real-world conditions, which can significantly impact performance. Although the systems did not consistently reach the target power output of 100 W at noon throughout the year under real-world test, it is still a positive outcome considering the various factors affecting system performance during the four-month test period. Further evaluation and optimization of the systems, as well as addressing the impact of high temperatures on the CPC/PCM system, would be necessary to improve performance and achieve the desired power output and efficiency levels consistently.

Table 7. 9 CPC/PCM system under 100 W power output in four months

Date	Time	Solar radiation (W/m^2)	CPC/PCM Power (W)	CPC/PCM Power ratio	CPC/PCM Fill factor	CPC/PCM solar cell Eff (%)	CPC/PCM Optical Eff (%)	CPC/PCM System Eff (%)	CPC/PCM Solar Cells T (°C)	Outdoor T (°C)
2022-08-19	12:08	773	107	2.40	0.73	30	90	12	45	16
2022-08-26	11:28	862	101	2.18	0.58	31	89	10	72	19
2022-08-26	11:46	896	103	2.12	0.55	30	95	9	82	18
2022-09-01	12:02	855	101	3.79	0.59	32	85	11	38	17
2022-09-01	12:08	877	100	2.85	0.59	30	83	10	62	18
2022-09-01	12:12	840	101	2.31	0.65	33	89	10	39	18
2022-09-02	11:52	802	104	3.47	0.59	35	84	11	44	17
2022-09-02	11:54	832	105	2.64	0.59	34	85	11	52	19
2022-09-02	11:56	798	102	2.32	0.60	33	82	10	46	17
2022-09-07	11:46	895	104	1.99	0.58	31	91	10	55	18
2022-09-07	11:50	771	106	5.72	0.69	37	81	12	47	17
2022-09-08	11:56	753	100	2.52	0.62	38	79	16	55	18
2022-09-08	12:10	723	105	2.44	0.58	39	77	12	52	20
2022-09-09	11:48	855	103	2.34	0.62	32	85	10	50	17
	Average	**824**	**103**	**2.79**	**0.61**	**33**	**85**	**11**	**53**	**18**

Table 7. 10 CPC system under 100 W power output in four month tested

Date	Time	Solar radiation (W/m^2)	CPC Power (W)	CPC Power ratio	CPC Fill factor	CPC Solar cell Eff (%)	CPC Optical Eff (%)	CPC System Eff (%)	CPC Solar Cells Temperature (ºC)	Outdoor T (ºC)
2022-08-16	12:24	776	102	2.42	0.65	35	90	11.07	55	17
2022-08-18	12:00	784	102	2.34	0.63	35	95	10.98	53	18
2022-08-19	11:08	873	102	2.33	0.64	31	86	9.81	27	14
2022-08-19	11:14	1045	113	3.11	0.65	29	95	9.10	38	16

2022-08-19	11:18	915	102	2.29	0.62	30	85	9.35	49	17
2022-08-19	12:08	831	112	2.52	0.57	36	93	11.33	39	16
2022-08-20	12:26	876	104	-	0.68	32	-	9.96	23	15
2022-08-21	11:26	870	103	-	0.59	32	-	9.94	61	16
2022-08-21	11:28	869	101	-	0.61	31	-	9.80	72	17
2022-08-21	11:30	885	105	-	0.58	32	-	9.97	73	20
2022-08-21	11:40	845	105	-	0.69	33	-	10.42	59	18
2022-08-24	12:24	745	101	2.33	0.61	36	95	11.39	57	17
2022-08-26	12:00	880	105	2.45	0.72	32	81	10.03	72	19
2022-09-01	12:02	820	105	3.94	0.60	34	78	10.75	35	17
2022-09-01	12:08	877	104	2.68	0.60	31	86	9.92	57	18
2022-09-01	12:10	863	102	2.28	0.61	32	92	9.93	39	16
2022-09-01	12:12	896	105	2.40	0.60	31	95	9.81	39	18
2022-09-01	12:14	810	102	2.25	0.60	33	97	10.53	49	18
2022-09-01	12:24	834	103	2.86	0.68	33	95	10.42	63	19
2022-09-02	12:00	730	103	2.74	0.76	38	86	11.86	38	17
2022-09-02	12:02	795	104	2.65	0.62	35	84	10.99	51	17
2022-09-07	11:50	771	112	2.89	0.63	39	83	12.14	45	17
2022-09-07	12:00	812	102	2.21	0.61	33	90	10.50	54	18
2022-09-08	11:26	819	100	2.47	0.60	33	84	10.26	45	18
2022-09-08	11:56	796	104	2.49	0.61	35	82	10.98	50	18
2022-09-08	12:06	815	103	3.74	0.62	34	86	10.62	50	19
2022-09-08	12:10	723	105	2.45	0.61	39	99	12.25	51	20
2022-09-09	11:48	855	110	2.48	0.62	34	79	10.78	43	17
2022-09-13	12:18	712	111	3.20	0.75	41	86	13.05	50	16
	Average	**832**	**104**	**2.65**	**0.63**	**34**	**88**	**10.62**	**50**	**17**

From table 7.9 and 7.10 the provided data shows that there were instances where the CPC/PCM and CPC systems reached high concentration ratios over 3 and up to 4. Table 7.11 presents instances where both the CPC/PCM and CPC systems reached a high concentration ratio of 3 or higher. This was significant because a higher concentration ratio indicated that the systems effectively focused more solar radiation onto the solar cells, increasing the efficiency and power output of the systems.

The concentration ratio was the ratio between the collected solar radiation and the solar radiation incident on the solar cells. A higher concentration ratio meant that a larger amount of solar radiation was concentrated onto a smaller area of solar cells. This was beneficial as it led to increased efficiency and reduced material costs for the solar cells.

In the cases presented in Table 7.11, the CPC/PCM and CPC systems achieved concentration ratios ranging from 3.11 to 5.72. This meant that the systems were able to concentrate the solar radiation by 3 to nearly 6 times, depending on the specific conditions and configuration.

When observing the solar cell and outdoor temperatures, it was apparent that the solar cells operated at a higher temperature than the outdoor ambient temperature. This temperature difference, which ranged from 21 to 34°C, resulted from the concentrated solar radiation increasing the temperature of the solar cells. While this could have been a concern for the long-term performance and efficiency of the solar cells, it demonstrated that the systems effectively concentrated the solar radiation.

Table 7. 11 Concentrator systems reached a concentration ratio of 3 or higher

System	Date	Time	Solar radiation (W/m^2)	Power (W)	Power Ratio	Solar Cell T (°C)	Outdoor T (°C)
CPC/PCM	2022-09-01	12:02	855	101	3.79	38	17
CPC/PCM	2022-09-02	11:52	802	104	3.47	44	17
CPC/PCM	2022-09-07	11:50	771	106	5.72	47	17
CPC	2022-08-19	11:14	1045	113	3.11	38	16
CPC	2022-09-01	12:02	820	105	3.94	35	17
CPC	2022-09-08	12:06	815	103	3.74	50	19
CPC	2022-09-13	12:18	712	111	3.2	50	16

7.3 Conclusion

Table 7.12 presents a comparison of the performance metrics of two solar concentrator systems (CPC and CPC/PCM) and a Reference system across different locations and conditions. The locations include Ferrara, Italy, and Mayo, Ireland (with clear sky, diffuse radiation, and a 4-month average). The performance metrics include average solar radiation, outdoor temperature, power output, power ratio, fill factor, solar cell efficiency, optical efficiency, system efficiency, and maximum solar cell temperature.

In Ferrara, Italy, the CPC system had a power output of 80 W, while the CPC/PCM system had a power output of 113 W, which was significantly higher than the Reference system's power output of 63 W. The solar cell efficiency was 25 % for the CPC system and 27 % for the CPC/PCM system, both of which were higher than the Reference system's 12 %. The system efficiency was 4 % for the CPC system and 9 % for the CPC/PCM system.

In Mayo, Ireland, under clear sky, the CPC system had a power output of 37 W and a power ratio of 1.86, while the CPC/PCM system had a power output of 33 W and a power ratio of 1.79. Both systems performed better than the Reference system, which had a power output of 19 W. The solar cell efficiency and system efficiency were also higher for both the CPC and CPC/PCM systems compared to the reference system.

Under diffuse radiation in Mayo, Ireland, the CPC system had a power output of 5 W and a power ratio of 2.07, while the CPC/PCM system had a power output of 5 W and a power ratio of 2.23. Both systems demonstrated higher solar cell efficiency and system efficiency compared to the Reference system.

Over four months in Mayo, Ireland, the CPC system had an average power output of 15 W, while the CPC/PCM system also had a power output of 15 W. The power ratio for the CPC/PCM system was 1.91. Both systems had higher fill factors, solar cell efficiencies, and system efficiencies compared to the reference system.
The maximum solar cell temperature for the CPC/PCM system was 67 ºC in Mayo, Ireland under direct radiation and 33 ºC for the four-month average.

In conclusion, the CPC and CPC/PCM systems demonstrated improved performance in terms of power output, solar cell efficiency, and system efficiency compared to the Reference system across different locations and conditions. The CPC/PCM system, in particular, showed higher power output and system efficiency in Ferrara, Italy, and better performance under diffuse radiation in Mayo, Ireland.

Table 7. 12 Conclusion from chapter 7, Mayo systems performance

Performance Metrics	Ferrara, Italy	Mayo, Ireland (Clear sky)	Mayo, Ireland (Diffuse Radiation)	Mayo, Ireland (4 Months)
Average Solar Radiation	823 W/m²	420 W/m²	50 W/m²	-
Average Outdoor Temperature	-	22 ºC	14 ºC	-
Power Output	CPC: 80 W	CPC: 37 W	CPC: 5 W	CPC: 15 W
	CPC/PCM: 113 W	CPC/PCM: 33 W	CPC/PCM: 5 W	CPC/PCM: 15 W
	Reference: 63 W	Reference: 19 W	Reference: 2 W	Reference: 8 W
Power Ratio	-	CPC: 1.86	CPC: 2.07	-
	CPC/PCM: 1.79	CPC/PCM: 1.77	CPC/PCM: 2.23	CPC/PCM: 1.91
Fill Factor	-	CPC: 0.62	CPC: 0.62	CPC: 0.67
	-	CPC/PCM: 0.59	CPC/PCM: 0.73	CPC/PCM: 0.69
	-	Reference: 0.76	Reference: 0.70	Reference: 0.71
Solar Cell Efficiency	CPC: 25 %	CPC: 20 %	CPC: 27 %	CPC: 25 %
	CPC/PCM: 27 %	CPC/PCM: 19 %	CPC/PCM: 29 %	CPC/PCM: 25 %
	Reference: 12 %	Reference: 12 %	Reference: 13 %	Reference: 13 %
Optical Efficiency	-	CPC: 69 %	CPC: 63 %	CPC: 63 %
	-	CPC/PCM: 72 %	CPC/PCM: 63 %	CPC/PCM: 64 %
System Efficiency	CPC: 4 %	CPC: 6 %	CPC: 8 %	CPC: 8 %
	CPC/PCM: 9 %	CPC/PCM: 6 %	CPC/PCM: 9 %	CPC/PCM: 8 %
	Reference: 4 %	Reference: 4 %	Reference: 4 %	Reference: 4 %
Max Solar Cell Temperature	-	CPC/PCM: 67 ºC	-	CPC/PCM: 33 ºC

Chapter 8 Conclusions and recommendations for further work

Truncated Asymmetric Compound Parabolic Photovoltaic Concentrator have been found the most suitable for using in building facades for the range of angular acceptance and have been proven to be an excellent option for electricity generation in buildings (Zacharopoulos et al, 2000; Mallick et al, 2004, Wu, 2009).

- Two Compound Parabolic Concentrator for façade integration to produce 100 W power output at noon during the year for two locations: Ferrara, Italy and Mayo, Ireland has been, has been designed.
- A ray trace simulation has been used to predict the optical and power performance of two Compound Parabolic Concentrator systems for two locations: Ferrara and Mayo.
- An extensive outdoor experiment was used to investigated the power output, power ratio and efficiencies of the compound parabolic concentrators with acceptance half angle of 22 º - 68 º, concentrator ratio of 3, 32 solar cells and power output 100 W suitable in Ferrara weather climate condition.
- An extensive outdoor experiment was used to investigated the power output, power ratio, efficiencies and thermal behavior of the compound parabolic concentrators with acceptance half angle of 12 º - 63 º, concentrator ratio of 3, 24 solar cells and power output 100 W suitable in Mayo weather climate condition.

8.1 Simulation

The simulation found that two CPC systems with different acceptance half-angles were suitable for building façade characterization in Ferrara, Italy and Mayo, Ireland. Both CPC systems outperformed the Reference system under global and diffuse radiation and demonstrated the ability to reach 100 W power output at noon throughout the year. The CPC system with acceptance half-angles of 22º - 68º, concentration ratio of 3 and 32 solar cells was the best for Ferrara, while the CPC system with acceptance half-angle of 12º - 63º, concentration ratio of 3 and 24 solar cells was the best for Mayo. The solar cell efficiency for the CPC system varied from 24 % to 41 % during the year, while the Reference system had an efficiency of 9 % to 21 %.

It is important to note that the maximum efficiency of silicon solar cells is typically around 30%. The 41 % efficiency predicted by the simulation might seem unrealistic at first glance. However, this value was likely obtained due to the concentration effect provided by the CPC system, which focuses solar radiation onto the solar cells, leading to increased efficiency. It is worth mentioning that the simulation results represent an ideal scenario, and the actual efficiency in real-world conditions might be lower due to various factors such as temperature, dust accumulation, and manufacturing tolerances. Therefore, the discrepancy between the

predicted and observed efficiencies can be attributed to these factors, as well as the inherent limitations of the simulation model.

Power ratio was stable and approximately 2.8 from February to September for both locations. The optical efficiency varied from 28 % to 74 % for Ferrara and 34 % to 70 % for Mayo, with the lowest values in summer and greatest in spring. The unique aspect of the simulation findings was that it identified and tailored two different CPC systems with distinct acceptance half-angles and concentration ratios to suit the specific building façade characteristics in Ferrara, Italy, and Mayo, Ireland. This customization allowed both systems to outperform the Reference system under global and diffuse radiation, and achieve 100 W power output at noon throughout the year.

8.2 Small prototype

Small prototype CPC systems were tested in outdoor conditions in Dublin, Ireland and compared to a Reference system with the same solar cell area and characteristics. The results showed that for both CPC systems, power output, power ratio and efficiencies were higher that Reference system. The solar cell temperatures were also higher in both CPC systems. The experimental results confirmed the simulation results for both locations. At maximum solar radiation, the CPC systems showed a power ratio of 1.34 and 1.43 for Ferrara, Italy and Mayo, Ireland respectively. As average values obtained during the tests, the CPC systems showed a power ratio of 2.8 and 2.57 for Ferrara, Italy and Mayo, Ireland.

This experimental validation was crucial for future large scale manufacturing for both locations (Ferrara, Italy and Mayo, Ireland). The higher power output, power ratio, and efficiencies observed in the CPC systems, along with increased solar cell temperatures, further supported the effectiveness of these systems compared to the Reference system.

The fact that the CPC systems performed well under actual outdoor conditions was a significant finding, as it demonstrated the potential for these systems to be utilized in real-world applications.

8.3 Design and manufacturing

While compound parabolic concentrators (CPC) and CPC systems with phase change materials (PCM) had been previously studied and developed, the uniqueness of this research lay in the tailored design and fabrication methods specifically for the distinct locations of Ferrara, Italy and Mayo, Ireland. The focus on optimizing the systems based on location-specific building façade characteristics and solar radiation conditions demonstrated a customized approach. Furthermore, this research involved large-scale manufacturing for integration into building façades, which added another layer of novelty to the project.
For each location, three types of systems were designed and fabricated:

Ferrara, Italy

- **CPC System:** Concentrating compound parabolic concentrator with 32 solar cells connected in series.
- **CPC/PCM System**: Concentrating compound parabolic concentrator with PCM containers located in the back of the solar cells with 32 solar cells.
- **Reference System:** Flat non-concentrating panel with 32 solar cells connected in series.

Mayo, Ireland:

- **CPC System:** Concentrating compound parabolic concentrator with 24 solar cells connected in series.
- **CPC/PCM System:** Concentrating compound parabolic concentrator with PCM containers located in the back of the solar cells with 24 solar cells.
- **Reference System:** Flat non-concentrating panel with 8 solar cells connected in series.

Although similar systems had been developed in the past, the tailored design and fabrication for these specific locations, as well as the large-scale manufacturing for integration into building façades, set this research apart from previous work in the field.

8.4 Experimental characterization

An extensive characterization between the concentrators and reference systems was carried out in Ferrara and Mayo over a period of 4 – 5 months to determine the performance. The detailed conclusion are as follows:

In Ferrara, Italy, the CPC system achieved a power output of 80 W, while the CPC/PCM system reached 113 W, significantly surpassing the Reference system's output of 63 W. Solar cell efficiency was 25 % for the CPC system and 27% for the CPC/PCM system, both outperforming the Reference system's 12 %. System efficiency stood at 4% for the CPC system and 9 % for the CPC/PCM system.

In Mayo, Ireland, under clear sky conditions, the CPC system had a power output of 37 W and a power ratio of 1.86, while the CPC/PCM system had a power output of 33 W and a power ratio of 1.79. Both systems outpaced the Reference system, which had a power output of 19 W. Solar cell efficiency and system efficiency were also higher for both the CPC and CPC/PCM systems compared to the Reference system.

Under diffuse radiation conditions in Mayo, Ireland, the CPC system had a power output of 5 W and a power ratio of 2.07, while the CPC/PCM system had a power output of 5 W and a power ratio of 2.23. Both systems displayed higher solar cell efficiency and system efficiency compared to the Reference system.

Over a four-month period in Mayo, Ireland, the CPC system had an average power output of 15 W, and the CPC/PCM system also had a power output of 15 W. The power ratio for the CPC/PCM system was 1.91. Both systems exhibited higher fill factors, solar cell efficiencies, and system efficiencies compared to the Reference system. The maximum solar cell temperature for the CPC/PCM system was 67 ºC under direct radiation in Mayo, Ireland, and 33 ºC for the four-month average.

When comparing the experimental test results with the simulation results for both locations, the following differences and similarities were observed:

Ferrara, Italy:

- **Solar Cell Efficiency:** The experimental test results had shown a solar cell efficiency of 25 % for CPC and 27 % for CPC/PCM systems, while the simulation results had predicted a range of 24 % to 41 %.
- **Power Ratio:** The experimental test results reported a power ratio of 1.79 for the CPC/PCM system. In the simulation results, the power ratio ranged from 1.42 in December to 2.80 from February to September.
- **Power Output:** The experimental test results reported 80 W for the CPC system and 113 W for the CPC/PCM system. The simulation had predicted a power output of 121 W at 1000 W/m² and 25 ºC.

Mayo, Ireland (Clear sky):

- **Solar Cell Efficiency:** The experimental test results had shown a solar cell efficiency of 20% for the CPC system and 19 % for the CPC/PCM system, whereas the simulation results had indicated a range of 31 % to 49 %.
- **Power Ratio:** The experimental test results reported a power ratio of 1.86 for the CPC system and 1.79 for the CPC/PCM system. The simulation results had shown a power ratio of 1.4 in January, 1.29 in December, and 2.82 from February to September.
- **Power Output:** The experimental test results had shown a power output of 37 W for the CPC system and 33 W for the CPC/PCM system. The simulation results had predicted a power output of 126 W at 1000 W/m² and 25 ºC.

The experimental test results and simulation results showed some discrepancies in solar cell efficiency and power ratio. However, both sets of results demonstrated that the CPC and CPC/PCM systems had performed better than the Reference system across different locations and conditions.

The full-scale tests conducted in this research have critical implications for commercial installation of such solar systems, shedding light on key considerations such as area requirements, costs, and potential payback.

- Area Requirements: The test revealed that the CPC and CPC/PCM systems require more space than conventional flat panel systems due to the inclusion of concentrators. This could be a significant factor in urban installations where available space is limited. However, in situations where ample space is available, such as in rural or industrial settings, these systems can be more beneficial as they can potentially harness more solar energy per unit area.

- Costs: The additional components (CPC and PCM) incorporated in these systems add to the overall cost. The fabrication, installation, and maintenance costs of these systems are higher than those of conventional systems. However, these initial costs could be offset by the higher efficiency and power output demonstrated by these systems, particularly the CPC/PCM system. Furthermore, the cost can be reduced in industrial manufacturing through economies of scale and material optimization.

- Likely Pay-back: Pay-back period will depend on several factors such as the local price of electricity, the amount of sunlight received, and any government subsidies or incentives available. Given their higher efficiency, the CPC and CPC/PCM systems could potentially have shorter payback periods in areas with high solar radiation like Ferrara. The extra energy generated can be sold back to the grid or used for thermal applications, thereby adding another revenue stream and reducing the payback period.

The full-scale tests have proven invaluable in understanding the real-world performance of these innovative solar systems. These insights can guide further development and commercialization of these systems. However, for commercial success, it is crucial to consider the local context - solar irradiation levels, available space, electricity prices, and available incentives. Future research could focus on optimizing the design and materials used to reduce costs and improve efficiency, thereby making these systems a more attractive option for commercial installations.

8.5 Contribution to knowledge

In conclusion, this thesis presented a comprehensive research study that aimed to enhance the power output, power ratio, and efficiency of solar cells in building-integrated façades using CPCs at two different locations. The study involved designing CPCs, conducting ray tracing, testing small prototypes, designing and manufacturing large-scale systems, and investigating the power output and efficiencies of the CPC systems in outdoor conditions.

The thesis made several significant contributions to the field of solar energy:

- It introduced a novel design approach for CPCs, capable of generating 100 W power output at noon throughout the year in both Ferrara, Italy, and Mayo, Ireland.
- It employed ray tracing to predict power and optical performance for different CPC systems, aiding the selection of the most suitable system for each location.
- It validated the results through small prototype testing and demonstrated their scalability through the design and manufacture of large-scale systems.
- It was the first time systems were built, installed, and monitored in real-world outdoor conditions to investigate power output, power ratio, efficiencies, and thermal behavior of the combined LDS/CPC/PCM systems.
- The concentrator systems achieved a concentration ratio of 3 or higher on multiple occasions, with the highest concentration ratio of 5.72 being recorded for the CPC/PCM system on September 7, 2022, under a solar radiation of 771 W/m².

By providing a better understanding of the effectiveness of CPCs in increasing the power output and efficiencies of solar cells for building-integrated façades, this research has the potential to significantly impact the reduction of buildings' carbon footprints and promote sustainable energy sources. The findings in this research could be used to inform future research and development in the field of solar energy and building design.

8.6 Recommendation for future work

- Anti-condensation system should be designed and integrated in the systems in order to avoid high condensation and better the transmissibility of the aperture for better optical efficiency. An anti-condensation system is a solution designed to prevent or minimize the formation of condensation on the surface of a solar panel or solar concentrator system. Condensation can reduce the transmissibility of the aperture, leading to lower optical efficiency and a decrease in the system's overall performance. Designing an effective anti-condensation system involves addressing the factors that contribute to condensation, including temperature differences and humidity. Examples of designs are as follows:

1. **Hydrophobic coating:** Applying a hydrophobic coating on the surface of the aperture can help reduce condensation by lowering the surface energy, causing water droplets to form beads and slide off the surface rather than adhering to it. This prevents the buildup of moisture and maintains the transmissibility of the aperture.

2. **Ventilation and air circulation:** Ensuring proper ventilation around the solar panel or concentrator system can help reduce condensation. By maintaining good air

circulation, the temperature and humidity levels near the panel's surface can be better controlled, minimizing the chances of condensation forming.

3. **Small fans for air circulation:** Integrating small fans into the solar concentrator system can help improve air circulation around the panel and aperture. By actively moving the air, fans can help maintain a consistent temperature and humidity level near the surface of the system, reducing the chances of condensation forming. The fans can be either solar-powered or connected to a low-power external source, ensuring minimal energy consumption while maximizing their effectiveness in promoting air circulation.

- Design a mechanism for easy opening and access to the systems in order to facilitate the maintenance and cleaning of the systems during the year. For example:

1. **Hinged frames:** Implementing hinged frames on the solar concentrator system allows for easy access to the interior components. The hinges can be secured with latches or locking mechanisms to keep the system closed during normal operation. When maintenance or cleaning is required, the latches can be released, and the frame can be opened like a door, providing full access to the solar cells, CPCs, and other internal components.

2. **Sliding panels:** Designing sliding panels on the system's enclosure can enable easy access to the interior without the need for hinges. The panels can be mounted on tracks or rails, allowing them to be smoothly opened and closed as needed. This approach also provides the benefit of minimal space requirements for maintenance access.

- Ensure the systems are installed with at least 500 mm between them in order to avoid over shadowing.

- Additional structure in order to correct the inclination of 46º with the south, so that the systems are perfectly oriented to the south.

- Changing the Perspex pieces in the frames for glass in order to improve the transmittance of solar radiation and reduce the Life Cycle Assessment (LCA) of the systems. LCA is a methodology used to evaluate the environmental impacts associated with a product, process, or service throughout its entire life cycle. It considers various factors, including raw material extraction, manufacturing, transportation, usage, and end-of-life disposal or recycling. By replacing Perspex with glass, the LCA of the solar concentrator systems can be reduced. Glass is generally more durable, less prone to degradation from UV exposure, and easier to recycle compared to Perspex. This can lead to a longer service life, reduced maintenance requirements, and a lower overall

environmental impact of the solar concentrator system. Additionally, it is important to consider the aluminum used in the construction of the solar concentrators. Aluminum has a high embodied energy and environmental impact during its production process; however, it is highly recyclable and durable. When evaluating the LCA of the solar concentrator systems, it is crucial to account for the potential environmental benefits of recycling aluminum and its long service life, which can offset its initial environmental impact.

- Water pipe cooling system integrated to the CPC/PCM systems should be used with temperature control system in order to reduce the temperature of the solar cell and increase the efficiency and power output. In addition, the hot water could be stored in a tank for building application

- Design of array of parabolas with focal line in the centre of the solar cells in order to avoid the loss of rays at the edges of the solar cells.

- The flux distribution in the solar cell could be improved adding an extra reflector perpendicular to the solar cell and located on the edge to eliminate multiple reflections and improve flux distribution.

- Three-dimensional CPC systems in small scale using 3D printing (figure 8.1) could be used in order to realize indoor characterization with controlled solar incident radiation. In addition, using biodegradable filaments can contribute to a more environmentally friendly approach. Biodegradable filaments are made from renewable resources such as PLA (polylactic acid), which is derived from cornstarch, sugarcane, or tapioca roots. These materials decompose naturally over time under the right conditions, reducing the environmental impact and waste associated with traditional, petroleum-based plastic materials. By employing biodegradable filaments for 3D printing small-scale CPC systems, the overall environmental footprint of these devices can be reduced, making them more sustainable and eco-friendly options for solar energy applications.

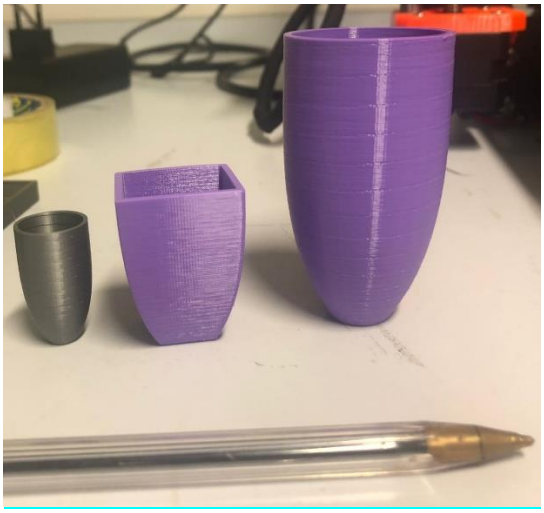

Figure 8. 1 Small scale 3D CPC system proposed for future work

- Large scale composite of small-scale CPCs integrated into mesh using 3D printers with algae-based filaments (figure 8.2). A grid of 3D CPC systems in series connection could be used as a potential building integrated application.

Figure 8. 2 Algae – based filament commercial available

- Dielectric CPC on a small scale 3D CPC system (figure 8.3) can be designed and manufactured using resins on SL 3D printers. Different colors can be tested in order to find the resin with the best performance. Clear resins can be used with controlled additions of dye in order to improve the concentration of the dielectric CPC.

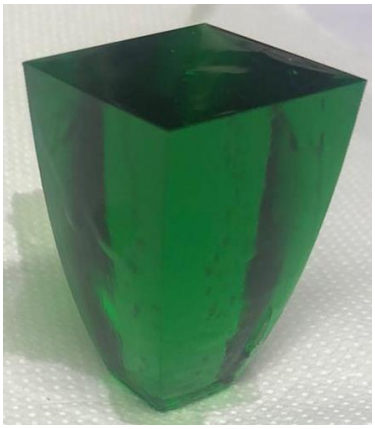

Figure 8. 3 Dielectric CPC printed using SL 3D printer

- As this research has demonstrated, the successful implementation of CPC and CPC/PCM systems depends on various factors, including reported power values, efficiency, and operational conditions. Moving forward, it would be advantageous to undertake a more comprehensive analysis that extends beyond reported power values to evaluate overall energy generation. While reported power values provide insight into peak performance, they do not necessarily indicate cumulative energy output, which is crucial for evaluating the system's viability in real-world conditions.

To better understand this dynamic, future research could focus on the following areas:

1. **Energy Generation Analysis:** Conduct an in-depth study on how the peak power generation conditions relate to the total energy generation. This would involve not only considering the maximum power output but also how long the system can maintain high output levels throughout the day and over different seasons.

2. **Operational Efficiency:** Investigate how factors such as temperature variations, solar irradiance levels, and system conditions (like the presence of shading or dust) affect the total energy output. This would provide a more robust understanding of the systems' performance in real-world conditions.

3. **Optimization of System Parameters:** Perform further studies to optimize the design and operational parameters of the CPC and CPC/PCM systems. This could include optimizing the concentrator's shape or orientation, the type of PCM used, or the system's cooling mechanism to enhance energy generation.

4. **Long-Term Performance:** Monitor and assess the long-term performance of the systems, including aspects like durability, maintenance needs, and performance degradation over time. This could provide valuable insights into the lifecycle costs and return on investment of these systems.

By focusing on these areas, future work can provide a more comprehensive understanding of the energy generation potential of CPC and CPC/PCM systems, guiding their development towards higher efficiency and commercial viability.

References

Ahmed, H., Kennedy, M., Doran, J., McCormack, S. J., Galindo, S., Voz, C., and Puigdollers, J., 2012. Lumogen Violet Dye as Luminescent Down-Shifting Layer for c-Silicon Solar Cells. In Proceedings of the 27th European Photovoltaic Solar Energy Conference and Exhibition, Frankfurt, Germany.

Ahmed, H. (2014). Materials Characterization and Plasmonic Interaction in Enhanced Luminescent Down-Shifting Layers for Photovoltaic Devices. (PhD thesis). Dublin Institute of Technology.

Ahmed H., McCormack S., Doran J., Plasmonic luminescent down shifting layers for enhacement of CdTe mini-modules performance. Solar Energy Journal, 2017:242-248.

Ames, W. D., 1983. Photovoltaic devices for producing electrical and heat energy. United States of America patent application.

Browne, M., Norton, B., McCormack, S., 2016. Heat retention of a photovoltaic/thermal collector with PCM. Sol. Energy 133, 533–548 ISSN 0038-092X.

Collares-Pereira, M., Goodman, N.B., Greenman, P., O'Gallagher, J., Rabl, A., Simmons, H., Wharton, L., Winston, R., 1978. Compound Parabolic Concentrators With Non-Evacuated Receivers - Prototype Performance and a Larger Scale Demonstration in a School Heating System., in: Proceedings of the International Solar Energy Society Congress. New Delhi, India, pp. 1227–1232. doi:10.1016/b978-1-4832-8407-1.50242-7

Devanayanan, K., Murugavel, K., 2014. Integrated collector storage solar water heater with compound parabolic concentrator-development and progress. Renew. Sustain. Energy Rev. 39, 51–64.

Duffie, J., Beckman, W., 1991. Solar engineering of thermal processes, Wiley y So. ed. New Jersey, USA.

Government of Ireland, 2023. https://www.gov.ie/en/ [Online]. [Accessed 15 March 2023].

Hasan, A., Mccormack, S. J., Huang, M. J., Norton, B., 2010. Evaluation of phase change materials for thermal regulation enhancement of building integrated photovoltaics. Solar Energy, 84, 1601-1612.

Hasan, A., Mccormack, S., Huang, M. & Norton, B., 2014. Energy and Cost Saving of a Photovoltaic-Phase Change Materials (PV-PCM) System through Temperature Regulation and Performance Enhancement of Photovoltaics. Energies, 7, 1318-1331.

Hovel, H. J., Hodgson, R. T., and Woodall, J.M., 1979. The Effect of Fluorescent Wavelength Shifting on Solar Cell Spectral Response. Solar Energy Materials, 2, 19-29.

Huang, M. J., Eames, P. C. & Norton, B., 2004. Thermal regulation of building-integrated photovoltaics using phase change materials. International Journal of Heat and Mass Transfer, 47, 2715-2733.

Ideas, 2023. https://www.horizon2020ideas.eu/ [Online]. [Accessed 02 February 2023].

Jaaz, A.H., Sopian, K., Gaaz, T.S., 2018. Study of the electrical and thermal performances of photovoltaic thermal collector-compound parabolic concentrated. Results Phys. 9, 500–510. doi:10.1016/j.rinp.2018.03.004

Klampaftis, E., Ross, D., McIntosh, K. R., and Richards, B., 2009. Enhancing the Performance of Solar Cell via Luminescent Down-Shifting of the Incident Spectrum: A Review. Solar Energy Materials & Solar Cells, 93, 1182-1194.

Kessentini, H., Bouden, C., 2013. Numerical and experimental study of an integrated solar collector with CPC reflectors. Renew. Energy 57, 577–586. doi:10.1016/j.renene.2013.02.015

Ling, Z., Zhang, Z., Shi, G., Fang, X., Wang, L., Gao, X., Fang, Y., Xu, T., Wang, S. & Liu, X., 2014. Review on thermal management systems using phase change materials for electronic components, Li-ion batteries and photovoltaic modules. Renewable and Sustainable Energy Reviews, 31, 427-438.

Luque, A., Sala, G.L., Araujo, 1995. Cost reducing potential of photovoltaic concentration. Int. J. Sol. Energy 16, 179–198.

Mallick, T., 2003. Optics and heat transfer for asymmetric compound parabolic photovoltaic concentrator for building integrated photovoltaics. PhD Thesis. University of Ulster, Newtownabbey, N.I.U.K.

Mallick, T., Eames, P., Norton, B., 2002. Asymmetric compound parabolic photovoltaic concentrators for building integration in the UK: An optical analysis, in: World Renewable Energy Congress-VII. Koln, Germany.

Mallick, T.K., Eames, P.C., Hyde, T.J., Norton, B., 2004. The design and experimental characterisation of an asymmetric compound parabolic photovoltaic concentrator for building façade integration in the UK. Sol. Energy 77, 319–327. doi:10.1016/j.solener.2004.05.015

Mallick, T.K., Eames, P.C., Norton, B., 2007a. Using air flow to alleviate temperature elevation in solar cells within asymmetric compound parabolic concentrators. Sol. Energy 81, 173–184. doi:10.1016/j.solener.2006.04.003

Mallick, T.K., Eames, P.C., Norton, B., 2007b. Power losses in an asymmetric compound parabolic photovoltaic concentrator. Sol. Energy Mater. Sol. Cells 91, 1137–1146. doi:10.1016/j.solmat.2007.03.020

Mallick, T.K., Eames, P.C., Norton, B., 2006. Non-concentrating and asymmetric compound parabolic concentrating building façade integrated photovoltaics: An experimental comparison. Sol. Energy 80, 834–849. doi:10.1016/j.solener.2005.05.011

Mills, D.R., Giutronich, J.E., 1978. Asymmetrical non-imaging cylindrical solar concentrators. Sol. Energy 20, 45–55.

Norton, B., Eames, P.C., Mallick, T.K., Huang, M.J., McCormack, S.J., Mondol, J.D., Yohanis,

Y.G., 2011. Enhancing the performance of building integrated photovoltaics. Sol. Energy 85, 1629–1664. doi:10.1016/j.solener.2009.10.004

Othman, M.Y.H., Yatim, B., Sopian, K., Abu Bakar, M.N., 2005. Performance analysis of a double-pass photovoltaic/thermal (PV/T) solar collector with CPC and fins. Renew. Energy 30, 2005–2017. doi:10.1016/j.renene.2004.10.007

R. Winston, 1978. Ideal flux concentrators with reflector gaps. Appl. Opt. 17, 1668–1669.

Rabl A, 1976a. Comparison of solar concentrators. Sol. Energy 18, 93–111.

Rabl A, 1976b. Optical and thermal properties of compound parabolic concentrators. Sol. Energy 18, 497–511.

Ross, D., Alonso-Álvarez, D., Klampaftis, E., Fritsche, J., Bauer, M., Debije, M. G., Fifield, R. M., and Richards, B. S., 2014. The Impact of Luminescent Down Shifting on the Performance of CdTe Photovoltaics: Impact of the Module Vintage. IEEE Journal of Photovoltaic, 4, 457-464.

Shanks, K., Senthilarasu, S., Mallick, T.K., 2016. Optics for concentrating photovoltaics: Trends, limits and opportunities for materials and design. Renew. Sustain. Energy Rev. 60, 394–407. doi:10.1016/j.rser.2016.01.089

Stultz, J. W. & Wren, L. C., 1978. Thermal performance testing and analysis of photovoltaic modules in natural sunlight, Pasadena, California, Jet propulsion laboratory.

SunPower, 2023. https://us.sunpower.com/ [Online]. [Accessed 02 February 2023].

Wang, Z., Jinjia Wei, G.Z., Xie, H., Khalid, M., 2019. Design and performance study on a large-scale hybrid CPV/T system based on unsteady-state thermal model. Sol. Energy 177, 427–439.

Welford, W., Winston, R., 1978. The optics of non-imaging concentrators. Light Sol. energy. Acad. Press.

Winston, R., 1974. Principles of solar concentrators of a novel design. Sol. Energy 16, 89–95.

Winston, R., Goodman, N., O´Gallagher, J., Pereira, M., Wharton, L., Rabl, A., 1978. Nonevacuated solar collectors with compound parabolic concentrators. Mankind's Futur. Source Energy 2, 1032.

Winston, R., O'Gallagher, J., 1986. Maximally concentrating optics for solar electricity generation, in: Roceedings of the Ninth Biennial Congress of the International Solar Energy Society. pp. 1669–1673.

Winston, R., O'Gallagher, J., Schertz, W., 1986. Integrated evacuated CPC´s for high temperature solar thermal systems, in: Proceedings of the Ninth Biennial Congress of the International Solar Energy Society. pp. 1148–1152.

Wu Y., 2009. Thermal Management of Concentrator Photovoltaics. PhD Thesis. University of Warwick, U.K.

Xie, H., Wei, J., Wang, Z., Yang, G., Ma, Q., 2016. Design and performance research on eliminating multiple reflections of solar radiation within compound parabolic concentrator (CPC) in hybrid CPV/T system. Sol. Energy 129, 126–146. doi:10.1016/j.solener.2016.01.037

Zacharopoulos, A., Eames, P.C., McLarnon, D., Norton, B., 2000. Linear dielectric non-imaging concentrating covers for PV integrated building facades. Sol. Energy 68, 439–452. doi:10.1016/S0038-092X(00)00013-X

Publications

Journals

Akbari, H., Browne, M.C., Ortega, A., Huang, M.J., Hewitt, N.J., Norton, B., McCormack, S.J., 2019. Efficient energy storage technologies for photovoltaic systems. Sol. Energy 192, 144–168. doi:10.1016/j.solener.2018.03.052

Carlini, M., McCormack, S.J., Castellucci, S., Ortega, A., Rotondo, M., & Mennuni, A. (2020). Modelling and Numerical Simulation for an Innovative Compound Solar Concentrator: Thermal Analysis by FEM Approach. Energy Journal. Received: 10 December 2019; Accepted: 20 January 2020; Published: 22 January 2020.

Sethi, A., Chandra, S., Ortega, A. et al. Outdoor Characterization of a Plasmonic Luminescent Solar Concentrator. Plasmonics 17, 725–734 (2022). https://doi.org/10.1007/s11468-021-01562-y

Ortega, A., Obasi, G., Chandra, S., Mangherini, G., Bernardoni, P., Huang, M., McCormack, S.J., 2023. Design and characterization of a large scale asymmetric compound parabolic solar concentrator for building façade in Italy. Solar Energy Journal. *In Review*

Martzeli, P., Centino, M., Ortega, A., & McCormack, S. (2023). Investigation of biomimetic designs and the use of phase change materials for improving the efficiency of solar energy applications. Renewable Energy and Environmental Sustainability. Manuscript Number: REES230018. *In Review*

Conferences

Ortega, A., Akbari, H., McCormack, S.J., 2017. Building Integrated Compound Parabolic Photovoltaic Concentrator: A review. BIRES, Build. Integr. Sol. Therm. Syst. 9. Dublin, Ireland

Ortega, A., Reid, I., Akbari, H., Chandra, S., Parfrey, E., McCormack, S., Design and Characterization of a Roof Mounted Compound Parabolic Concentrator with Phase Change Material, *14th International Conference on Energy Storage*, 25-28 April 2018, Adana, Turkey.

Ortega, A., Chandra, S., McCormack, S.J., Design and Characterization of a Roof-Mounted Compound Parabolic Concentrator, *World renewable Energy Congress*, 13 – 18 September 2020, Lisboa, Protugal.

Saers, S., Ortega, A., Chandra, S., McCormack, S., Compound Parabolic Concentrator Design : Assessment of Performance Enhancement for Building-Integrated Photovoltaic, *World renewable Energy Congress*, 13 – 18 September 2020, Lisboa, Protugal.

Bacaoanu, A., Ortega, A., McCormack, S., n.d. Phase Change for a Radiant Floor Coupled to a Heap Pump and a Geothermal Heat Exchanger. In World Renewable Energy Congress XXI: Energy and Environment. Murdoch University, Western Australia.

Flynn, T., Chandra, S., Ortega, A., & McCormack, S. (2022). Assessment of large-area luminescent solar concentrators as building-integrated geodesic dome panels. In World Renewable Energy Congress XXI: Energy and Environment (pp. 4-9). Murdoch University, Western Australia.